


For Reference

NOT TO BE TAKEN FROM THIS ROOM

Ex LIBRIS
UNIVERSITATIS
ALBERTAENSIS





Digitized by the Internet Archive
in 2024 with funding from
University of Alberta Library

<https://archive.org/details/Arvidson1973>

THE UNIVERSITY OF ALBERTA

RELEASE FORM

NAME OF AUTHOR WAYNE DOUGLAS ARVIDSON.....
TITLE OF THESIS WATER FLOW INDUCED BY SOIL FREEZING.....
.....
DEGREE FOR WHICH THESIS WAS PRESENTED M.Sc.....
YEAR THIS DEGREE GRANTED1973.....

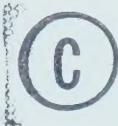
Permission is hereby granted to THE UNIVERSITY OF
ALBERTA LIBRARY to reproduce single copies of this
thesis and to lend or sell such copies for private,
scholarly or scientific research purposes only.

The author reserves other publication rights, and
neither the thesis nor extensive extracts from it may
be printed or otherwise reproduced without the author's
written permission.

THE UNIVERSITY OF ALBERTA

WATER FLOW INDUCED BY SOIL FREEZING

by



WAYNE DOUGLAS ARVIDSON

A THESIS

SUBMITTED TO THE FACULTY OF GRADUATE STUDIES AND RESEARCH
IN PARTIAL FULFILLMENT OF THE REQUIREMENTS FOR THE DEGREE
OF MASTER OF SCIENCE

DEPARTMENT OF CIVIL ENGINEERING

EDMONTON, ALBERTA

FALL, 1973

THE UNIVERSITY OF ALBERTA
FACULTY OF GRADUATE STUDIES AND RESEARCH

The undersigned certify that they have read,
and recommend to the Faculty of Graduate Studies and
Research, for acceptance, a thesis entitled "Water Flow
Induced by Soil Freezing," submitted by Wayne Douglas
Arvidson in partial fulfillment of the requirements for
the degree of Master of Science.

TO DONNA
WITH LOVE

ABSTRACT

An experimental study was conducted to determine the freezing behavior of Ottawa sand and a locally occurring silt. The soils were frozen under varied pressure, stress history, drainage and temperature boundary conditions.

The results demonstrated that freezing behavior of a soil can be predicted by short term freezing tests in which heave and net change in sample porewater volume or porewater pressure were measured. Results indicate that sands expel porewater upon freezing. Freezing behavior of fine grained soils is influenced by both soil properties and external factors. Freezing behavior of the fine grained soils varied from sucking in water leading to ice segregation and lensing, to expulsion of porewater. It was found that the freezing behavior of the fine grained soils depended on overburden pressure, stress history, step temperature, grain size distribution, porosity and permeability.

Results indicate that heave and heave pressure are not a unique freezing soil property. Experimental results support a theory of freezing soils based on the net heat flow from a soil sample and on the stress difference across

across the ice-water interface.

Guidelines for a revised frost susceptibility criterion are given.

ACKNOWLEDGEMENTS

I would like to express my gratitude to the following people:

Dr. N. R. Morgenstern for his guidance and continued enthusiasm throughout the project.

Mr. E. McRoberts for suggesting the topic.

Mr. B. P. Shields and the Research Council of Alberta for providing financial support.

Mr. J. F. Dixon and Mr. W. D. Roggensack for their helpful suggestions and discussions of all aspects of the project.

Mr. A. Muir, Mr. O. Wood and their staff for their help in building and modifying the apparatus.

Mrs. M. Wahl, typist and Mr. J. Maher, draftsman for their part in preparing the thesis.

My wife, Donna, who helped weather the setbacks and successes.

TABLE OF CONTENTS

	PAGE
LIBRARY RELEASE FORM	i
TITLE PAGE	ii
APPROVAL PAGE	iii
DEDICATION	iv
ABSTRACT	v
ACKNOWLEDGEMENT	vii
TABLE OF CONTENTS	viii
LIST OF TABLES	xi
LIST OF FIGURES	xii
CHAPTER I - INTRODUCTION	1
CHAPTER II - LITERATURE SURVEY AND FREEZING THEORY . .	5
2.1 Selected Literature Review	5
2.1.A Freezing Mechanism	5
2.1.B Ice Segregation and Ice Lensing . .	10
2.1.C Frost Heaving	16
2.1.D Heaving Pressures	18
2.1.E Pore Pressures at the Freezing Front	22
2.1.F Frost Susceptibility of Soils . . .	25
2.2 Theory of Freezing of Soils	26
2.2.A Assumptions	27
2.2.B Development of Theory	30

CHAPTER	PAGE
CHAPTER III - TEST PROCEDURE AND DESCRIPTION OF	
OF EQUIPMENT	41
3.1 Test Procedure	41
3.1.A Materials and Sample Preparation .	41
3.1.B Test Procedure	41
3.2 Description of Equipment	43
3.2.A General	43
3.2.B Oedometer	45
3.2.C Freeze System	51
3.2.D Loading and Backpressure Systems .	51
3.2.E Temperature Measurement System . .	52
3.2.F Pore Pressure Measurement System .	53
3.2.G Volume Change Measurement System .	53
3.2.H Vertical Displacement Measurement	
System	55
3.2.I Heave Pressure Measurement System .	55
3.2.J Equipment Assessment and	
Recommendations	55
CHAPTER IV - TEST RESULTS AND CALCULATIONS	58
4.1 Introduction	58
4.2 Test Results	58
4.2.A Ottawa Sand	58
4.2.B Devon Silt	61
4.2.C Modified Devon Silt	78

CHAPTER	PAGE
4.3 Calculations	82
4.3.A Soil Property Calculations	82
4.3.B Freezing Test Calculations	84
CHAPTER V - DISCUSSION AND CONCLUSIONS	99
5.1 Discussion	99
5.1.A Equipment	99
5.1.B Testing Procedure	101
5.1.C Experimental Results	103
5.2 Conclusions	118
LIST OF REFERENCES	124
APPENDIX A - SUMMARY OF SOIL PROPERTIES	129
APPENDIX B - TYPICAL FREEZING TEST CALCULATIONS	134
APPENDIX C - EQUIPMENT SPECIFICATIONS	143
APPENDIX D - SUMMARY OF DATA - OTTAWA SAND	146
APPENDIX E - SUMMARY OF DATA - DEVON SILT (NORMALLY CONSOLIDATED)	153
APPENDIX F - SUMMARY OF DATA - DEVON SILT (OVER CONSOLIDATED)	173
APPENDIX G - SUMMARY OF DATA - MODIFIED DEVON SILT (OVER CONSOLIDATED)	200

LIST OF TABLES

TABLE		PAGE
2.1	Summary of Williams (1967) Data	23
4.1	Rates of Penetration of Freezing Front . . .	89
4.2	Unfrozen Water Content Calculated from Sample Water Balance	94
4.3	Observed and Theoretical Freezing Behavior .	95
4.4	Observed and Calculated Heave	97
4.5	Heave Pressure Data	98
5.1	Experimental P_o Values	112

LIST OF FIGURES

FIGURE		PAGE
2.1	Effective Grain Size, D_{10} , Versus Heave Pressure	21
2.2	Schematic Freezing Model	28
3.1	Schematic Diagram, Test Apparatus	44
3.2	Oedometer	46
3.3	Freeze Piston-Reaction Head and Load Collar. .	47
3.4	Freeze Piston - Heat Exchanger	48
3.5	Freeze Piston - Base Plate	49
3.6	Ambient Temperature - Time Log	54
4.1	Net Change in Sample Porewater Volume - Soil Type	60
4.2	Porewater Pressure - Stress History	65
4.3	Net Change in Sample Porewater Volume - Stress History	69
4.4	Net Change in Sample Porewater Volume - Step Temperature	74
4.5	Penetration of 0°C Isotherm	88
4.6	Comparison of Average Frost Penetration Rates	90
4.7	Schematic Freezing Situation	92
5.1	Comparison of P_o and Preconsolidation Pressure	109

CHAPTER 1

INTRODUCTION

Whenever the mean air temperature drops below freezing for a significant period of time, the effects of frost action are of concern in geotechnical engineering. To date a large number of facilities constructed in the Canadian Arctic have been successfully designed on the basis of engineering judgement. Winter construction techniques in the more southerly regions have similarly been largely developed through experience. With the rapidly increasing development of the Arctic regions larger and more complex facilities are being proposed for which design precedents are not available and accumulated experience is inadequate. There is an urgent need for a basic understanding of the behavior of freezing soils.

Freezing behavior of soils such as heave, heave pressure and frost susceptibility, are well known and easily identified. The bulk of the work that has been carried out on freezing soils is concerned with the analysis of the fundamentals of freezing soils. Few studies to date are concerned with the phenomenological behavior of soils subjected to controlled freezing conditions. The purpose of this thesis is to present some observations on

the behavior of freezing soils.

Initially, the basic outline and goals of the study were conceived by McRoberts (1972) as a basis for analyzing landslides in Northern Canada. That study was concerned with the concept of expulsion of porewater by granular soils proposed by Mackay (1972). Field studies of subsurface ice conducted by Mackay (1972) revealed that sand and gravel underlay 95% of the ice masses investigated. Furthermore, in the remaining 5 per cent of the cases the ice was underlain by a clay layer which in turn rested on sands and gravels.

A field case given by Mackay (1972) illustrates the porewater expulsion phenomenon. In this instance a large lake, which remains partly unfrozen during the winter, is partially drained by natural processes resulting in the formation of 3 smaller lakes in the original lake basin. In the subsequent period of 36 years, 3 pingos developed where the smaller lakes occurred. The underlying basin of the large lake was also composed of sands and gravels. Mackay (1972) believed that as the large lake drained the exposed ground surface began to freeze everywhere except under the three small lakes. He proposed that the aggrading permafrost resulted in the expulsion of porewater from the lake basin sands and gravels resulting in an excess of water in areas underlying the as yet unfrozen smaller lakes.

However, in time these smaller lakes became sufficiently shallow, to freeze completely and to allow the permafrost to aggrade in these areas as well. The ensuing result was a mound with a core of ice, a pingo.

The significance of the porewater expulsion concept has many important practical implications. Frost heave and heave pressure are known to result when water is sucked into the soil sample resulting in segregated ice and ice lensing. The expulsion of porewater is the reverse effect and would indicate that no heave or heave pressure would occur during these conditions. The present classification of frost susceptible soils, by Casagrande (1931), is based on the relative tendency of a soil to heave or to generate heave pressures. If a soil expels water then it would appear that it would not heave and hence be classified as non-frost susceptible. Clearly the mechanism which controls whether a soil will suck in or expel porewater is of vital importance in understanding and predicting the behavior of freezing soils.

The following study investigates the concept of porewater expulsion by freezing soils. The study concentrates on determining which factors, viz., applied pressure, grain size, grain size distribution, temperature, and stress history, influence the expulsion/sucking in mechanism of freezing soils and the relative importance of these factors.

Fundamental research into the actual freezing mechanism is not part of this study but a mathematical model based upon the thermal balance occurring during freezing is investigated.

CHAPTER 2

LITERATURE SURVEY AND FREEZING THEORY

2.1 Selected Literature Review

2.1.A. Freezing Mechanism

The basic mechanism of the freezing of soils is well established qualitatively and generally accepted. Whenever a negative temperature gradient is imposed on a soil, the volumetric heat is removed causing a drop in the bulk temperature. When all of the volumetric heat has been removed and the bulk temperature is 0 degrees Centigrade nucleation of ice occurs with a subsequent release of latent heat. If supercooling of the porewater occurs nucleation of the ice will occur at some temperature lower than 0 degrees Centigrade. The ice crystals grow in the direction of heat removal, (Taber, 1929) and impinge and apply pressure against any restraining boundary. The pressure is relieved by heaving of the soil in the direction of least resistance (Kaplur, 1970). The heave is in response to the 9 per cent volume change at crystallization of the porewater.

After nucleation the freezing front moves in accordance with the relative balance or imbalance of the heat supplied to the heat removed from the soil sample

(Anderson and Morgenstern, 1973). If the rate of heat removal is greater or less than the rate of heat supplied, the freezing front advances or recedes respectively. A receding freezing front results in the melting of the frozen soil from the freezing front upwards. An advancing freezing front results in the engulfment of soil particles by ice crystals or in situ freezing. If the rate of heat removal equals the rate of heat supplied the freezing front becomes immobile, a stationary freezing front.

Once the freezing front becomes stationary and water in sufficient quantity is available to the freezing front the ice crystals grow by freezing the adjacent water. Due to the rigidity and perfection of the ice crystals, soil particles are rejected by the ice resulting in the segregation of ice and soil particles (Anderson, 1968). Any change however, in the heat balance/imbalance will result in a corresponding change in the behavior of the freezing front.

Sources of heat to a soil sample are heat conducted by the soil sample from the surrounding environment and heat released by the porewater, and any water flowing into the sample. Heat released by the porewater is volumetric heat and latent heat of fusion. The latent heat of fusion is the major source of heat (Nixon, 1972).

Basic factors that influence the freezing behavior of soils according to Taber (1929) and Penner (1972) are: thermal conditions, water supply and nature of the porous media. Thermal conditions include the thermal gradient imposed on the soil, and the direction or directions of heat removal. The amount of heat present and potentially present in the soil depends on the degree of saturation, initial water content prior to freezing, unfrozen water content during freezing, and availability of water in quantity. Osler, (1967) expresses the availability of water under field conditions in terms of the depth to the water table from the freezing front. If the water table is at a great depth and the freezing front is unable to induce water migration, closed system freezing conditions are approached. Water migration is a necessary condition of ice lensing and theories used to explain the mechanisms involved are discussed in Section 2.1.B. The nature of the porous media depends on the soil type, size and shape of voids, soil stress history, and permeability as determined by the grain size and grain size distribution. Water solutes and minerals present in the soil system also influence the freezing behavior of soil.

The amount of water whose freezing temperature is less than 0 degrees Centigrade expressed as a percentage of the weight of the soil solids is called the unfrozen water

content. Unfrozen water content is an indicator of the amount of supercooling occurring as a soil is in the process of freezing. Hence depending on the amount of supercooling (unfrozen water content) of a soil type the freezing may follow or lag behind the 0°C isotherm.

Neresova (1963) has shown that clean sands freeze at 0 degrees Centigrade while clays and silts may freeze at temperatures lower than 0 degrees Centigrade. The unfrozen water content of a soil is a function of temperature, Anderson (1968), and a function of soil type and corresponding surface area Anderson (1968), Anderson, Tice and McKim (1973), Dillon and Andersland (1966), and Williams (1967). The application of pressure at a constant temperature increases the unfrozen water content (Hoekstra and Keune, 1967). To date unfrozen water contents have been correlated to surface area, Anderson and Tice and McKim (1973), Atterberg Limits, freezing point depression, clay mineralogy, and activity ratio, Dillon and Andersland (1966).

Two equations, the Clausis-Clapeyron and Kelvin equations, may be used to describe conditions at the freezing front. Glasstone and Lewis (1964), derive the Clausis-Clapeyron equation from basic thermodynamics. The equation governs conditions under which a system remains in equilibrium at all times as it is being transformed from one phase to another as a result of external influences. Changes of

state may be caused by the removal of heat or by variations in pressure on the system. Anderson and Morgenstern (1973) have related the equation to freezing soil conditions in the form:

$$\frac{dP}{dT} = \frac{\Delta \bar{H}_{fs}}{T \Delta \bar{V}} \quad 2.1$$

where:

dP = change in pressure across the freezing front

dT = change in temperature across the freezing front

$\Delta \bar{H}_{fs}$ = difference in latent heat of the two phases, latent heat of fusion of ice

T = freezing temperature of the soil

$\Delta \bar{V}$ = change in specific volume occurring during phase transformation

The Kelvin equation expresses the pressure relation at the interface for small crystals in their own melt. Williams (1967), applies the equation to the situation of developing ice in a capillary in the form:

$$P_i - P_w = \frac{2\sigma_{iw}}{r_{iw}} \quad 2.2$$

where:

P_i = pressure on ice, overburden pressure

P_w = pressure in porewater

σ_{iw} = pressure differential across the ice-water interface

r_{iw} = radius of the ice-water interface, taken positive on the ice side of the interface

For conditions of optimum heat removal, temperature conditions, soil structure and access to a water supply, pressures generated by enlarging ice crystals may be predicted by the Clausius-Clapeyron equation. Equation 2.1 may also be used to predict the pressure melting of ice in frozen soil from which an estimate of the change in unfrozen water content can be made. The Kelvin equation (2.2) can be used to predict the decrease (or increase) in the porewater pressure whenever the freezing front encounters a pore with a radius r , larger than (or smaller than) r_{iw} , for a constant overburden pressure.

2.1.B. Ice Segregation and Ice Lensing

Segregated ice may be defined as a continuous body of pure ice that has developed in but separate from a mass of soil particles. Segregated ice may occur in the order of microinches in thickness, inches in thickness as ice

lenses or up to tens of feet in thickness as massive ice bodies. A genetic classification of ground ice has been published by Mackay (1972). Segregated ice is generally observed in fine-grained soils whether cohesive or non-cohesive Taber (1929), Beskow (1935). It has been shown that the intensity of segregated ice varies directly with initial degree of saturation (Haley, 1953), and varies inversely with overburden pressure (Aitken, 1963).

Ice segregation may occur whenever a continuous water supply is available to the freezing front for a sufficient length of time under the prevailing temperature gradient and pressure differential across the ice-water interface. The capability of a soil to supply water to the freezing front is a necessary condition for ice lensing. If water flow to the freezing front is inadequate, particle trapping and ice proliferation may result (Wissa and Martin 1968). Consequently a lot of work has been carried out investigating the mechanism by which a soil is able to supply water to the freezing front. Two theories, film theory and capillary theory, have been postulated in an attempt to explain the phenomenon. The two theories are in fact complimentary with the capillary theory being a component part of the more general film theory.

It is now well established that soil particles are engulfed by an adsorbed layer of water with different

properties than that of the void water, (Anderson and Morgenstern, 1973). Taber (1929) was the first to propose this concept while (Corte, 1962) was the first to demonstrate it. The thickness of the film is a function of temperature (Anderson, 1968).

According to the film theory when a temperature gradient is imposed on a soil the water molecules of the film crystallize and leave the film. In order to maintain the film thickness water molecules from the unfrozen void water are absorbed by the film. A process is thereby set up to move water molecules to the freezing front.

Kaplar (1970) postulated the development of negative film pore pressures. He believed that a quasi-liquid layer, 'active film layer', must be present to provide the drive force for ice segregation. The water molecules in contact with the ice have a high degree of polar orientation with the ice lattice and hence have a rigid ordered structure. The adsorbed soil water is also formed by strong adsorption forces and has a high structural rigidity. During freezing the water molecules in the active film undergo a physical readjustment of their position, creating a negative pressure in the process, in order to fit into the ice crystal lattice. At the time of this readjustment the film force balance is disturbed resulting in a rearrangement of the remaining film water molecules, and the absorption of void water

molecules to restore equilibrium. The demand for replacement molecules in the active film layer is governed by the volumetric rate of phase transformation within the layer. Freezing of water molecules in the film occurs simultaneously with the freezing of void water molecules.

The initial mechanism in ice lensing is the rejection and exclusion of soil particles by the growing ice crystals (Anderson and Morgenstern, 1973). Water is drawn to the freezing front by negative pressures at the ice-water interface and by the imposed negative temperature gradient. The ice crystals begin to grow by the freezing of this water and the accumulation of these ice crystals. At crystallization the energy that is released is transformed into work lifting the overburden, and into heat released at the interface which tends to moderate the rate of ice formation. The energy involved in the work of the frost heave is due to the difference in energy states of ice and water; the latent heat of fusion (Anderson, 1968).

Chronologically the capillary theory was the first theory to describe the migration of water to the freezing front. The hydraulic theory of Taber (1929) and Beskow (1935) was in effect the capillary theory. The basis of the theory is that water in small capillaries freezes at temperatures lower than 0 degrees Centigrade and that the stress difference across the ice-water interface is inversely

proportional to the radius of the ice-water interface.

These relations are given by the Kelvin equation, equation 2.2, and equation 2.3 given below.

In Williams' (1967) development of the theory the soil is considered to be a series of capillaries. The radius of the capillary (r_c) in part controls the behavior of the freezing front. According to the capillary theory the freezing front continues to advance as long as the capillary radius, r_c , is greater than the radius of the interface, r_{iw} , or $r_c > r_{iw}$. When the capillary radius r_c is smaller than r_{iw} , the interface radius ($r_c < r_{iw}$), the freezing front cannot enter the capillary and its advance would be halted. At this point the cooling of the pore fluid would continue lowering the fluid temperature below 0 degrees Centigrade without crystallization. The pore fluid would then be supercooled. The depression of the freezing point is given by the relation:

$$T - T_o = \frac{V_e \frac{2\sigma_{iw} T_o}{r_{iw} L}}{2.3}$$

where:

T = is the freezing point in degrees Kelvin

T_o = normal freezing point

V_e = specific volume of water at the freezing temperature

σ_{iw} = stress difference across the ice-water interface

r_{iw} = radius of the ice-water interface taken positive on the side of the ice

L = latent heat of fusion of water

Due to the reduction in the radius of the ice-water interface the porewater pressure would subsequently decrease according to the Kelvin equation, equation 2.2. This reduction in the porewater pressure at the ice-water interface is the force that sucks the void water to the freezing point. The freezing of this water results in the growth of ice lenses.

Jackson and Chalmers (1958, 1966) postulated that supercooling supplied the force required to transport water to the freezing front. Based on studies of porous media they concluded that supercooling controls the free energy of a freezing system. Upon the freezing of a soil a reduction in free energy occurs in proportion to the amount of supercooling. Hence the force that draws water to the freezing front is derived from the system free energy change during freezing.

The capillary theory has several shortcomings and is not capable of describing all known freezing conditions. Some of these are: (1) It is not universally accepted that supercooling is the source of energy that sucks water to

the freezing front. Anderson (1968) contends that the difference in energy states, the latent heat of fusion, is the source of this energy. (2) The capillary theory is based on a uniform pore size or uniform particle size distribution. Considering soils with a non-uniform particle size distribution, as in virtually all cases, difficulties arise in assigning a typical capillary pore radius to use in the theory. This seriously limits the applicability of the theory. (3) The capillary theory is a static theory based on grain size, pressure and interface stress differences. The theory is based on the premise that pore radius or grain size and grain size distribution is the unique parameter that controls the ice lensing capability of a soil. The theory does not account for any other factors affecting the freezing soil system, i.e. temperature gradient, and is incapable of accounting for any changes in these factors.

2.1.C. Frost Heaving

When individual ice crystals form and enlarge they impinge on confining boundaries generating crystallization pressures. Depending on the boundary this pressure is often relieved by displacement of the soil surface in the direction of least resistance. Displacement usually occurs by lifting the overburden or to a lesser extent in a

compressible soil by compressing the soil structure.

As the freezing front penetrates, engulfing the soil particles and freezing the porewater in situ, freezing pressures and/or heave result entirely from phase transformation. Whenever the freezing front becomes stationary however, resulting in ice segregation and lensing, heave is a direct result of the buildup of ice lenses. Substantial heave as observed in the field can only be accounted for in terms of ice lensing and segregation and not as a result of phase transformation (Taber, 1929). Ice lensing and hence heave may continue indefinitely as long as temperature, pressure and water supply conditions remain suitable. Whenever one of these conditions is altered, say a decrease in the water supply, or an increase in temperature gradient, the freezing front will advance until a favorable balance of conditions is achieved again and the freezing front becomes stationary once more. Heaving would be minimal while the freezing front is advancing but would continue as before once the freezing front stabilizes. Repetition of this process results in rhythmic ice banding (Martin, 1959).

The amount and the rate of frost heave is a function of many factors. Beskow (1935) and Kaplar (1970) showed that heave rate is dependent on the rate of heat extraction or freezing front penetration. Penner (1972) found that by

increasing the rate of heat extraction, heave rate increases to a maximum after which it decreases to a point where heave is a result of the expansion of porewater at phase transformation. These studies also showed that the response of the heave rate to increasing heat removal rates differed depending on the soil type. Heaving occurs in the direction of heat extraction or crystal growth and total heave was reduced by increasing the overburden load (Kaplar, 1970). Field studies by Aitken (1963) provided field evidence of the effectiveness of surcharge loading in reducing heave. Heave is also dependent on water content (Taber, 1929), and can be prevented by inducing high tensions in the porewater (Gold, 1957), (Penner, 1958, 1966).

2.1.D. Heaving Pressures

Upon freezing under constant volume conditions pressures are created due to the volumetric expansion associated with phase transformation, and due to ice segregation and lensing. It is common practice in the literature to refer to heaving pressures as those pressures which are caused by ice lensing. Heave pressures occur in the direction of heat removal and originate at the freezing front. Heave pressures are dependent on particle size (Gold, 1957), with the smaller particle sizes responsible for the maximum heave pressures (Penner, 1968). Miller et al. (1960) and Everett and Haynes (1965) developed

empirical formulations, based on a study using glass beads which related heave pressures to particle or pore size.

A summary of the findings of several people relating grain size and heave pressure is shown on Figure 2.1. It was generally found that the effective diameter, D_{10} , gave the best correlation with heaving pressure and so is used on the figure.

The heaving pressures plotted were determined from freezing tests with no overburden loading and open drainage conditions. Only Sutherland and Gaskin used a back pressure. Preparation of the soil samples varied; Hoekstra et al. used a compacted sample, Penner densified the sample by vibration, Sutherland and Gaskin consolidated the sample from a slurry, Yong placed and froze the sample in a 'loose' condition, and Kinoshita 'packed' the sample into the soil container. Yong also measured heave pressure using proving rings of varied stiffness. All samples were reported as being saturated prior to freezing. Discrepancies between the data are likely a result of less than 100 per cent saturation for the duration of the freeze test, variation in sample preparation and hence stress history, and a difference in freezing rates. Kinoshita reported results that were determined by both open and closed system freezing tests. It would appear however, from the equipment description, that Kinoshita froze under closed drainage conditions.

Applying the formulations of Everett and Haynes (1965) and the capillary model, Penner (1968) envisaged an undulating freezing front which extended as far as possible into the larger pores and, which was stopped by the smaller pores. He maintained that maximum heave pressure was generated when the freezing front everywhere rested on the small pores. The tendency for heaving pressures to become very large for the smaller particle sizes is shown in Figure 2.1. This condition of maximum heave pressure likely occurred when the freezing front became stationary after a period of rapid penetration.

Penner (1970) showed that maximum heave pressures developed when the soil macrostructure was completely broken down and the freezing front was relatively stationary. These studies also indicated that the higher the soil density the larger the heave pressures. Measurement of heave pressures were influenced by the compliance (Kaplar, 1971) and small heave movements were sufficient to prevent the buildup of large heave pressures in the laboratory. Penner (1970) noted that the buildup of large heave pressures in the field were dissipated in cracks and discontinuities.

□ Sutherland and Gaskin (1973)

△ Penner (1968)

▽ Penner (1967)

× Yong and Osler (1971)

+ Hoekstra et al (1965)

○ Test Results, Arvidson (1973)

▲ Penner (1966)

■ Kinoshita (1966)

● Williams (1967)

×_a stiff proving ring

×_b medium proving ring

×_c soft proving ring

■_a -10°C

■_b -5°C

○_a Normally consolidated

○_b Over consolidated, $P_C = 5 \text{ Kg/cm}^2$

○_c Over consolidated, $P_C = 7.7 \text{ Kg/cm}^2$

+ 5.06 Kg/cm^2

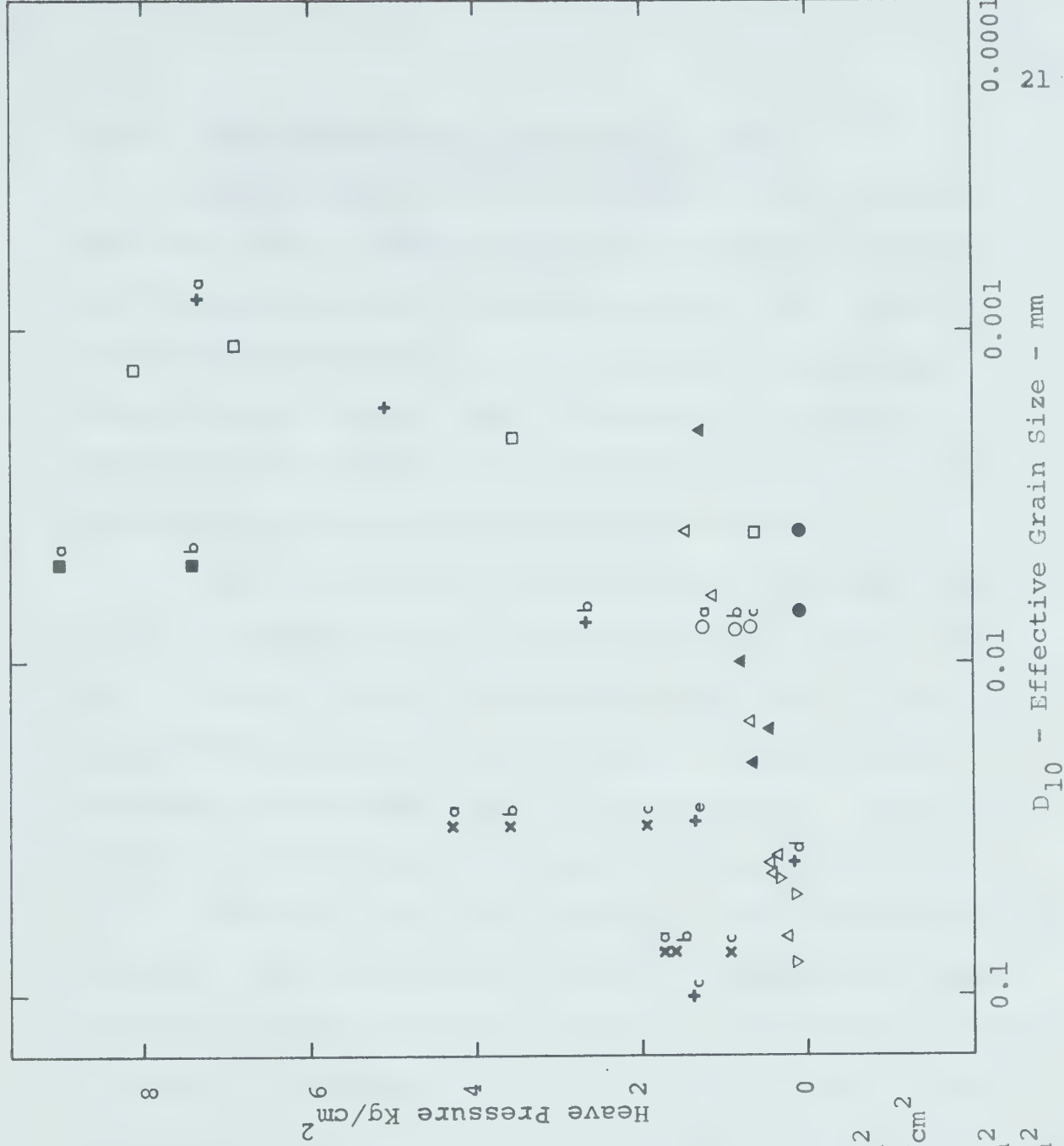
+_a 7.39 Kg/cm^2

+_b 2.65 Kg/cm^2

+_c 1.40 Kg/cm^2

+_d 0.18 Kg/cm^2

+_e 1.34 Kg/cm^2



EFFECTIVE GRAIN SIZE, D_{10} , VERSUS HEAVE PRESSURE

2.1.E. Pore Pressures at the Freezing Front

The existence of pore pressures at the freezing front are clearly demonstrated by the expulsion of pore-water (Balduzzi, 1959; Wissa and Martin, 1968), and by the attraction of water to the soil sample during open system freezing tests. Negative porewater pressures at the freezing front are the forces that draw water to the freezing front resulting in ice segregation and lensing.

Based on theoretical developments the magnitude of the pore pressures varies inversely with pore size, Gold (1957), Penner (1958), and have been evaluated in terms of the capillary model by Penner (1966). Williams (1967) presented data showing that the air intrusion value could be used to estimate pore pressures at the freezing front.

Williams (1967) froze samples 1 and 2 centimeters in height by imposing a temperature of -8 degrees Centigrade under open system conditions. Results obtained on 2 natural silts with a uniformity coefficient (C_u) of about 80 for silt E and 8 for silt 64/15-25, and graded fraction $49_\mu - 73_\mu$ are shown on Table 2.1.

Sutherland and Gaskin (1973) showed that pore pressure at the freezing front in compressible and incompressible soils could be reasonably predicted using grain size and capillary pore size. Work was done on pulverized flyash, coefficient of uniformity $C_u = 3$, (referred

TABLE 2.1

Summary of Williams (1967) Data

Sample	Rate of Freezing Hours	Water Intake cm ³	Gas Pressure P _g Kg/cm ²	P _g +0.02-U _i Kg/cm ²	Air Intrusion P _a - P _w Kg/cm ²
Graded Fraction 49 - 73 _μ	15 (ca.)	0.76	0	0.134	$\begin{cases} 0.27 \\ 0.32 \\ 0.27 \end{cases}$
Natural Soil Silt E	15 (ca.)	0.34	0	0.075	0.13
Silt 64/15-25	15 (ca.)	0.24	0	0.056	0.08

to as soil 1); Kaolin $C_u = 5.5$ and 6.5 , soils 2 and 3; and a mixture of flyash and kaolin $C_u = 5.2$, soil 4. The soil specimens were frozen uniaxially by applying cold temperature of -17 degrees Centigrade under closed system conditions. Results reported show:

Soil	P_i KN/M ²	P_w KN/M ²	Max. drop in P_w KN/M ²
1	1011	1007	62
2	1062	1035	465
3	1075	1071	491
4	1080	1080	240

Data on predicted and measured values of maximum drop in porewater pressure for air entry tests were also reported as follows:

Soil	Maximum Drop in Porewater Pressure KN/M ²	
	Predicted	Measured
1	40	62
2	100	465
3	143	491
4	57	240

Based on these results the authors concluded that predicted values of the drop in porewater pressures using the air entry method grossly underestimated the actual measured values.

2.1.F. Frost Susceptibility of Soils

Fine grained soils and coarse or medium grained soils with fines were observed by early workers to be the most susceptible to frost action. As a means of classifying soils in terms of their susceptibility to frost action a criterion based on grain size was established. The Casagrande criterion for frost susceptibility was one of the earliest published. The criterion stated that non-uniform soils containing more than 3 per cent of grains smaller than 0.02 millimeters and very uniform soils containing more than 10 per cent smaller than 0.02 millimeters were considered frost susceptible. This criterion was based on local materials in New Hampshire and has been widely used around the world since 1931. Not all materials in other parts of the world, however, behaved similarly to the New Hampshire materials and modified criteria were designed to match local conditions. As a result a great multitude of criteria were developed in various parts of the world backed by the experience of people like Beskow, Croney, Schiable, Linell and Kaplar, and organizations such as the U. S. Civil Aeronautics Administration, and the U.S. Army Corps of

Engineers, (Townsend and Csathy, 1963). Each criterion met the needs of the person/organization involved but none proved to be a significant improvement over the Casagrande criterion and none were as widely accepted.

All frost susceptibility criteria are based on the capillary model of soil freezing and hence are subject to the limitations of the theory. The Casagrande frost susceptibility criterion based solely on grain size is useful as a guide to the frost susceptibility of a material but is inaccurate and incapable of predicting all frost action phenomenon for all soil types. An improved frost susceptibility criterion is needed.

2.2. Theory of Freezing of Soils

The literature cited above is capable only of presenting qualitative and some quantitative theories for the formation of ice lenses during the freezing of certain soil types. A large gap exists between these theories and a comprehensive theory capable of describing the freezing of soils as observed in the field and laboratory. A theory is presented below in an attempt to fill this gap.

The theory developed below describes the behavior of a soil subjected to freezing conditions. Equilibrium conditions are assumed to exist when the soil is in quasi-thermal equilibrium with the surroundings. This condition occurs in

a one dimensional system whenever the freezing front is stationary with an ice lens actively growing or in the trivial situation of an unfrozen soil with a uniform temperature distribution. The theory predicts the behavior of a soil when this thermal equilibrium is upset. The theory is developed in terms of soil mechanics and heat transfer principles.

2.2.A. Assumptions

The freezing situation is assumed as shown in Figure 2.2. Assumed conditions are:

(1) A unit quantity of soil is being frozen. The following soil properties are known or assumed: n , porosity; w , water content; C_u , coefficient of uniformity ($C_u = D_{60}/D_{10}$); C_v , coefficient of consolidation; k , permeability; γ_d , dry density, and S , degree of saturation ($S = 100\%$).

(2) Soil is being uniaxially frozen from the top downward with the imposition of a negative temperature at the soil surface.

(3) A net heat balance exists at all times within the soil freezing system or Heat out (q_o) = Heat in (q_i).

(4) Freezing front elevation is given by the distance X , from the top of sample. Soil at a depth less than X is frozen while soil at a depth greater than X is unfrozen. Unfrozen water content is assumed to equal to zero.

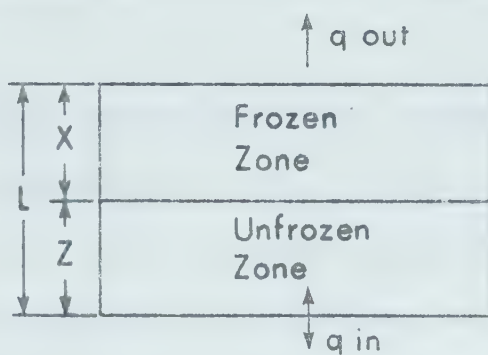


Figure 2.2A

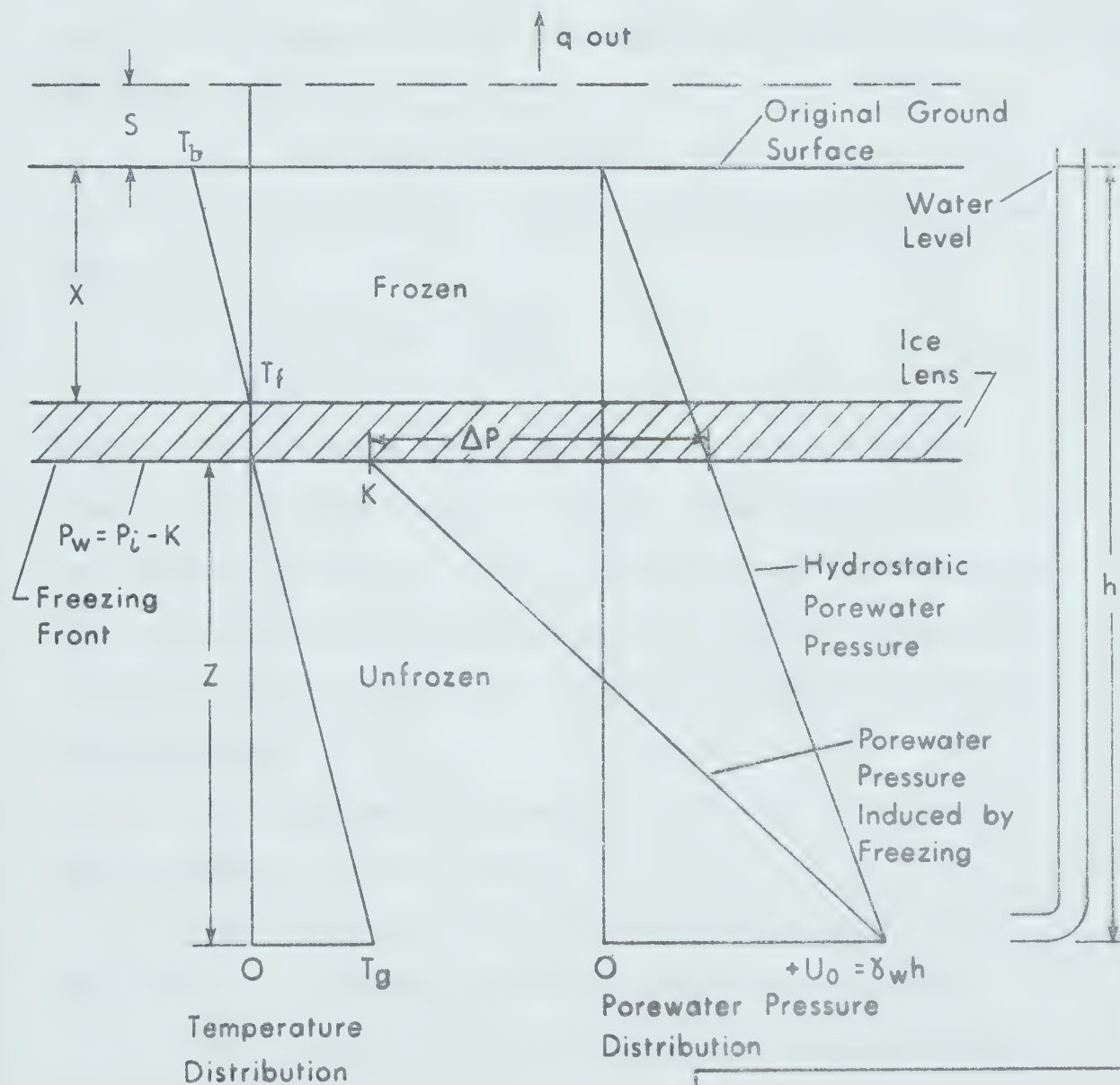


Figure 2.2B

SCHEMATIC
FREEZING MODEL

FIGURE 2.2

(5) A temperature gradient exists in the soil with below freezing temperatures, T_b , at the soil surface, freezing temperature, T_f , at the freezing front and above freezing temperature, T_g , at the base of the soil sample. The freezing temperature may be equal to or less than 0 degrees Centigrade. Heat flow out of the soil sample is only due to conduction and is proportional to the temperature gradient.

(6) The water level in the soil is known and water flow within the unfrozen soil obeys the Darcy flow law:

$$q = v A = k i A \left[\frac{\text{Cm}^3}{\text{sec}} \right] \quad 2.4$$

where q is the quantity of water in cubic centimeters flowing through the soil; v , is the flow velocity in centimeters per sec; A , is the cross-sectional area of the soil sample in square centimeters; k , is the permeability in centimeters per sec; and i , is the pressure gradient, dimensionless.

(7) Drainage of the soil system is controlled, open system or closed system.

(8) Soil particles are engulfed by a film of water that has a state different from the void water.

(9) A stress difference occurs across the ice-water interface.

2.2.B. Development of Theory

Applying surface tension physics to an ice lensing system, the pressure difference across the ice-water interface for small crystals in their own melt is given by the Kelvin equation, equation 2.2:

$$P_i - P_w = \frac{2\sigma_{iw}}{r_{iw}} \quad 2.2$$

For the case of freezing soils it appears from the work of Williams (1967) and Sutherland and Gaskin (1973) that the stress difference $P_i - P_w$ is nearly constant. For the mechanistic model presented here it is postulated that the stress difference is equal to or less than a certain constant during the growth of an ice lens or

$$P_i - P_w \leq K \quad 2.5$$

where K is a characteristic value depending on the soil.

K may be determined analytically, (Williams 1967; Sutherland and Gaskin 1973) or experimentally. To find K experimentally two types of freezing tests, open or closed system may be run. The closed system tests measures the porewater pressure and by substituting this value into equation 2.5 K may be determined. On the other hand if one assumes that P_w in equation 2.5 is equal to zero then K is equivalent to the overburden pressure P_o . The porewater pressure in open system tests is equal to zero whenever no flow

of water into or out of soil sample occurs. By running a series of open system tests to find the stress, P_i , at which no water flow occurs, K may be found directly.

Conditions governing the magnitude of P_w may be evaluated in terms of soil mechanics parameters and soil system temperature and pressure conditions.

A basic heat balance may be written for conditions shown in Figure 2.2A:

$$\text{Heat out} = \text{Heat in} + \text{Heat of phase change}$$

or

$$q_o = q_i + q_p \quad \left[\frac{\text{cal}}{\text{sec}} \right] \quad 2.6$$

where:

q_o - is the heat conducted away from the soil sample by the imposition of a negative temperature gradient at the soil surface.

q_i - is the heat of the system, volumetric heat and any heat conducted into the soil from the outside environment by the soil itself or by water flowing into the soil. When water flows out of the soil a net reduction of q_i results.

q_p - is the heat of phase change or latent heat of fusion that is released by the porewater upon crystallization. q_p depends on the amount of water freezing at the freezing front, water content and degree of saturation of the unfrozen soil, and the amount of water that is sucked into the soil during freezing. q_p can be several orders of magnitude larger than q_i .

The heat conducted out of the soil sample is proportional to the temperature gradient imposed or

$$q_o = K_f \frac{dT}{dX} A \quad \left[\frac{\text{cal}}{\text{sec}} \right] \quad 2.7$$

where K_f - conductivity of the frozen soil [$\text{cal}/^\circ\text{Ccm sec}$]

dT - temperature gradient that exists in the soil sample [$^\circ\text{C}$]

dX - thickness of soil sample [cm]

A - cross-sectional area of the soil sample [cm^2]

The heat of phase change is in direct proportion to the volume of water sucked into the soil sample, frozen or

$$q_p = \frac{L \cdot V}{t} = \frac{L}{t} (vAt) = Lki A \quad 2.8$$

where:

L - latent heat of fusion of the water flowing to the freezing point - [cal/gm]

V - volume of soil frozen $[\text{cm}^3]$ per unit time
 which equals $vA = kiA$ from equation 2.4.

t - time [sec]

The pressure gradient, i , is equal to the difference in pressure, Δp , causing water to flow to the freezing front, through the thickness of the soil sample, z , or:

$$i = \frac{\Delta p}{\gamma_w z} \quad 2.9$$

From figure 2.2B, Δp equals the difference in pressure between the hydrostatic water level at a distance x from the freezing front, P_x , and the pressure in the water at the freezing front, P_w or

$$\Delta p = P_x - P_w \text{ [gm/cm}^2\text{]} \quad 2.10$$

$$\text{where } P_x = P_h - P_z \text{ [gm/cm}^2\text{]} \quad 2.11$$

Hence the pressure gradient, i , may be expressed as:

$$i = \frac{(P_h - P_z) - P_w}{z \gamma_w} \quad 2.12$$

substituting equation 2.12 into equation 2.8:

$$q_p = \frac{LkA}{\gamma_w} \frac{(P_h - P_x) - P_w}{z} \text{ [} \frac{\text{cal}}{\text{sec}} \text{]} \quad 2.13$$

Volumetric heat is proportional to the initial soil bulk temperature, the difference between the bulk temperature and the ambient air temperature, and the net

change (gain or loss) of porewater, ΔV , from the system during open system tests.

Specific heat of soil and water flowing into the soil is given by:

$$q_1 = \frac{Q}{t} = \frac{1}{t} [C_s V_s (T_{bs} - T_{fs}) + C_w \Delta V (T_w - T_{fw})] \quad 2.14$$

where

C_s - volumetric specific heat of soil

[cal/°C cm³] given by:

$$C_s = \gamma_d (0.2 + 1.0 W)$$

where γ_d - unit weight of dry soil

[gm/cm³]

W = water content [%]

C_w - volumetric specific heat of water

(= 1 cal/°C cm³)

V_s - volume of soil sample [cm³]

ΔV - volume of water sucked into or expelled from soil sample [cm³]

T_{bs} - initial bulk soil temperature [°C]

T_w - initial temperature of ΔV [cm³] of water in [°C]

T_{fs} - freezing temperature of soil [°C]

T_{fw} - freezing temperature of water [$^{\circ}\text{C}$]

Amount of heat, q_2 , conducted by the unfrozen soil sample is given by

$$q_2 = K_u \frac{dT}{dz} A \quad 2.15$$

where

K_u - conductivity of unfrozen soil [$\text{cal}/^{\circ}\text{C cm sec}$]

dT - temperature differential existing in the unfrozen soil [$^{\circ}\text{C}$] due to step temperature

dz - thickness of unfrozen soil [cm]

A - cross-sectional area of soil sample [cm^2]

Total volumetric heat, q_i , is the sum of equations 2.14 and 2.15 or

$$q_i = \frac{C_s V_s}{t} (T_{bs} - T_{fs}) + \frac{C_w \Delta V}{t} (T_w - T_{fw}) + k_u \frac{dT}{dz} A \quad 2.16$$

Substituting equations 2.7, 2.13 and 2.16 into equation 2.6 yields:

$$K_f \frac{dT}{dx} A = \frac{Lk}{\gamma_w} A \left(\frac{P_h - P_x - P_w}{z} \right) + \frac{C_s V_s}{t} (T_{bs} - T_{fs}) + \frac{C_w \Delta V}{t} (T_w - T_{fw}) + K_u \frac{dT}{dz} A \quad 2.17$$

Solving for porewater pressure, P_w :

$$P_w = \frac{\gamma_w Z}{LkA} \left[\frac{C_s V_s}{t} (T_{bs} - T_{fs}) + \frac{C_w \Delta V}{t} (T_w - T_{fw}) + K_u \frac{dT}{dz} A - K_f \frac{dT}{dx} A \right] + (P_h - P_w) \quad 2.18$$

Substitution of P_w determined in equation 2.18 into equation 2.5:

$$P_i - P_w \leq K \quad 2.5$$

enables one to determine whether active ice lensing will occur. For example for a $P_w = 0$, if P_i is greater than K ($P_i > K$) no ice lens growth will occur, but if P_i is less than or equal to K ($P_i \leq K$) ice lenses could grow. K is determined from subsequent test data.

The growth of an ice lens may be halted by any one of a combination of factors. These factors are: (1) low soil permeability, K , resulting in a small insufficient discharge to the freezing front; (2) overburden pressure high so that the pressure differential across the freezing front does not create sufficient suction to induce water movement to the freezing front, the pressure differential may even be positive resulting in flow away from the freezing front; (3) suction at the freezing front may be limited by cavitation at minimal overburden pressures such as near the surface; and (4) water supply is inadequate as often occurs when the water table is at a great depth.

The magnitude of heave, S , may be calculated from considerations of a balance of soil porewater volumes. Heave is proportional to the increase in sample porewater volume upon freezing. Initial sample porewater volume, V_o , is equivalent to (assuming $S = 100\%$):

$$V_o = nV \quad 2.17$$

where n is porosity and V is the total volume of the soil sample. Volume of sample porewater after freezing, V_1 , is given by:

$$V_1 = V_f + V_u + V_a \quad 2.18$$

where:

V_f - volume of ice in frozen zone (reduced
accordingly for unfrozen water)

V_u - volume of water in unfrozen zone

V_a - volume of ice frozen as a result of water,
 V_{aw} , being sucked into the soil sample to
build an ice lens.

From Figure 2.2 the volume of ice in the soil sample frozen to a depth x (assuming all water is frozen) is:

$$V_f = 1.09 \frac{x}{\ell} nV \quad 2.19$$

where ℓ is the total depth of sample. Volume of porewater in the unfrozen zone is

$$V_u = \frac{z}{\ell} nV \quad 2.20$$

where z is the thickness of the unfrozen zone and equal to $z = \ell - x$. Equation 2.20 then becomes:

$$V_u = \left(1 - \frac{x}{\ell} \right) nV \quad 2.21$$

V_a , volume of ice frozen as a result of water being sucked into the soil to build an ice lens is:

$$V_a = 1.09 V_{aw} \quad 2.22$$

where V_{aw} is volume of water sucked into the soil sample. The change in sample porewater volume, ΔV_f , may then be written:

$$\begin{aligned} \Delta V_f &= V_1 - V_0 \\ &= 1.09 \frac{x}{\ell} nV + \left(1 - \frac{x}{\ell} \right) nV + 1.09 V_{aw} - nV \\ &= 0.09 \frac{x}{\ell} nV + 1.09 V_{aw} \end{aligned} \quad 2.23$$

ΔV_f may also be written as:

$$\Delta V_f = SA \quad 2.24$$

By equating equations 2.23 and 2.24 and solving for heave:

$$S = \frac{1}{A} \left(0.09 \frac{x}{\ell} nV + 1.09 V_{aw} \right) \quad 2.25$$

The depth of the freezing front, x , in Figure 2.2 is proportional to the square root of time. See equation 4.8.

The rate at which a volume of water, V_{aw} , is sucked into the soil sample is dependent on the rate of heat removal and the surcharge loading and stress history of the soil at the time of freezing. The volume of water V_{aw} may be calculated in terms of heat removal. The total heat released, Q_i , by a volume of water that has been sucked into the soil sample is (assuming specific heat of water is very small)

$$Q_i = q_i t = L_w V_{aw} \quad 2.26$$

where t - time

L_w - latent heat of fusion of water

From equation 2.6 the heat in, q_i , is equivalent to:

$$q_i = q_o - q_p \quad 2.27$$

Assuming that q_i of equation 2.27 is the latent heat of fusion then equations 2.26 and 2.27 may be equated to give:

$$L_w V_{aw} = q_o - q_p$$

or

$$V_{aw} = \frac{t}{L_w} (q_o - q_p) \quad 2.28$$

The heat out, q_o , is given by equation 2.7, and q_p , the heat of phase change is given by equation 2.13.

Substituting equations 4.8 and 2.28 into equation 2.25 we have as a function of time is recovered:

$$S = \frac{1}{A} \left[0.09 \frac{\alpha \sqrt{t}}{\ell} nV + 1.09 \frac{t}{L_w} (q_o - q_p) \right] \quad 2.29$$

The rate of heave, ΔS , may be deduced from equation 2.29 by differentiating heave with respect to time:

$$\Delta S = \frac{ds}{dt} = \frac{1}{A} \left[0.045 \frac{\alpha nV}{\sqrt{t}\ell} + 1.09 \left(\frac{q_o - q_p}{L_w} \right) \right] \quad 2.30$$

Total heave and rate of heave are also dependent on the freezing temperature of the soil (i.e. unfrozen water content). When the soil freezing temperature is less than 0 degrees Centigrade the heave and heave rate would be reduced accordingly.

CHAPTER 3

TEST PROCEDURE AND DESCRIPTION OF EQUIPMENT

3.1 Test Procedure

3.1.A. Materials and Sample Preparation

Testing was carried out using Ottawa sand and Devon silt. A summary of material properties is given in Appendix A. Ottawa sand was chosen because of its low susceptibility to frost action and in order to verify the test program hypothesis. Devon silt was chosen because of its high frost susceptibility and general similarity to silty materials found in northern regions. The bulk of the testing was done on Devon silt.

Both materials were prepared as a slurry. Devon silt was slurried at roughly 1 1/2 times its Liquid Limit for ease of handling. The slurries were deaired to ensure saturation, Ottawa sand by vigorously boiling and Devon silt by means of a vacuum pump. Distilled water was used at all times.

3.1.B. Test Procedure

The procedure followed during testing was: (1) allow temperature of soil sample to reach a constant equilibrium value, (2) apply back pressure to the soil

porewater, (3) impose freezing test boundary conditions, and (4) freeze the soil sample.

A back pressure was applied to all samples to ensure 100 percent saturation. Back pressures of 45 and 50 pounds per square inch were used. While a back pressure was applied, sample temperatures were allowed to stabilize and come to equilibrium with the ambient air temperature of the cooling chamber or styrofoam cabinet. Samples were usually left overnight, for 8 to 14 hours, in order to ensure temperature equilibrium.

Samples were then consolidated to a desired effective stress. All Ottawa sand samples were normally consolidated whereas tests were run on both normally consolidated samples and overconsolidated samples of Devon silt.

Prior to freezing the soil sample, desired freeze test drainage and displacement conditions were imposed. Two drainage boundary conditions were imposed on the soil sample, open and closed. Either of two displacement boundary conditions, restrained or unrestrained, were further imposed on each drainage condition. Open system drainage occurred when the soil sample had free access to an outside water source. The volume of fluid entering or leaving the soil was measured by a volume change indicator, described below. During closed system drainage conditions the soil sample had no access to an outside water source. Porewater

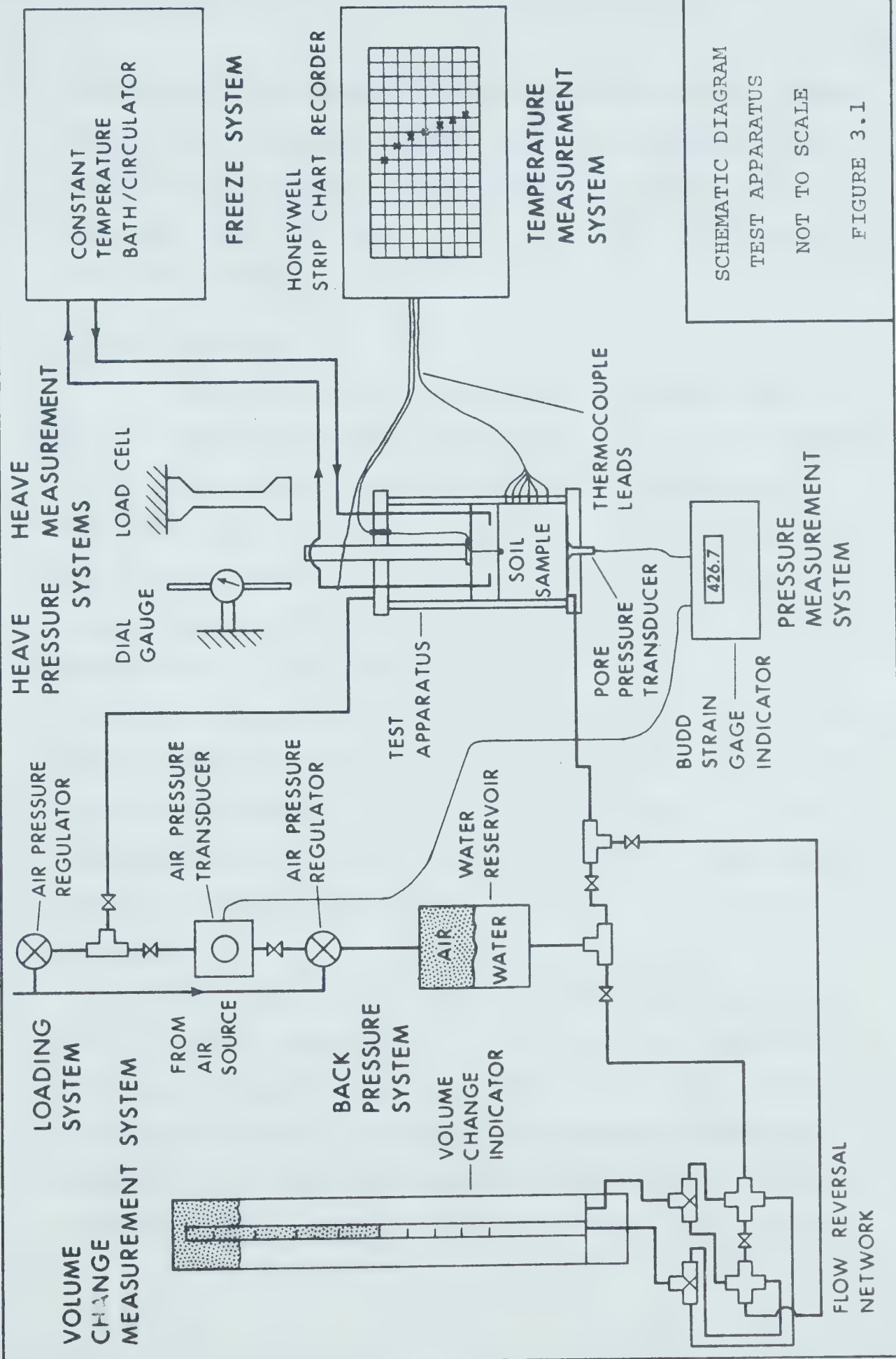
pressures were measured in this case. Depending upon whether the vertical displacement of the freezing piston was restrained or not, heave pressure or heave was recorded respectively. Methods used to measure pore pressure, heave pressure and heave are discussed under the equipment section. The bulk of the testing was conducted under open system, unrestrained vertical displacement conditions.

To simulate field conditions, samples were frozen uniaxially from the top downward by imposing a negative step temperature on the soil surface. The step temperature was held constant while the resultant freeze rate depended on the temperature gradient and sample water content. A constant step temperature was used to facilitate calculation and prediction of the advance of the freezing front (Appendix B). The movement of the 0°C isotherm was deduced from soil temperature data. Other parameters monitored were volume change or pore pressure, depending on drainage conditions and heave.

3.2 Description of Equipment

3.2.A. General

The experimental apparatus was basically a modified oedometer designed for controlled temperature conditions. A schematic diagram of the equipment is shown in Figure 3.1. Appendix C lists equipment manufacturers and some specifications.



SCHEMATIC DIAGRAM
TEST APPARATUS
NOT TO SCALE
FIGURE 3.1

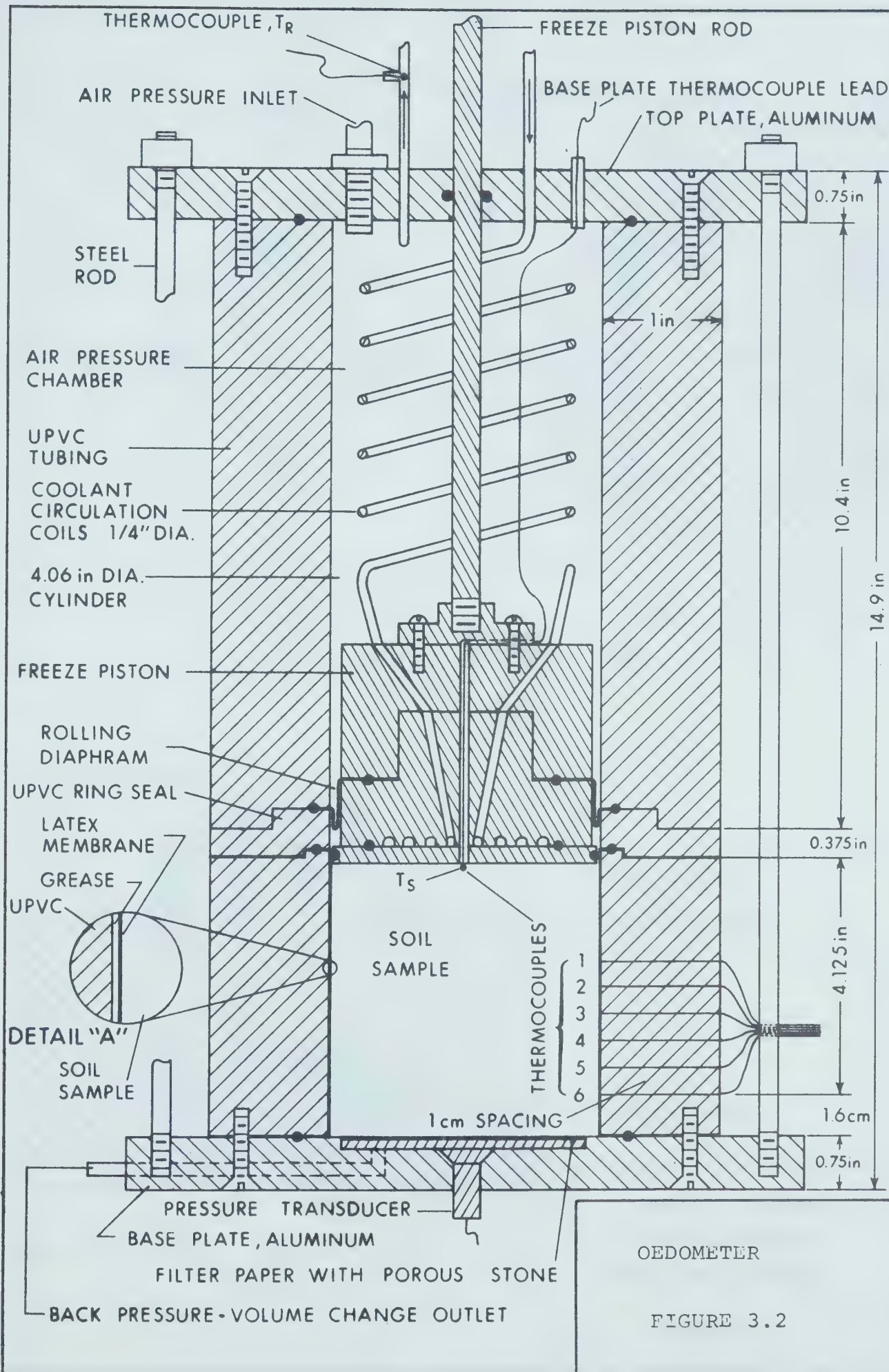
Components of the apparatus were: oedometer, freeze system, load and back pressure systems, and the measurement systems. The various measurement systems monitored temperature, porewater pressure, volume change, vertical displacement, and heave pressure.

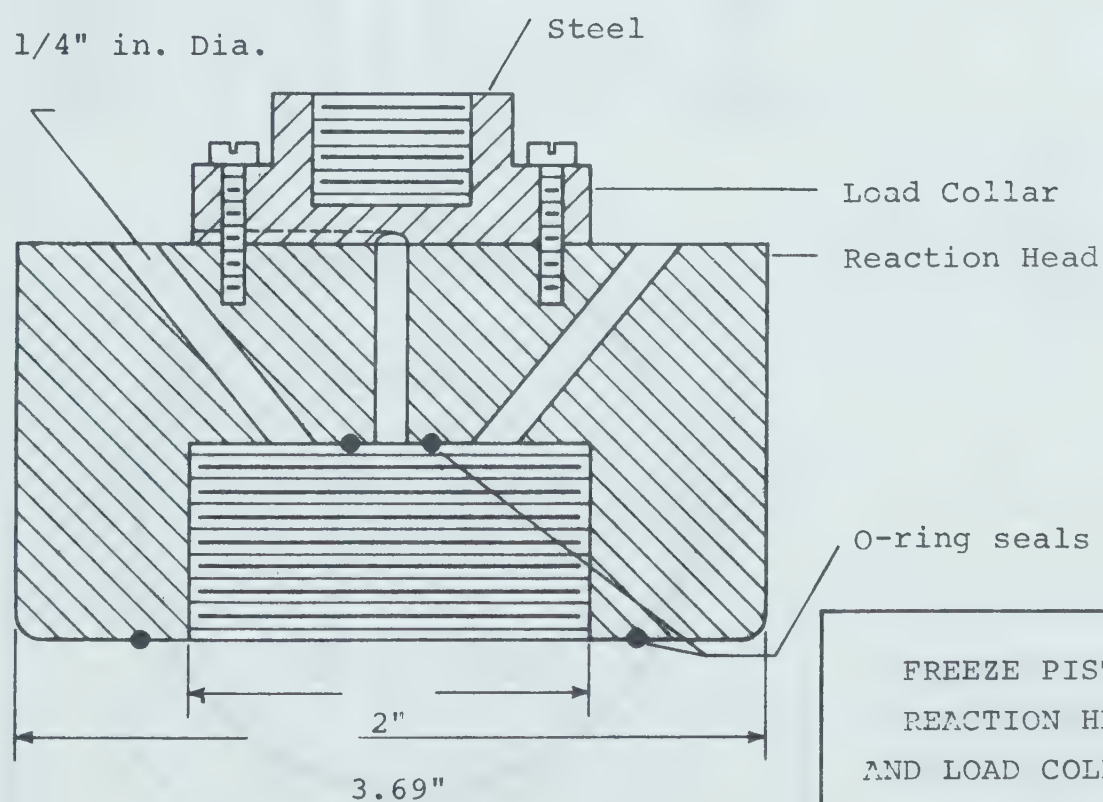
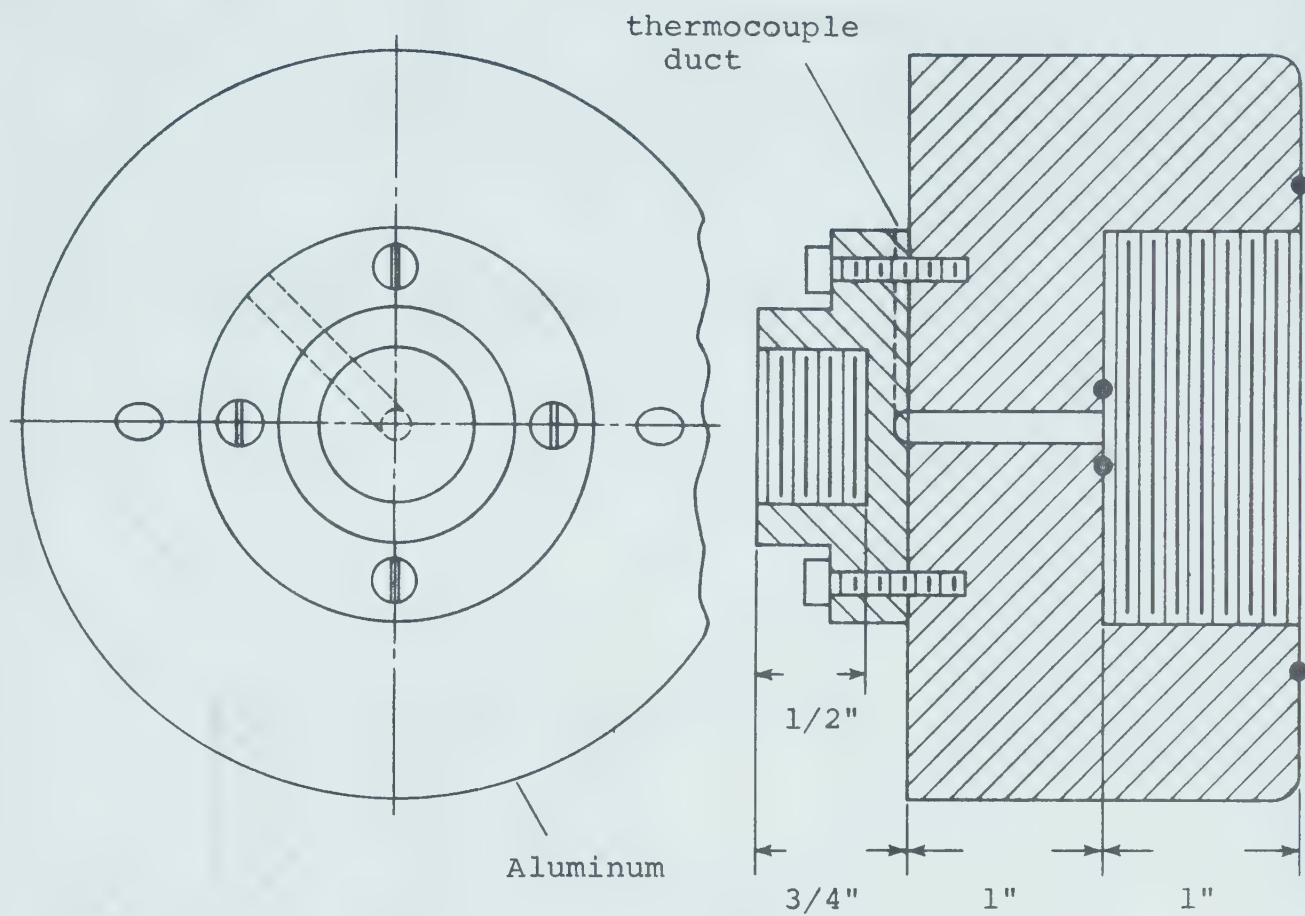
3.2.B. Oedometer

Figure 3.2 shows the oedometer. Noteable features are the rolling diaphragm, freeze piston, and rubber membrane.

The rolling diaphragm was a rubber impregnated fiberglass mesh sold commercially under the name Bellofram. The diaphragm acted as a pressure and water seal around the freeze piston, and provided virtually frictionless movement, excluding frictional resistance due to the O-ring seal on the freeze piston rod, of the freeze piston. The membrane used was designed to withstand a 300 pound per square inch pressure differential with negligible deformation. The placement position of the diaphragm provided 1/2 inch upward and 2 1/2 inch downward piston travel for a net total of 3 inches.

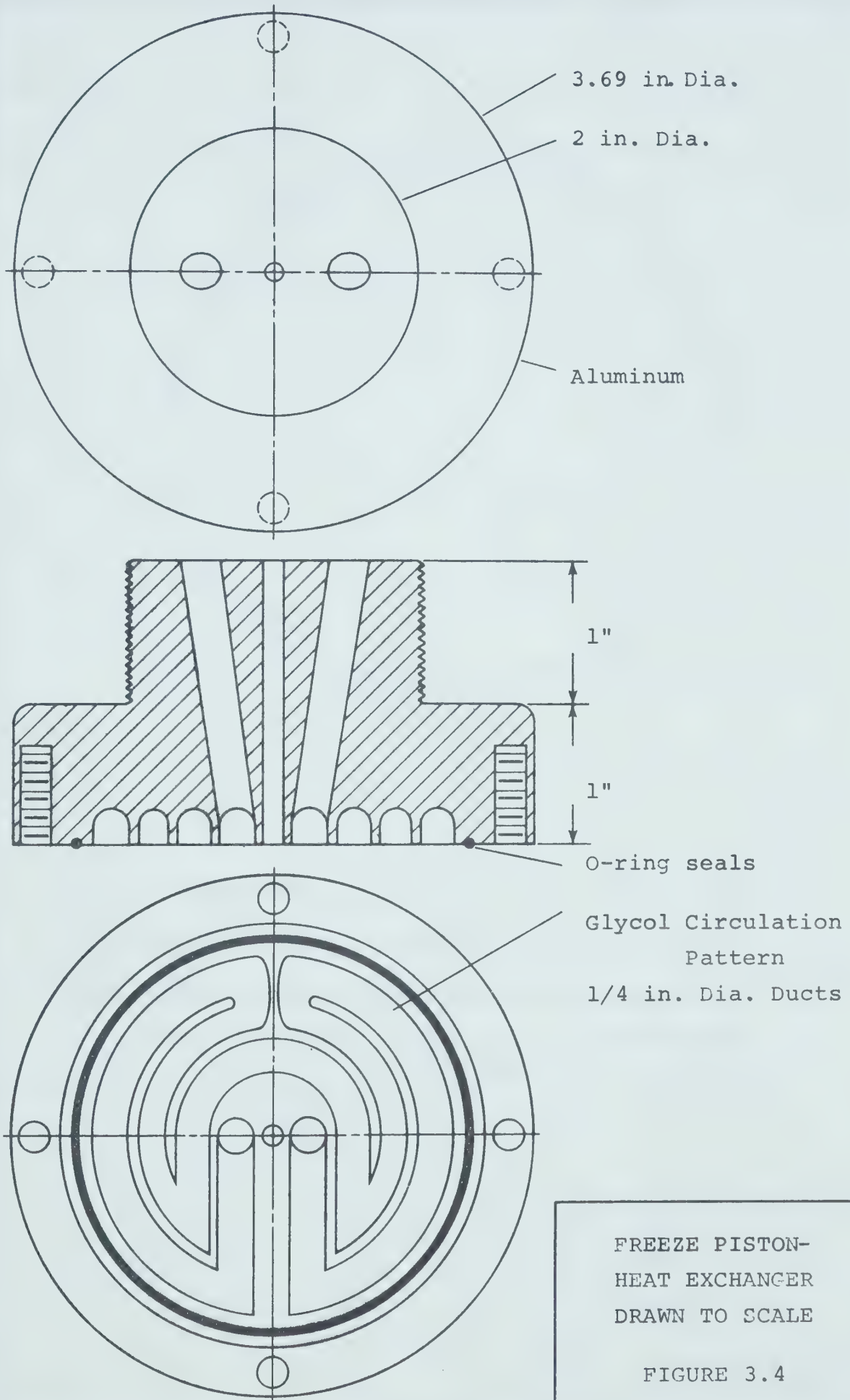
The freeze piston transferred the applied load to the soil sample and acted as a heat sink. The sections of the freeze piston are shown in Figures 3.3, 3.4, and 3.5. The rolling diaphragm was cemented to the top of the heat exchanger unit. The exchange unit contained the coolant circulation maze and functioned as the heat sink. To gain

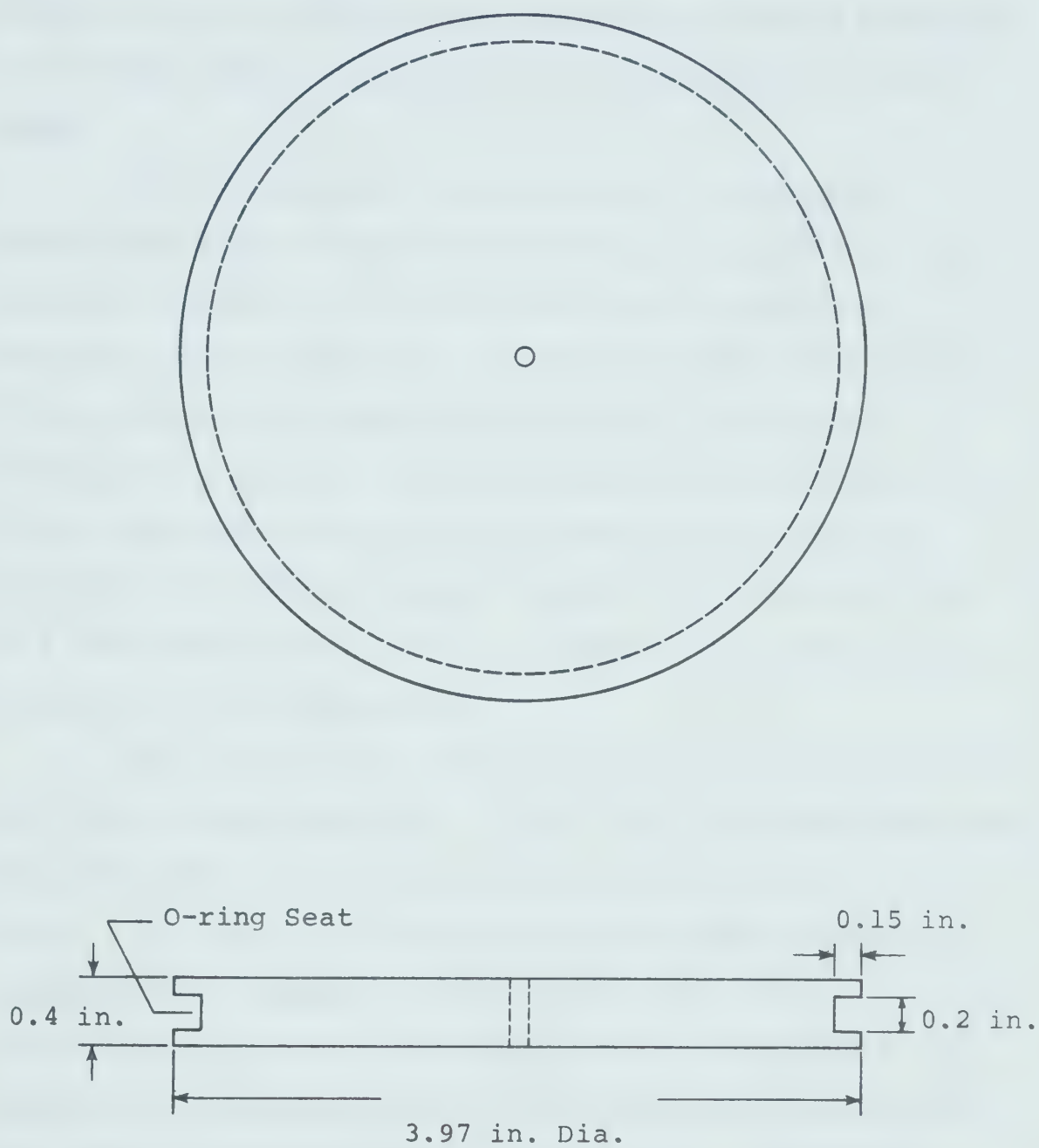




FREEZE PISTON-
REACTION HEAD
AND LOAD COLLAR

FIGURE 3.3





FREEZE PISTON -
BASE PLATE

FIGURE 3.5

maximum heat transfer efficiency the circulation maze was located below the rolling diaphragm and as close as possible to the soil sample; circulation maze length was also maximized.

The freeze piston base plate bore on the soil surface and fitted to the bottom of the heat exchange unit enclosing the maze. An O-ring was seated around the perimeter of the base plate in order to impede the movement of the soil slurry upwards past the base plate during consolidation loading. Side friction due to the adfreezing of this extruded material to the freeze piston was thus minimized. To further reduce friction the O-ring was set in a slot enabling the O-ring to slide in response to movement of the freeze piston.

The inside of the sample container was lined with a thin latex rubber membrane. A thin layer of grease separated the container wall and the membrane as shown in Detail 'A', Figure 3.2. Due to the inability of the grease layer to transfer shear stresses created by the freezing soil, friction generated along the sides of the soil sample was minimized. Pressures required to extrude the frozen soil from the soil container were measured to be as low as 2 pounds per square inch.

3.2.C. Freeze System

The freeze system is shown in Figure 3.1. Freezing of the soil sample was accomplished by imposing a negative step temperature on the soil surface. This was achieved by the circulation of a precooled coolant through the heat exchanger maze situated on top of the soil surface. An ethylene-glycol and water mixture (50-50 mix by volume) was used as coolant. The coolant was circulated by and maintained at the desired temperature by a constant temperature bath/circulator. The coolant was pumped at a rate of 6 3/4 gallons per hour and temperature maintained to ± 0.1 degrees Centigrade.

The rate of freezing of the soil sample depended on the negative temperature gradient imposed on the soil and the rate of circulation of the coolant.

3.2.D. Loading and Backpressure Systems

Air pressure, regulated by Nullmatic Pressure Regulators and monitored by a pressure transducer, was used to apply both load and back pressure to the sample. The two air pressures were delivered to the soil sample by two separate systems as shown in Figure 3.1. The loading of the sample was accomplished by an air pressure chamber situated above the freeze piston. Consolidation loads and freezing surcharge loads are listed for each test in Appendices D, E, F, and G. Application of back pressure to the

soil sample was achieved by applying air pressure to a water reservoir which was connected to the base of the soil container. Back pressures of 40 to 50 pounds per square inch, as given on each of the test summaries in Appendices D, E, F, and G.

3.2.E. Temperature Measurement System

Thermocouples were used to monitor soil sample temperatures. Temperatures were recorded by a Honeywell Elektronik 15* Strip Chart Recorder. Temperatures were measured to $\pm 1/2$ degree Fahrenheit. Sample temperature-time logs and penetration of 0°C isotherm for each test are given in Appendices, D, E, F and G.

Soil sample temperatures were monitored by six thermocouples set in the wall of the sample container. See Figure 3.2. The thermocouples were vertically spaced 1 centimeter apart with the lowest thermocouple 1.6 centimeters from the sample bottom. Starting from the uppermost thermocouple the thermocouples were numbered from 1 to 6 consecutively. Thermocouple temperature data collected during each test were identified by number in Appendices D, E, F and G.

A thermocouple located in the freeze piston base plate measured the soil surface temperature. Temperature interference due to the base plate was avoided by setting the tip of thermocouple below the plate. This thermocouple

is labelled T_s , surface temperature, in Appendices D, E, F, and G.

Heat removed from the soil sample was calculated from thermocouple data collected in the entry and exit lines of the heat exchange unit. One thermocouple, labelled T_b , was placed in the reservoir of the constant temperature bath/circulator and measured the 'cold' temperature of the coolant. The second thermocouple, labelled T_R , was situated just past the heat exchanger unit in the return line of the coolant circulation tubing. The heat removed from the soil sample was in direct proportion to the rise in the coolant temperature recorded.

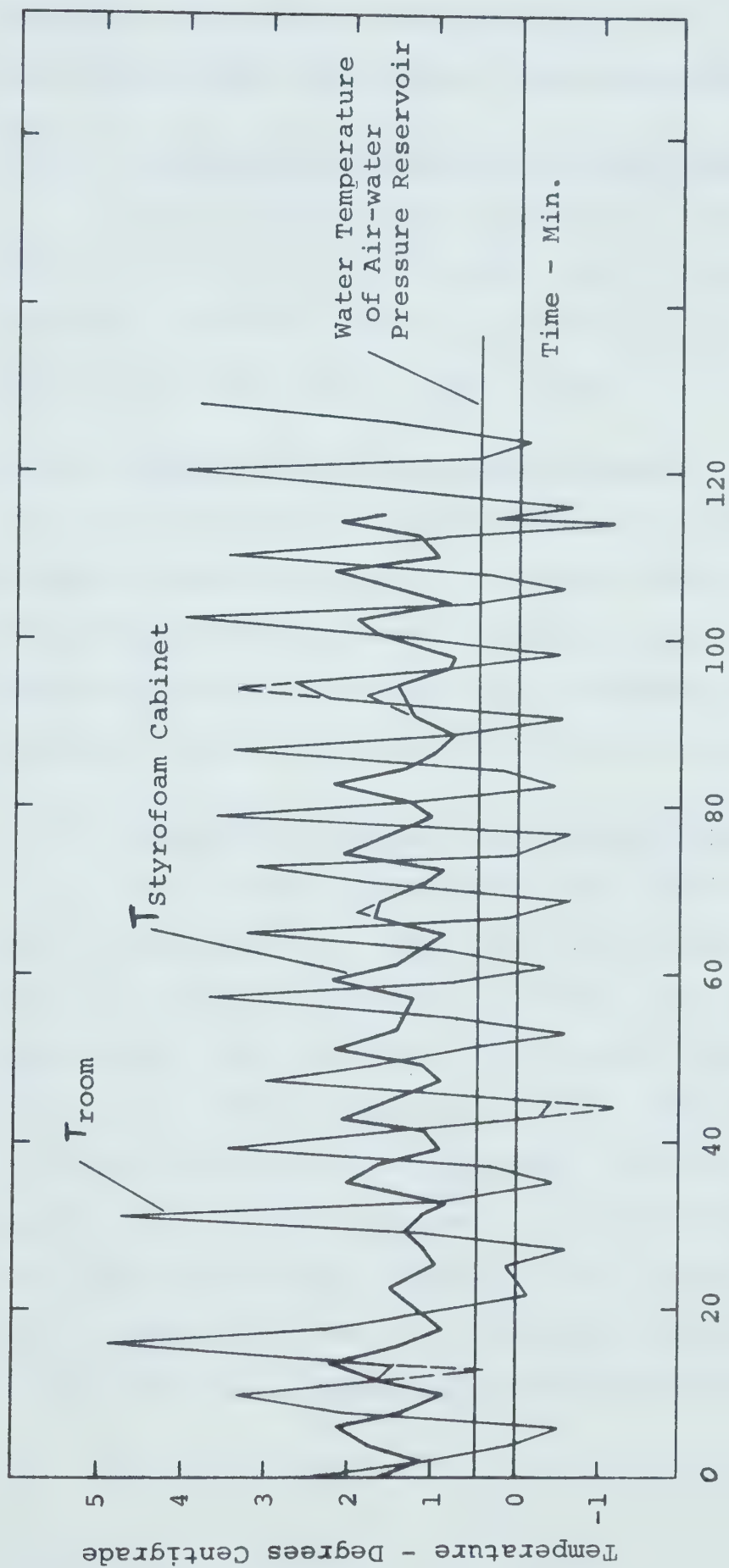
The cold room and/or styrofoam cabinet temperatures were also measured and are shown in Figure 3.6.

3.2.F. Pore Pressure Measurement System

Porewater pressures were monitored by a pressure transducer located in the base plate of the sample container as shown in Figure 3.2. The transducer was calibrated to 0.01 pounds per square inch. Pore pressure measurements were taken during closed system freeze tests.

3.2.G. Volume Change Measurement System

Volume change of the soil sample, in terms of pore fluid entering or leaving, was measured by a 25 cubic centimeter burette. Back pressure could be applied to



AMBIENT TEMPERATURE - TIME LOG

FIGURE 3.6

the burette system, as shown in Figure 3.1. Volume change measurements were taken during open system freeze tests.

3.2.H. Vertical Displacement Measurement System

A dial gage measured the vertical displacement of the soil surface to 0.001 inches. Soil surface displacements were monitored during consolidation and freezing tests for both open and closed system tests.

3.2.I. Heave Pressure Measurement System

A load cell was designed to attach to the freeze piston rod and to be fixed to a rigid frame to measure anticipated heave pressures. The load cell was made of machined aluminum and calibrated to measure ± 0.01 pounds per square inch. The load cell is shown in Figure 3.1.

3.2.J. Equipment Assessment and Recommendations

The rolling diaphragm performed satisfactorily and added a high degree of flexibility to the type of freeze test that could be conducted. Initial familiarization, installation and sealing of the diaphragm proved quite troublesome. The system used to anchor the diaphragm to the freeze piston could be improved to provide faster installation of new diaphragms. Under the present arrangement with the diaphragm cemented to the freeze piston, a day is required to replace a damaged diaphragm, and time is lost. In the original design the bellofram was anchored

by fitting the freeze piston base plate and heat exchange unit together, squeezing the bellofram between the two sections. This system proved unsatisfactory and was abandoned. This problem is minor in nature but to reduce lost experimental time the latter system is more desirable.

The attainment of a 100 per cent pore pressure response (B value equals 1.0) to the applied consolidation loading proved to be a problem and an area that should be improved. The crux of the problem concerns the rolling - O-ring seal on the freeze piston base plate (Figure 3.5). The O-ring was set to provide maximum impedance to the soil slurry from moving upwards past the base plate during consolidation loading without creating excessive normal pressures and hence friction against the sample container. The O-ring seating used satisfactorily impeded drainage and generated acceptable amounts of friction but was incapable of confining the pressure within the soil chamber. Consequently the air space between the rolling diaphragm and freeze piston base plate introduced a compressible component into the pressurized zone resulting in a finite reduction of the soil container pressure. This problem occurred only during the consolidation loading stage and ceased to exist once a plug of frozen soil develops. A new design is needed that will confine the soil pressures without creating excessive side friction. One solution might be to attach

the rubber latex membrane surrounding the soil sample to the freeze piston.

Rate of heat removal is another area that could be improved. The heat removal capacity of the freeze system is a direct function of the rate of coolant circulation. Higher flow rates could be achieved by reducing the resistance to flow by using large diameter circulation tubing and heat exchange maze flow channels, and by using a less complex circulation maze in the heat exchange unit. These diameters must be optimized with respect to dimensions of the freezing piston.

CHAPTER 4

TEST RESULTS AND CALCULATIONS

4.1 Introduction

A general outline of testing procedure was given in Chapter 3. Details of the testing program, and processing of the data are given below.

Data for each soil type are given in the following appendices: Ottawa sand data are summarized in Appendix D, Devon silt data are listed in Appendices E and F, and modified Devon silt data are summarized in Appendix G. Whenever more than one type of test was conducted on a soil type, the test was identified by the series number and test number. For example, Test E-1-2 refers to test 2 of series 1 listed in Appendix E.

Results of calculations are also summarized below with typical calculations given in Appendix B.

4.2 Test Results

4.2.A. Ottawa Sand

Three freezing tests were run on Ottawa sand to verify the concept that during freezing cohesionless granular soils expel water. Soil properties of Ottawa sand are given in Appendix A. Summaries of soil data and

freezing test data are given in Tables 1 and 2, Appendix D, respectively. A summary of freezing test results for Ottawa sand is given in Figure 4.1.

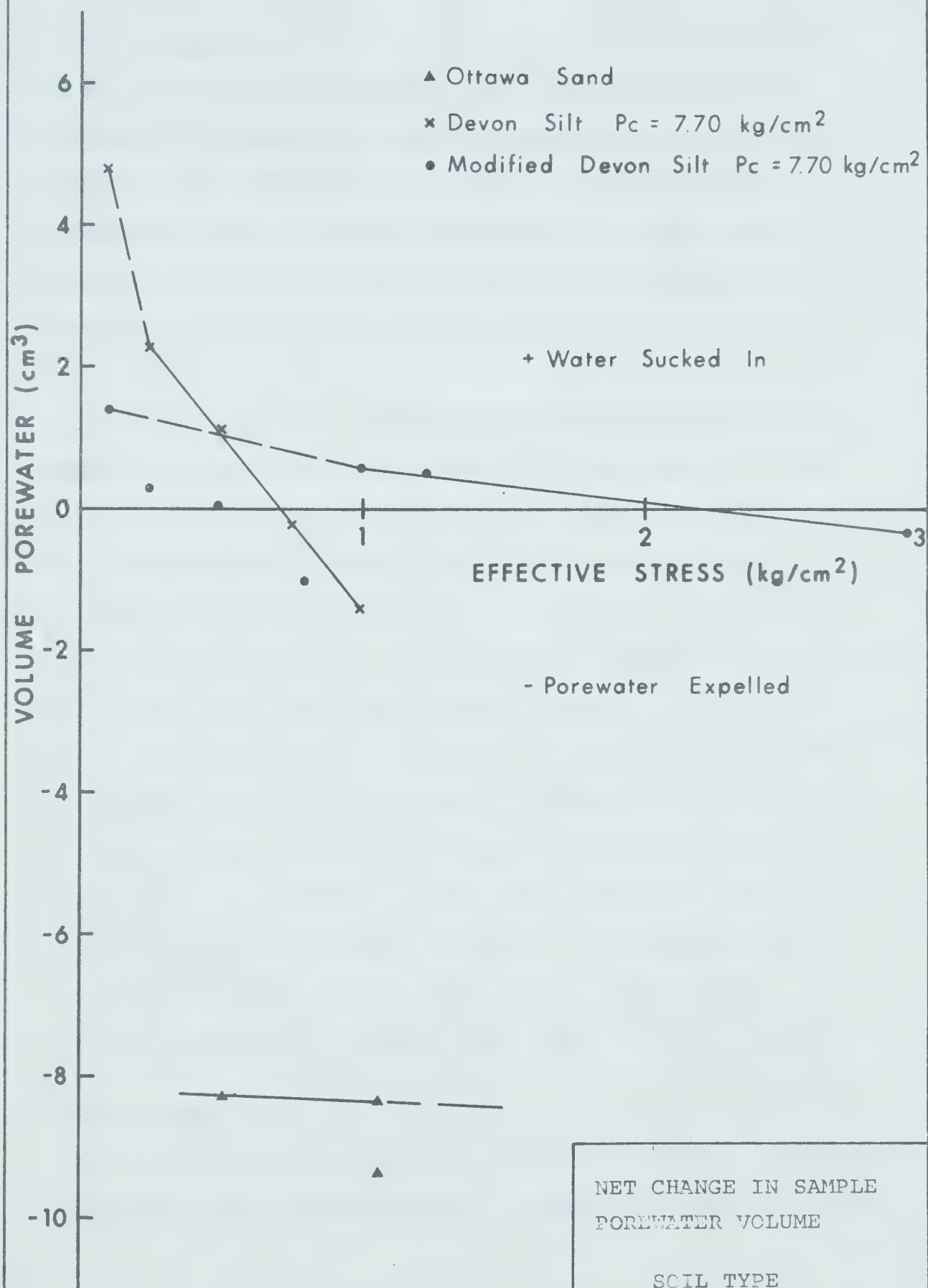
All freezing tests carried out on Ottawa sand were conducted under open drainage and unrestrained heave conditions. Details of stress history and freezing step temperature for each test are as follows:

Test D-1

A slurry was placed in the soil container and allowed to consolidate under an effective stress of 1.04 Kg/cm^2 . A step temperature of -10°C was imposed on the soil surface. Freezing test data are given in Appendix D, (Figure D-1).

Test D-2

A slurry was placed in the soil container and densified by tapping the sides of the container. The purpose of this test was to investigate the influence of porosity on the freezing behavior of sand. The slurry was allowed to consolidate under an effective stress of 1.04 Kg/cm^2 . A step temperature of -10°C was applied to the soil surface. Data for this test are given in Appendix D, (Figure D-2).



Test D-3

A slurry was placed in the soil container and allowed to consolidate under an effective stress of 0.50 Kg/cm². This test was run to check the influence of overburden load on freezing behavior. The soil was subjected to a -9.39°C step temperature. Freezing test data are given in Appendix D, (Figure D-3).

At the end of these tests the dimensions of the sample container and arrangement of thermocouples in the container wall were changed to those shown in Figure 3.2. The cross-sectional area of the sample container was changed from 81 cm², used above, to 83.4 cm². The height of the sample container was reduced to accommodate the freeze piston and the large consolidation strains of the silts which were used for the remainder of the testing program. The thermocouples were arranged in three sets of pairs in the above tests. The thermocouple arrangement shown in Figure 3.2 was adopted to gain a more detailed soil temperature profile during freezing. Thermocouple T_R, was also installed in the return line of the glycol circulation tubing to monitor the amount of heat removed.

4.2.B. Devon Silt

Devon silt was used to test the porewater expulsion concept on fine grained soils. A summary of the mechanical

properties of this soil is given in Appendix A. Freezing tests were conducted on normally consolidated and overconsolidated samples. Summaries of data obtained for normally consolidated samples are given in Appendix E, (Tables 1 and 2), and for overconsolidated samples in Appendix F, Tables (1 and 2). Void ratio versus effective stress plots are given in Appendix E, (Figure E-0-1) for normally consolidated samples and in Appendix F, (Figures F-0-1, F-0-2, F-0-3) for overconsolidated samples. Details of test series run on Devon silt are as follows:

(1) Test Series E-1

The purpose of Test Series E-1 was to investigate the freezing behavior of normally consolidated Devon silt. Freezing tests were run at varied effective stresses and void ratios. As summarized in Appendix E, (Table 1) a series of freezing test, Tests E-1-1 to E-1-7, were carried out under effective stresses ranging from 0.72 to 2.42 Kg/cm². Freezing test data for each of these tests are summarized in Appendix E, (Table 2). A summary of test results for this test series is given in Figure 4.1.

For each test of this series a slurry having a liquidity index between 3.5 and 4.0 was placed in the sample container and consolidated to the desired effective stress. Consolidation data are summarized in Appendix E,

(Table 1 and Figure E-0-1). The samples were frozen by imposing a step temperature of -4.44°C on the soil surface. All freezing tests were conducted under open drainage and unrestrained heave conditions. Data for tests E-1-1 to E-1-7 are shown in Appendix E, (Figures E-1-1 to E-1-7 respectively).

Test E-1-2 was conducted at roughly the same effective stress as Test E-1-1 to demonstrate repeatability of results.

(2) Test Series E-2

This test series was conducted under closed drainage conditions in order to investigate the freezing behavior of normally consolidated Devon silt in terms of porewater pressure generation. It was anticipated that the freezing behavior mapped in Test Series E-1 and E-2 would be consistent.

In a procedure similar to Test Series E-1, freezing tests E-2-1 to E-2-5 inclusive of series E-2 were carried out under effective stresses ranging from 0.97 to 1.47 Kg/cm^2 respectively. For each test a slurry having a liquidity index between 3.1 to 3.9 was placed in the sample container and consolidated to the desired effective stress. Consolidation data are summarized in Appendix E, (Table 1 and Figure E-0-1). A step temperature of -4.44°C was applied to the soil surface and the soil frozen under unrestrained

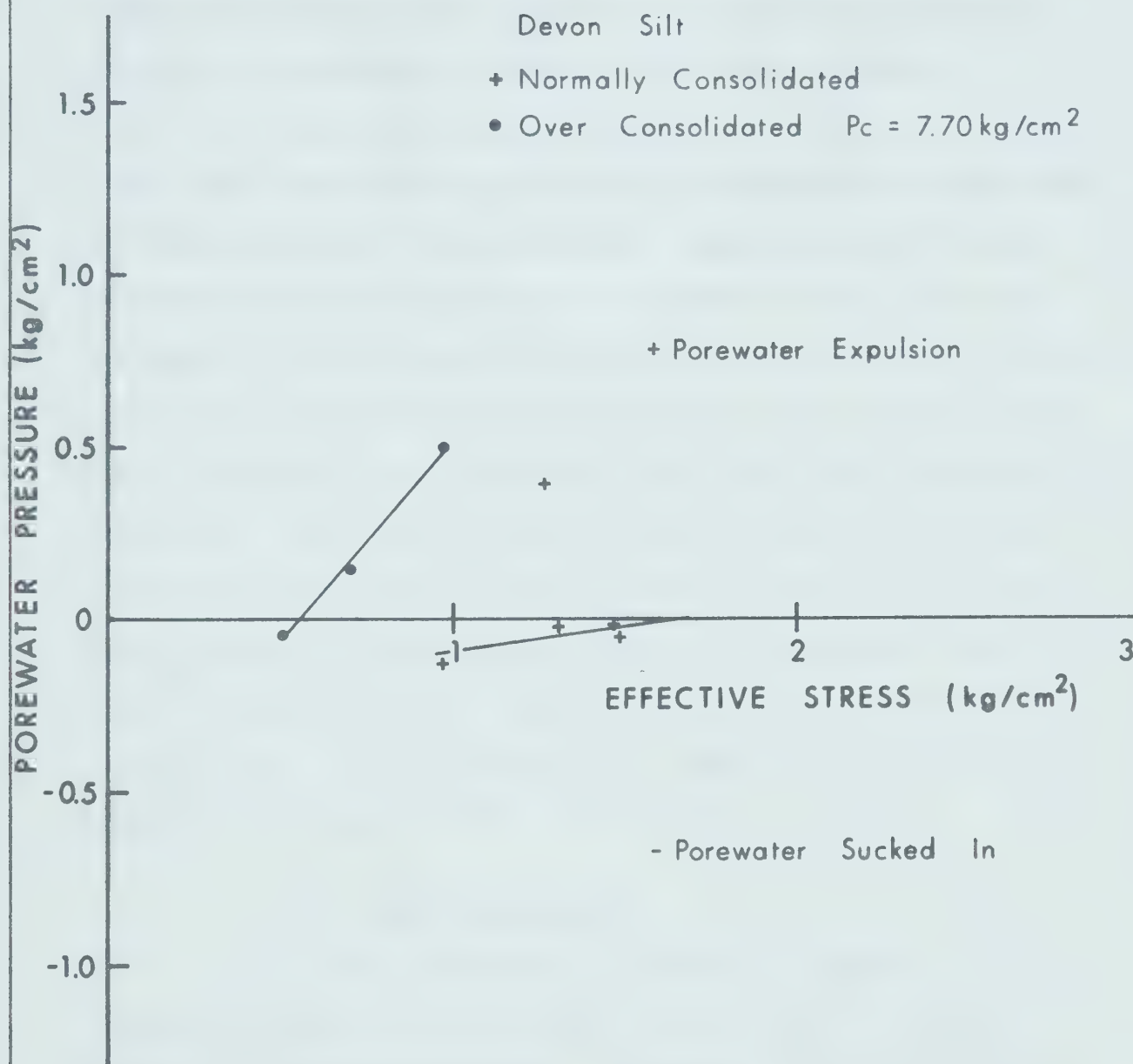
heave and closed drainage conditions. Data for this series, Tests E-2-1 to E-2-5, are shown in Appendix E, (Figures E-2-1 to E-2-5 respectively). A summary of test results for this test series is given in Figure 4.2.

Tests E-2-4 and E-2-5 were run at roughly the same effective stress to demonstrate reproducibility. Pore-water pressure results of Test E-2-2 cannot be fully explained.

(3) Test Series E-3

Boundary conditions of both tests in this series were changed while the freezing process was in progress. Freezing was initiated in Tests E-3-1 and E-3-2 under open drainage and unrestrained heave conditions and were continued until a consistent set of porewater expulsion data points was generated. At this time the sample drainage was stopped and the freezing test continued under closed drainage conditions. The purpose of these tests was to attempt to measure the porewater pressure (closed drainage conditions) that caused the porewater expulsion under open drainage conditions, and to see if freezing conditions were different for open and closed drainage cases.

Again for each test a slurry at a liquidity index of 3.8 and 3.5, for Tests E-3-1 and E-3-2 respectively, was placed in the sample container. The slurries were then consolidated under the chosen effective stresses. The consolidation stress of 1.47 Kg/cm^2 for Test E-3-1 and 1.96



POREWATER PRESSURE
STRESS HISTORY

FIGURE 4.2

Kg/cm² for Test E-3-2 were chosen to ensure expulsion of porewater during freezing. (These values were based on results obtained in Test Series 1). Consolidation data are given in Appendix E, (Table 1 and Figure E-0-1).

As stated above freezing was initiated in both tests under open drainage and unrestrained heave conditions, and continued until the porewater expulsion rate became constant. The drainage was then closed in both tests and porewater pressures were measured. Once consistent pressures were being recorded the drainage system was opened in both tests, allowing free drainage. Test E-3-1 was terminated at this stage. After a period of free drainage the drainage system was closed for a second time in Test E-3-2 and porewater pressures measured once again. Step temperatures of -4.44°C and -5.00°C were used in Tests E-3-1 and E-3-2 respectively. Data collected for these tests are given in Appendix E, (Figures E-3-1 and E-3-2).

(4) Test Series F-1

In Test Series F-1 a sample of Devon silt was overconsolidated to investigate the influence of stress history on freezing behavior. Series F-1 is the first of several test series conducted to investigate this relationship.

A slurry at a liquidity index of 3.6 was placed in the sample container and consolidated under an effective

stress of 7.70 Kg/cm^2 . The applied stress was then reduced to 0.1 Kg/cm^2 and the sample allowed to rebound. A number of freezing tests were subsequently conducted at various effective stress conditions. All freezing tests of this series were run under open drainage and unrestrained heave boundary conditions. Details of stress path followed and applied step temperature for each test of the series are as follows:

Test F-1-1

Prior to freezing in this test the sample was allowed to consolidate under an effective stress of 7.70 Kg/cm^2 and then allowed to rebound under an effective stress of 0.1 Kg/cm^2 as described above. Consolidation data are presented in Appendix F, (Figure F-0-1). A step temperature of -4.44°C was applied to the soil surface. The data for this test is presented in Appendix F, (Figure F-1-1).

Test F-1-2

After completion of test F-1-1 the effective stress was increased to 0.25 Kg/cm^2 and the sample allowed to consolidate under the higher load. Consolidation data are summarized in Appendix F, (Figure F-0-1). A surface temperature of -4.94°C was applied to the soil surface. Test data for Test F-1-2 are shown in Appendix F, (Figure F-1-2).

Test F-1-3

The applied effective stress was doubled to 0.5 Kg/cm² and the sample allowed to consolidate. Consolidation data are presented in Appendix F, (Figure F-0-1). A step temperature of -4.44°C was imposed on the soil surface. The data for this test are presented in Appendix F, (Figure F-1-3).

Test F-1-4

The applied stress was increased to 0.74 Kg/cm² and the sample allowed to consolidate. A step temperature of -5.00°C was imposed on the soil surface. This test was the first to show that porewater could be expelled by freezing an overconsolidated silt. Data for this test is contained in Appendix F, (Figure F-1-4).

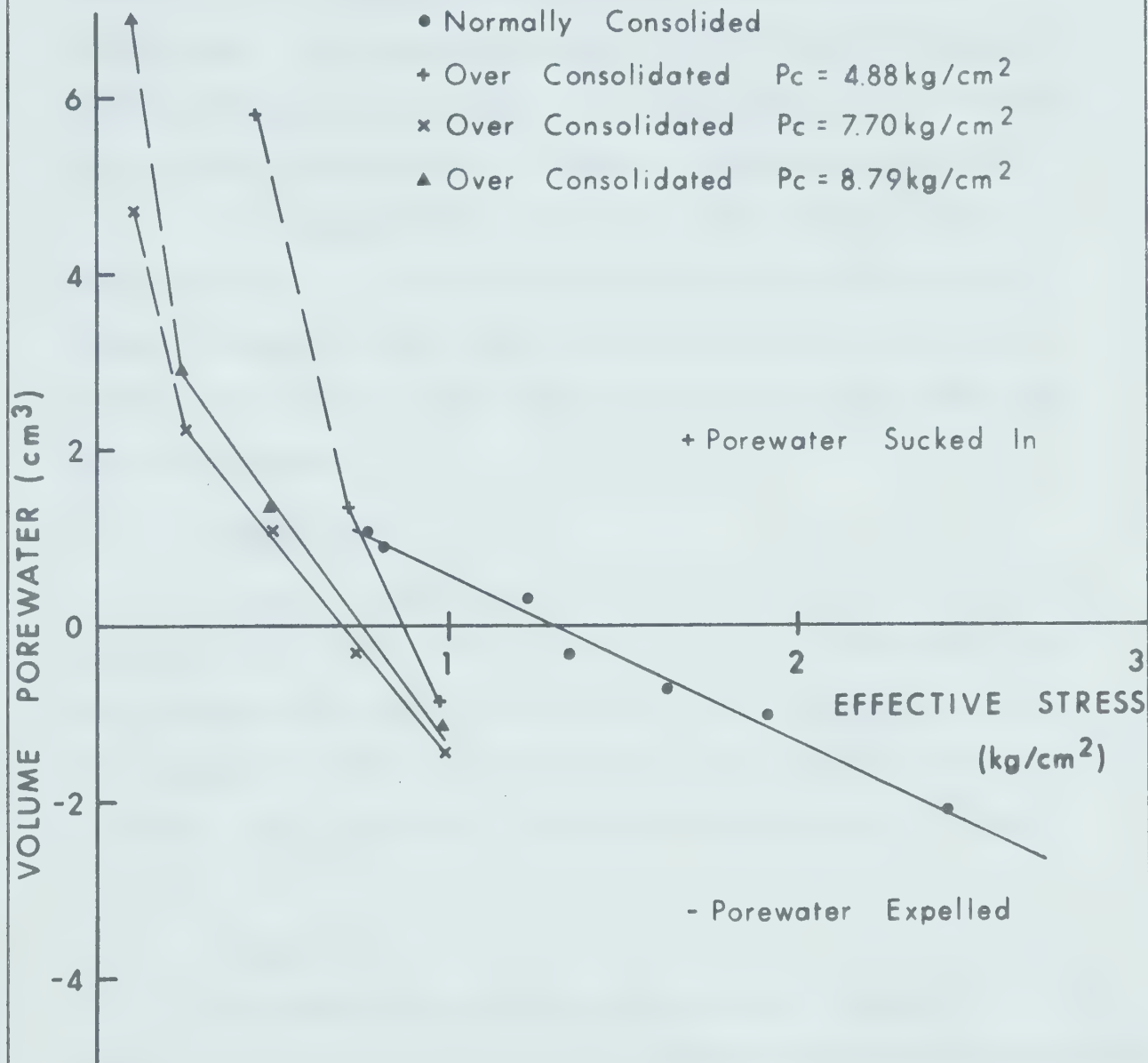
Test F-1-5

The applied effective stress was increased to 0.98 Kg/cm², the sample was allowed to consolidate and then frozen. A step temperature of -4.79°C was used. Test data is given in Appendix F, (Figure F-1-5).

A summary of test results for this test series is given in Figure 4.3.

Devon Silt

- Normally Consolidated
- + Over Consolidated $P_c = 4.88 \text{ kg/cm}^2$
- x Over Consolidated $P_c = 7.70 \text{ kg/cm}^2$
- ▲ Over Consolidated $P_c = 8.79 \text{ kg/cm}^2$



NET CHANGE IN SAMPLE
POREWATER VOLUME -

STRESS HISTORY

FIGURE 4.3

(5) Test Series F-2

In this test series the sample used in Test Series F-1 was frozen under closed system drainage conditions. The purpose of this series was to determine whether the porewater expulsion phenomenon of Test Series F-1 could be duplicated in terms of porewater pressures.

Consolidation data are shown in Appendix F, (Figure F-0-1). All tests of series F-2 were conducted under closed drainage and unrestrained heave conditions. Stress path and surface temperature details for each test are as follows:

Test F-2-1

Prior to freezing the applied effective stress was reduced from 0.98 Kg/cm^2 of Test F-1-5 to 0.50 Kg/cm^2 and the sample was allowed to rebound. The sample was frozen by imposing a step temperature of -4.44°C on the soil surface. Test data are presented in Appendix F, (Figure F-2-1).

Test F-2-2

The applied effective stress was increased to 0.98 Kg/cm^2 in an attempt to generate positive porewater pressures during freezing. After consolidation was complete a step temperature of -4.94°C was applied to the soil surface. Freezing test data are given in Appendix F, (Figure F-2-2).

Test F-2-3

The applied effective stress was reduced to 0.70

Kg/cm^2 , the sample was allowed to rebound, in an attempt to repeat the generation of negative porewater pressures measured in test F-2-2. A step temperature of -5.00°C was used. Data for this test are given in Appendix F, (Figure F-2-3).

A summary of test results for this test series is given in Figure 4.2.

(6) Test Series F-3

For this test series the step temperature used in previous test series was roughly doubled. The sample used previously in Test Series F-1 and F-2 was also used for this series. Consolidation data are given in Appendix F, (Figure F-0-1). All freezing tests were conducted under open drainage and unrestrained heave conditions. Stress path and surface temperature data for each test are as follows:

Test F-3-1

The effective stress of 0.70 Kg/cm^2 used in Test F-2-3 was maintained and used in this test. The sample was frozen by applying a step temperature of -9.72°C . Test data are given in Appendix F, (Figure F-3-1). Due to the reduced time required to freeze the soil sample all summarized data were extrapolated to time $t = 160$ minutes for comparison with previous data.

Test F-3-2

The effective stress was reduced to 0.25 Kg/cm^2

and the soil allowed to rebound. A step temperature of -9.72°C was applied to the soil surface. The data for this test is presented in Appendix F, (Figure F-3-2).

Test F-3-3

The soil sample was consolidated under an effective stress of 0.50 Kg/cm^2 . The soil surface was subjected to a -9.78°C step temperature. Data for this test is presented in Appendix F, (Figure F-3-3).

A summary of test results for this test series is given in Figure 4.4.

(7) Test Series F-4

In this series freezing tests were run on a moderately overconsolidated Devon Silt sample. The purpose of the series was to further investigate the influence of stress history on freezing behavior.

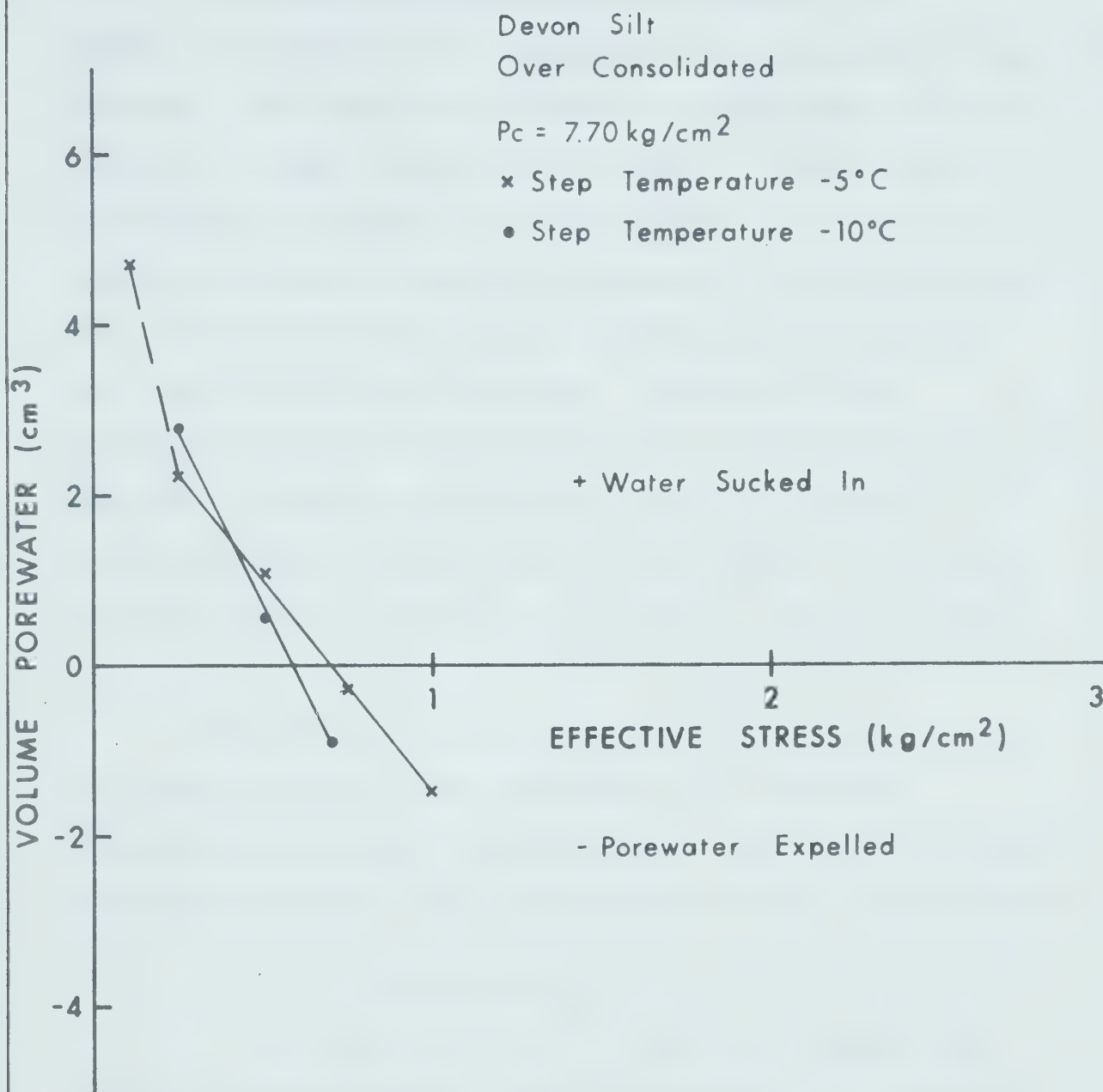
Prior to freezing the soil sample was consolidated under an applied effective stress of 4.88 Kg/cm^2 and then allowed to rebound under a stress of 0.46 Kg/cm^2 . Consolidation data are summarized in Appendix F, (Figure F-0-2). All freezing tests in this series were conducted under open drainage and unrestrained heave conditions. Details of stress path and surface temperature for each test are as follows:

Test F-4-1

A slurry having a liquidity index of 3.6 was placed in the sample container, allowed to consolidate then rebound under effective stresses of 4.88 and 0.46 Kg/cm² respectively. The sample was subjected to a step temperature of -7.36°C for the first 30 minutes and of -4.83°C for the remainder of the test. The change in the step temperature was a result of problems experienced with the regulation of glycol flow prior to the test. Due to the collapse of the circulation tubing the flow rate was significantly reduced. In order to maintain the same rate of heat extraction used in previous tests the step temperature was increased in proportion to the decrease in glycol flow. However, as test F-4-1 progressed it became evident, from frost penetration data, that a glycol flow rate roughly equivalent to earlier tests had been achieved by the equipment modifications. The step temperature was then increased to -4.83°C. Data for this test are given in Appendix F, (Figure F-4-1).

Test F-4-2

The applied effective stress on the sample was increased to 0.82 Kg/cm² and the sample was allowed to consolidate. The sample was frozen by applying a step temperature of -5.24°C. Data for this test is presented in Appendix F, (Figure F-4-2).



NET CHANGE IN SAMPLE
POREWATER VOLUME -
STEP TEMPERATURE

FIGURE 4.4

Test F-4-3

The effective stress was increased to 1.07 Kg/cm² in an attempt to cause porewater expulsion during freezing. The sample was allowed to consolidate and then frozen by a step temperature of -4.72°C. After roughly 50 minutes of testing a city wide power failure occurred and the test was necessarily terminated. The soil sample was removed because of feared contamination by kerosene from the volume change indicator. Because of the consistency of the expulsion porewater results and the favorable agreement with earlier tests, the author extrapolated the data to time $t = 160$ minutes. The data for this test is presented in Appendix F, (Figure F-4-3).

Because the results of Series F-4, tests F-4-1 to F-4-3, and as a whole were consistent with previous observations this test series was not repeated. A summary of test results for this test series is given in Figure 4.3.

(8) Test Series F-5

In Test Series F-5 a Devon silt sample was heavily overconsolidated, prior to freezing, to complete the study of stress history on freezing behavior. Heave was monitored in the first 4 tests of this series; heave pressure was measured in the last test, Test F-5-5.

A slurry at a liquidity index of 3.7 was placed in the soil container and allowed to consolidate under an effective stress of 8.79 Kg/cm^2 . The applied stress was then reduced to 0.1 Kg/cm^2 and the sample allowed to rebound. Consolidation data are shown in Appendix F, (Figure F-0-3). Details of stress path and freezing boundary conditions for each test are as follows:

Test F-5-1

As mentioned above the slurry was consolidated then allowed to rebound under effective stresses of 8.79 and 0.1 Kg/cm^2 respectively. A step temperature of -5.56°C was applied to the soil surface and the sample frozen under open drainage, unrestrained heave conditions. Data for this test are given in Appendix F, (Figure F-5-1).

Test F-5-2

The applied effective stress was increased to 0.24 Kg/cm^2 , the sample was consolidated and then frozen under open drainage and unrestrained heave boundary conditions. A step temperature of -4.78°C was used. Test data are shown in Appendix F, (Figure F-5-2).

Test F-5-3

The sample was allowed to consolidate under an effective stress of 0.49 Kg/cm^2 . The sample was subjected to a step temperature of -5.00°C and frozen under open

drainage and unrestrained heave conditions. Data for this test are given in Appendix F, (Figure F-5-3).

Test F-5-4

The applied effective stress was increased to 0.97 Kg/cm² and the sample allowed to consolidate. A step temperature of -5.17°C was applied to the soil surface and the sample frozen under open drainage and unrestrained heave conditions. Test data are shown in Appendix F, (Figure F-5-3).

A summary of test results for tests F-5-1 to F-5-4 of this series is given in Figure 4.3.

Test F-5-5

In this test heave pressure was measured by restraining the heave displacement of the soil surface using a load cell fixed to a rigid load frame as shown in Figure 3.1.

The purpose of this test was to measure heave pressure of a sample at an effective stress at which no net change in sample porewater volume occurs. Based on results of previous tests of this series an effective stress of 0.69 Kg/cm² was applied to the sample. The sample was allowed to rebound under this reduced stress and frozen under open drainage and restrained heave conditions. A step

temperature of -5.17°C was used. Any vertical movement of the freeze piston due to load frame compliance was monitored for control purposes. Test data are shown in Appendix F, (Figure F-5-5).

4.2.C. Modified Devon Silt

The grain size distribution of Devon silt was artificially changed in order to study the influence of grain size distribution on freezing behavior. Modification of the characteristic grain size distribution was accomplished by increasing the proportion of finer silt sizes and clay sizes. The finer particle sizes were removed from a second Devon silt sample by elutriation. Grain size distribution plots of typical Devon silt and Modified Devon silt are shown in Appendix A, (Figure A-1).

A slurry prepared at a liquidity index of 5.1 was placed in the soil container and allowed to consolidate and rebound under effective stresses of 7.7 and 0.1 Kg/cm^2 respectively. Consolidation data are contained in Appendix G, (Table 1 and Figure G-0). Details of stress path and freezing boundary conditions for each test are as follows:

Test G-1

As described above the slurry was allowed to consolidate and rebound under effective stresses of 7.70 and 0.1 Kg/cm^2 respectively. A step temperature of -5.22°C

was applied to the sample surface. Freezing occurred under open drainage and unrestrained heave conditions. Data for this test are given in Appendix G, (Figure G-1).

Test G-2

The effective stress was increased to 0.24 Kg/cm^2 and the sample allowed to consolidate. Freezing was carried out under open drainage and unrestrained heave conditions. A step temperature of -4.87°C was used. Data for this test are given in Appendix G, (Figure G-2).

The volume of porewater sucked in during this test was less than anticipated. The validity of the test data is open to question due to a suspected leak in the volume change indicator.

Test G-3

The effective stress was increased to 0.49 Kg/cm^2 . After sample consolidation was completed the sample was frozen under open drainage and unrestrained heave conditions. A step temperature of -4.72°C was used. Data for this test are given in Appendix G, (Figure G-3). The porewater volume results for this test are also questionable as the leak in the volume change indicator was not successfully stopped.

Test G-4

The sample was consolidated under an effective stress of 0.73 Kg/cm^2 . Step temperature of -4.79°C was applied to the soil surface. The soil was frozen under open drainage and unrestrained heave conditions. Test data are contained in Appendix G, (Figure G-4). The pore-water volume results are also questionable for this test. Again the leak in the volume change indicator was not successfully stopped.

Test G-5

The effective stress was increased to 0.98 Kg/cm^2 and the sample allowed to consolidate. Freezing was conducted under open drainage and unrestrained heave conditions. A step temperature of -4.89°C was used. Data for this test are shown in Appendix G, (Figure G-5).

Test G-6

The effective stress was increased to 1.22 Kg/cm^2 and the sample allowed to consolidate. Freezing was conducted under open drainage and unrestrained heave conditions. A step temperature of -5.00°C was used. Data for this test are given in Appendix G, (Figure G-6). Results of this test are consistent with Tests G-1, and G-5.

Test G-7

The effective stress was increased to 2.23 Kg/cm^2 in an attempt to expel porewater during freezing. The sample was allowed to consolidate under this pressure and frozen under open drainage and unrestrained heave conditions. A step temperature of -5.00°C was used. Data for this test are shown in Appendix G, (Figure G-7).

A summary of test results for tests G-1 to G-7 of this series is given in Figure 4.1.

Test G-8

Test G-8 consisted of measuring the heave pressure generated by a freezing soil with free drainage. As in Test F-5-5 the effective pressure at which this test was carried out at would not result in any net change in sample porewater volume. Based on results of Tests G-1, G-5, 6, and 7, an effective stress of 2.24 Kg/cm^2 was used.

The sample was allowed to rebound under this effective stress of 2.24 Kg/cm^2 . The sample was subjected to a step temperature of -4.50°C and frozen under open drainage and restrained heave conditions. Vertical movement of the freeze piston, due to compliance, was monitored for control purposes. Test data for this test are contained in Appendix G, (Figure G-8).

The apparent correlation of results of Tests G-1, 2, 3 and 4 is recognized by the author. The leak that occurred in the volume change indicator during Tests G-2, 3 and 4 was very small but its possible effect on test results must be acknowledged. Because of this possibility of error and the satisfactory duplication of results of Tests G-5 and G-6 the relationship shown in Figure 4.1 is recommended.

4.3 Calculations

Soil property and freezing test calculations are presented below.

4.3.A. Soil Property Calculations

Initial height of the slurry sample was the average of nine vernier measurements. The height of sample at any time during testing was determined by adding or subtracting the net change in the dial gage reading to the initial height.

The void ratio, e , at any time is:

$$e = \frac{H - H_o}{H_o} \quad 4.1$$

where H is the sample height [cm]

H_o is the height of soil solids [cm] or

$$H_o = \frac{W_s}{G \gamma_w A}$$

where W_s is the weight of the dry soil [cm]

G is the specific gravity of the soil solids

γ_w is the unit weight of water = 1[gm/cm³]

A is the cross-sectional area of the sample

container [cm²] ($A = 81 \text{ cm}^2$ for sand and

$A = 83.4 \text{ cm}^2$ for the silts).

The degree of saturation at the beginning of the test, S_o was calculated from the initial water content and void ratio by

$$S_o = \frac{W_o G}{e_o} \quad 4.2$$

where W_o is the initial water content

e_o is the initial void ratio.

S_o for virtually all tests was equal to 100%.

The coefficient of consolidation, C_v , was determined from $e - \log$ time plots in the conventional manner:

$$C_v = \frac{0.848 H^2}{t_{90}} \quad [\text{cm}^2/\text{sec}] \quad 4.3$$

where H is the average sample height

t_{90} is the time at which 90% of total consolidation

has been completed.

Actual t_{90} data are of little significance to this study and have been omitted from data summaries.

Permeability, k , was then determined by:

$$k = \gamma_w C_v m_v \quad [\text{cm/sec}] \quad 4.4$$

where m_v is the compressibility

$$m_v = \frac{1}{1+e} \frac{\Delta e}{\Delta \sigma}, \quad [\text{cm}^2/\text{gm}] \quad 4.5$$

Prior to the freezing tests, void ratio e_f , was calculated from equation 4.1 by substituting the sample height prior to freezing for H . Porosity was then calculated:

$$n = \frac{e_f}{1 + e_f} \quad 4.6$$

As shown in Table 1 in each of Appendices D, E, F and G, S_o calculated from equation 4.2 was virtually equal to 100 per cent in all cases. Consequently water content prior to freezing, w_f , was calculated from equation 4.2, assuming $S_o = 100\%$ or

$$w = \frac{e}{G} \times 100\% \quad 4.7$$

4.3.B. Freezing Test Calculations

(1) Penetration of 0°C Isotherm

The movement of the freezing front in a soil subjected to a step decrease in temperature has been described by Neumann and is given by Carslaw and Jaeger (1947). Assuming that the properties of the frozen and

thawed regions are homogeneous and independent of temperature, the movement of the 0°C isotherm through the unfrozen soil is:

$$X = \alpha \sqrt{t} \quad 4.8$$

where X is the depth of frost penetration

t is time

α is a constant which is determined as a root of the transcendental equation

$$\frac{e^{-\frac{\alpha^2}{4k_u}}}{\operatorname{erf}\left(\frac{\alpha}{2\sqrt{k_u}}\right)} - \frac{T_g}{T_s} \frac{K_f}{K_u} \sqrt{\frac{k_u}{k_f}} \frac{e^{-\frac{\alpha^2}{4k_f}}}{\operatorname{erfc}\left(\frac{\alpha}{2\sqrt{k_f}}\right)} = \frac{L \sqrt{\pi\alpha}}{2\sqrt{k_u} C_u T_s} \quad 4.9$$

where $\operatorname{erf}(\)$ is the error function

$$\operatorname{erfc}(\) = 1 - \operatorname{erf}(\)$$

k_u, k_f are the diffusivities of unfrozen and frozen soil [cm^2/sec]

K_u, K_f are the thermal conductivities of unfrozen and frozen soil [$\text{cal}/^\circ\text{C cm sec}$]

C_u, C_f are the volumetric heat capacities of unfrozen and frozen soil [$\text{cal}/^\circ\text{C cm}^3 \text{ soil}$]

T_g is the uniform initial ground temperature [$^\circ\text{C}$]

T_s is the applied constant surface step temperature [$^\circ\text{C}$], L is the volumetric latent heat of the soil [$\text{cal}/\text{cm}^3 \text{ soil}$].

Assuming a linear temperature distribution in the frozen zone and ignoring the temperature profile in the unfrozen zone Stefan solved equation 4.8 in the form

$$x = \sqrt{\frac{2K_u T_s}{L}} \sqrt{t} \quad 4.10$$

from which the constant term can also be written in the dimensionless form:

$$\frac{\alpha}{2\sqrt{k_u}} = \sqrt{\frac{St_e}{2}} \quad 4.11$$

where $St_e = \frac{C_u T_s}{L}$ and is called the Stefan number.

Volumetric heat capacity of unfrozen soil, C_u , and volumetric latent heat of the soil, L , may be determined as follows:

$$C_u = \gamma_d \left(C_m + \frac{1.0w}{100} \right) \quad 4.12$$

where 1.0 = heat capacity of water [cal/gm°C]

$$L = \gamma_d w (1-w_u) L' \quad 4.13$$

The terms of equation 4.12 and 4.13 are defined as:

C_m denotes the heat capacity of the soil grains
[cal/gm°C]

γ_d denotes the dry density of the soil [gm/cm³]

w denotes water content [%]

w_u denotes unfrozen water content [gm water/gm
(ice + water)]

L' denotes latent heat of water [= 79.6 cal/gm]

The test equipment was designed to impose a step temperature on the soil surface. Figure 4.5 shows the penetration of the 0°C isotherm for several selected freezing tests. Penetration data of Figure 4.5 was monitored by thermocouples. Appendix B, (Table 1) summarizes the X , \sqrt{t} data plotted in Figure 4.5.

The curves shown in Figure 4.5 are bi - and trilinear and hence do not follow the relation described by equation 4.8. An average rate of penetration, α_a , is calculated for each selected test in Appendix B, (Table 1). Table 4.1 summarizes the calculated α_a values.

For each test shown in Figure 4.5, theoretical α values were calculated using equation 4.10. Unfrozen water contents (w_u) of 0 and 5% were assumed in the calculations. A sample calculation is contained in Appendix B, (Section 1). A summary of calculated α values is given in Table 4.1.

To this point, the discussion has been concerned with depth of frost penetration as determined by thermocouple measurements of the sample temperature distribution. For normally consolidated tests the penetration of the freezing front was also measured by Vernier at the end of

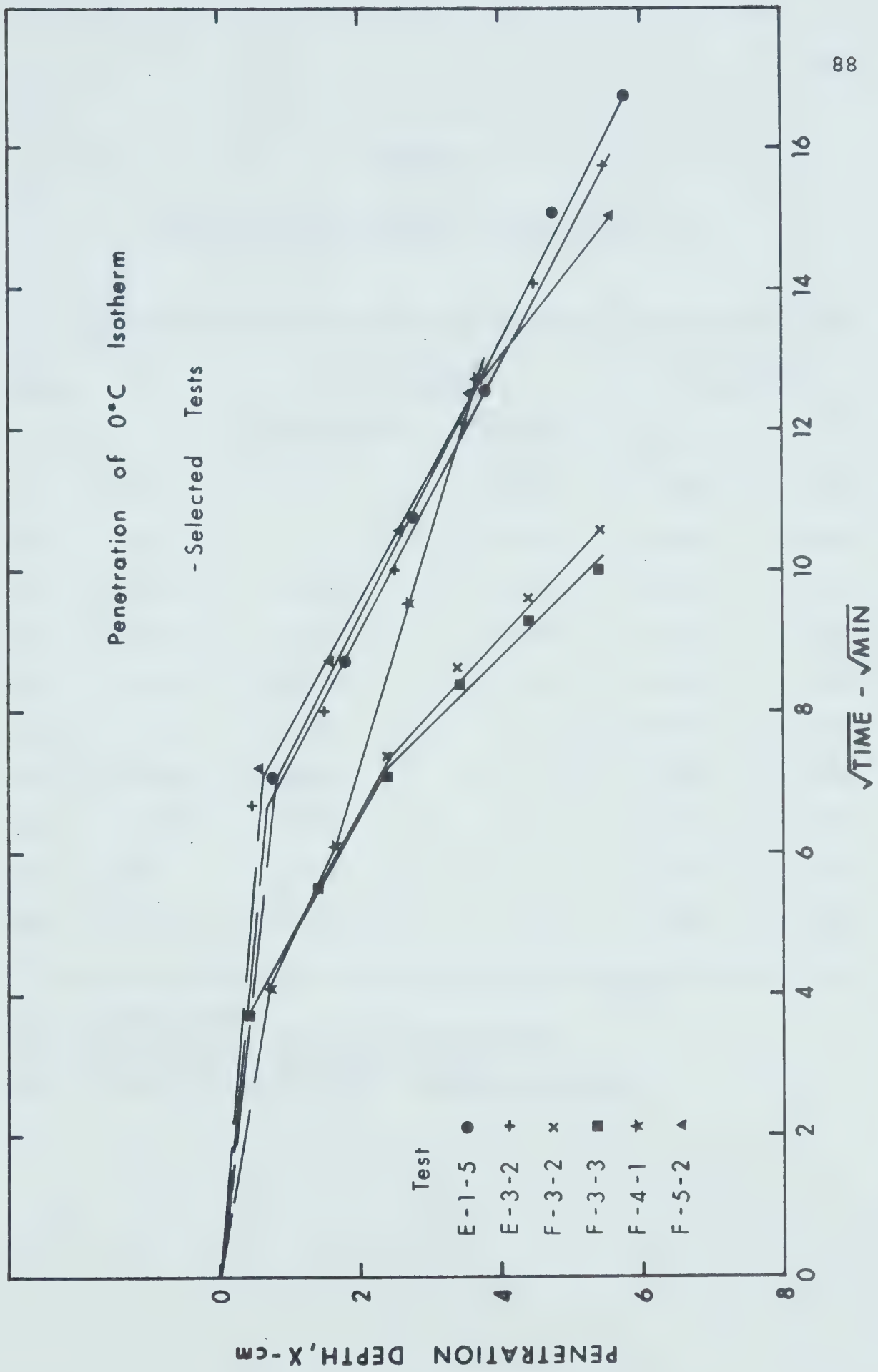


FIGURE 4.5

TABLE 4.1

Rates of Penetration of Freezing Front

Soil Type	Test	Experimental α_a [cm/ $\sqrt{\text{min}}$]		Theoretical α_a [cm/ $\sqrt{\text{min}}$]	
		Thermocouple	Measured	$w_u = 0\%$	$w_u = 5\%$
OS	D-1	-	0.323	0.220	0.226
OS	D-2	-	0.341	0.203	0.208
DS	E-1-2	0.342	0.267	0.261	0.268
DS	E-1-3	0.407	0.299	0.236	0.242
DS	E-1-4	0.376	0.271	0.233	0.239
DS*	F-1-3	0.384	-	0.233	0.239
DS*	F-1-4	0.381	-	0.232	0.239
DS*	F-1-5	0.375	-	0.226	0.232
MDS	G-7	0.378	-	0.246	0.252
MDS	G-8	0.276	-	0.247	0.253

OS - Ottawa Sand

DS - Devon Silt - normally consolidated

DS*- Devon Silt - overconsolidated

MDS - Modified Devon Silt - overconsolidated

each test. An average α value, α_a , could thus be calculated. (This method was not applicable to over-consolidated samples). A comparison of average α values determined in these two ways is presented in Figure 4.6.

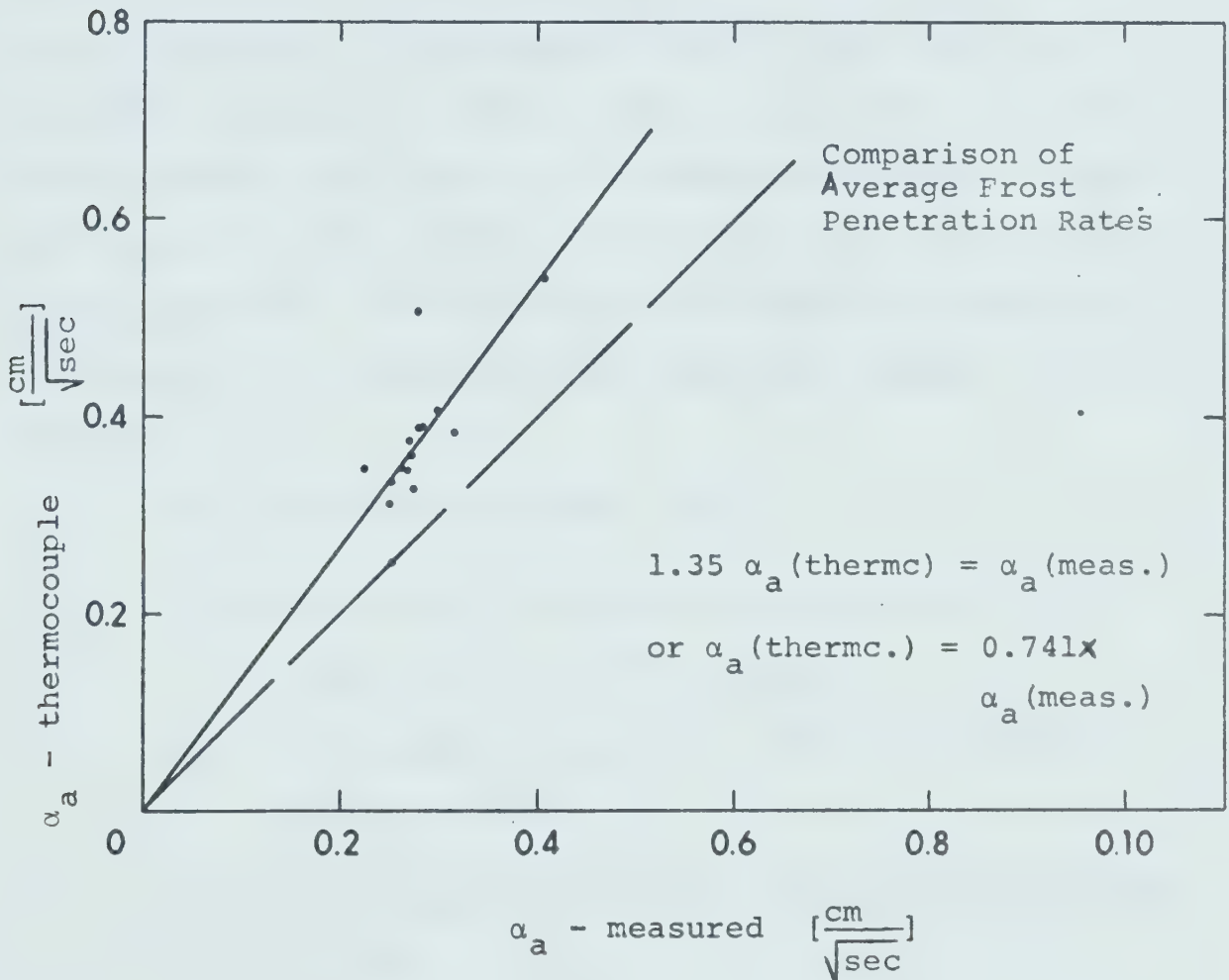


FIGURE 4.6

(2) Sample Water Balance

At any given time during the freezing test volume change of the sample is a result of the volume

change accompanying freezing of the porewater and of the volume of water sucked into or expelled from the soil sample. It was assumed that the volume change due to the freezing of the soil solids is negligible. The volume change accompanying freezing of the porewater was assumed to be equivalent to the volume of water sucked into or expelled from the soil sample, and to the volume displaced by the heaving soil surface. By knowing the depth of frost penetration and the porosity of the soil, the volume change of the porewater (in both frozen and unfrozen states) may be equated to (or balanced with) the actual change in sample volume.

As illustrated in Figure 4.7,

V_o is the volume of frozen soil defined by the depth, X , of the 0°C isotherm.

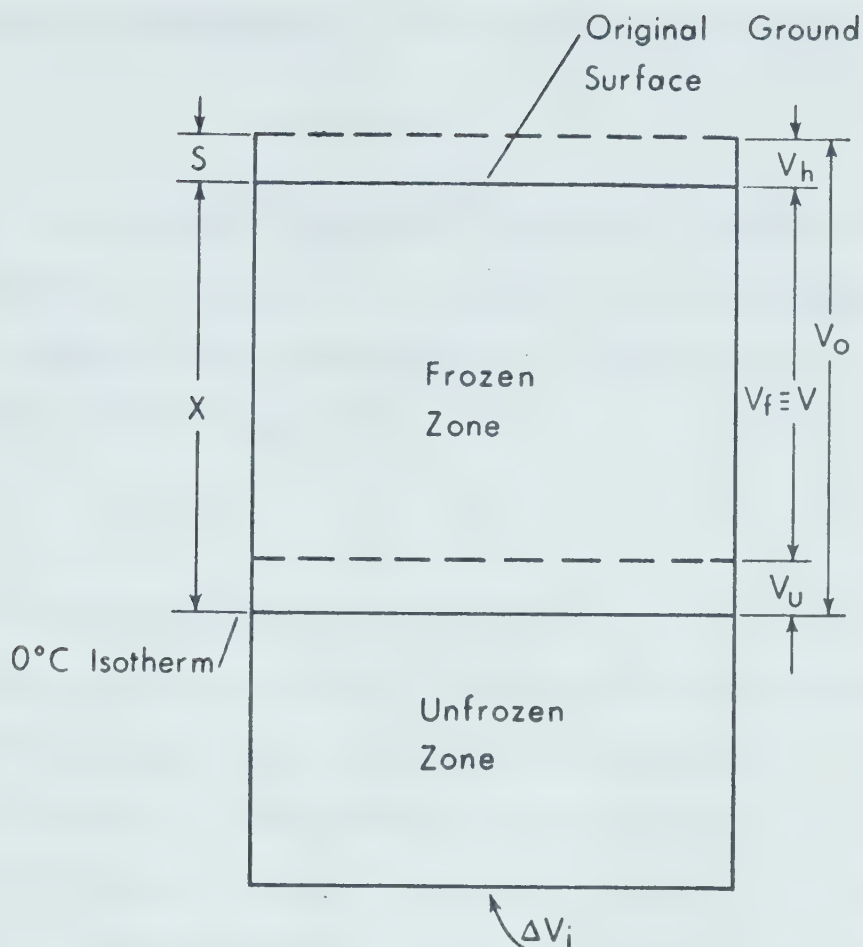
V_f is the volume portion of V_o that is actually frozen at 0°C .

V_u is the volume portion of V_o that remains unfrozen at 0°C .

V is defined as a volume of soil that is completely frozen at 0°C .

ΔV_i is a volume of water that is sucked into the soil sample during the freezing process.

V_h is the volume displaced by the heave displacement of the soil surface.



SCHEMATIC FREEZING SITUATION

FIGURE 4.7

The volume of water in the unfrozen soil zone is assumed constant throughout the freezing test and therefore is not included in the calculations. Hence we may write:

$$V_o = V_f + V_u \quad 4.14$$

where V_o , assuming $w_u = 0$, may also be written

$$V_o = 0.09 n XA \quad 4.15$$

The total volume increase of the soil sample is directly measured in terms of V_h and ΔV_i . If this volume increase is assumed to be equivalent to a known (defined) volume of frozen soil we may write:

$$0.09 n V = V_h + \Delta V_i \quad 4.16$$

By definition V is equivalent to V_f . Hence by substituting V into equation 4.14 the volume of unfrozen water in the zone of frozen soil, V_u , may be determined. V_u is usually expressed as a percentage of the weight of soil solids and is defined as the unfrozen water content of a soil (w_u).

Unfrozen water content calculations were made for several tests and the results summarized in Table 4.2. A sample calculation of w_u is given in Appendix B, (Section 2).

(3) Porewater Pressure, P_w

Porewater pressures that theoretically developed during various freezing tests were calculated using equation 2.18. The calculated P_w 's were then substituted into equation 2.5 and a theoretical K calculated. Results of these calculations together with experimental observations made during the tests are summarized in Table 4.3. A

TABLE 4.2

Unfrozen Water Content Calculated
From Sample Water Balance

Soil	Test	Unfrozen Water Content	
		Thermocouple	Measured
DS	E-1-3	7.96	5.11
DS	E-1-4	8.20	5.30
DS*	F-1-3	5.20	3.88
DS*	F-2-3	10.00	6.40
DS*	F-5-3	6.00	-
MDS	G-7	14.70	-
MDS	G-8	13.8	-

DS - Devon Silt - normally consolidated
DS* - Devon Silt - overconsolidated
MDS - Modified Devon Silt - Overconsolidated

TABLE 4.3

Observed and Theoretical Freezing Behavior

Soil Type	Test	P_i [Kg/cm ²]	Observed		Theoretical	
			K [Kg/cm ²]	Behavior	P_w [Kg/cm ²]	K [Kg/cm ²] Behavior
OS	D-1	1.04	-	Expel	+0.004	1.03 Expel
OS	D-2	1.04	-	Expel	+0.008	1.03 Expel
DS	E-1-2	0.76	1.25	Suck In	-0.31	1.07 Suck In
DS	E-1-3	1.25	1.25	O	-0.26	1.51 Expel
DS	E-1-4	1.34	1.25	Expel	-0.30	1.75 Expel
DS*	F-1-3	0.50	0.71	Suck In	-0.13	0.63 Suck In
DS*	F-1-4	0.74	0.71	Expel	-0.12	0.86 Expel
DS*	F-1-5	0.98	0.71	Expel	-0.17	1.15 Expel
MDS	G-7	2.93	2.20	Expel	-1.19	4.12 Expel
OS - Ottawa Sand DS - Devon Silt - normally consolidated						
DS* - Devon Silt - overconsolidated			MDS - Modified Devon Silt - overconsolidated			

sample calculation of P_w and K is presented in Appendix B, (Section 3).

(4) Heave Calculation

Heave was calculated for several freezing tests using equation 2.25. Results of these calculations along with observed heave values are summarized in Table 4.4. A sample calculation of heave is presented in Appendix B, (Section 4).

(5) Heave Pressures

Results of the two heave pressure tests, Tests F-5-5 and G-8, are summarized in Table 4.5. Also listed in the table is the volume change due to freezing, V_F , equal to the volume of porewater expelled plus the heave displacement volume, and the theoretical 9% volume change of the frozen soil zone, V_9 . A comparison of V_F and V_9 indicates the unfrozen water content of the soil, w_u . Theoretically for $w_u = 0$ percent V_F should equal V_9 .

TABLE 4.4

Observed and Calculated Heave

Soil Type	Test	P_i [Kg/cm ²]	Heave [cm]	
			Observed	Calculated
OS	D-1	1.04	0.040	0.200
OS	D-2	1.04	0.040	0.197
DS	E-1-2	0.76	0.152	0.232
DS	E-1-3	1.23	0.126	0.190
DS	E-1-4	1.30	0.112	0.164
DS*	F-1-3	0.50	0.114	0.200
DS*	F-1-4	0.74	0.088	0.162
DS*	F-1-5	0.98	0.061	0.202
MDS	G-7	2.93	0.038	0.163

OS - Ottawa Sand

DS - Devon Silt - normally consolidated

DS* - Devon Silt - Overconsolidated

MDS - Modified Devon Silt - Overconsolidated

TABLE 4.5

Heave Pressure Data

Test	P_i Kg/cm^2	Heave Pressure Kg/cm^2	Water Expelled $\Delta V, \text{cm}^3$	Heave S, cm	$V_F + S$ $\Delta V, \text{cm}^3$	V_9 cm^3
F-5-5	0.69	1.62	3.93	0.016	5.27	16.1
G-8	2.24	1.18	0.52	0.010	1.35	10.8

CHAPTER 5

DISCUSSION AND CONCLUSIONS

5.1 Discussion

5.1.A. Equipment

Once operational, the equipment performed satisfactorily. Reproducibility of test results, as for Tests E-1-1 and E-1-2 and Tests E-2-1 and E-2-2, was good.

The major aspect of the equipment requiring improvement is the pressure sealing system around the freezing piston. Some problems occur as a result of the sliding O-ring design. One problem is that initial pressure applied to the soil sample cannot be maintained in the sample container. When pressure is first applied to the soil sample a B value of 0.95 is usual but with time this pressure dissipates ($B = 0.85$) and remains at this lower pressure. Secondly, whenever pressure is applied to the soil sample a small portion of the soil sample is extruded upwards past the sliding O-ring. Because of this capability of the porewater to extrude past the O-ring, some drainage of the top of the sample occurs. This water at a later time may go back into the soil resulting in a higher water content in the upper areas of the soil as compared to the remainder of the sample.

This excess water affects the freezing rate of the soil and is responsible for the bi-linear penetration of the freezing front with respect to the square root of time. See Figure 4.5. Initially the rate of penetration is rather slow, as evidenced by the flat slope of the X, \sqrt{t} curve, whereas below this 'wet' zone the penetration rate is nearly twice as fast. The average of the two experimental penetration rates, however, compares favorably with the theoretical rate of penetration. The difference in freezing rates between the upper portion and the remainder of the sample does not appear to be reflected in the heave or net change in volume porewater results.

Friction occurred in three areas of the equipment but was minimal. The first location was between the freezing-piston rod and the O-ring seal. Lubrication was frequently applied to this area and any friction that developed would be minimal. Friction also developed around the sliding O-ring seal located in the freezing piston base plate. This area was also lubricated to minimize friction. Some friction may also have developed in the sample container due to the movement of the soil mass. To minimize this friction however, a latex membrane, encasing the soil sample, was separated from the sample container by a layer of grease. Pressures as low as 2 pounds per square inch were sufficient to extrude a frozen soil sample (plus membrane) from the sample container.

The author believes that errors in experimental results due to the pressure seal at the freezing piston base plate and due to friction were small and likely did not influence the freezing behavior of the sample significantly.

5.1.B. Testing Procedure

The application and maintainance of a step temperature on the soil surface was effectively achieved by the constant temperature bath/circulator apparatus used in the testing program. This method afforded excellent control over the freezing process, though not the freezing rate, as recommended by Penner (1972). The freezing rate varied from sample to sample depending on the water content, density and of course step temperature. The actual step temperatures used were chosen arbitrarily on the basis of practicality. The experimental step temperatures agreed fairly well with temperatures that were reported in the literature. Typical temperatures reported in the literature were -2 to -12°C by Kaplar (1971) and -17°C by Sutherland and Gaskin (1973).

Although the length of the experimental freezing tests were short, the tests proved capable of demonstrating the freezing behavior of a soil. It was found that as the tests progressed the freezing behavior trend that was established in the first hour of testing continued for the

duration of the test and hence indefinitely depending on the sample height. The short term tests were thus justified.

The freezing tests, varied from 120 minutes to 360 minutes, were usually 160 to 200 minutes in length. The length of freezing tests were thus in the order of 1 hour to 10 or more hours shorter than tests reported in the literature by people and agencies such as Penner (1972), Williams (1967), and the Corps of Engineers, U.S. Army (see Townsend and Csathy 1963). For each freezing test the results recorded at 160 minutes (after application of the step temperature) were recorded and used for the comparison of the various freezing tests. The time, 160 minutes, was chosen arbitrarily by the author since the freezing front was located in the middle third of the sample (height) and any effects due to the proximity of the bottom or top of the sample were minimal.

If the tests were not terminated at 160 minutes they were terminated when the freezing front was 1.6 centimeters from the base of the sample. The freezing front was not allowed to penetrate any deeper to prevent damaging the base transducer. If this depth of penetration was reached in less than 160 minutes, as in the case of the large step temperature, the test results were extrapolated to 160 minutes.

As shown on the data summary tables the initial water content and void ratio varied for each test. This variation occurred as a result of the sample preparation procedure. A slurried sample was prepared at a water content of 45% (for Devon silt) and then placed in the sample container which was partly filled with water. The variations in initial water contents listed arises from the different amounts of water absorbed by the slurry prior to testing. The author feels that these variations in water content and void ratio did not affect the freezing test results significantly and is only of interest in terms of sample preparation control.

5.1.C. Experimental Results

Experimental results indicate that the freezing behavior of a soil can be described in terms of net change in sample porewater volume, porewater pressure and heave. Results also indicate that soil type, grain size, grain size distribution, permeability, stress history, overburden pressure and step temperature influence the freezing behavior of a soil.

The difference in the freezing behavior of coarse and fine-grained soils is clearly shown in Figure 4.1. The Ottawa sand data indicate that under all freezing test conditions porewater is expelled. The freezing behavior of Devon silt however depended on the test conditions. The

Devon silt expelled water under certain effective stress conditions, roughly 15 to 20% (by volume) of that of the Ottawa sand. This difference in freezing behavior can be attributed to differences in shape and surface area of the soil particles, and permeability as determined by grain size and grain size distribution.

The freezing behavior of Devon silt shown in Figure 4.1 should be noted. The results show that the freezing behavior of Devon silt is determined primarily by the grain size, as implied by the capillary theory, but is strongly dependent on the applied effective stress during freezing. As illustrated in Figure 4.1 Devon silt may behave in three different ways during freezing tests: (1) increase total sample porewater volume, (2) decrease total sample porewater volume, or (3) maintain the total sample porewater volume. These freeze test data further imply that a linear relation between change in total sample porewater volume and effective stress exists, and that the freezing behavior is a continuous phenomenon with a smooth transition from one behavior mode to another.

The results show that at a particular pressure, P_o , there is no net change in total volume of sample porewater. Under these freezing conditions it is likely that all volume change, due to the 9 per cent volume increase at phase transformation, be expressed in terms of heave by the soil

sample. At pressures less than P_o , water is sucked into the sample by the freezing front, increasing the total sample porewater volume. This action, if allowed to continue under the same conditions, could lead to ice segregation and lensing. At pressures greater than P_o , porewater is expelled from the sample thereby decreasing the total porewater volume. Under these conditions in situ freezing results; ice segregation and lensing can occur.

The preceding results are consistent with the Theory of Freezing Soils proposed in Section 2.2 and predicted by equation 2.5. When no net change in sample porewater occurs, the porewater pressure P_w , is equal to zero, or P_w of equation 2.5 and of the freezing sample is equal to zero. The effective pressure, P_o , of Figure 4.1 then is equal to P_i which in this case is also equal to K of equation 2.5. Thus terms of K and P_o are interchangeable.

At $P_w = 0$ equation 2.5 and the accompanying theory predict that water would be sucked into the soil sample and ice lensing would result. This phenomenon was not verified experimentally and warrants further study.

It should be noted that in all tests shown in Figure 4.1 and in the testing program the freezing plane was continually moving through the soil. At first this

appears inconsistent with the theory and observations reported in the literature that ice lensing or the sucking in of water during freezing occurs only when the freezing front is stationary. However, the apparent inconsistency is likely due only to the scale of the sample height, step temperature and freezing time used in the freezing tests. The freezing front in these tests is advancing because the rate of heat removal is greater than the rate of heat supply. For a similar sample of infinite height and subjected to the same step temperature, the freezing front would advance and suck in water until the heat exchange and/or pressure conditions changed significantly. This freezing phenomenon is defined as 'imperfect segregation' by Arakawa (1966). As the freezing front advanced the rate of heat removal would decrease in proportion to the depth until the rate of heat removal was equal to the rate of heat supplied. The freezing front would then become stationary. At any time during this advance of the freezing front the sample would continue to suck in water as long as the overburden pressure P_i was less than P_o . At this time the freezing front would become stationary and continue to suck in water, assuming the difference in pressure $P_i - P_w$ of equation 2.5 was still less than (or equal) to K .

Equating equations 2.2 and 2.5 we see that K may be calculated in terms of:

$$K = \frac{2\sigma_i w}{r_{iw}} \quad 5.1$$

Sutherland and Gaskin (1973) suggest using:

$$\sigma_{iw} = 0.03 \text{ N/M} = 3.06 \times 10^{-5} \text{ Kg/cm}$$

$$r/r_i = 5.4 \quad 5.2$$

where σ_{iw} - stress across the ice-water interface

r_i - radius of the ice crystal interface

r - radius of the soil pore = $0.5 (D_{10})$

From Appendix A, D_{10} of Devon silt is 0.00016 mm.

Substitution of r into equation 5.2, and equation 5.2 into equation 5.1 a value of 41 kg/cm^2 is determined for K .

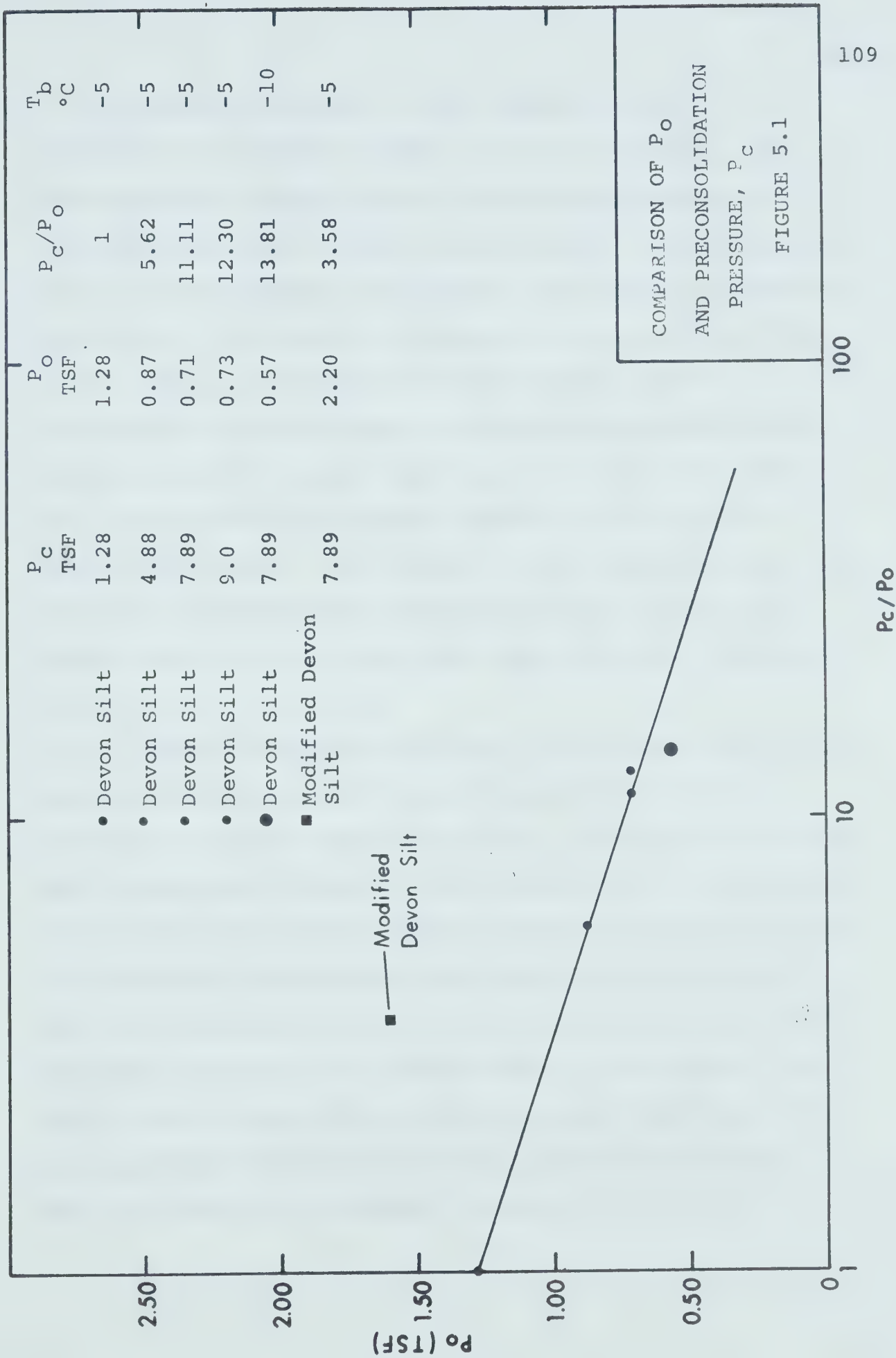
The experimental K value for normally consolidated Devon silt is 1.30 kg/cm^2 .

Further to Figure 4.1 it should be noted that the linear relation between net change in sample porewater volume, ΔV , and effective stress, σ' , exhibited by Devon silt also holds true for the finer-grained modified Devon silt. The slope of the $\Delta V - \sigma'$ curve of the modified Devon silt is less than, and the effective stress intercept, P_o , is greater than the corresponding values for Devon silt. It appears then from Figure 4.1 that the slope of the $\Delta V - \sigma'$ curve and the P_o intercept are unique characteristics of a soil type. It would also follow that the characteristics of the $\Delta V - \sigma'$ plot are dependent on soil type, grain size, grain size distribution and percentage of fines. Again

the role of soil permeability should be noted.

It is also evident from the test data that the freezing behavior of a soil is dependent on the stress history of that soil. From Figure 4.3 it can be seen that the slope of the $\Delta V - \sigma'$ curve increases, and the P_o intercept decreases as a result of overconsolidation of the Devon silt. The plot also shows that the slope of the $\Delta V - \sigma'$ curve increases and the P_o intercept decreases with an increasing degree of consolidation. The $\Delta V - \sigma'$ curve plotted for Test Series F-5 where the preconsolidation pressure, P_c , equals 8.79 Kg/cm^2 is inconsistent with the above observations. This inconsistency is likely due to experimental error.

Replotting the results shown on Figure 4.3 indicates that P_o is inversely proportional to the \log_{10} of the ratio of P_c/P_o where P_c is the preconsolidation pressure. It can be seen from Figure 5.1 that once the P_o of a soil type is known the influence of stress history on that P_o can be determined. Results gained from tests run on Devon silt at an increased step temperature and tests run on modified Devon silt do not correspond to the Devon silt data points. This would indicate that the $P_o - \log_{10} P_c/P_o$ curve is unique for a soil type being frozen under certain temperature freezing conditions. Figure 5.1 has many practical implications.



Further to Figure 4.3 the effects of the difference in testing procedure should be examined. For the test series run on normally consolidated samples a new sample was used for each freezing test. For the series run on the overconsolidated samples, one sample was used for each series, and therefore subjected to several freeze-thaw cycles. As shown by the test result curves the $\Delta V - \sigma'$ relationship is linear once the sample had been subjected to one freeze-thaw cycle. However, the slope of the same curve is significantly steeper between the 1st and 2nd freeze-thaw cycles. This change in slope indicates that the effect of the freeze-thaw consolidation of a soil is much greater for the first freeze-thaw cycle than for subsequent cycles.

Hence a comparison of the P_o of normally consolidated samples determined on the initial freezing of a sample should not be strictly made with the P_o of an overconsolidated sample subjected to several freeze-thaw cycles. Consequently the normally consolidated samples should have been subjected to at least one freeze-thaw cycle prior to determining a P_o value for comparison with the P_o of overconsolidated samples. The author recognizes this shortcoming in the results. The author also believes that if the more valid procedure for normally consolidated soils had been followed the result would have been a P_o intercept occurring at a larger

effective stress and a flatter slope on the $\Delta V - \sigma'$ curve. This prediction is based on the shape of the lower portion as compared to the initial portion of the overconsolidated $\Delta V - \sigma'$ curves. The comparison of normally and overconsolidated test result data shown in Figure 4.3 is nonetheless useful.

Freezing tests conducted under close system drainage conditions were run to determine if the freezing behavior of a soil was affected by the drainage boundary conditions. Closed system freezing tests are also a practical alternate testing procedure. Test data for normally consolidated and overconsolidated Devon silt samples are shown in Figure 4.2. Test results for the normally consolidated samples are somewhat erratic and hence may be questioned. Data for the overconsolidated samples are more consistent. The difference between the quality of results is believed due to the higher compressibility of the normally consolidated samples.

The trends of the closed system freeze results are consistent with open system freeze tests discussed earlier. The results show that porewater pressures are equal to zero at a particular effective stress, P_o ; at stresses greater than P_o , the porewater pressure is positive (or porewater would be expelled from the sample); and at stresses less than P_o the porewater pressures are negative (or water

would be sucked into the soil sample). The P_o values of closed system freezing tests do not favorably compare with those of open system freezing tests. Table 5.1 summarizes the experimental P_o values.

TABLE 5.1

Experimental P_o Values

Stress History	P_o for Freezing Test [Kg/cm^2]	
	Open Drainage	Closed Drainage
Normally Consolidated	1.28	1.70
Over Consolidated $P_o = 7.70 \text{ Kg}/\text{cm}^2$	0.71	0.55

As can be seen in Table 5.1 the freezing behavior of Devon silt appears to be dependent on the drainage boundary conditions of the freezing test.

During the progress of Tests E-3-1 and E-3-2 the drainage boundary condition was changed to further check the influence of the drainage boundary condition on the freezing behavior. Results of these tests were inconclusive. The freezing behavior of the Devon silt was unaffected by the

change in drainage boundary conditions in Test E-3-2. However, the freezing behavior of Devon silt in Test E-3-1 was completely reversed. In Test E-3-1 the sample expelled water under open system drainage, showed a steadily decreasing porewater pressure under closed system drainage, and then sucked in water when the drainage system was opened again.

Because of the inconclusiveness of the closed drainage system freezing tests, this type of testing was abandoned and efforts were concentrated on open drainage freeze tests. Further work on closed system freezing tests is warranted.

As illustrated in Figure 4.4 the freezing behavior of Devon silt is dependent on the step temperature. When the step temperature was doubled the same freezing behavior, as discussed earlier, was followed. The slope of $\Delta V - \sigma'$ curve was steeper, however, and P_o was less than the corresponding curve for a step temperature of -5°C .

Devon silt does not completely freeze at 0°C . The unfrozen water content of Devon silt was determined in two ways: by measurement of the advance of the 0°C isotherm using thermocouples and by vernier, and secondly by determining a sample porewater balance and back calculating the unfrozen water content. Calculated unfrozen water contents ranged from 4 to 6 percent. These values compared favorably with

an unfrozen water content of 5 percent for a comparable silt at the same freezing or step temperature by Anderson, Tice and McKim (1973). Because of this unfrozen water the total change in sample volume during freezing was always less than the 9 percent volume change of water at nucleation.

Based on the general agreement between predicted and observed freezing behavior, the porewater pressure at the freezing front can be estimated from the net supply and removal of heat from the soil sample. All calculated porewater pressures listed in Table 4.3 were determined by equation 2.18. Substitution of the calculated porewater pressures into equation 2.5 enabled the author to predict freezing behavior. The results of these calculations indicate that equations 2.5 and 2.16 are useful. These equations can predict the freezing behavior of a soil if the step temperature, water content, permeability, thermal properties, dry density, water table conditions and the K value of the soil are known.

With the exception of two tests all samples 'heaved' during the freezing process. The two samples that did not heave were tested under restrained heave conditions. A small amount of vertical displacement in these two tests did occur however due to compliance. The vertical displacement or 'heave' measured during the remainder of the

freezing tests was likely due to the 9 percent volume increase at phase transformation. Tests in which water was being sucked in would develop segregated ice and ice-lenses if the tests were allowed to continue for a sufficient period of time. The vertical displacement in this case would correctly be termed heave as is done in the literature. The samples which expelled porewater during freezing tests would displace vertically little more than recorded. These samples would not heave. As expected the greatest displacement occurred under the smallest overburden pressures. These results indicate that heave is merely a volumetric response along with the expulsion/attraction of water to the freezing of the soil porewater in conjunction with the applied boundary conditions. The results imply that the magnitude of heave is not unique to the particular soil sample tested.

Calculation of vertical displacement, based on the volume increase at phase transformation of the amount of porewater frozen during the freezing process, was attempted. Calculated results were in poor agreement with the observed heave. The reason for this discrepancy is likely because the overburden loading was not accounted for in the calculations.

The 'heave' pressure results are summarized in Table 4.5. The summary shows that both samples expelled

water during the freezing tests or in other words neither sample was developing ice lenses during the freezing tests. Therefore the measured pressures were a result of the 9 percent volume increase at phase transformation. For the sake of clarity these pressures will be referred to as transformation pressures.

Since the applied overburden pressures used in both tests were such that no expulsion of porewater would occur during freezing, the transformation pressures were responsible for the expulsion of porewater. This can be seen from the test results; the largest volume of porewater expelled corresponded with the largest transformation pressure measured. The results also show that the largest transformation pressure was developed by the sample with the smallest overburden pressure. Therefore heave pressure depends on overburden pressure. Contrary to Gold (1957), the 'coarser' Devon silt sample generated larger transformation pressures than the finer modified Devon silt sample. This is likely due to a higher unfrozen water content and the lower permeability of the modified Devon silt.

Movement of the freezing piston was also recorded and summarized in Table 4.5. This vertical movement is a measure of the compliance of the rigid frame. Any upward or compliant movement of the rigid frame resulted in lower transformation pressures being measured. This reduction

in pressure undoubtedly happened in both tests but the effect of this reduction appears to be minor in comparison to any change in overburden pressure.

In summary, heave pressure is pressure developed when vertical displacement is restrained due to the generation of transformation pressures plus pressures resulting from the development of ice lenses (also called heave pressure). From the test results quoted it appears that heave pressure is dependent on soil type, permeability, grain size, and grain size distribution, and overburden pressure.

Based on the above summary, results, and discussion the following theory on the mechanism of heave pressure is outlined.

Whenever the soil surface is restrained during an open system drainage test the ice crystals displace the soil porewater. These ice crystals may occur as an ice lens or individually as after crystallization. The resistance to flow that the porewater encounters is the basis of heave pressure. Bounds may then be set on the flow resistance, in terms of pressure, of various soils: (1) in coarse grained soils with a high permeability the resistance to flow would be minimal, (2) in a fine grained soil with a very low permeability near infinite pressures are required to initiate flow.

Therefore in the case of the granular soil, as the soil freezes the ice would fill the voids and the displaced porewater would be able to move freely throughout and even leave the soil sample. The pressures generated on the soil surface would be negligible as would be the vertical displacement. For the fine grained soil however, the porewater being displaced by the growing ice crystals (or lenses) would encounter significant resistance to flow. Initially no flow would occur but as the ice crystals enlarged increased pressures in the voids would result. When the pressure in the void became larger than the soils' resistance to flow the porewater would move out of that pore space. The pressure generated to cause this flow could be measured on the soil surface and would be defined as heave pressure.

In summary, heave pressure would be measure of the degree of the free drainage capability of a soil system. In the field then if a soil permitted free drainage, open system drainage conditions would be approached; whereas if the soil permitted practically no flow then closed system drainage conditions would be approached.

5.2. Conclusions

Experimental results indicate that the short term freezing tests conducted during the testing program proved to be an effective procedure in determining freezing behavior of a soil. Therefore the running of prolonged freezing does

not appear necessary. The application and maintainance of a step temperature on the soil surface, as opposed to varying the surface temperature to maintain a constant rate of penetration of the freezing front, is a very effective method of maintaining experimental control over freezing tests. Application of a step temperature is also a simpler and more practical method of freezing samples.

For the soils tested, the running of open system drainage tests, measuring net change in sample porewater volume and heave, and closed system drainage tests measuring porewater pressure and heave, proved to be effective methods of determining the freezing behavior of a soil. The diversity of experimental results obtained and of testing boundary conditions used show that the freezing behavior of a soil cannot be accurately predicted on the basis of one soil property, i.e. grain size, or one freezing characteristic, i.e. heave pressure. Therefore in describing the freezing behavior of a soil the boundary conditions such as step temperature, drainage and pressure conditions, and soil properties should be listed. Care should be taken when comparing data obtained from open and closed system freezing tests as experimental results indicate the freezing behavior of a soil is influenced by the testing boundary conditions. Further study of these affects is needed.

Soil properties that affect the freezing behavior of a soil are: soil type (specific surface area), grain size,

grain size distribution, density, porosity, water content and permeability. Test results also demonstrated that the freezing behavior of a soil is dependent on external factors such as: overburden pressure, stress history, drainage boundary conditions and step temperature. The relative importance of these factors for the soil types tested is as follows:

Cohesionless soils used with no fines, expel water upon freezing. This phenomenon appears insensitive to changes in overburden pressure, porosity or dry density.

The freezing behavior of a fine grained soil (silt) is not only dependent on soil properties but is also dependent on external factors. The freezing behavior exhibited by the silt varied from sucking in to expulsion of porewater in open system freezing tests.

A definite relationship was shown to exist, for the soils tested, between the net change in sample porewater volume, ΔV , and effective stress, σ' . At a particular stress level, P_0 , no net change in the sample porewater volume occurred. (This however was not verified experimentally). At stresses less than P_0 water is sucked into the sample which would result in ice segregation, lensing and significant heaving if allowed to continue indefinitely. At stresses greater than P_0 , porewater is expelled during freezing resulting in situ freezing and insignificant heaving if allowed to continue

indefinitely. The test results indicated that the freezing behavior of the Devon silt was a continuous phenomenon with a smooth transition from one type of behavior to another.

Results of tests run on the modified silt further indicated that the $\Delta V - \sigma'$ relation was unique to a particular soil type and that the slope of the curve and the P_o intercept is influenced by grain size distribution and permeability. It was shown that the slope of the $\Delta V - \sigma'$ curve decreases and that the P_o intercept increases as the percentage of fines in a soil increases, or in other words as the permeability of a soil decreases.

Besides being stress dependent the freezing behavior of the silt was also shown to be dependent on stress history. Overconsolidation of the silt increased the slope of the $\Delta V - \sigma'$ curve and decreased the P_o intercept. Furthermore it was shown that the slope of the $\Delta V - \sigma'$ increased and the P_o intercept decreased as the degree of overconsolidation increased.

When the 'stress history' data were replotted it was found that P_o was inversely proportional to the $\log_{10} (P_c/P_o)$ where P_c is the preconsolidation pressure. The data indicated that this curve was also unique for a soil type and was dependent on step temperature. This relation between P_o and the $\log_{10} (P_c/P_o)$ has important practical implications, i.e. in estimating the depth of burial (overburden) required to prevent frost heaving of a pipeline.

Test result data also demonstrate that the freezing behavior of a fine grained soil is dependent on step temperature. It is shown that the slope of the $\Delta V - \sigma'$ curve increased and the P_0 intercept decreased when the step temperature was increased.

Closed system freezing tests on the silt demonstrated that freezing behavior could also be monitored in terms of porewater pressures at the freezing front. Freezing behavior of the silt exhibited the same trends but did not duplicate the behavior shown in the open system tests. Based on the experimental data it appears that freezing conditions are not identical under open and closed drainage conditions.

The validity of the assumptions and theory of freezing soils described earlier was demonstrated by the experimental results. Theoretical predictions of freezing soil behavior developed in terms of the relative heat flow into and out of the soil sample and of the stress difference across the ice-water interface were verified by experimental results.

Little success was achieved in predicting the heave of a soil. This is likely due to the limitations of the theory and due to the influence of the unfrozen water content and the omission of overburden stress in the development of the heave equations. The test results indicated that heave was not a property of a freezing soil but is a response of a freezing soil dependent on the overburden pressure and

drainage boundary conditions.

Similarly the test data showed that heave pressure is not a soil property but is also a response to the restrained displacement, drainage and overburden boundary conditions. The amount of porewater expelled during the heave pressure tests appeared to be linked to the heave pressure measured.

The experimental data demonstrated the diversity of freezing behaviors that a soil (fine grained) can exhibit depending on the boundary conditions. The experimental data also showed that for the soils used the freezing behavior of granular soils does not vary within the same limits as the fine grained soils. This evidence clearly indicates that the present frost susceptibility criteria, based on grain size, is inadequate and needs revision. It was clearly demonstrated that a fine grained soil cannot be (in absolute terms) classed as frost or non-frost susceptible. The freezing behavior of a soil is dependent on many factors and in order to classify the degree of frost susceptibility of a soil these factors must be dealt with. A new frost susceptibility criteria should set definite limits on freezing soil behavior in terms of soil properties, drainage, temperature and applied stress boundary conditions.

REFERENCES

LIST OF REFERENCES

- Aitken, G. W., 1963. Reduction of Frost Heave by Surcharge Loading. CRREL Tech. Rept. 184, Hanover, New Hampshire.
- Anderson, D. M., 1967. "Ice Nucleation and the Substrate-Ice Interface." Nature, Vol. 216, pp. 563-566.
- Anderson, D. M., 1968. "Undercooling, Freezing Point Depression and Ice Nucleation of Soil Water." Israel Journal of Chemistry, Vol. 6, pp. 349-355.
- Anderson, D. M. and Morgenstern, N.R., 1973. "Physics, Chemistry and Mechanics of Frozen Ground." Proc. 2nd. Int. Permafrost Conf., Yakuskt, in press.
- Anderson, D. M., Tice, A. R. and McKim, H.L., 1973. "The Unfrozen Water in Frozen Soils." Proc. 2nd. Int. Permafrost Conf., Yakuskt, in press.
- Arakawa, K., 1966. "Theoretical Studies in Ice Segregation in Soil." J. Glaciology, Vol. 6, pp. 255-260.
- Balduzzi, F., 1959. "Experimental Investigations of Soil Freezing" (in German). Translated by Sinclair. N.R.C., TT 912, 1960.
- Beskow, G., 1935. "Soil Freezing and Frost Heaving." Swedish Geol. Soc. Ser. C26th Year Book, No. 3. Translation by Osterberg, Evanston, Illinois, 1947.
- Corte, E., 1962. "The Frost Behavior of Soils II Horizontal Sorting." Highway Research Board, Bull. 331, pp. 46.
- Csathy, T. I. and Townsend, D. L., 1962. "Pore size and Field Performance of Soils." Highway Research Board, Bull. 331.
- Dillon, H. B. and Andersland, O. B., 1966. "Predicting Unfrozen Water Contents in Frozen Soil." Canadian Geotechnical Journal, Vol. 3, No. 2, pp. 53-60.

- Everett, D. H. and Haynes, J. M., 1965. "Capillary Properties of Some Model Pore Systems With Reference to Frost Damage." Rilem Bull., New Series, 27, pp. 28-31.
- Gold, L. W., 1957. "A Possible Force Mechanism Associated With Freezing of Water in Porous Materials," Highway Research Board, Bull. 168, pp. 65.
- Glasstone, S. and Lewis, D., 1964. Elements of Physical Chemistry, 2nd Ed. Toronto, Ont.: Van Nostrand Co., Inc.
- Haley, J. F., 1953. "Cold Room Studies of Frost Action in Soils, a Progress Report." Highway Research Board. Spec. Rept. No. 2.
- Hoekstra, P., 1969. "Water Movement and Freezing Pressures." Soil. Sci. Soc. Amer. Proc. Vol. 33, pp. 512-518.
- Hoekstra, P., Chamberlain, E. and Frate, A., 1965. Frost Heaving Pressures. CRREL Res. Rept. 176. Hanover, New Hampshire.
- Hoekstra, P. and Keune, R., 1967. "Pressure Effects on the Conductance of Frozen Montmorillonite Suspensions." in Clays and Clay Minerals, Vol. 15, pp. 215-225, New York: Pergamon Press.
- Jackson, K. A. and Chalmers, B., 1958. "Freezing of Liquids in Porous Media with Special Reference to Frost Heave in Soils." J. Applied Physics, Vol. 29, No. 9, pp. 1178.
- Jackson, K. A., Uhlmann, D. R. and Chalmers, B., 1966. "Frost Heave in Soils." J. Applied Physics, Vol. 37, No. 2, pp. 848.
- Kaplar, C. W., 1962. "Laboratory Evaluation of Frost Heave Characteristics of a Slag-Flyash-lime Base Course Mixture." Highway Research Board, Bull. 331.
- Kaplar, C. W., 1970. "Phenomenon and Mechanism of Frost Heaving." Highway Research Board, Rec. 304.
- Kaplar, C. W., 1971. Experiments to Simplify Frost Susceptibility Testing of Soils. CRREL Tech. Rept. 223.
- Kinosita, S., 1967. "Heaving Force of Frozen Soils." In Physics of Snow and Ice (Ed. E. H. Oura), Hokkaido University, pp. 1345-1360.

- Linnell, K. A., 1959. "Factor of Soil and Material Type in Frost Action." Highway Research Board, Bull. 225.
- Mackay, J. R., 1972. "The World of Underground Ice." Annals of the Assoc. of Amer. Geographers, Vol. 62, pg. 1-22.
- MaGaw, R., 1971. "Frost Heaving versus Depth to Water Table." Highway Research Board, Rec. 393.
- Martin, R. T., 1959. "Rhythmic Ice Banding in Soil." Highway Research Board. Bull. 218, pg. 11-24.
- McRoberts, E., 1972. Personnal Communication.
- Neresova, Z. A., 1963. "Unfrozen Water in Frozen Soils." Proc. 1st. Int. Permafrost Conf., pg. 172-176.
- Miller, R. D., Baker, J. H. and Kolaian, J. H., 1960. "Particle Size, Overburden Pressure, Porewater Pressure and Freezing Temperature of Ice Lenses in Soil." Trans. 7th Int. Cong. Soil Science, 1, pg. 122-128.
- Nixon, J. F., 1972. Personnal Communication.
- Osler, J. C., 1967. "Influence of Depth of Frost Penetration on Frost Susceptibility of Soils." Can. Geotech. J., Vol. 4., No. 3, pg. 334-346.
- Palmer, A. C., 1967. "Ice Lensing, Thermal Diffusion and Water Migration in Freezing Soil." J. of Glaciology, Vol. 6, No. 47, pg. 681.
- Penner, E., 1957. "Soil Moisture Tension and Ice Segregation." Highway Research Board, Bull. 168, pg. 50.
- Penner, E., 1958. "Pressures Developed in a Porous Granular System as a Result of Ice Segregation." Highway Research Board., Spec. Rept. 40, pg. 191-199.
- Penner, E., 1966. "Pressures Developed During the Unidirectional Freezing of Water-Saturated Porous Materials." Conf. on Physics of Snow and Ice, Sapporo, Japan, pg. 1401, Part 2.
- Penner, E., 1967. "Heaving Pressure in Soils During Unidirectional Freezing." Can. Geot. J., Vol. IV, No. 4, pg. 398.

- Penner, E., 1968. "Particle Size as a Basis for Predicting Frost Action in Soils." Soils and Foundations, Vol. Vlll, Dec. No. 4, pg. 21.
- Penner, E., 1970. "Frost Heaving Forces in Leda Clay," Can. Geot. J. Vol. 7, pg. 8.
- Penner, E., 1971. "Heave and Heaving Pressures in Frozen Soils, Discussion." Can. Geot. J., Vol. 8, pg. 499.
- Penner, E., 1972. "Influence of Freezing Rate on Frost Heaving." Highway Research Board, Rec. 393, pg. 56-64.
- Sutherland, H. B. and Gaskin, P. N., 1973. "Pore Water and Heaving Pressures in Partially Frozen Soils." Proc. 2nd. Int. Permafrost Conf., Yakuskt, in press.
- Taber, S., 1929. "Frost Heaving." J. of Geology, Vol. 37, pg. 428.
- Townsend, D. L., and Csathy, T. I., 1963. Soil Type in Relation to Frost Action. Queens University, Kingston, Ontario.
- Williams, P. J., 1964. "Specific Heat and Apparent Specific Heat of Frozen Soils." Geotechnique, Vol. 14, No. 2, pg. 133-142.
- Williams, P. J., 1966. "Pore Pressures at a Penetrating Frost Line and Their Prediction." Geotechnique, Vol. 16, pg. 187-208.
- Williams, P. J., 1967. Properties and Behavior of Freezing Soils. Norwegian Geotechnical Inst., Publication No. 72.
- Wissa, A. E. Z. and Martin R. T., 1968. Behavior of Soils Under Flexible Pavements: Development of Rapid Frost Susceptibility Tests. Massachusetts Institute of Technology Res. Rept. R68-77, Soils Publ 224.
- Yong, R. N. and Osler, J. C., 1971. "Heave and Heaving Pressures in Frozen Soils." Can. Geot. J., Vol. 8, May 1971, pg. 272.

APPENDICES

APPENDIX A
SUMMARY OF SOIL PROPERTIES

APPENDIX A

OTTAWA SAND

Specific Gravity		2.67
γ Dense *	gm/cm ³	1.76
γ Loose *	gm/cm ³	1.54
% Passing	P ₂₀₀	0%
D ₁₀	mm	0.35
Coefficient of Uniformity, C _u , (D ₆₀ /D ₁₀)		1.71

DEVON SILT

Specific Gravity		2.68
Liquid Limit		30.2%
Plastic Limit		22.5%
% Passing P ₂₀₀		83%
D ₁₀ mm		0.00016
Coefficient of Uniformity, C _u		238

MODIFIED DEVON SILT

Specific Gravity	2.70
Liquid Limit	36.0%
Plastic Limit	20.9%
% Passing P_{200}	94
D_{60} mm	0.03
Coefficient of Uniformity, C_u	353

*Source: Personal Communication - H. K. Mittal

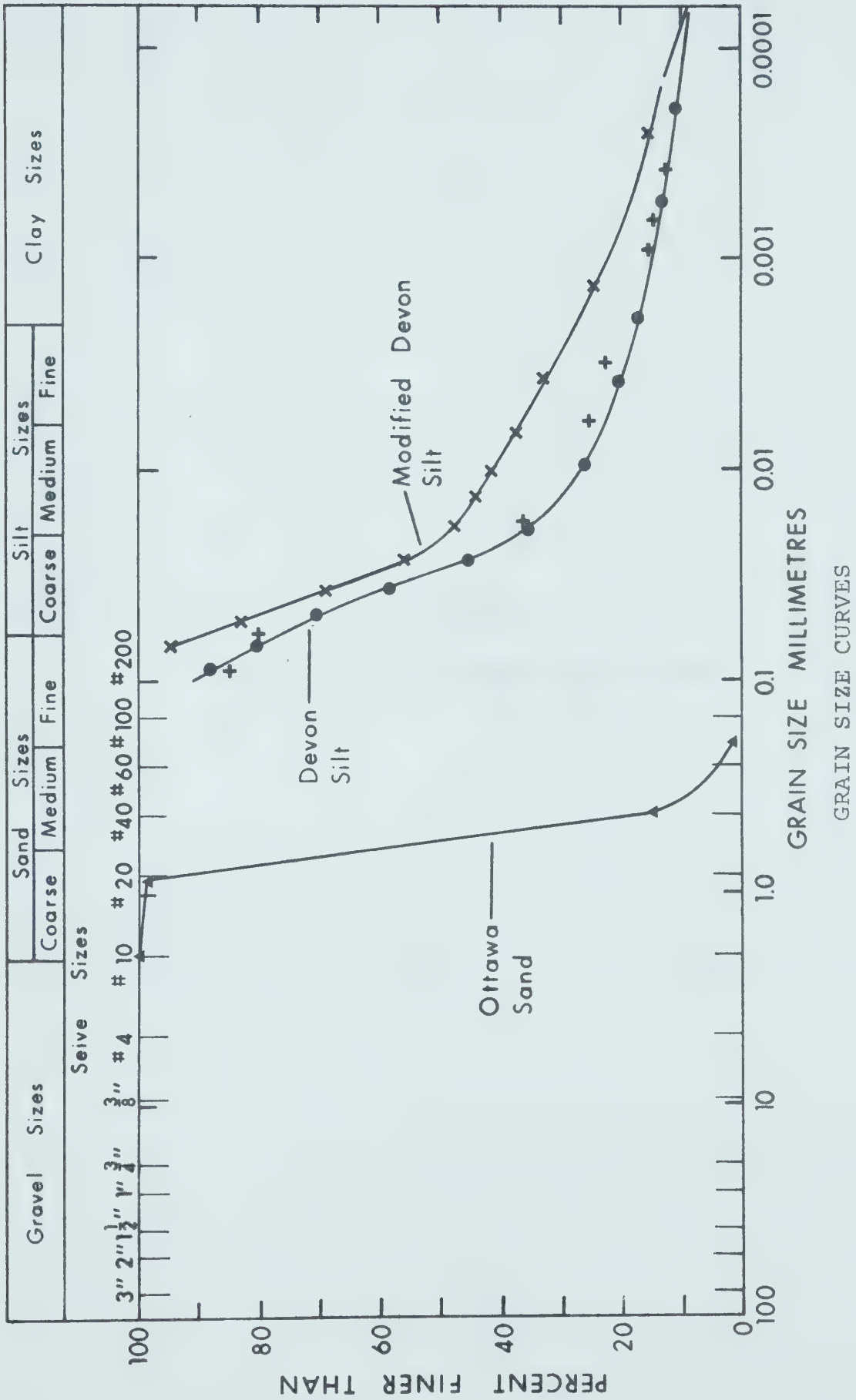


FIGURE A-1

APPENDIX B
TYPICAL FREEZING TEST CALCULATIONS

APPENDIX B

TABLE 1

Summary of Selected 0°C Isotherm Penetration Data

NOTE: $\sqrt{t_c}$ is defined as the latest time that $T_s = 0^\circ\text{C}$
on the temperature time curves

Test E-1-5		Test E-3-2	
$t_c = t - 0$		$t_c = t - 0$	
$\frac{\sqrt{t_c}}{\sqrt{\text{min}}}$	X cm	$\frac{\sqrt{t_c}}{\sqrt{\text{min}}}$	X cm
0	0	0	0
7.06	0.75	6.64	0.45
8.70	1.75	8.00	1.45
10.69	2.75	10.00	2.45
12.56	3.75	12.05	3.45
15.09	4.75	14.05	4.45
16.74	5.75	15.75	5.45
$\alpha_a = \frac{5.75}{16.74} = 0.344 \frac{\text{cm}}{\sqrt{\text{min}}}$		$\alpha_a = \frac{5.45}{15.75} = 0.346 \frac{\text{cm}}{\sqrt{\text{min}}}$	

Test F-3-2

$$t_c = t - 0$$

$\frac{\sqrt{t_c}}{\sqrt{\text{min}}}$	$\frac{X}{\text{cm}}$
0	0
3.77	0.40
5.48	1.40
7.35	2.40
8.60	3.40
9.59	4.40
10.58	5.40
$\alpha_a = \frac{5.40}{10.58} = 0.511 \frac{\text{cm}}{\sqrt{\text{min}}}$	

Test F-3-3

$$t_c = t - 0$$

$\frac{\sqrt{t_c}}{\sqrt{\text{min}}}$	$\frac{X}{\text{cm}}$
0	0
3.74	0.40
5.48	1.40
7.09	2.40
8.37	3.40
9.28	4.40
10.00	5.40
$\alpha_a = \frac{5.40}{10.00} = 0.540 \frac{\text{cm}}{\sqrt{\text{min}}}$	

Test F-4-1

$$t_c = t - 1.0$$

$\frac{\sqrt{t_c}}{\sqrt{\text{min}}}$	$\frac{X}{\text{cm}}$
0	0.0
4.12	0.67
6.08	1.67
9.53	2.67
12.59	3.67
$\alpha_a = \frac{3.67}{12.59} = 0.291 \frac{\text{cm}}{\sqrt{\text{min}}}$	

Test F-5-2

$$t_c = t - 0$$

$\frac{\sqrt{t_c}}{\sqrt{\text{min}}}$	$\frac{X}{\text{cm}}$
0	0
7.20	0.58
8.70	1.58
10.94	2.58
12.48	3.58
14.06	4.58
15.04	5.58
$\alpha_a = \frac{5.58}{15.04} = 0.370 \frac{\text{cm}}{\sqrt{\text{min}}}$	

APPENDIX B

1. Sample Calculation - Theoretical Frost Penetration

Rate

$$\alpha_a = \sqrt{\frac{2K_f T_s}{L}}$$

Considering Test E-1-2

By using Simpson's Integration formula the T_s -time plot shown in Appendix E, (Figure E-1-2) was integrated and an equivalent temperature T_s was determined or:

$$T_s = \frac{\int_0^{280} T_s dt}{t_{280}} = -3.65^\circ\text{C}$$

From Nixon (1973):

$$K_f = 5.3 \times 10^{-3} \left[\frac{\text{cal}}{^\circ\text{Ccmsec}} \right]$$

TEST DATA: $w = 27.5\%$

$$\gamma_d = 1.55 \text{ gm/cm}^3$$

$$L = \gamma_d w (1 - w_u) L'$$

for $w = 5\%$

$$L = 1.55 \left[\frac{\text{gm}}{\text{cm}^3} \right] \times .275 \times (1 - .05) \times 79.6$$

$$= 32.3 \left[\frac{\text{cal}}{\text{cm}^3} \right]$$

$$\alpha_{5\%} = \sqrt{\frac{2 \times 5.3 \times 10^{-3} \times 3.65}{32.3}} = 0.068 \text{ [cm}/\sqrt{\text{min}}]$$

APPENDIX B

2. Water Balance - Sample Calculation

Consider Test E-1-4

Test Data

$$\begin{aligned}
 h &= 6.916 \text{ [cm]} & A &= 83.4 \text{ [cm}^2\text{]} \\
 n &= 0.402 & W_s &= 918.0 \text{ [gms]} \\
 X \text{ (thermocouple)} &= 5.316 \text{ [cm]} & t &= 200 \text{ min} \\
 X \text{ (measured)} &= 4.516 \text{ [cm]} & t &= 280 \text{ [min]} \\
 S &= 0.112 \text{ [cm]} & \Delta V_i &= -0.11 \text{ [cm}^3\text{]}
 \end{aligned}$$

Heave Volume V_h ,

$$V_h = 0.112 \text{ [cm]} \times 83.4 \text{ [cm}^2\text{]} = 9.35 \text{ [cm}^3\text{]}$$

(a) Using X (thermocouple)

$$V_o = X A = 5.316 \text{ [cm]} \times 83.4 \text{ [cm}^2\text{]} = 443.0 \text{ [cm}^3\text{]}$$

from equation 4.16

$$V = V_f = \frac{V_h + \Delta V_i}{0.09n} = \frac{9.35 - 0.11}{0.09 \times 0.402} = 256.0 \text{ [cm}^3\text{]}$$

Substituting into equation 4.14

$$V_u = V_o - V_f = 443.0 - 256.0 = 187.0 \text{ [cm}^3\text{]}$$

$$\begin{aligned}
 W_u &= \frac{W}{W_s} = \frac{nV_u}{W_s} = \frac{0.402 \times 187.0}{918.0} \frac{\text{[gms]}}{\text{[gms]}} \\
 &= 8.2\%
 \end{aligned}$$

(b) Using X (measured)

$$V_O = X A = 4.516 \text{ [cm]} \times 83.4 \text{ [cm}^2\text{]} = 377.0 \text{ [cm}^3\text{]}$$

Substituting in equation 4.14

$$V_u = V_v - V_f = 377.0 - 256.0 = 121.0 \text{ [cm}^3\text{]}$$

$$W_u = \frac{nV_n}{W_s} = \frac{0.402 \times 121.0}{918.0} \text{ [}\frac{\text{gm}}{\text{gm}}\text{]}$$

$$= 5.3\%$$

3. Porewater Pressure - Sample Calculation

$$P_W = \frac{\gamma_w Z}{LkA} \left\{ \frac{C_s M_s}{t} (T_{bs} - T_f) + \frac{C_w \Delta V}{t} (T_w - T_f) + K_u \frac{dt}{dz} A - K_f \frac{dT}{dX} A \right\} + P_h - P_x \quad 2.18$$

Consider Test F-1-4

Test Data:

$$t = 200 \text{ [min]} = 1.2 \times 10^4 \text{ [sec]}$$

$$X = 5.402 \text{ [cm]}$$

$$Z = 1.60 \text{ [cm]}$$

$$k = 0.123 \times 10^{-6} \text{ [cm/sec]}$$

$$C_s = \gamma_d (0.2 + w) = 1.66 (0.2 + 0.229) = 0.712$$

$$\left[\frac{\text{cal}}{^\circ\text{Ccm}^3} \right]$$

$$L = \gamma_d w(1 - w_u) L' = 1.66 \times 0.229 (1-0) 79.6$$

$$= 30.2 \left[\frac{\text{cal}}{\text{cm}^3} \right]$$

$$\Delta V = -0.23 \text{ [cm}^3\text{]}$$

$$P_h = 7.002 \text{ [gm/cm}^2\text{]}$$

$$P_x = 5.402 \text{ [gm/cm}^2\text{]}$$

$$V_s = \frac{W_s}{G_s} = \frac{970.0}{2.68} = 362.0 \text{ [cm}^3\text{]}$$

$$V_w = w W_s = 0.229 \times 970.0 = 222.0 \text{ [cm}^3\text{]}$$

$$V_T = V_s + V_w = 362.0 + 222.0 = 584.0 \text{ [cm}^3\text{]}$$

from Nixon (1973):

$$K_u = 4.0 \times 10^{-3} \left[\frac{\text{cal}}{^\circ\text{Ccmsec}} \right]$$

$$K_f = 5.2 \times 10^{-3} \left[\frac{\text{cal}}{^\circ\text{Ccmsec}} \right]$$

$$T_{bs} = 1.89^\circ\text{C}$$

By using Simpson's Integration formula the T_s - time plot shown in Appendix F, (Figure F-1-4) was integrated and an equivalent temperature T_s was found or:

$$T_s = \frac{\int_0^{200} T_s dt}{t_{200}} = -2.56^\circ\text{C}.$$

From Figure 3.6 $T_w = 0.5^\circ\text{C}$

Hence calculating terms

$$\begin{aligned} \frac{\gamma_w z}{LkA} &= \frac{1 \left[\frac{\text{gm}}{\text{cm}^3} \right] \times 1.6 \text{ [cm]}}{30.2 \left[\frac{\text{cal}}{\text{cm}^3} \right] \times 0.123 \times 10^{-6} \left[\frac{\text{cm}}{\text{sec}} \right] \times 83.4 \text{ [cm}^2\text{]}} \\ &= 50.9 \times 10^2 \cdot \frac{\left[\frac{\text{gm}}{\text{cm}^2} \right]}{\left[\frac{\text{cal}}{\text{sec}} \right]} \end{aligned}$$

$$\begin{aligned}\frac{C_{sM}}{t} (T_{bs} - T_f) &= \frac{0.712 \left[\frac{\text{cal}}{^{\circ}\text{Ccm}^3} \right] \times 584 \text{ [cm}^3\text{]} (1.89 - 0) \text{ [}^{\circ}\text{C]}}{1.2 \times 10^4 \text{ [sec]}} \\ &= 6.55 \times 10^{-2} \left[\frac{\text{cal}}{\text{sec}} \right]\end{aligned}$$

$$\begin{aligned}\frac{C_w \Delta V}{t} (T_w - T_f) &= 1 \left[\frac{\text{cal}}{^{\circ}\text{Ccm}^3} \right] \frac{(-0.23) \text{ [cm}^3\text{]} \times (0.5 - 0) \text{ [}^{\circ}\text{C]}}{1.2 \times 10^4 \text{ [sec]}} \\ &= -0.958 \times 10^{-5} \left[\frac{\text{cal}}{\text{sec}} \right]\end{aligned}$$

$$\begin{aligned}K_u \frac{dT}{dz} A &= 4 \times 10^{-3} \left[\frac{\text{cal}}{^{\circ}\text{Ccmsec}} \right] \frac{0.5}{1.6} \left[\frac{^{\circ}\text{C}}{\text{cm}} \right] \times 83.4 \text{ [cm}^2\text{]} \\ &= 10.91 \times 10^{-2} \left[\frac{\text{cal}}{\text{sec}} \right]\end{aligned}$$

$$\begin{aligned}-k_f \frac{dT}{dx} A &= 5.2 \times 10^{-3} \left[\frac{\text{cal}}{^{\circ}\text{Ccmsec}} \right] \frac{2.65-0.}{5.402} \left[\frac{^{\circ}\text{C}}{\text{cm}} \right] \times 83.4 \text{ [cm}^3\text{]} \\ &= -19.75 \times 10^{-2} \left[\frac{\text{cal}}{\text{sec}} \right]\end{aligned}$$

$$P_h - P_w = 7.002 - 5.402 = 1.600 \text{ [gm/cm}^2\text{]}$$

Substituting the terms back into equation 2.18:

$$\begin{aligned}P_w &= 50.9 \times 10^2 \left[\frac{\text{gm}}{\text{cm}^2} \right] \left\{ 6.55 \times 10^2 - 0.958 \times 10^{-5} \right. \\ &\quad \left. + 10.91 \times 10^{-2} - 19.75 \times 10^{-2} \right\} \left[\frac{\text{cal}}{\text{sec}} \right] + 1.6 \left[\frac{\text{gm}}{\text{cm}^2} \right] \\ P_w &= -0.12 \text{ [Kg/cm}^2\text{]}\end{aligned}$$

Substituting P_W into equation 2.5

$$P_i - P_W = 0.74 - (-0.12) = 0.86 \text{ [Kg/cm}^2\text{]}$$

4. Sample Heave Calculation

$$S = \frac{1}{A} \left[0.09 \frac{x}{\ell} nV + 1.09 V_{aw} \right]$$

Consider Test F-1-3

Test Data:

$$\ell = 7.029 \text{ [cm]} \quad n = 0.382$$

$$x = 5.429 \text{ [cm]} \quad V_{aw} = +1.13 \text{ [cm}^3\text{]}$$

$$A = 83.4 \text{ [cm}^2\text{]}$$

$$V = \ell A = 7.029 \text{ [cm]} \times 83.4 \text{ [cm}^2\text{]} = 589 \text{ [cm}^3\text{]}$$

$$\begin{aligned} S &= \frac{1}{83.4} \left[0.09 \times \frac{5.429 \text{ [cm]}}{7.029 \text{ [cm]}} \times 0.382 \times 589 \text{ [cm}^3\text{]} + 1.13 \right] \\ &= 0.200 \text{ [cm]} \end{aligned}$$

APPENDIX C
EQUIPMENT SPECIFICATIONS

APPENDIX C

CONSTANT TEMPERATURE BATH/CIRCULATOR MODEL 334

Available from HOTPACK (CANADA) LTD.

385 Phillip Street N., Waterloo, Ontario.

TEMPERATURE RECORDER

HONEYWELL ELECTRONIK 15 STRIP CHART MULTIPOINT

RECORDER 15303836 -24-04-0-000-004 10

Available from HONEYWELL INDUSTRIAL PRODUCTS GROUP

Wayne and Windrim Avenue, Philadelphia 44, Pa.

'BELLOFRAM' FLEX-WEAVE MEMBRANE

Catalogue No. 3-400-244 DBT

Available from ANTEUS LABORATORY EQUIPMENT INC.

Malden Mass. 02148

JAYCOR UNSATURATED POLYVINYL CHLORIDE (UPVC) PIPE

Thermal conductivity at 20°C = $4 \times 10^{-4} \left[\frac{\text{cal}}{\text{cm}^2 \text{ sec } ^\circ\text{C}} \right]$

Specific Heat 0.24 $\left[\frac{\text{Btu}}{\text{lb. } ^\circ\text{F}} \right]$

Specific Gravity 1.47 $[\text{gm/cm}^3]$

Modulus of Elasticity - tension 350,000 [p.s.i.]

- flexure 400,000 [p.s.i.]

Thermal Expansion $3.6 \times 10^{-5} \left[\frac{\text{in}}{\text{in}^\circ\text{F}} \right]$
41°F to 140°F

Available from JOHNSTON INDUSTRIAL PLASTICS

9537 - 62nd Ave.

Edmonton, Alberta.

NULLMATIC PRESSURE REGULATORS MODEL 40

Available from MOORE PRODUCTS, . Rexdale, Ontario.

APPENDIX D
SUMMARY OF DATA
OTTAWA SAND

APPENDIX D

TABLE 1
Summary of Soil Mechanics Data
Ottawa Sand

Figure- Test	σ Kg/cm ²	U_b Kg/cm ²	Drainage	h_o cm	W_s gms	C_u	γ_d gm/cm ²
D-1	1.04	0	Open	11.34	1433	1.71	1.56
D-2	1.04	0	Open	11.62	1605	1.71	1.70
D-3	0.50	0	Open	10.66	1490	1.71	1.72

APPENDIX D

(Table 1 Continued)

Figure - Test	w _O %	e _O	S %	w _f %	e _f	n	k cm/sec
D-1	37.1	0.716	140	26.5	0.708	0.415	3.9×10^{-3}
D-2	31.6	0.560	151	27.8	0.741	0.426	3.12×10^{-3}
D-3	29.2	0.549	142	25.8	0.688	0.408	3.12×10^{-3}

APPENDIX D

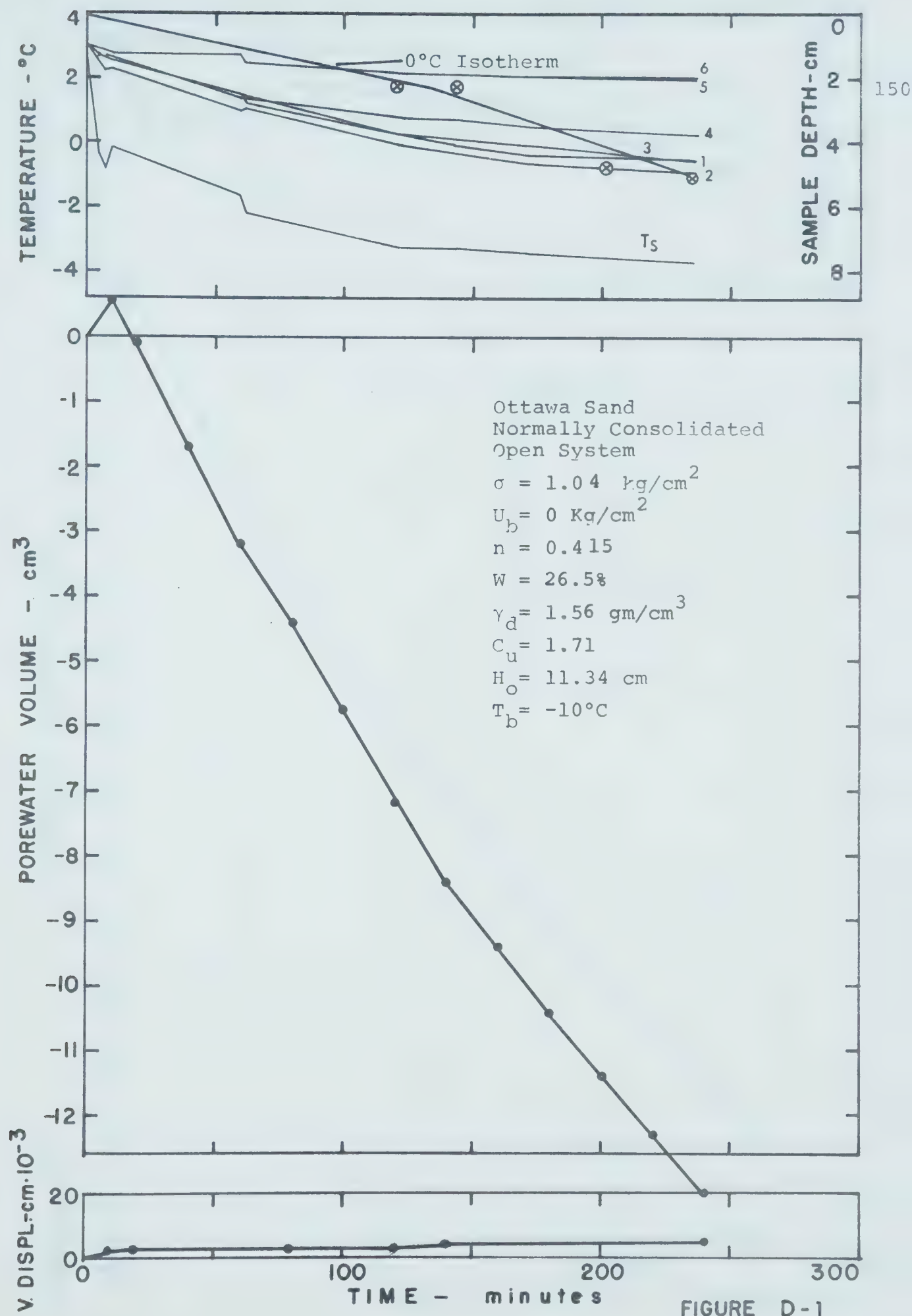
TABLE 2

Summary of Freezing Test Data

Ottawa Sand

Figure - Test	T _b °C	t min	X cm (th*)	t min	X cm (meas**)	α_a cm/ $\sqrt{\text{min}}$ (th*)	α_a cm/ $\sqrt{\text{min}}$ (meas**)	at t = 160 min	
								ΔV cm ³	Heave S, cm x10 ⁻³
D-1	-10	-	-	240	5.0	-	0.323	-9.4	4.57
D-2	-10	224.5	5.01	250	5.4	0.334	0.341	-8.4	4.83
D-3	-9.39	255	4.07	260	5.1	0.272	0.316	-8.3	2.28

NOTE: - ΔV - porewater expelled
+ ΔV - water sucked in
th* - thermocouple
meas** - measured



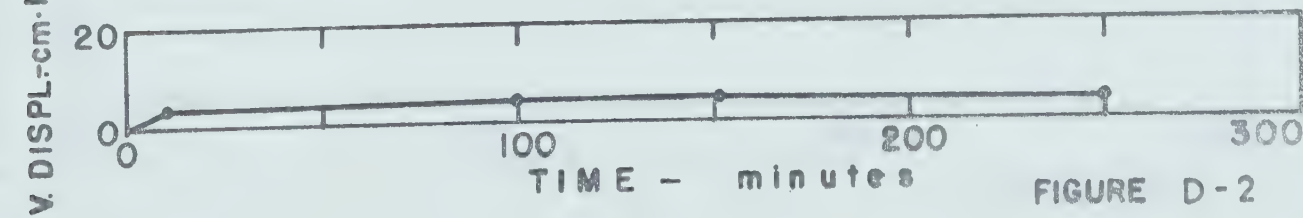
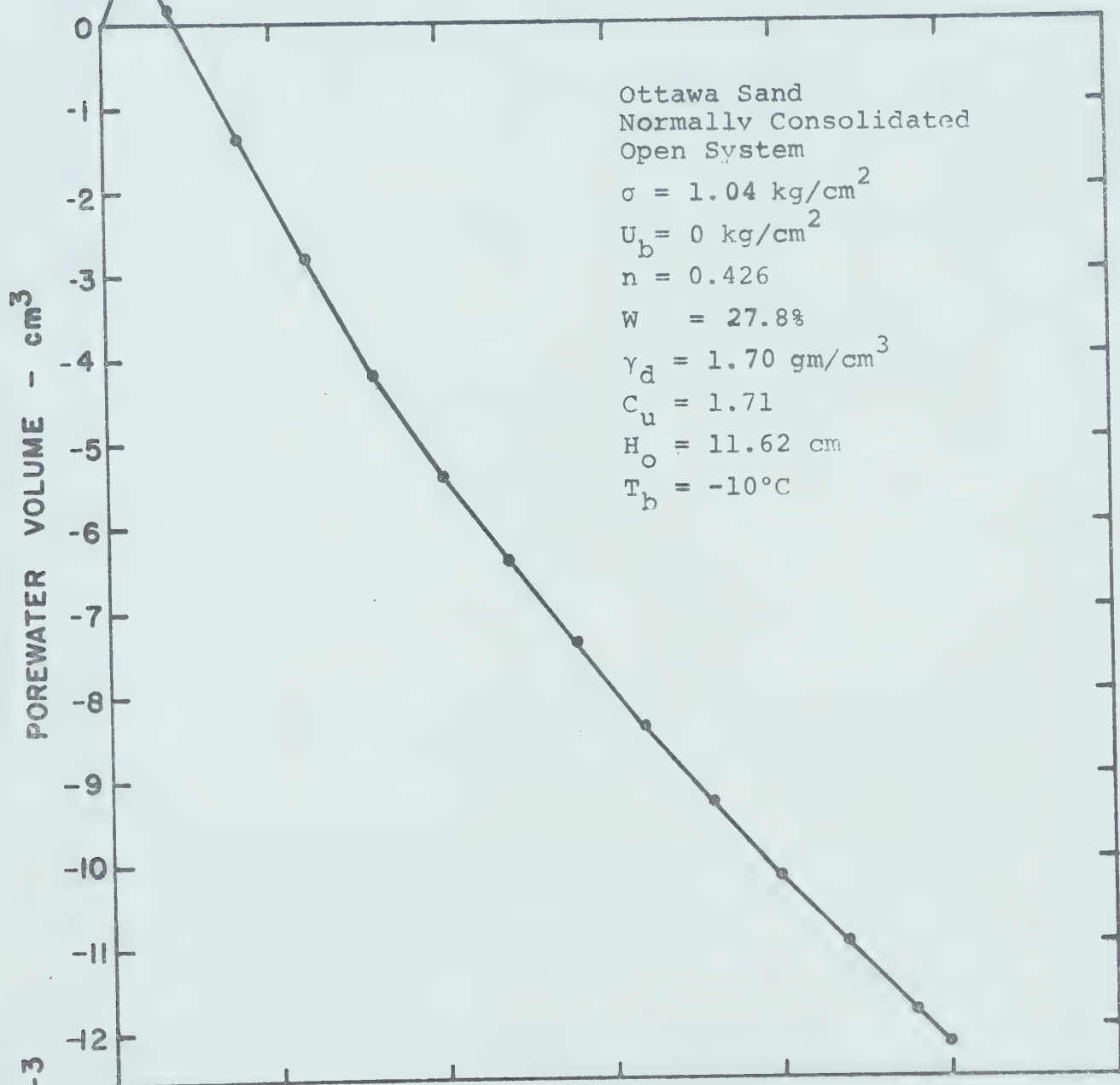
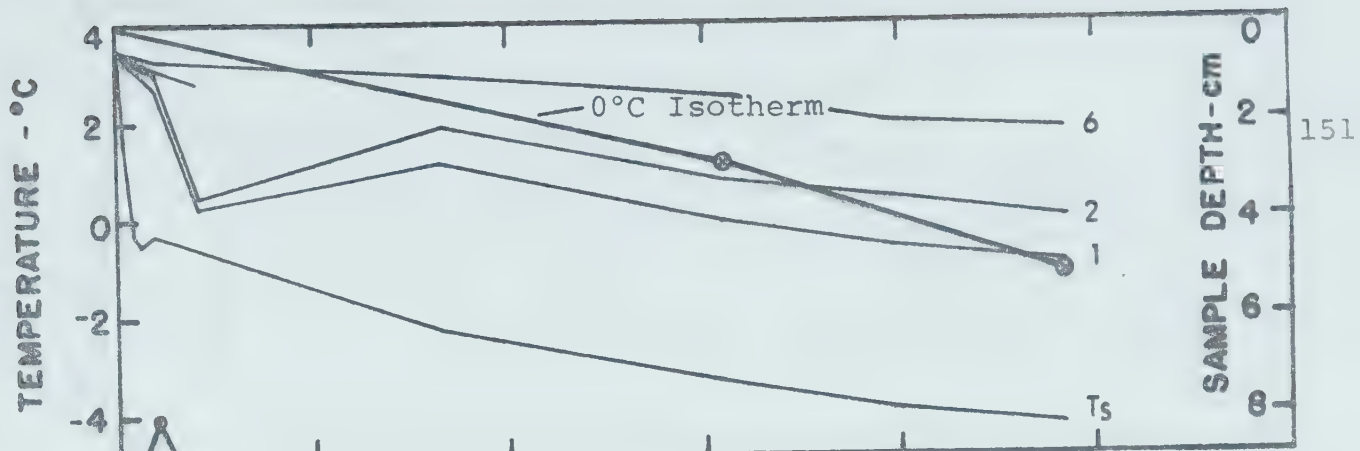


FIGURE D-2

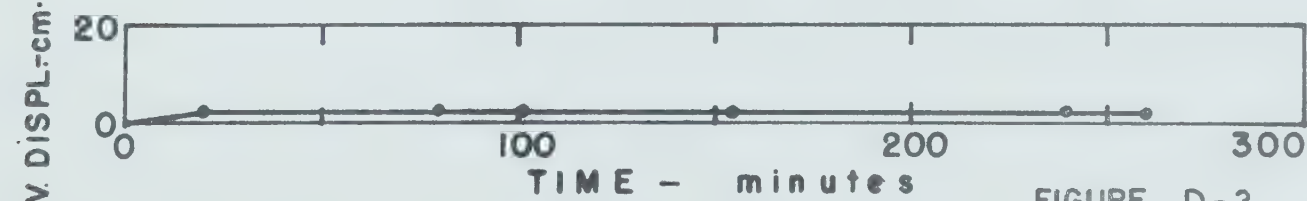
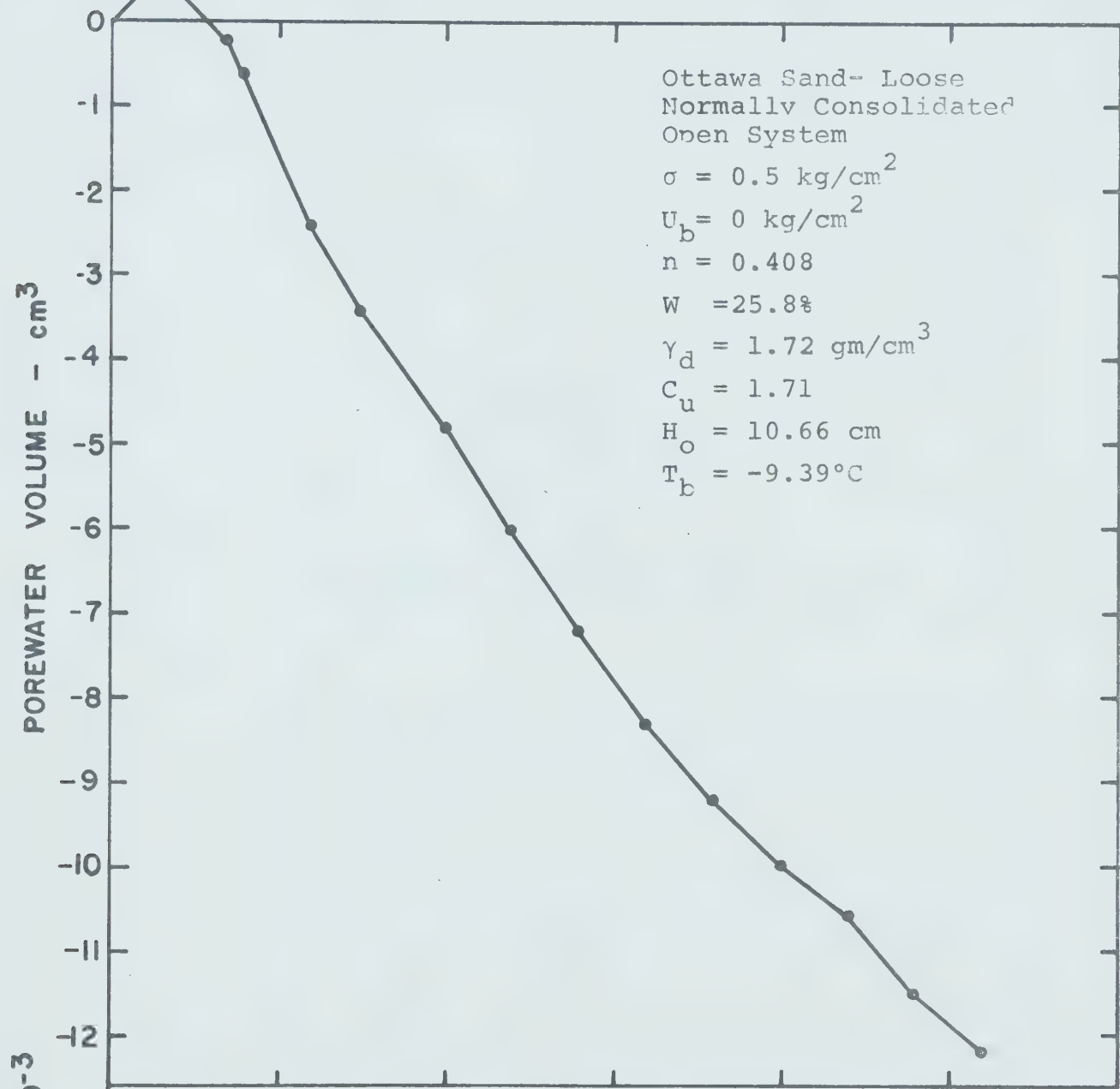
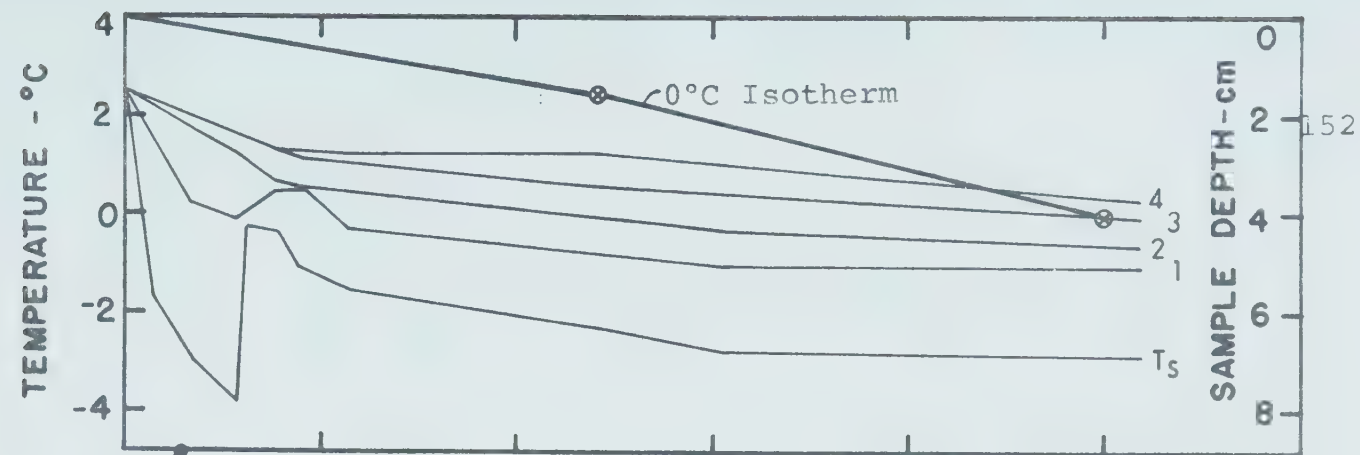


FIGURE D-3

APPENDIX E
SUMMARY OF DATA
DEVON SILT
(NORMALLY CONSOLIDATED)

APPENDIX E

TABLE 1

Summary of Soil Mechanics Data

Devon Silt - Normally Consolidated

Figure- Test	σ Kg/cm ²	U_b Kg/cm ²	Drainage	h_o cm	W_s gm	C_u	γ_d gm/cm ³	w_o %
E-1-1	3.82	3.10	0	7.081	915.0	238	1.55	51.1
E-1-2	3.92	3.16	0	7.047	908.0	238	1.55	50.2
E-1-3	4.23	3.00	0	7.072	915.5	238	1.55	51.4
E-1-4	4.44	3.10	0	6.916	918.0	238	1.59	50.4
E-1-5	4.56	2.94	0	7.347	978.0	238	1.60	49.2
E-1-6	5.04	3.13	0	6.711	896.7	238	1.61	53.0
E-1-7	5.50	3.08	0	6.866	926.0	238	1.62	50.4
E-2-1	3.96	2.99	C	7.346	953.5	238	1.55	51.6
E-2-2	4.35	3.08	C	6.963	1005.7	238	1.74	46.4
E-2-3	4.71	3.38	C	6.895	915.0	238	1.59	52.7
E-2-4	4.46	3.00	C	7.222	949.0	238	1.58	52.7
E-2-5	4.49	3.02	C	7.133	921.5	238	1.55	52.9
E-3-1	4.58	3.11	0 & C	7.323	942.5	238	1.54	51.6
E-3-2	5.06	3.10	0 & C	7.046	955.0	238	1.62	49.2

APPENDIX E

(TABLE 1 Continued)

Figure - Test	e _o	S %	w _f %	e _f	n	C _y (cm ² /sec) x10 ⁻³	k (cm/sec) x 10 ⁻⁶
E-1-1	1.349	102.0	27.2	0.731	0.422	1.010	0.429
E-1-2	1.349	99.9	27.5	0.739	0.424	1.145	0.450
E-1-3	1.392	98.0	27.1	0.725	0.420	1.395	0.367
E-1-4	1.350	100.0	25.2	0.676	0.402	1.680	0.424
E-1-5	1.331	98.2	25.4	0.680	0.405	1.845	0.370
E-1-6	1.411	101.0	25.0	0.670	0.401	1.645	0.312
E-1-7	1.351	100.0	24.5	0.657	0.397	2.075	0.296
E-2-1	1.390	99.5	26.8	0.717	0.418	-	-
E-2-2	1.197	103.0	20.2	0.544	0.353	1.930	0.529
E-2-3	1.460	97.4	25.6	0.686	0.407	1.429	0.404
E-2-4	1.410	100.0	26.2	0.703	0.413	1.55	0.366
E-2-5	1.421	100.0	27.1	0.726	0.422	-	-
E-3-1	1.405	98.5	27.4	0.735	0.432	1.26	0.278
E-3-2	1.320	99.9	24.2	0.650	0.395	-	-

O - Open drainage
C - Closed Drainage

APPENDIX E

TABLE 2

Summary of Freezing Test Data

Devon Silt - Normally Consolidated

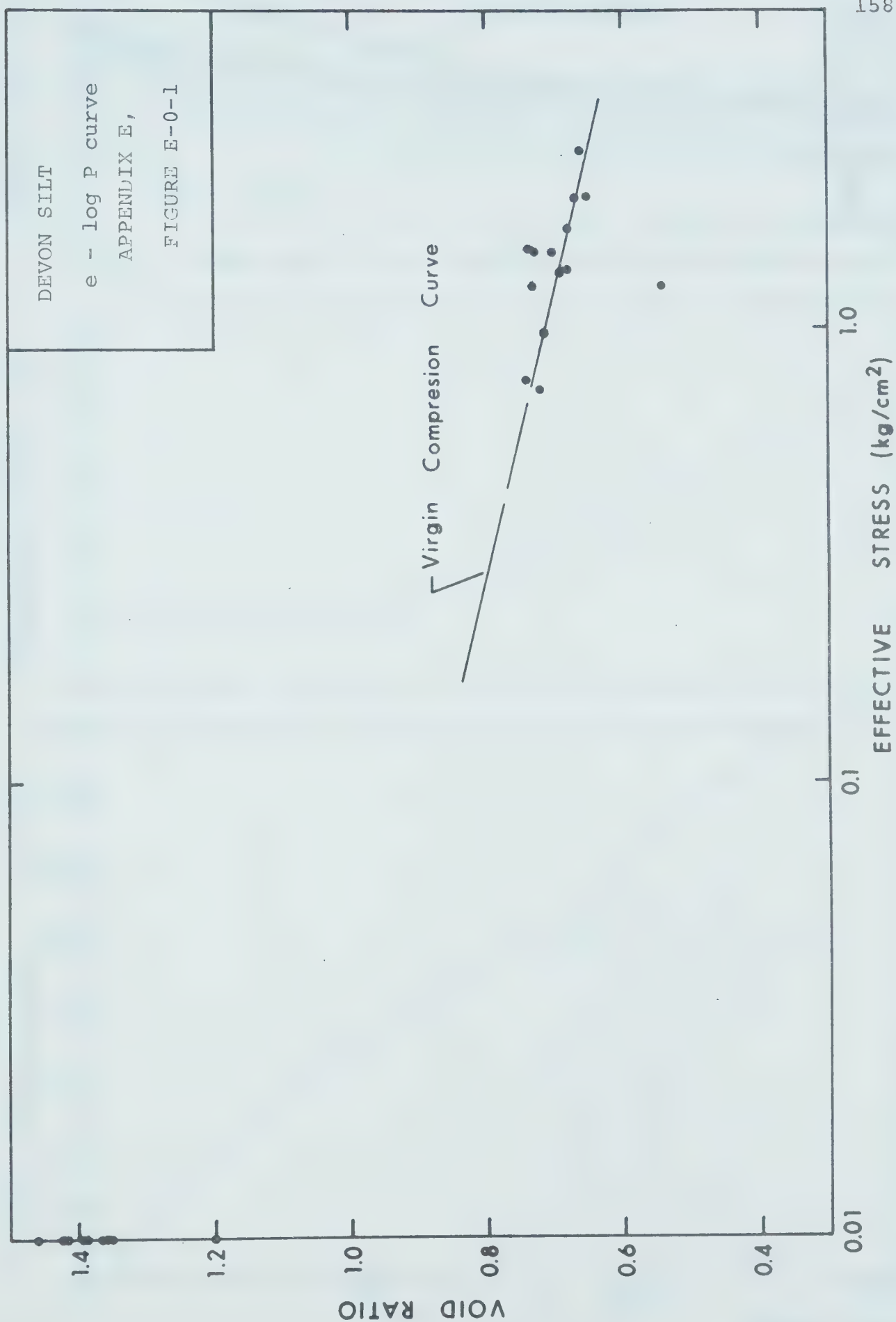
Figure- Test	T _b °C	t min	X thmc* cm	t min	X meas** cm	α_a thmc* cm/ $\sqrt{\text{min}}$
E-1-1	-4.44	302	4.481	360	4.08	0.258
E-1-2	-4.44	170	4.474	342	4.95	0.342
E-1-3	-4.44	180	5.472	250	4.72	0.407
E-1-4	-4.44	200	5.316	280	4.52	0.376
E-1-5	-4.44	180	5.745	280	4.41	0.344
E-1-6	-4.44	228	5.111	260	4.02	0.335
E-1-7	-4.44	196	5.266	260	4.37	0.361
E-2-1	-4.44	131	5.746	200	3.95	0.501
E-2-2	-4.44	259	5.363	310	4.46	0.333
E-2-3	-4.44	296	5.295	310	4.38	0.306
E-2-4	-4.44	210	5.622	236	4.52	0.388
E-2-5	-4.44	212	5.533	200	4.43	0.381
E-3-1	-4.44	209	4.723	370	5.27	0.327
E-3-2	-5.00	248	5.446	330	4.05	0.347

APPENDIX E

(TABLE 2 Continued)

Figure- Test	α_a meas** cm/ $\sqrt{\text{min}}$	at t = 160 min		Porewater Pressure, u Kg/cm ²
		ΔV cm ³	Heave S, cm	
E-1-1	0.254	+ 1.05	0.099	-
E-1-2	0.267	+ 0.90	0.097	-
E-1-3	0.299	+ 0.30	0.091	-
E-1-4	0.271	- 0.31	0.078	-
E-1-5	0.264	- 0.75	0.071	-
E-1-6	0.249	- 1.01	0.061	-
E-1-7	0.271	- 2.11	0.046	-
E-2-1	0.278	-	0.089	-0.13
E-2-2	0.254	-	0.067	+0.39
E-2-3	0.248	-	0.072	-0.02
E-2-4	0.294	-	0.082	-0.02
E-2-5	0.313	-	0.080	-0.05
E-3-1	0.274	- 0.90	0.080	decreasing
E-3-2	0.222	- 1.30	0.076	increasing

NOTE: porewater expelled: - ΔV , + u
porewater sucked in: + ΔV , - u
thmc* - thermocouple
meas** - measured



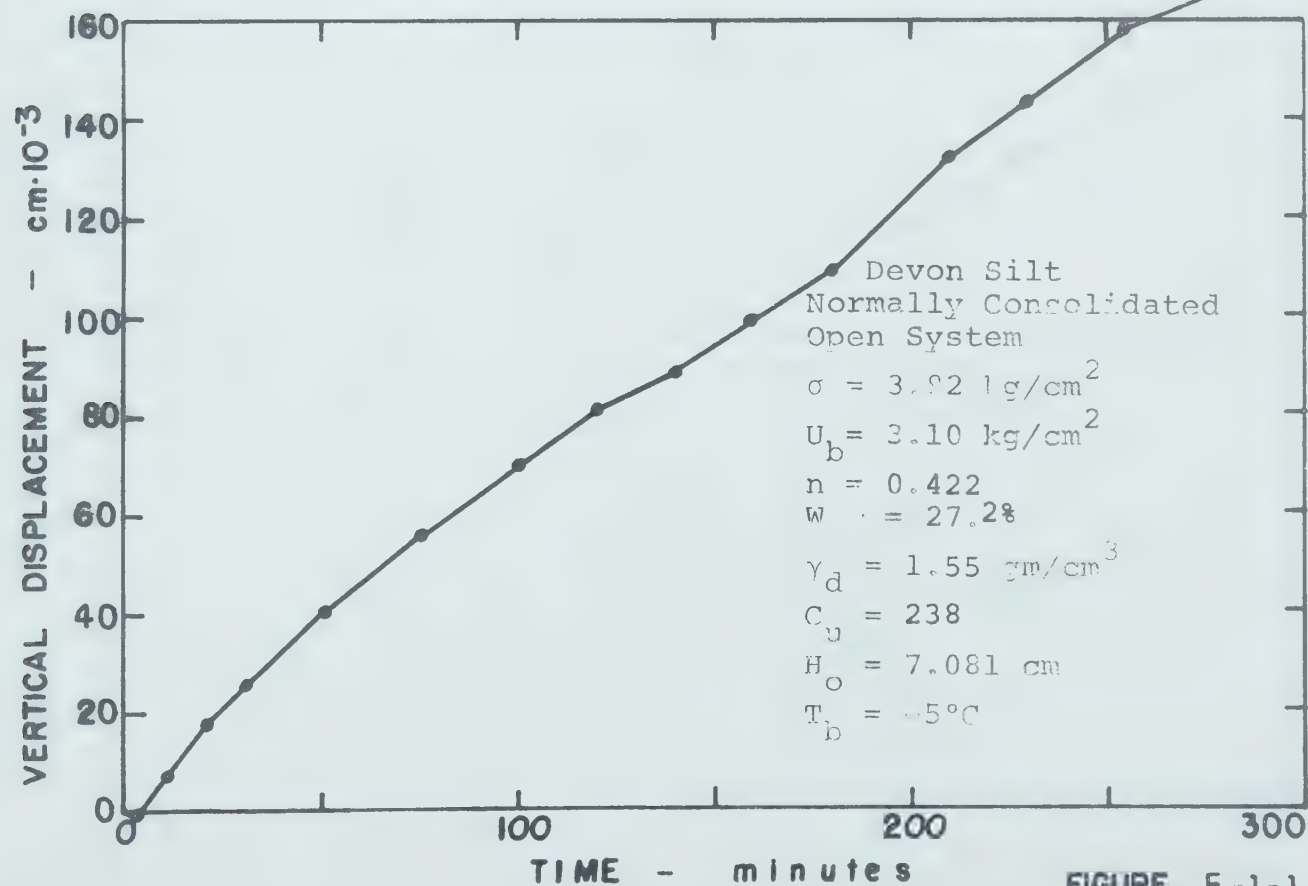
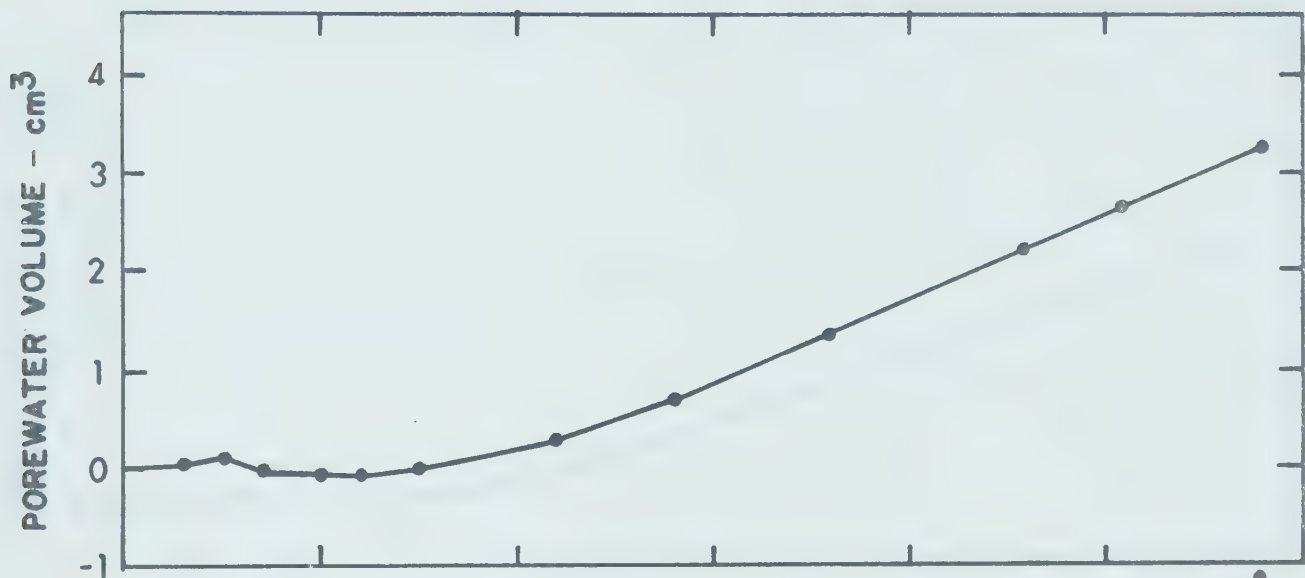
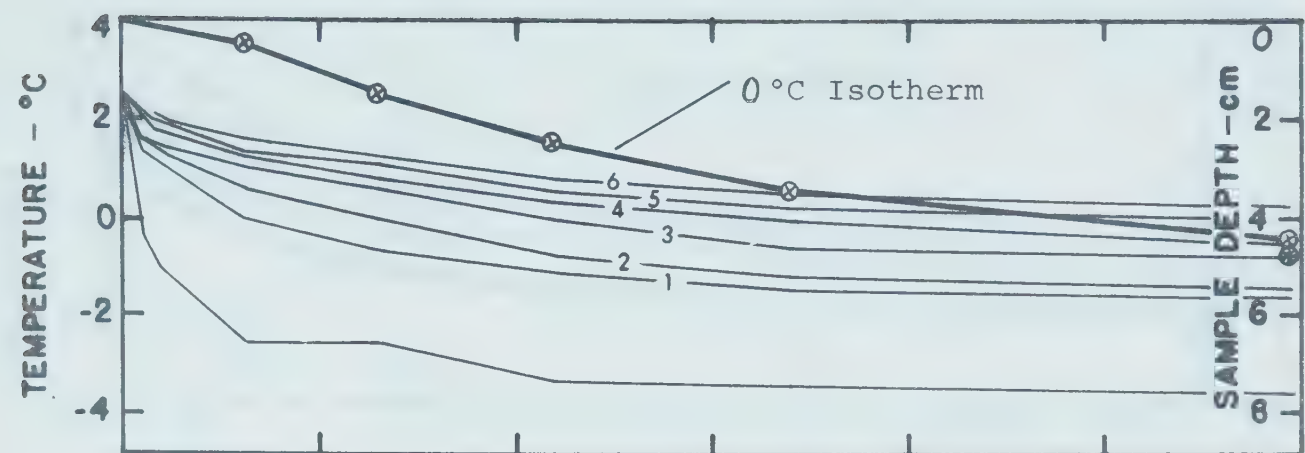


FIGURE E-1-1

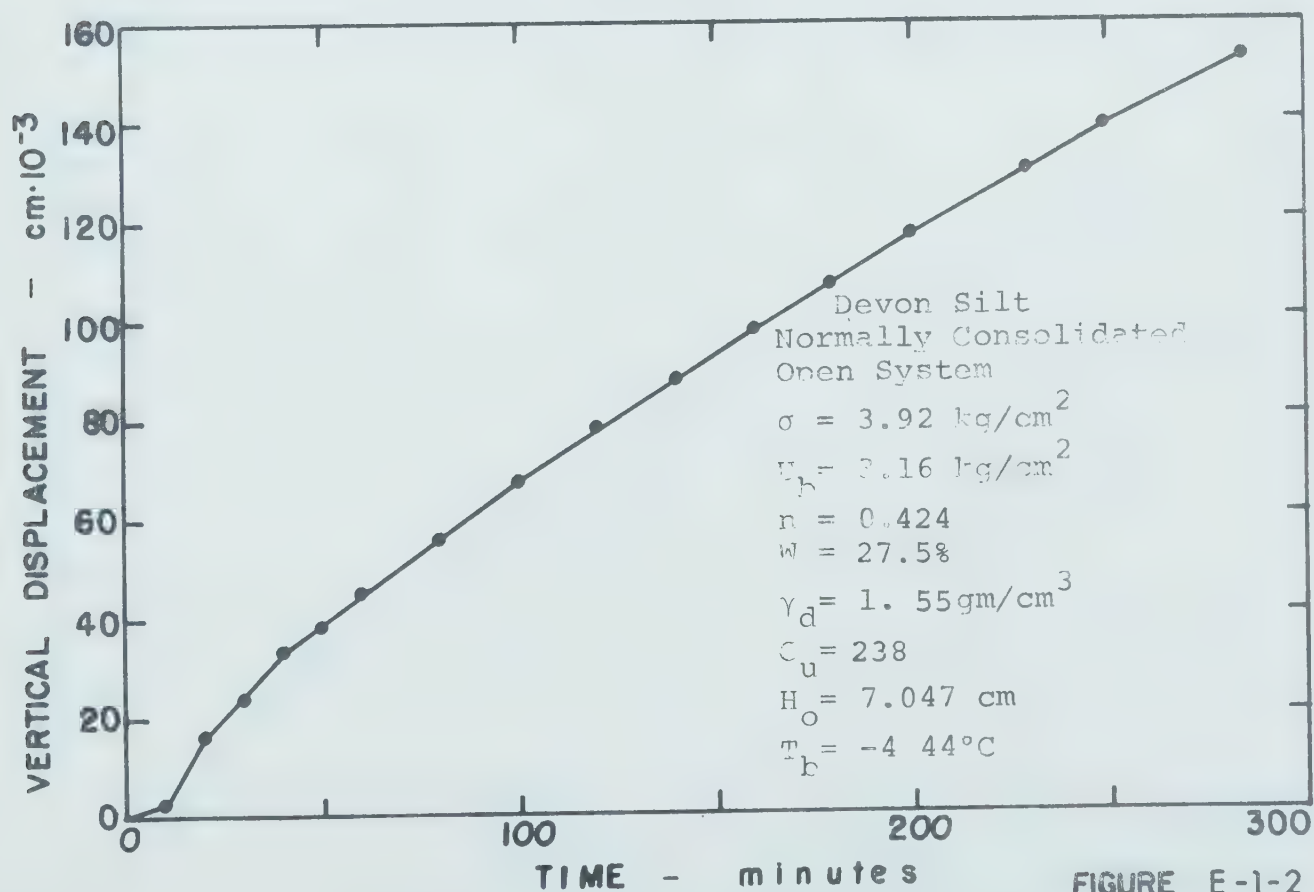
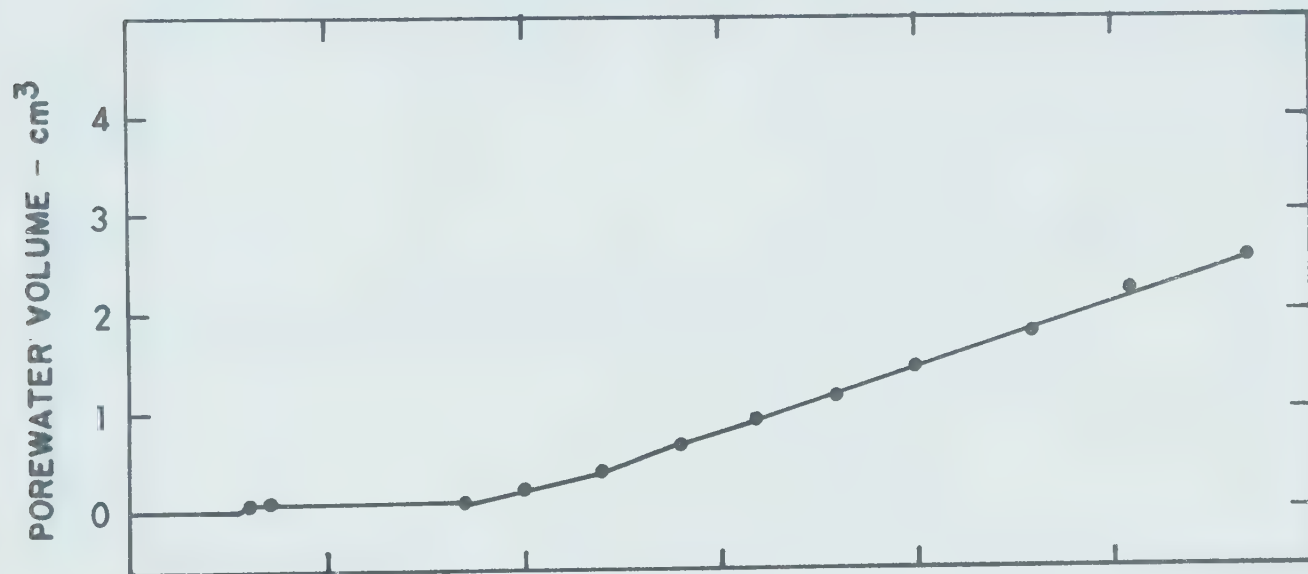
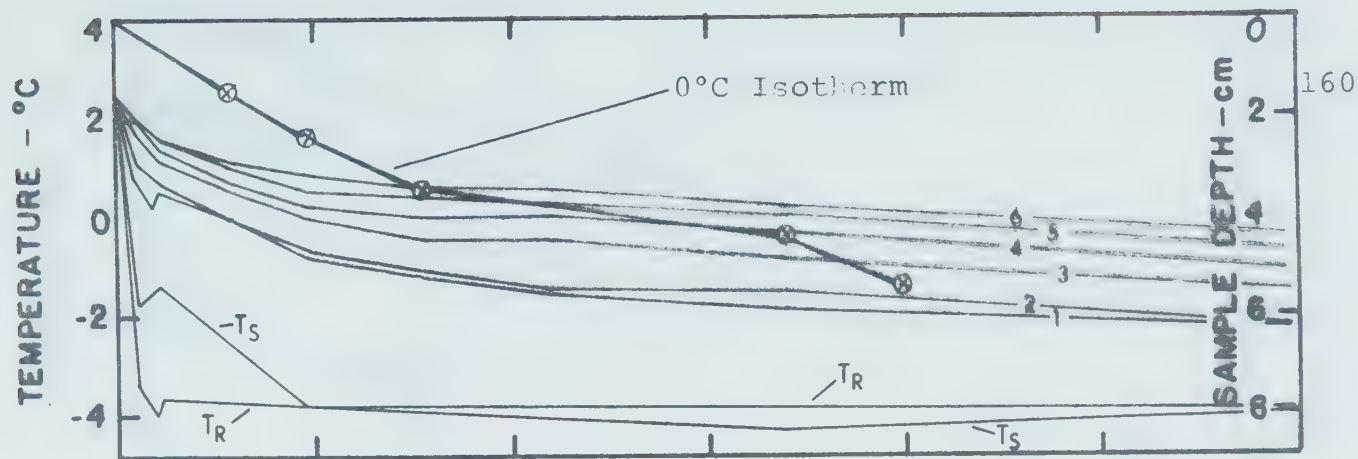


FIGURE E-1-2

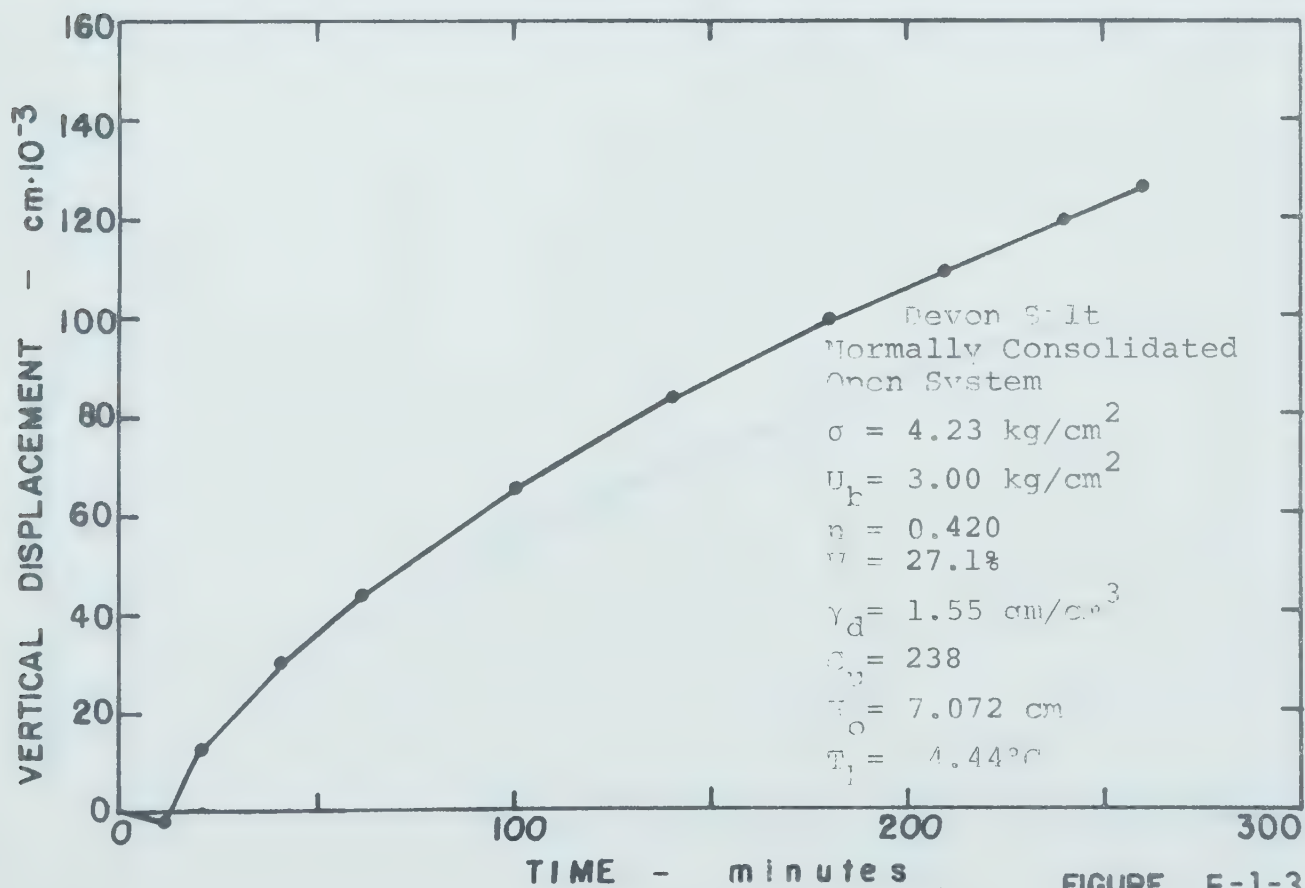
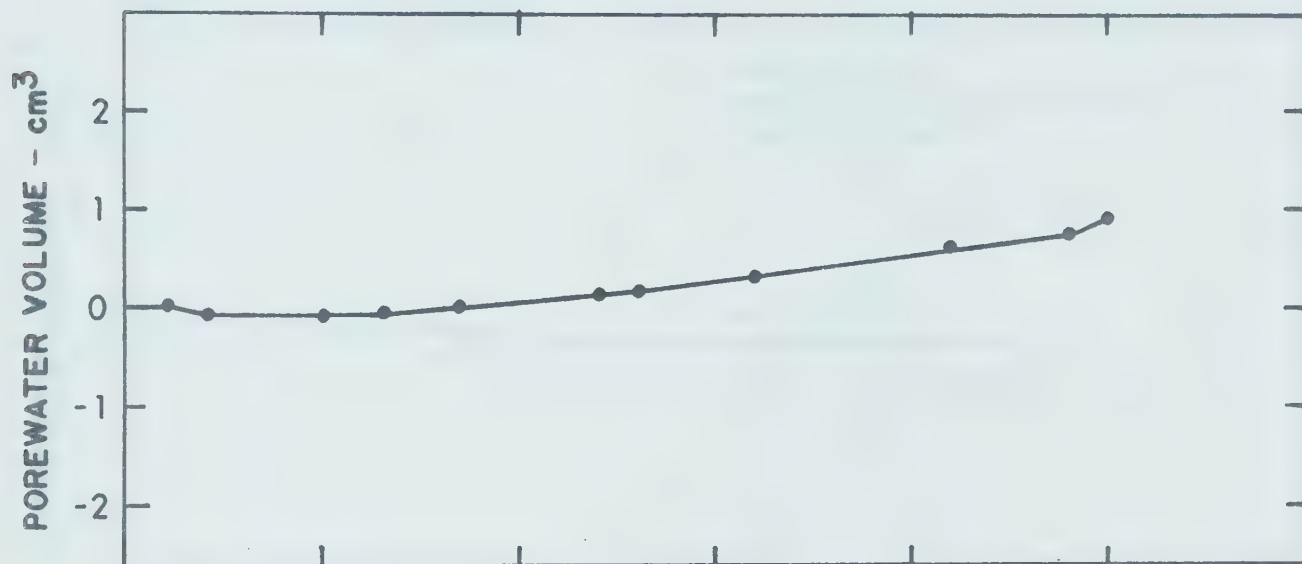
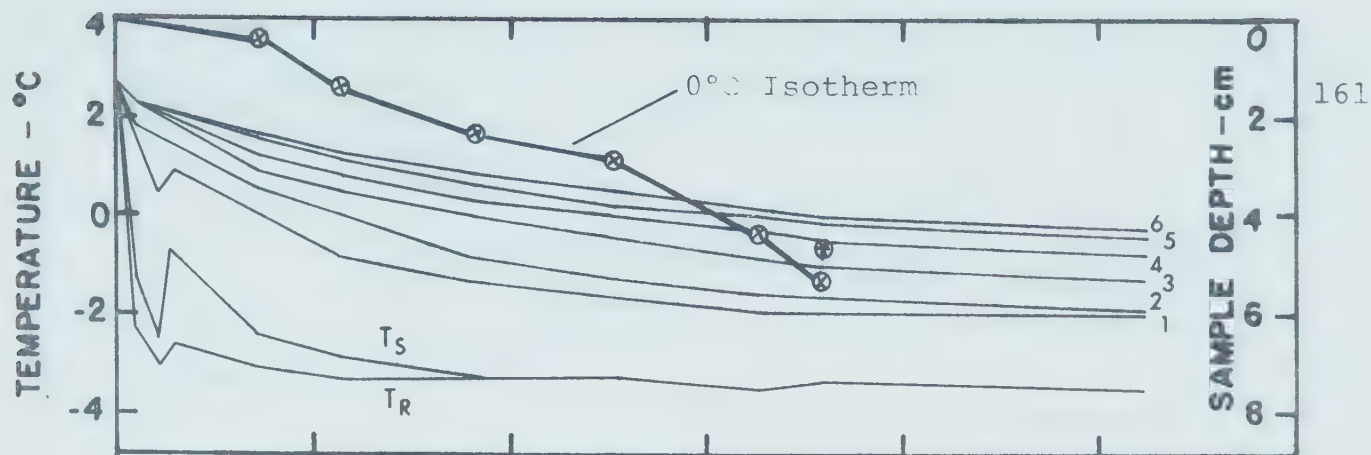


FIGURE E-1-3

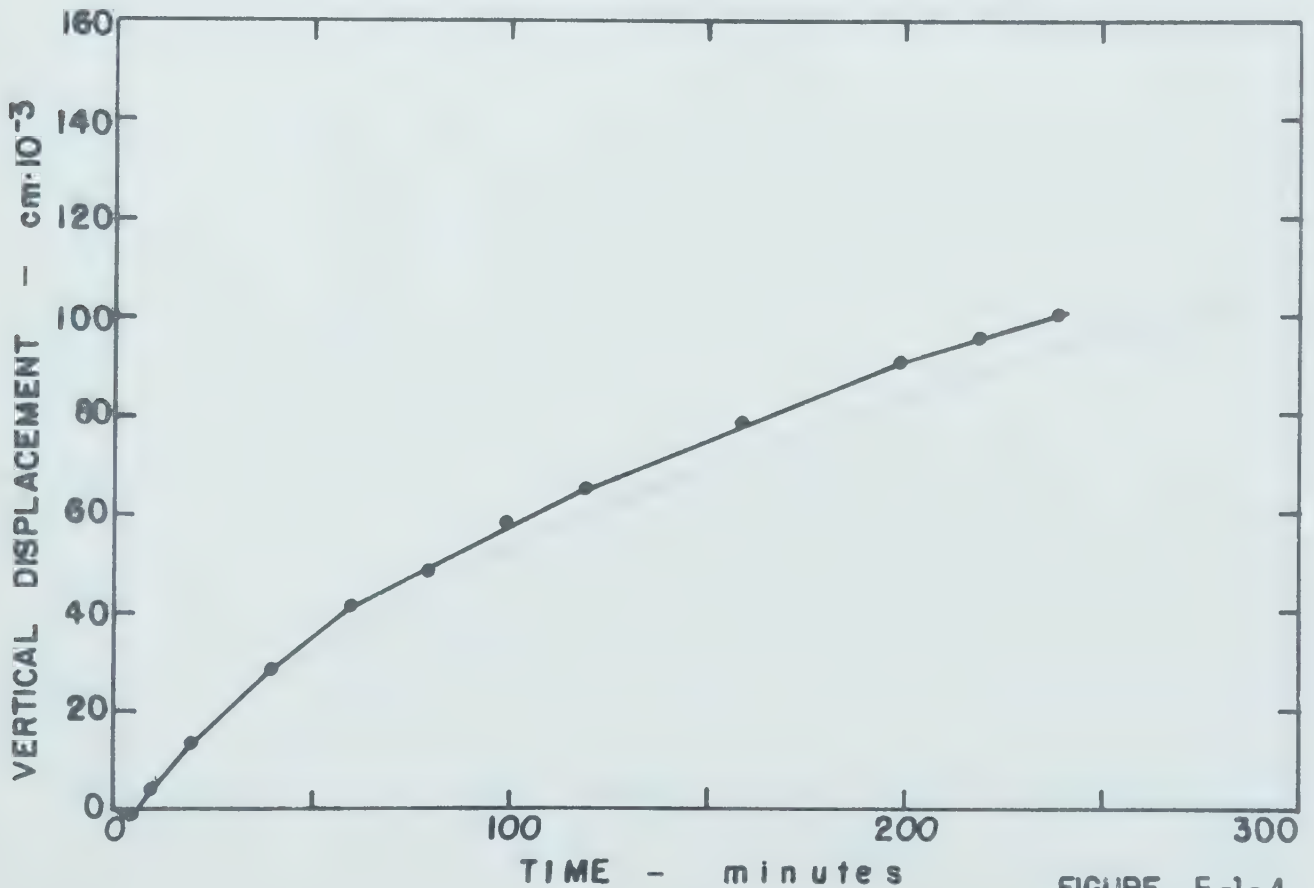
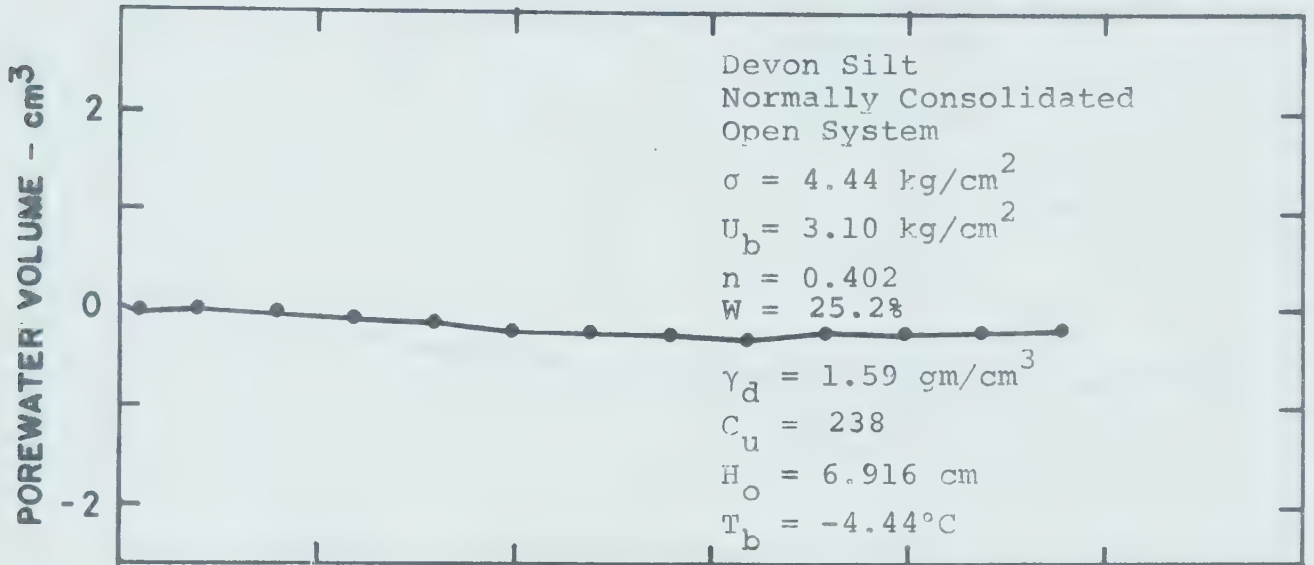
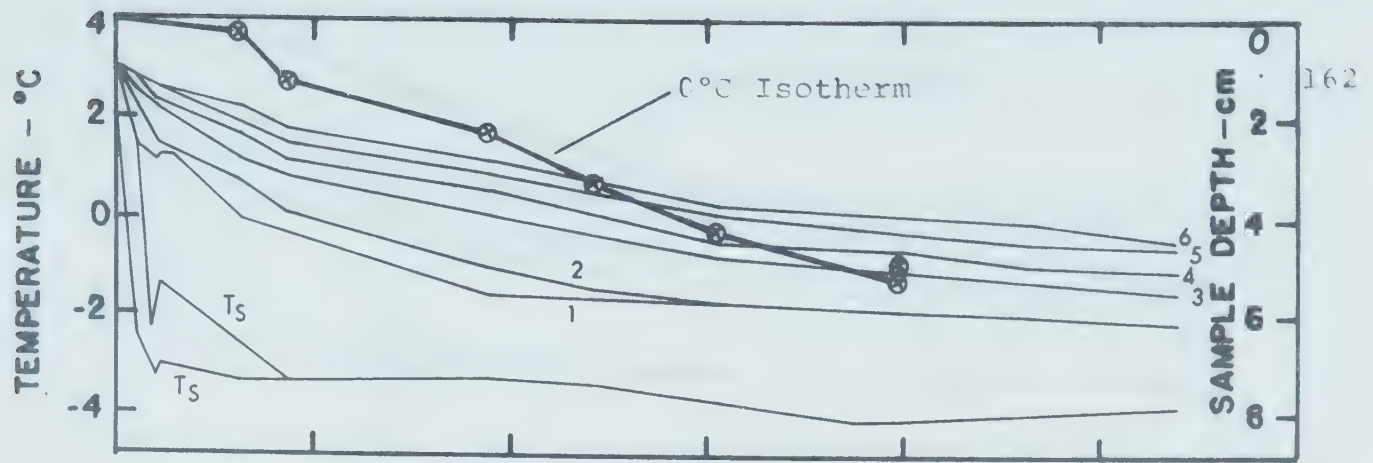


FIGURE E-1-4

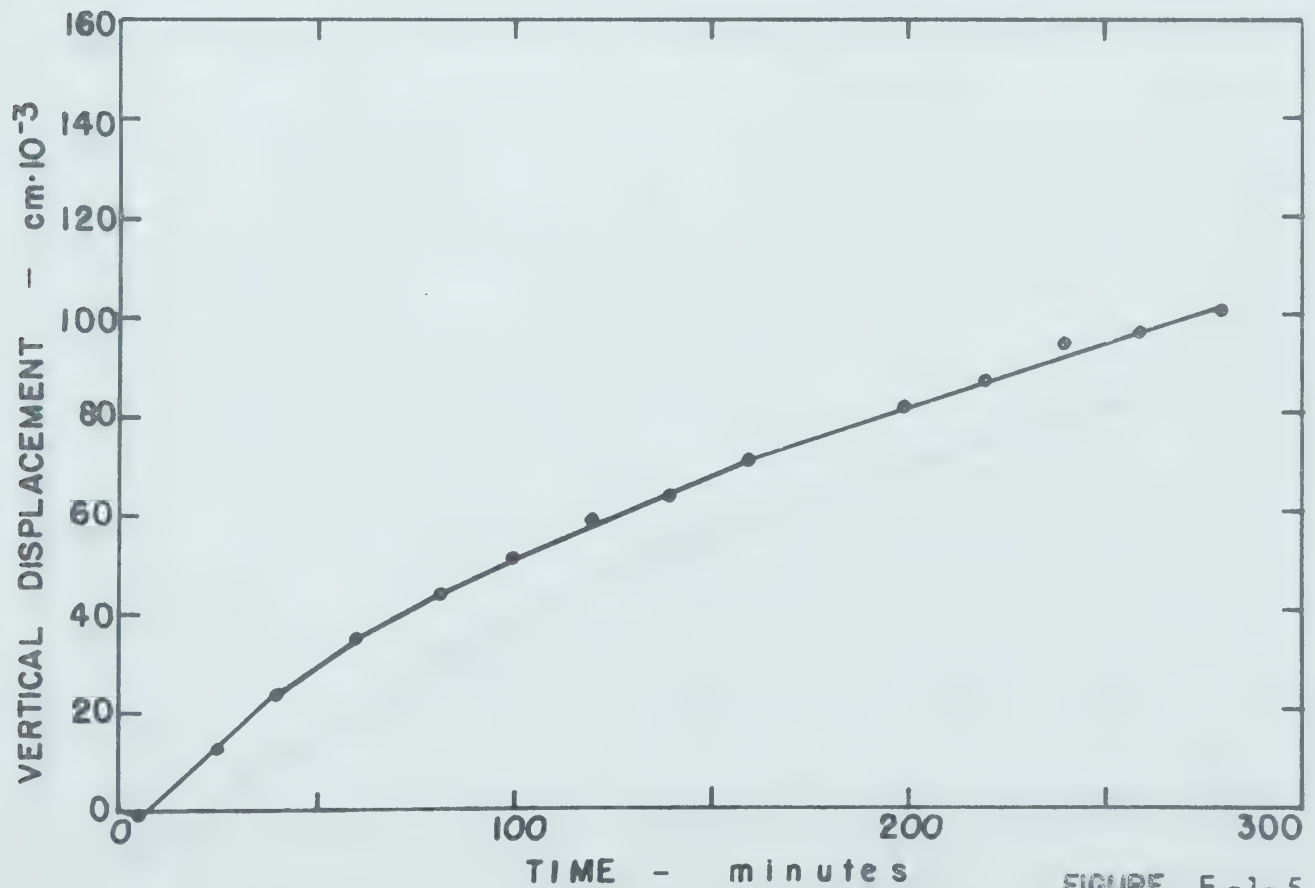
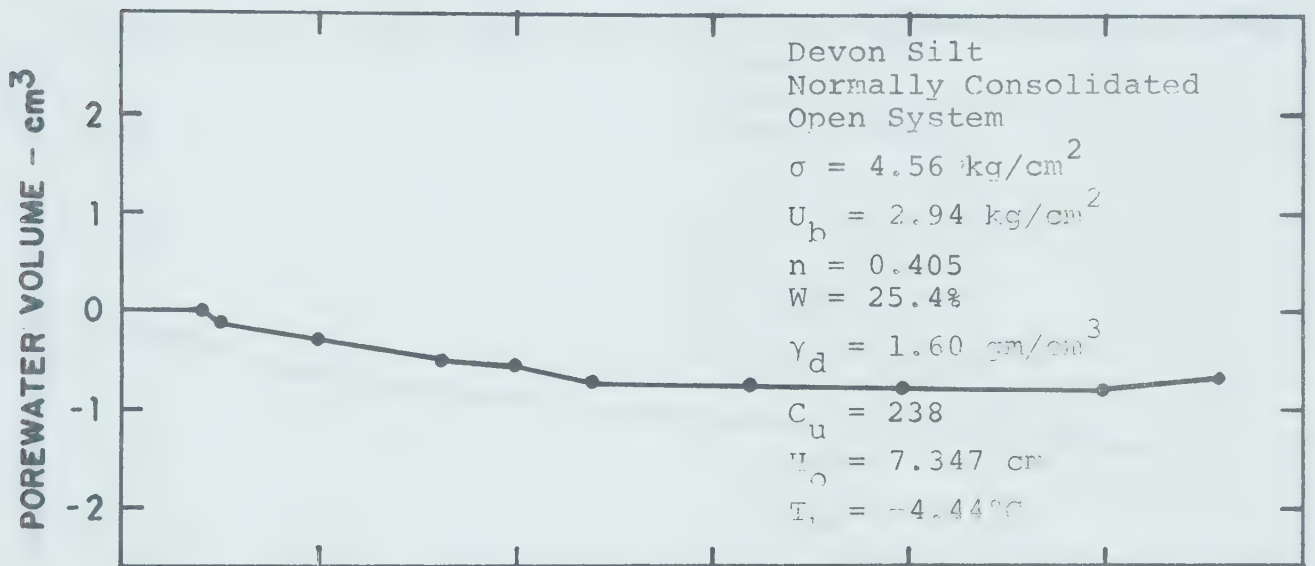
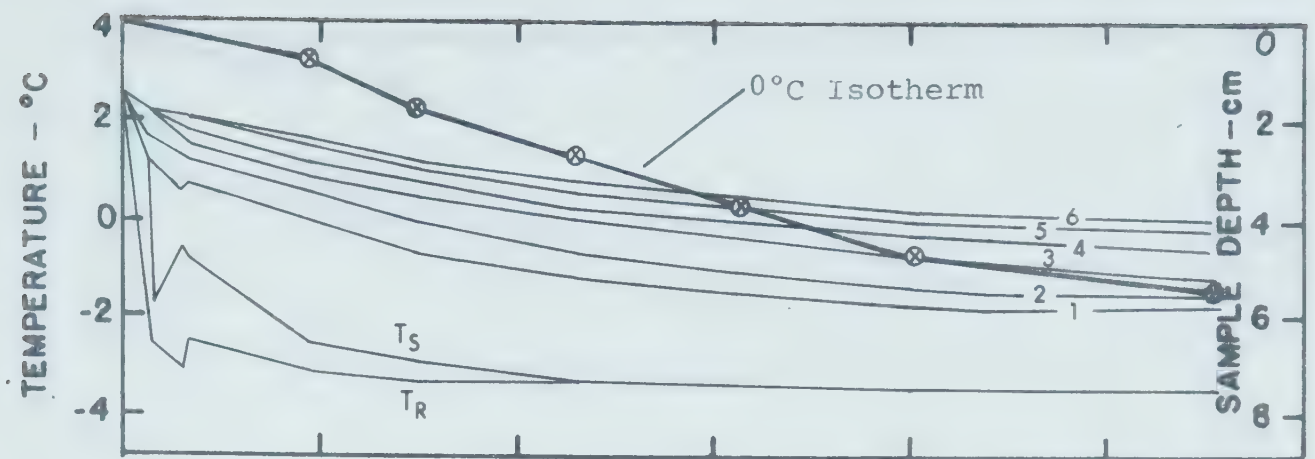


FIGURE E-1-5

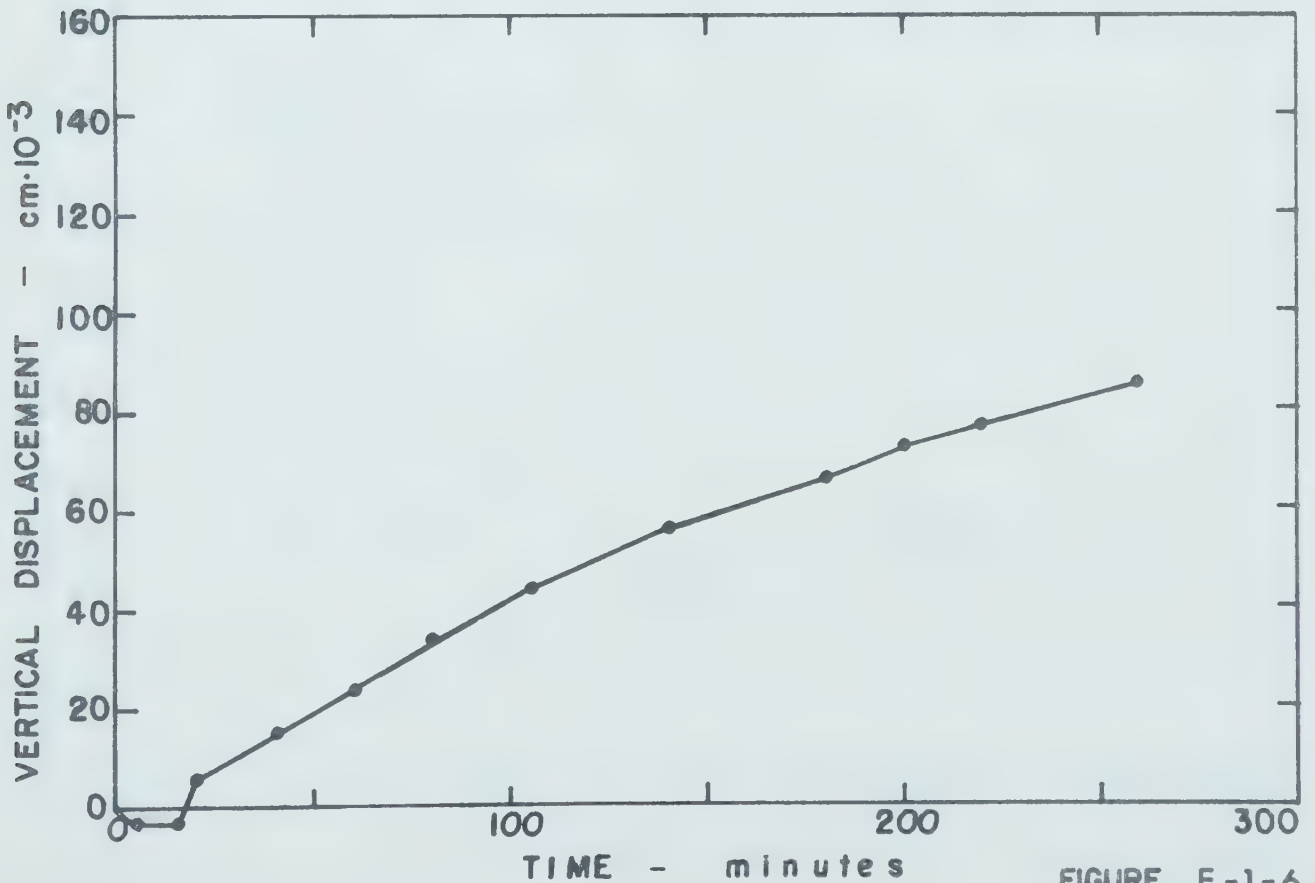
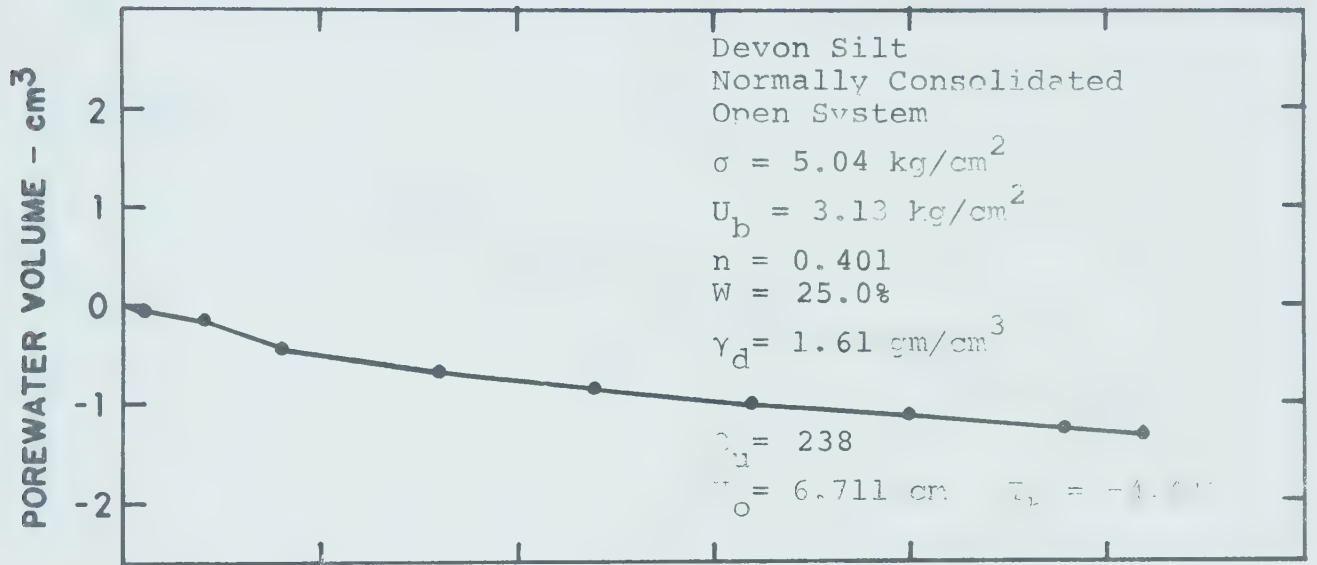
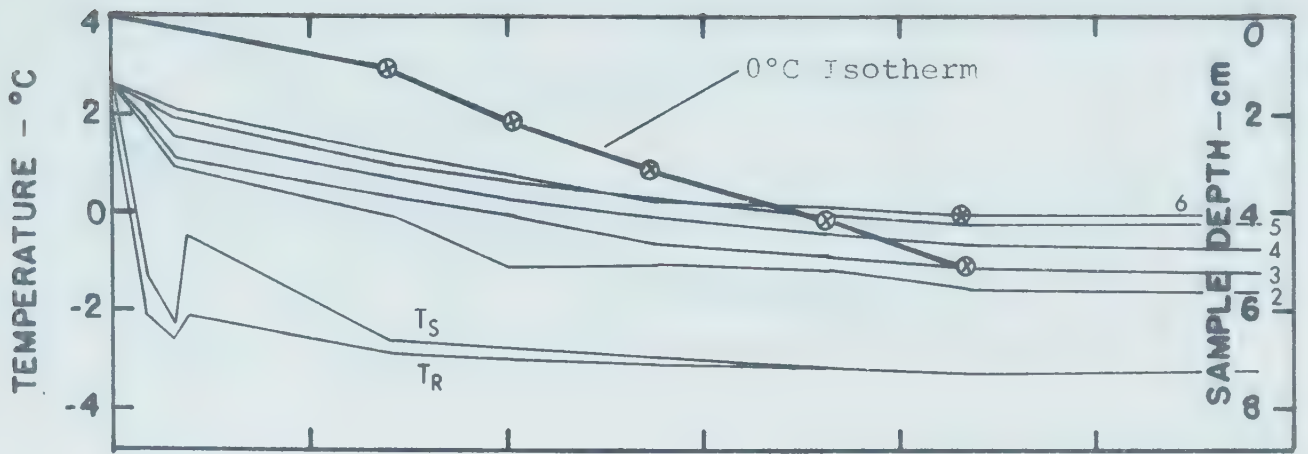


FIGURE E-1-6

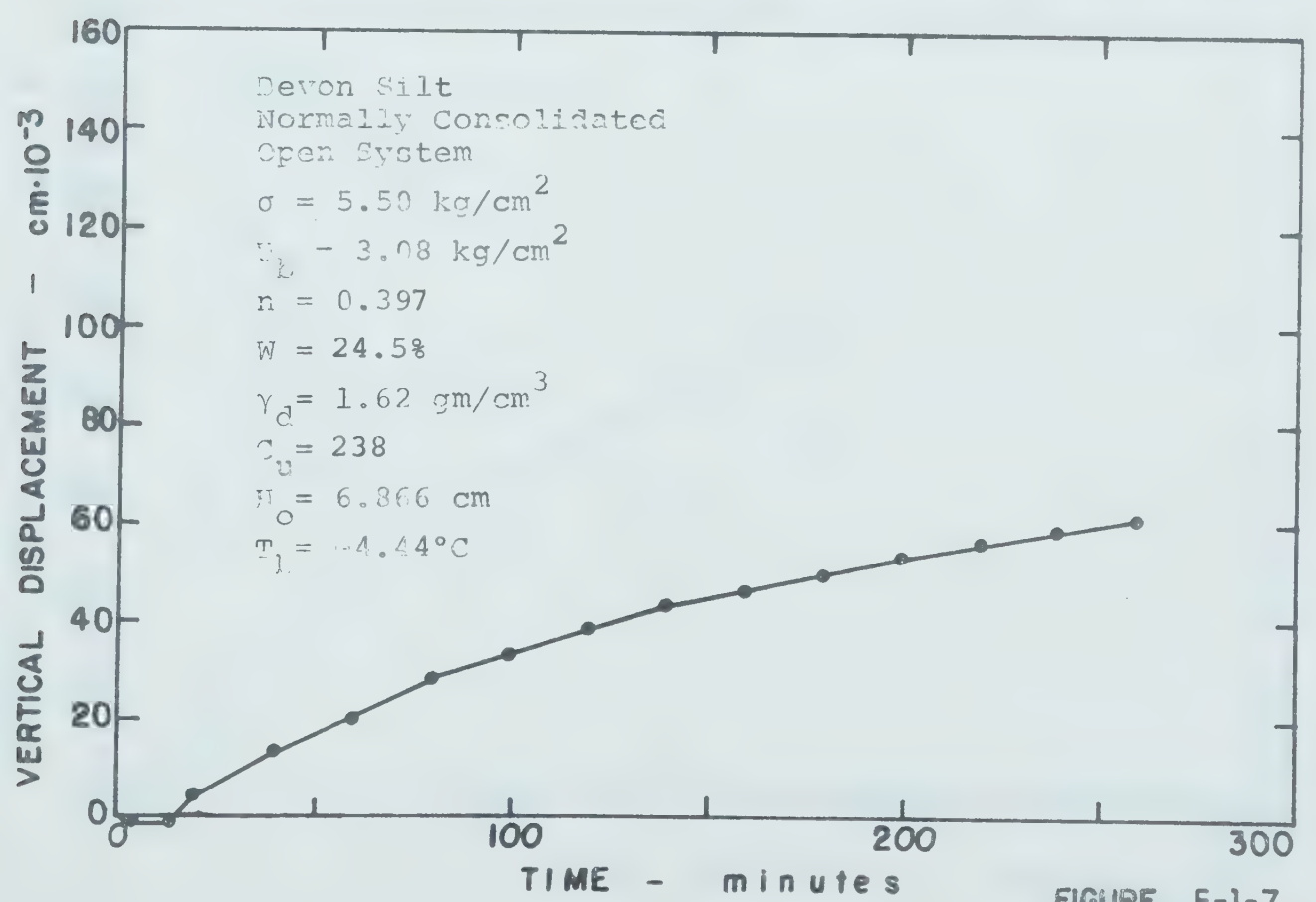
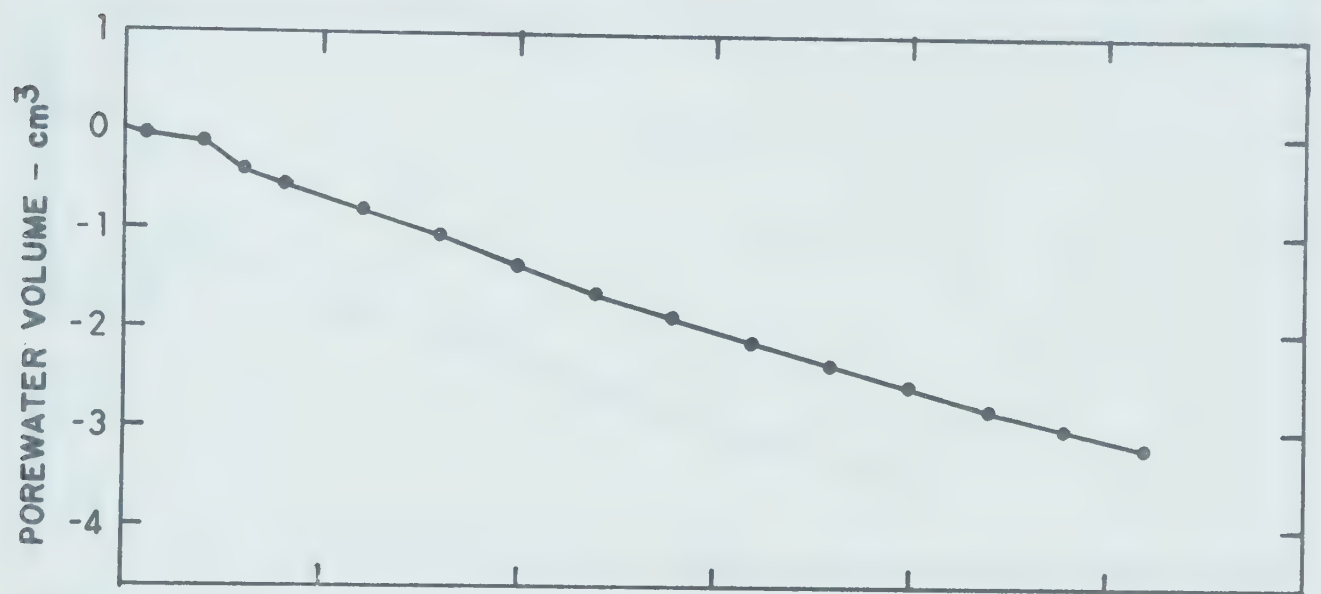
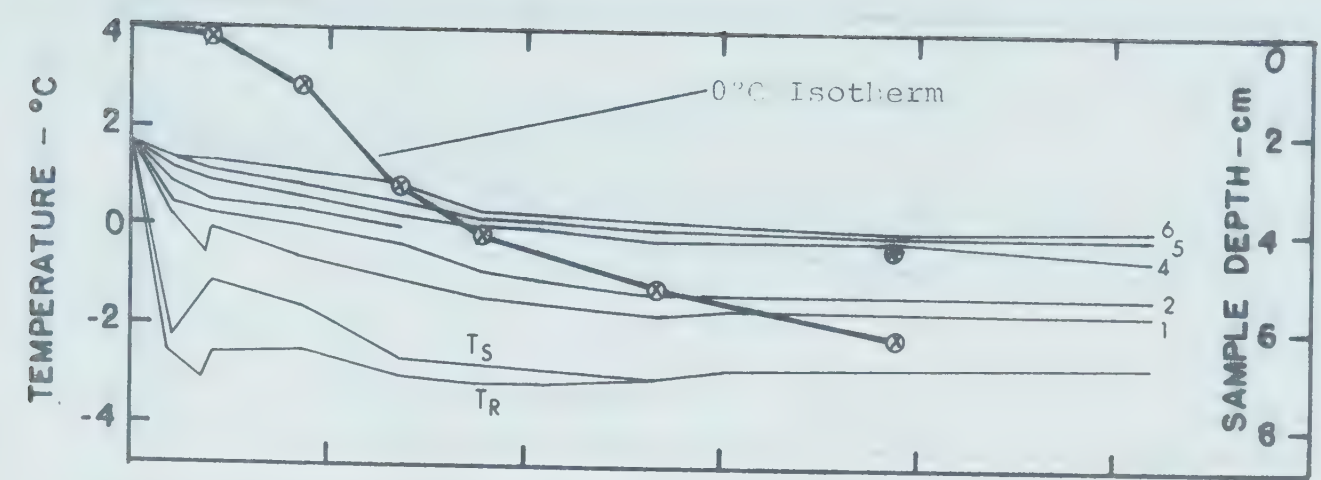


FIGURE E-1-7

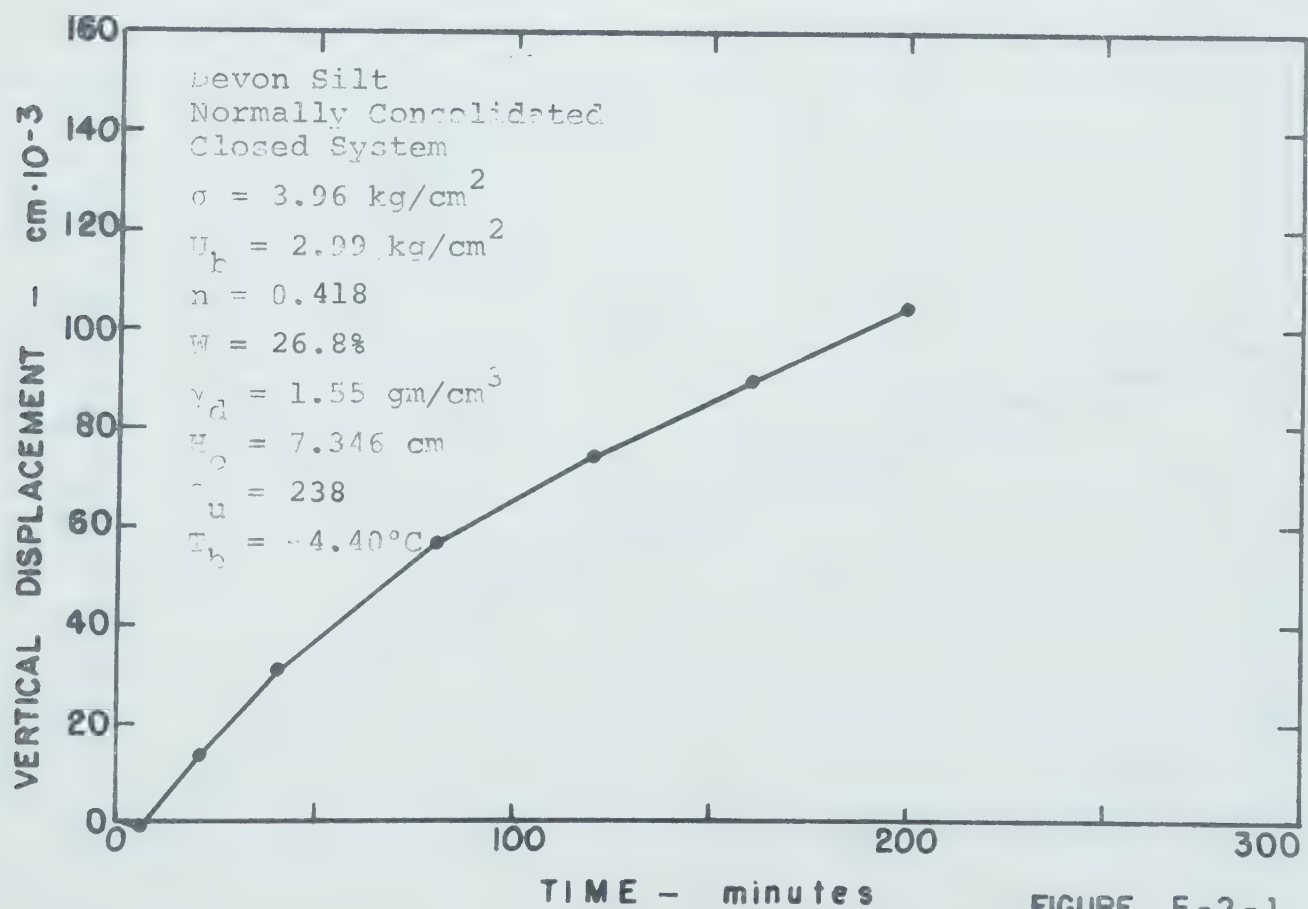
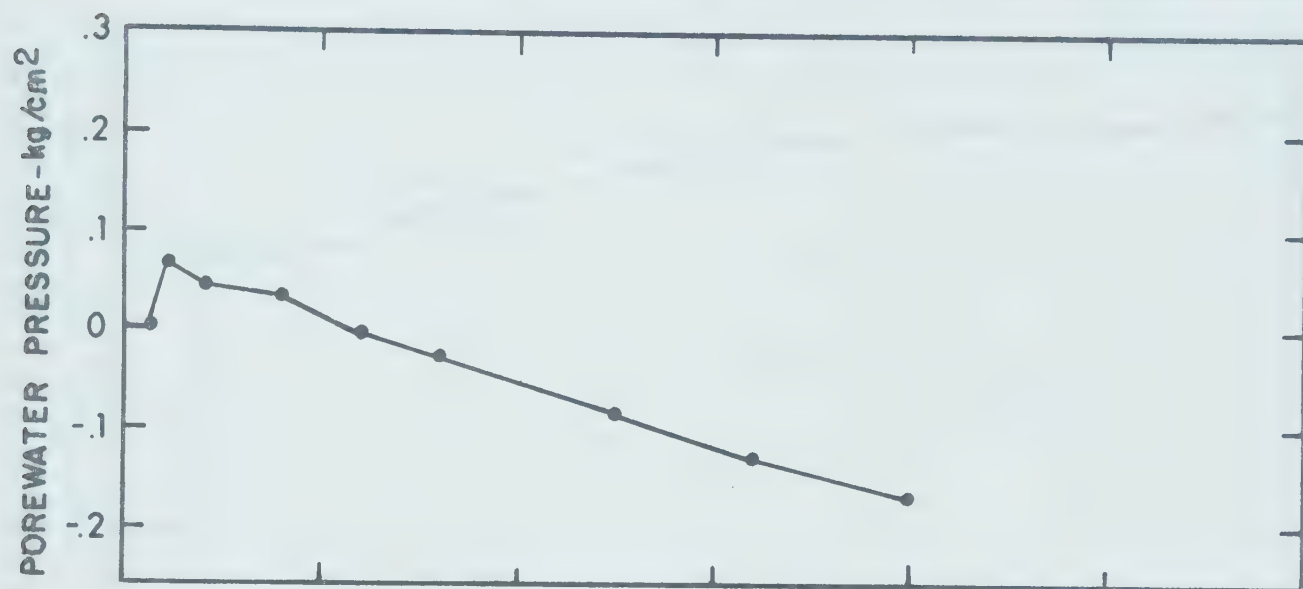
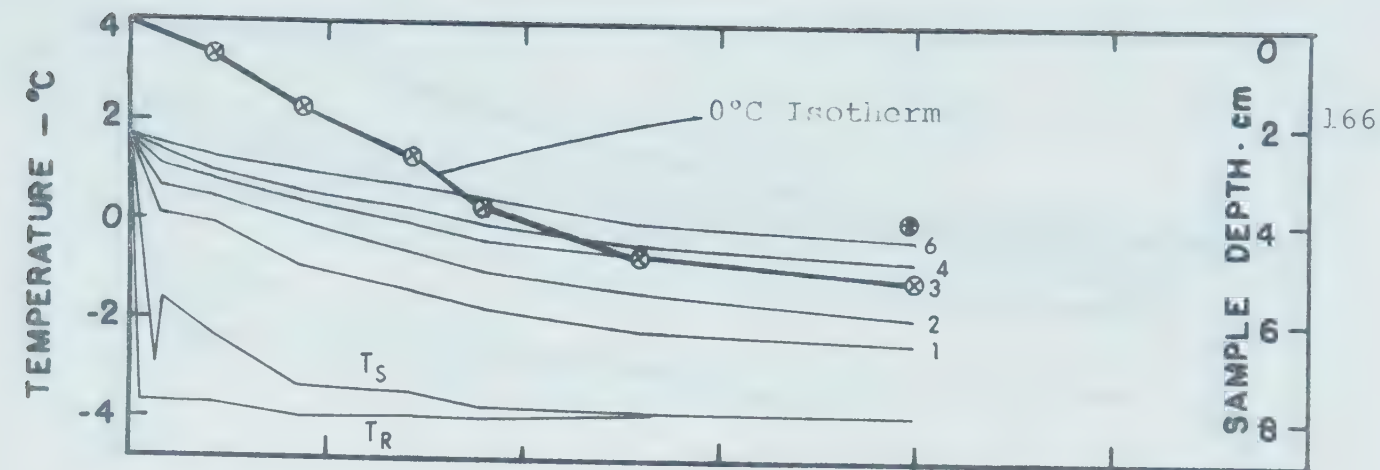


FIGURE E-2-1

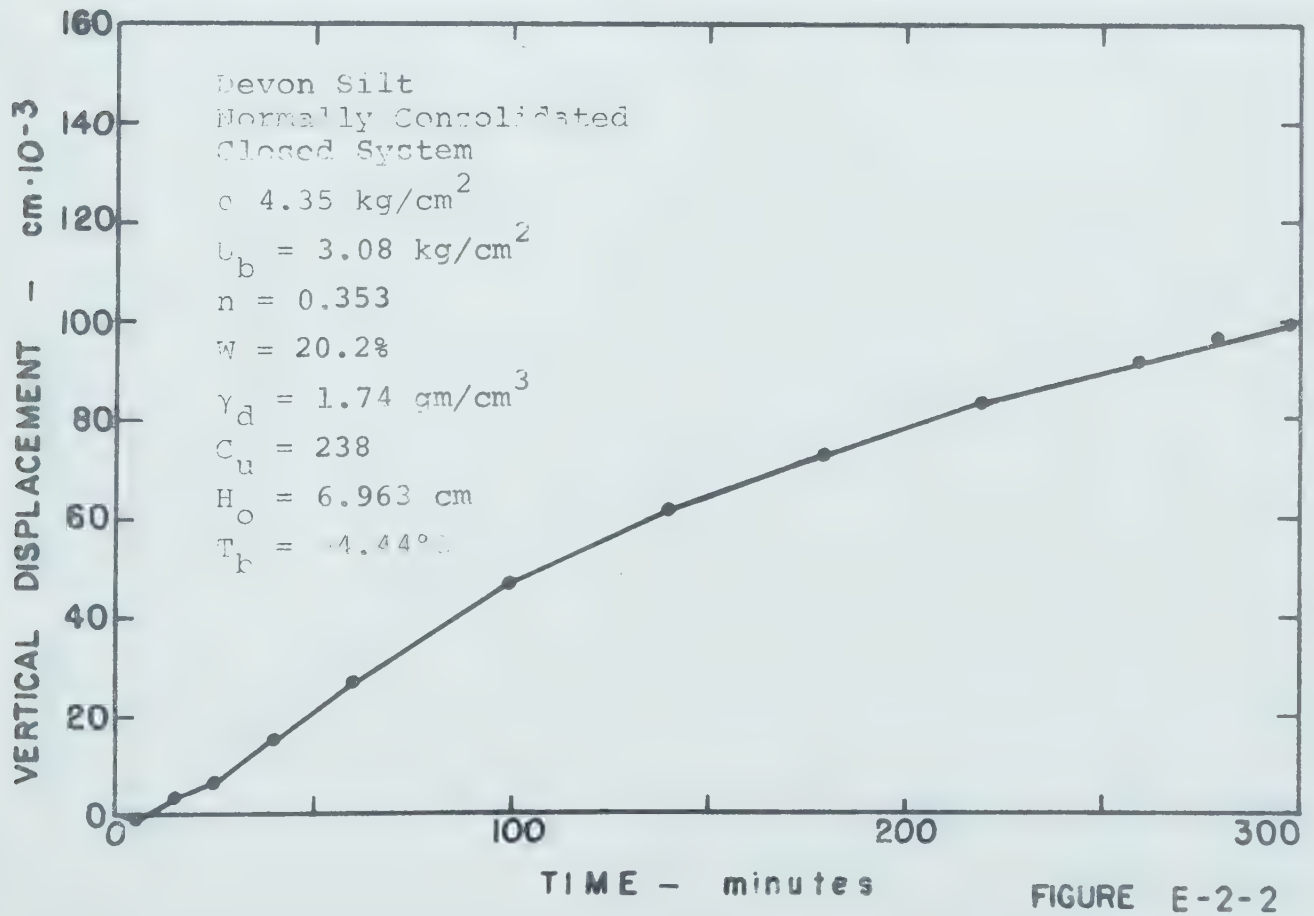
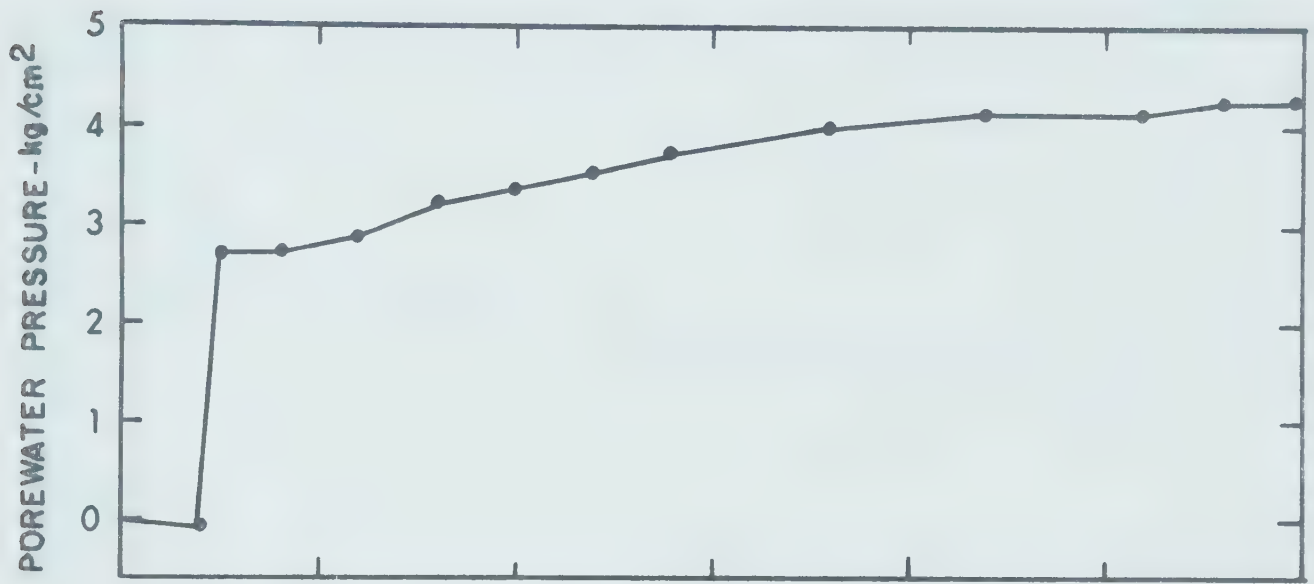
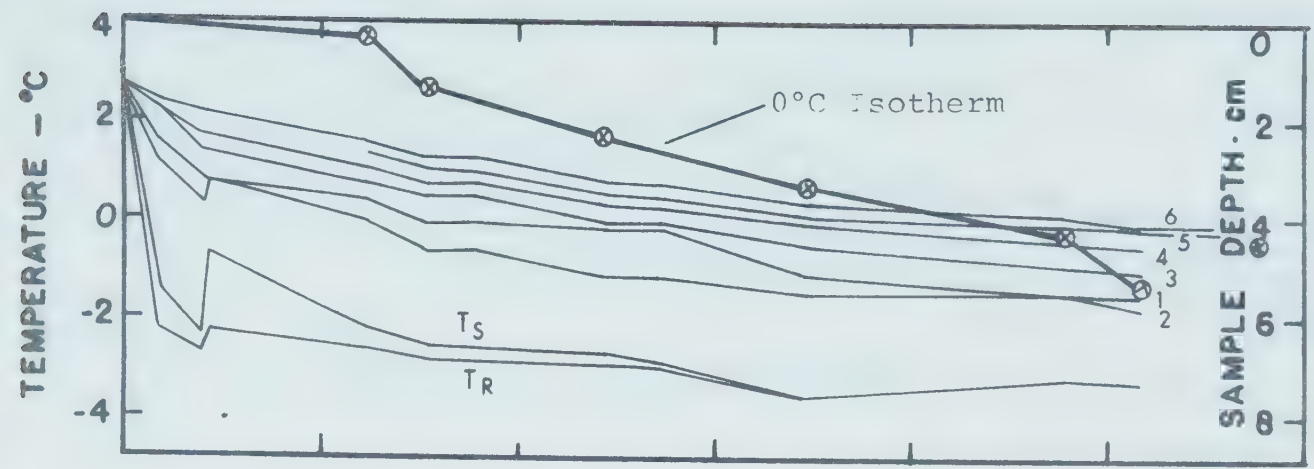


FIGURE E-2-2

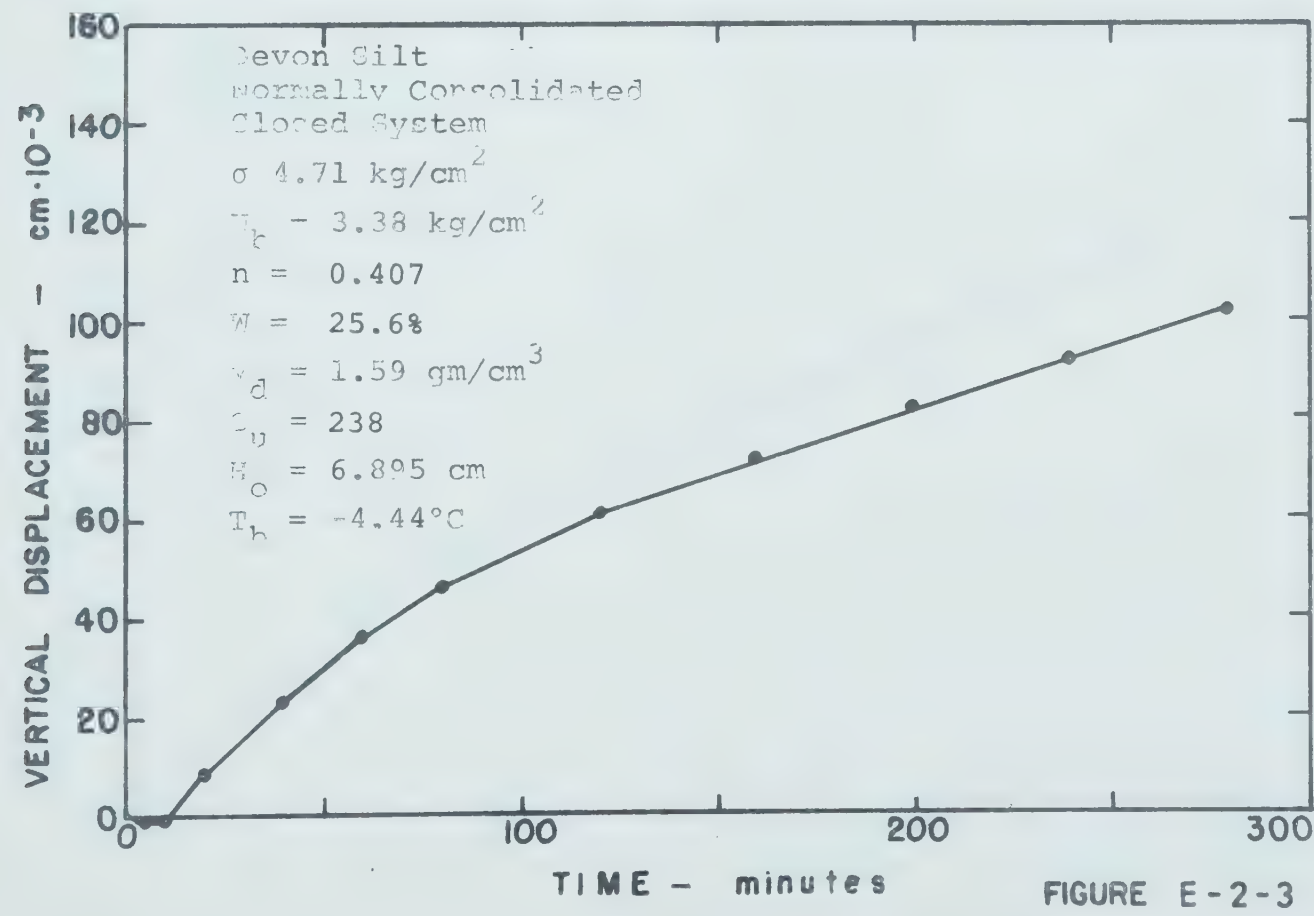
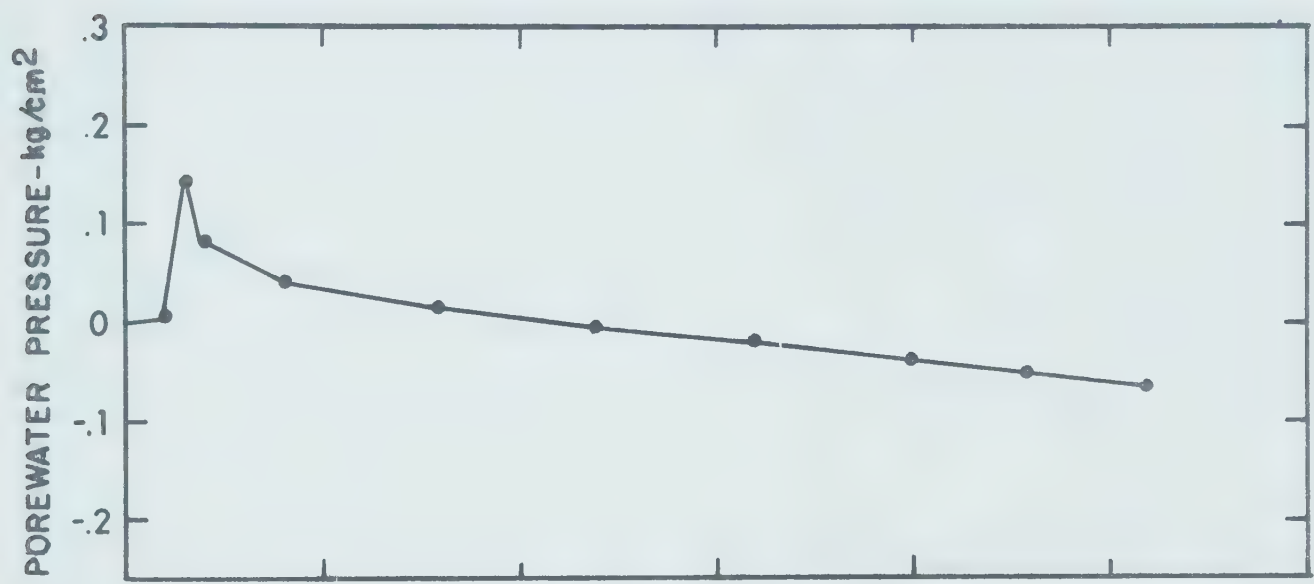
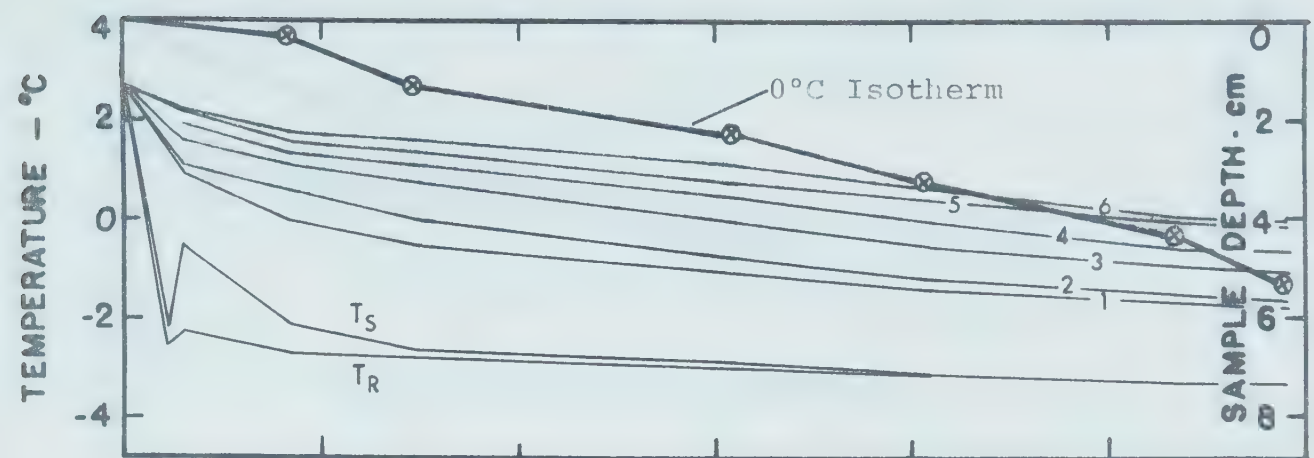


FIGURE E-2-3

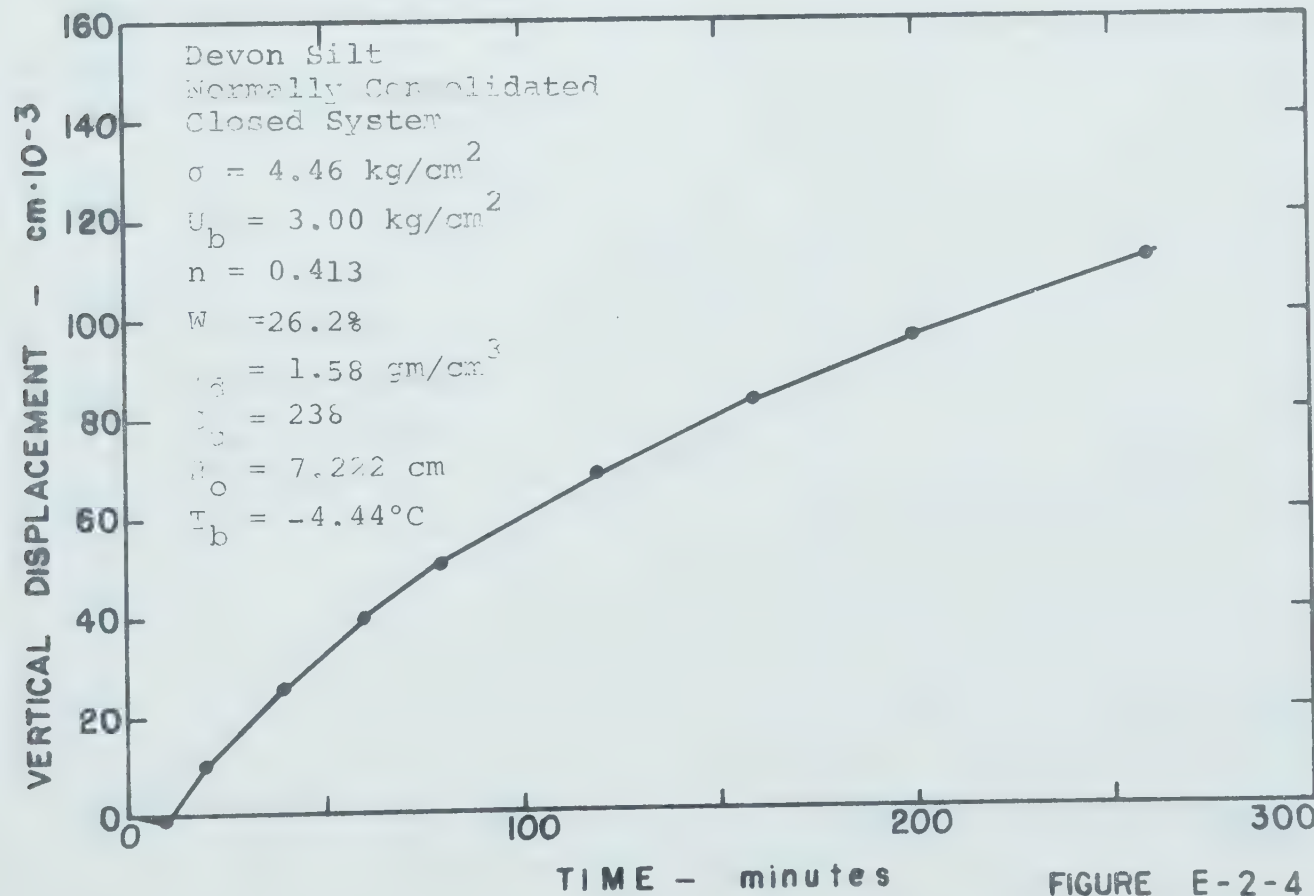
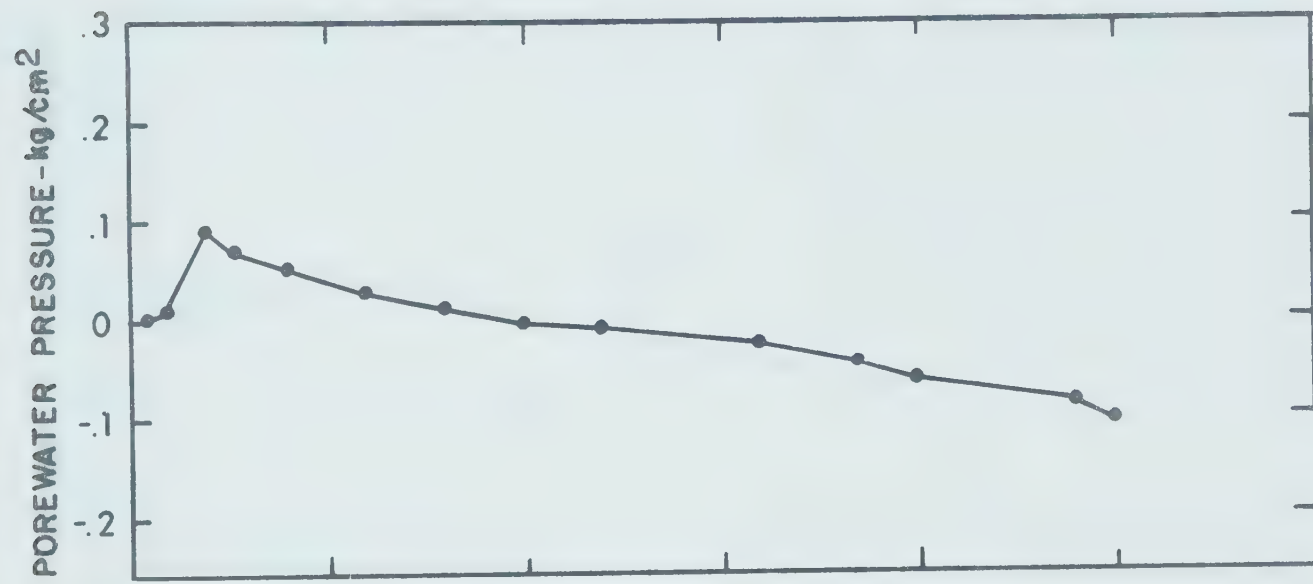
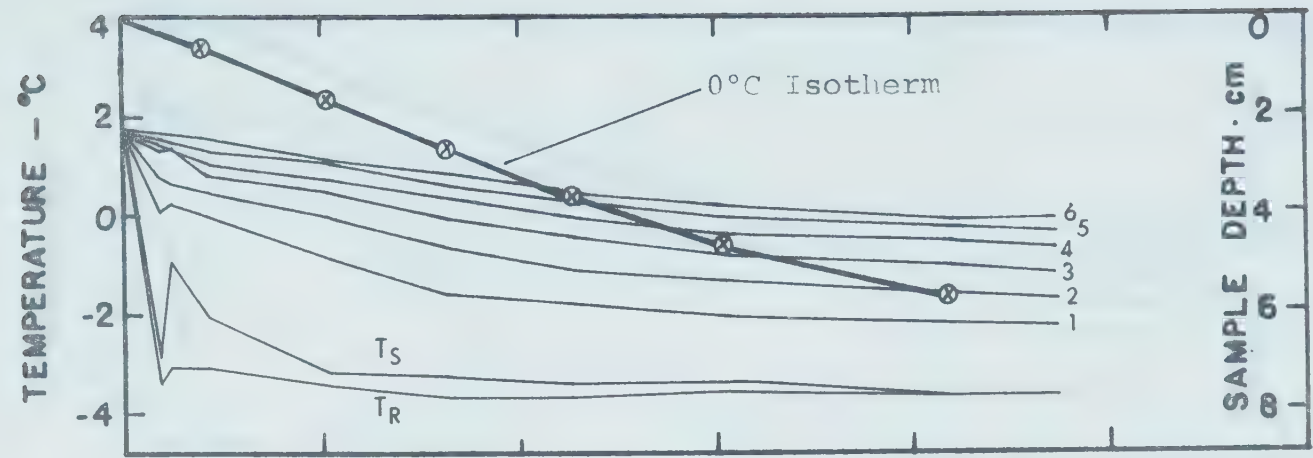


FIGURE E-2-4

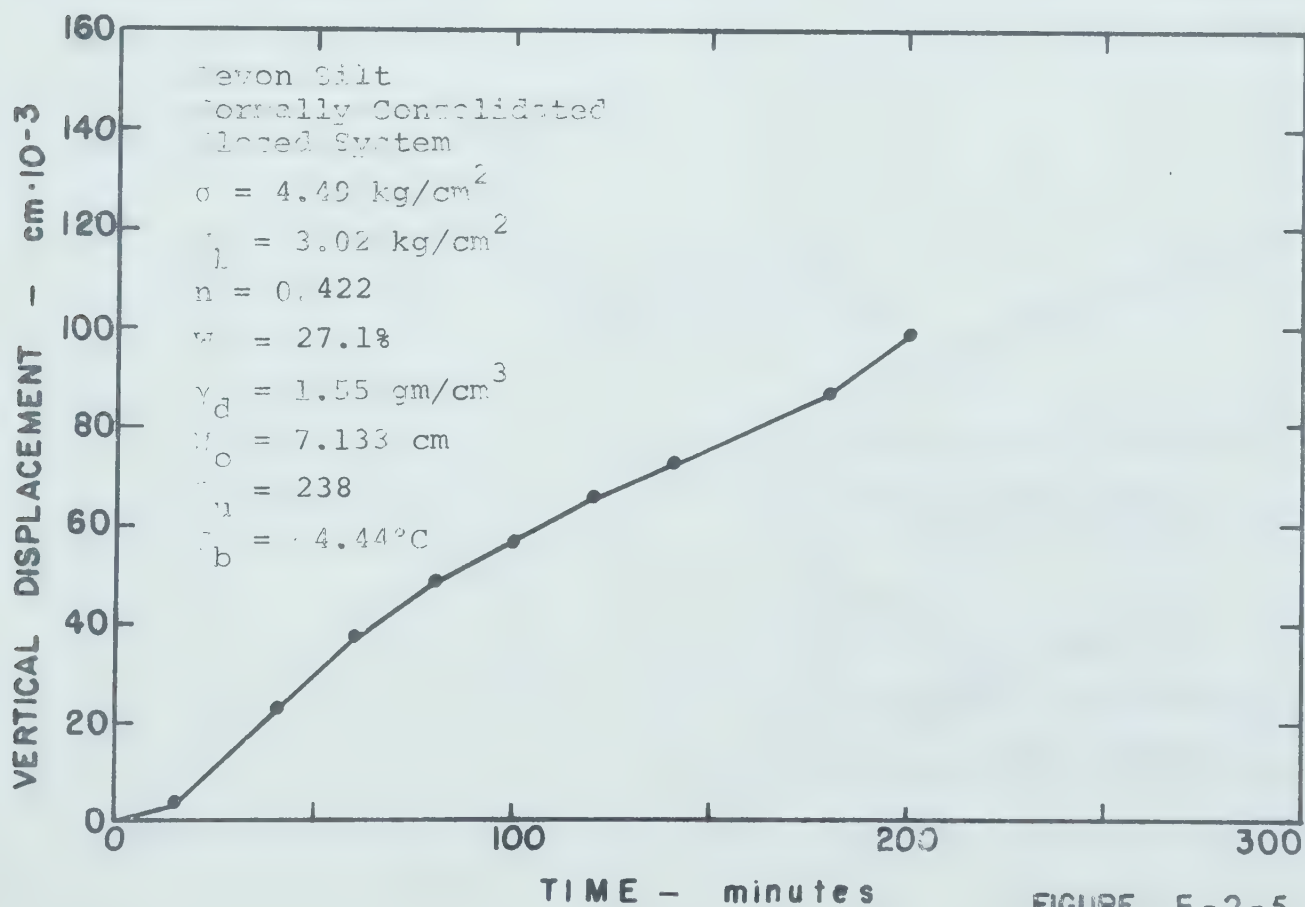
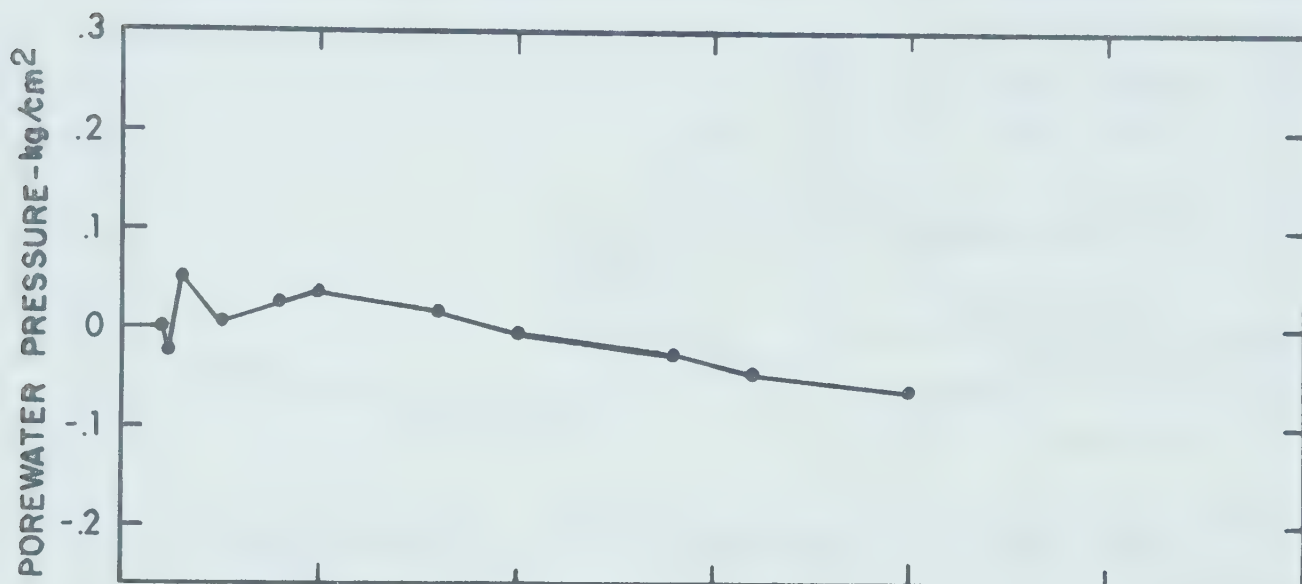
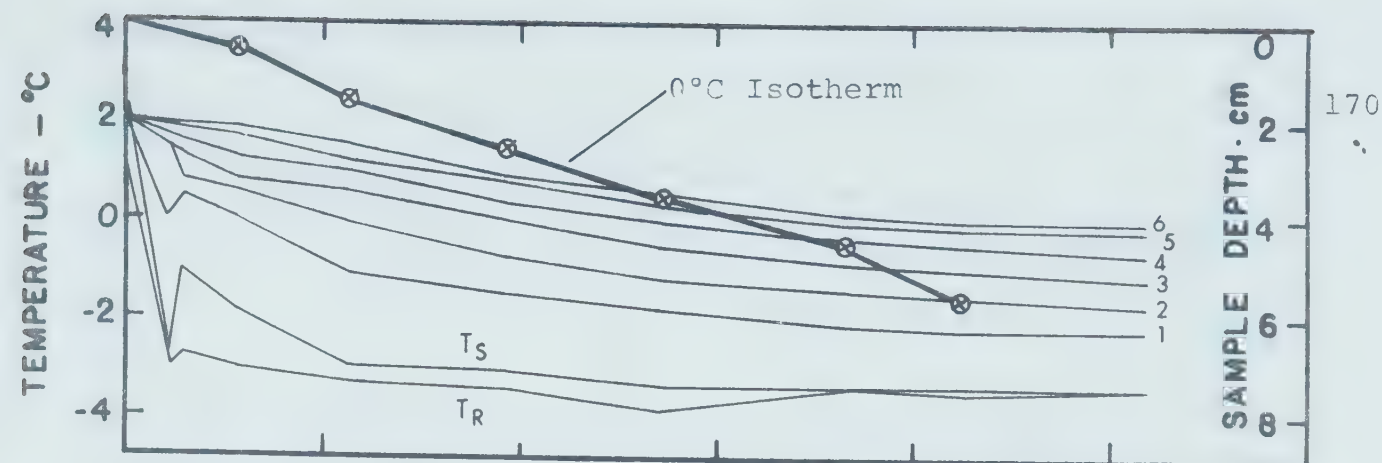


FIGURE E-2-5

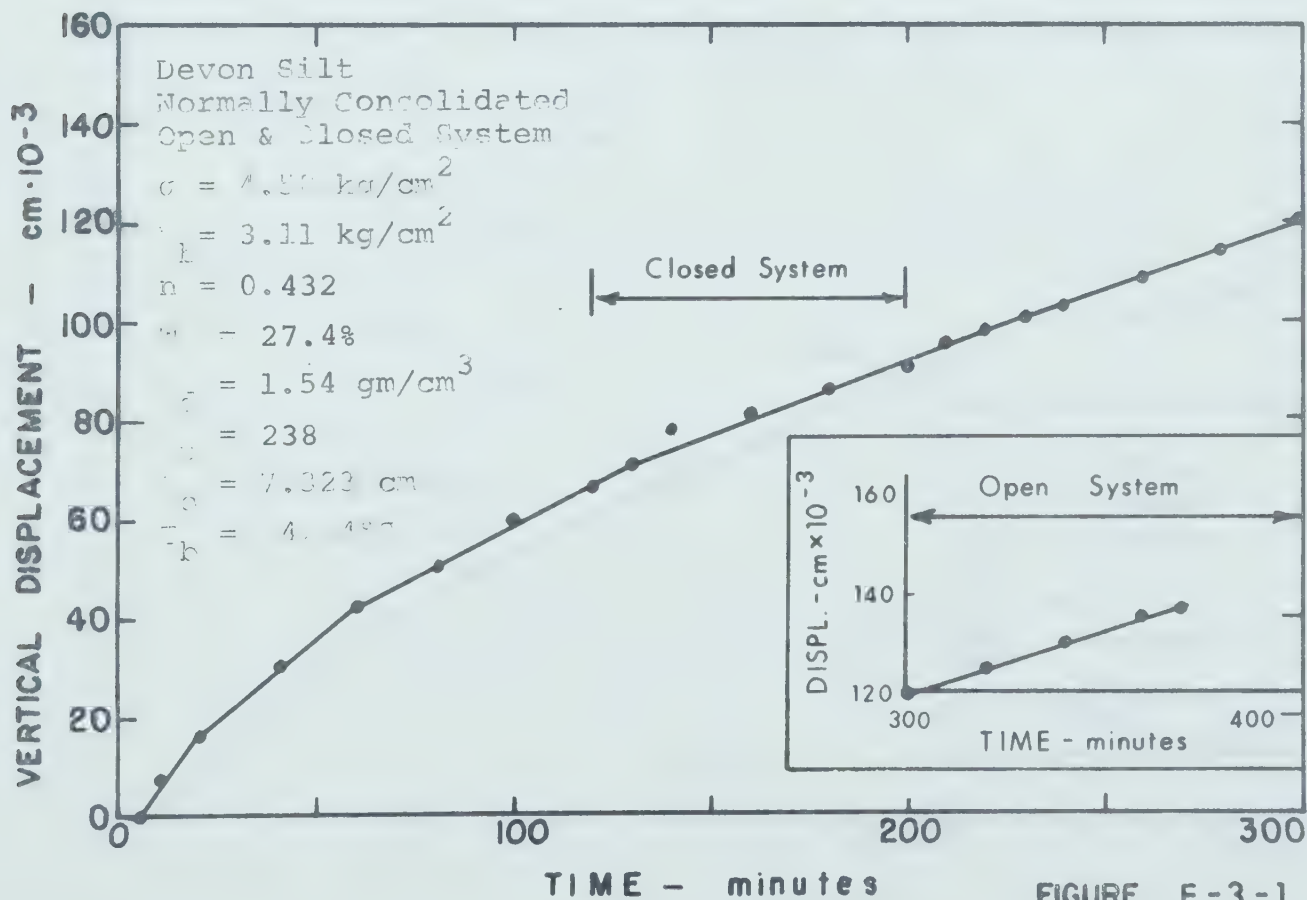
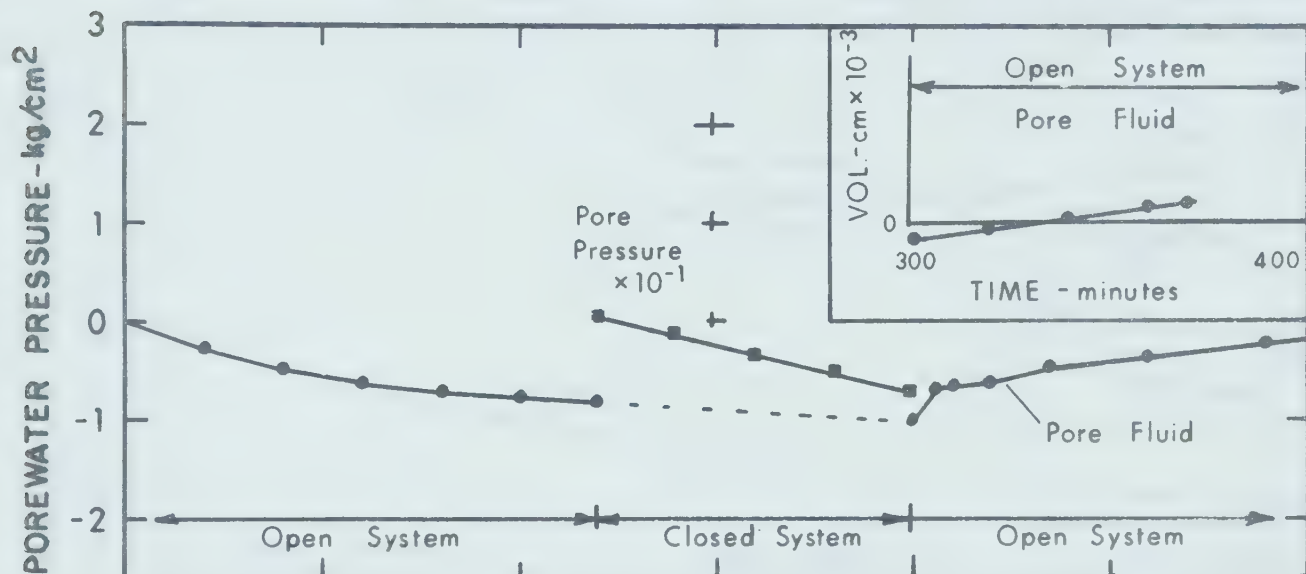
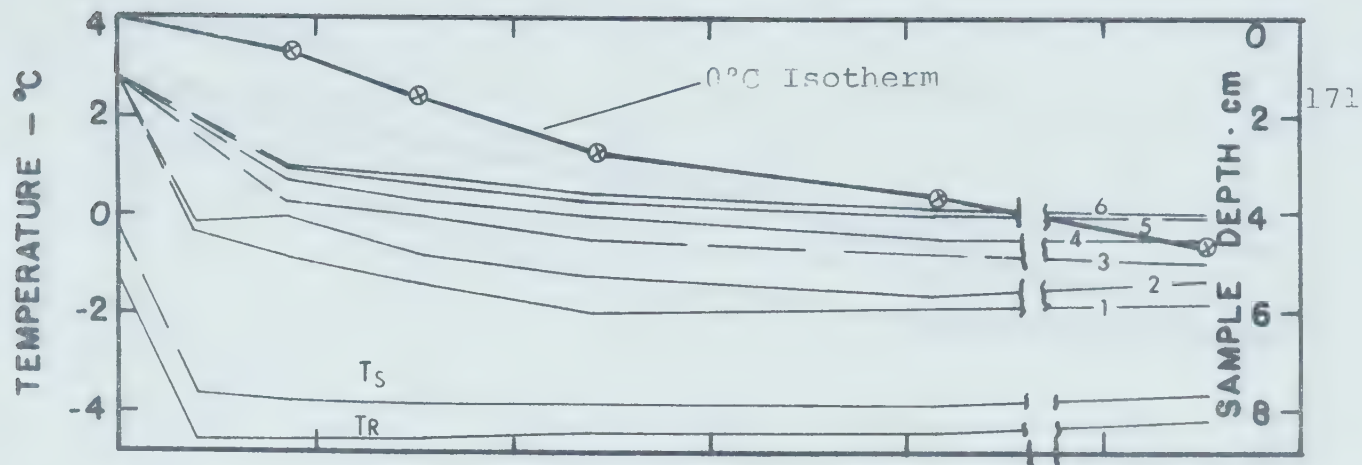


FIGURE E-3-1

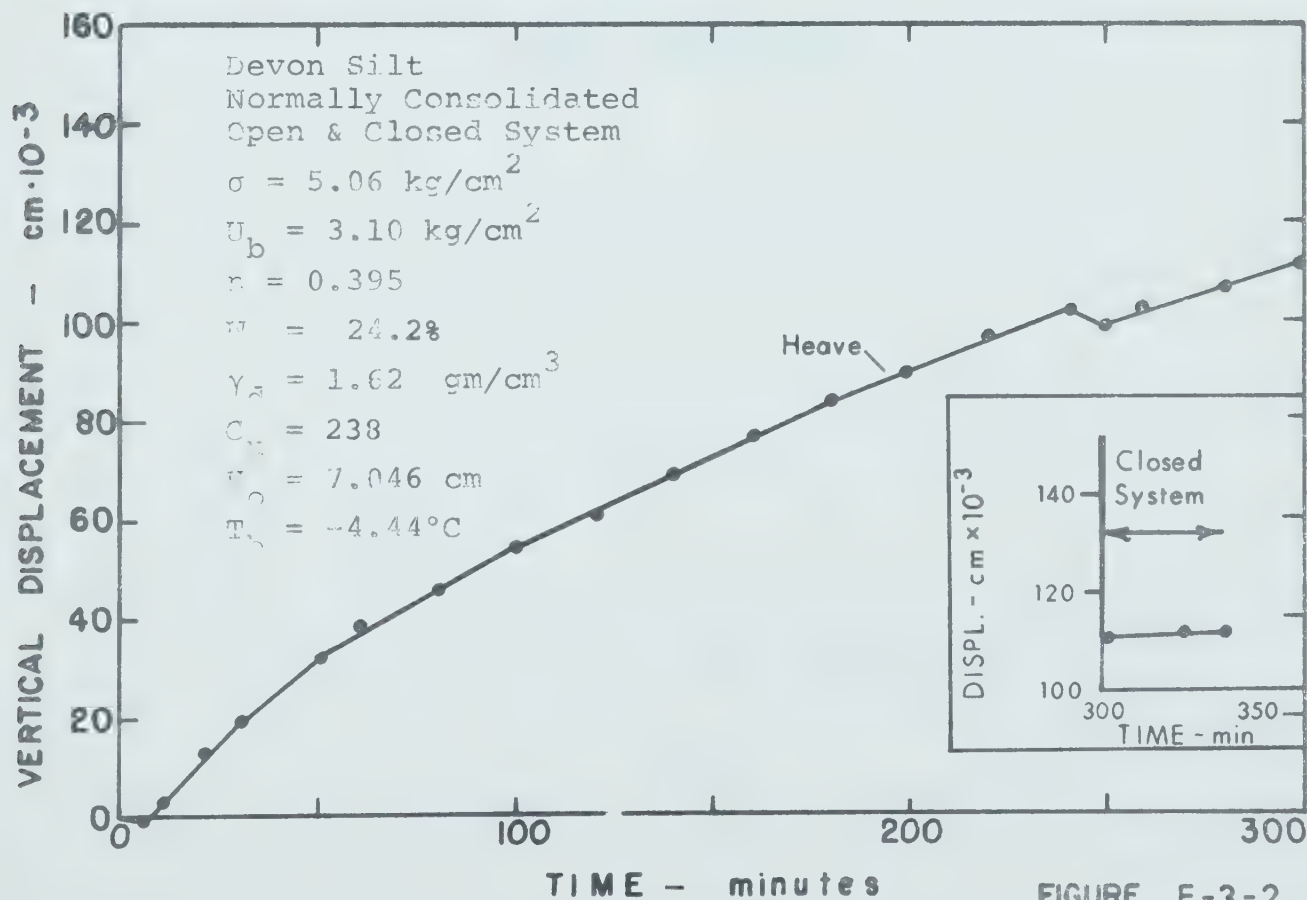
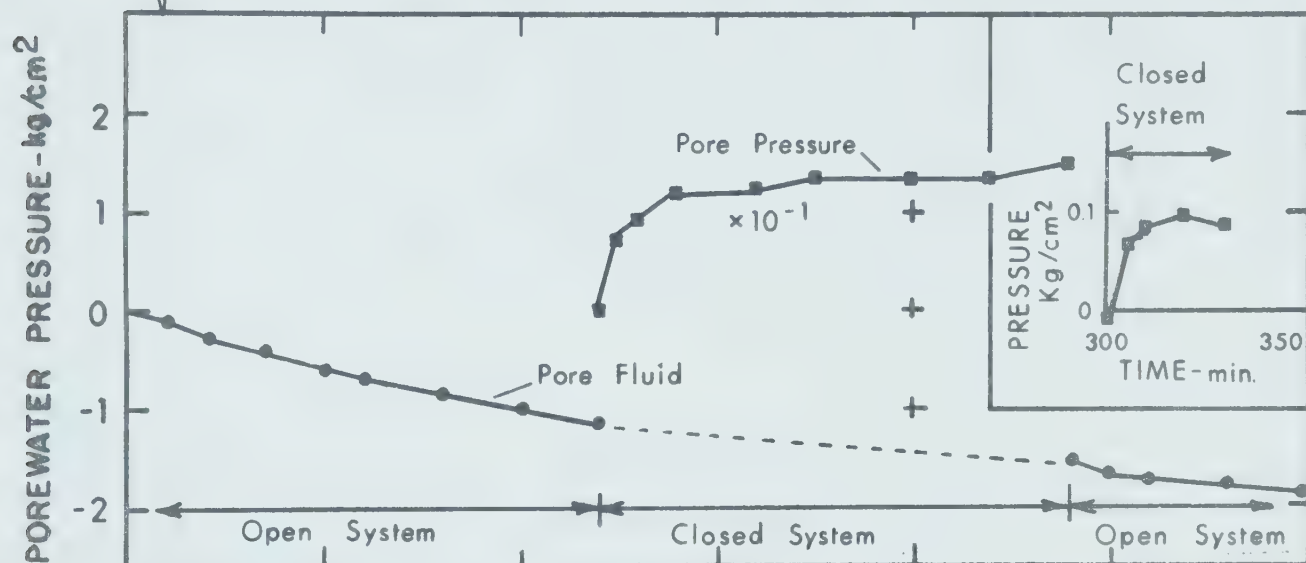
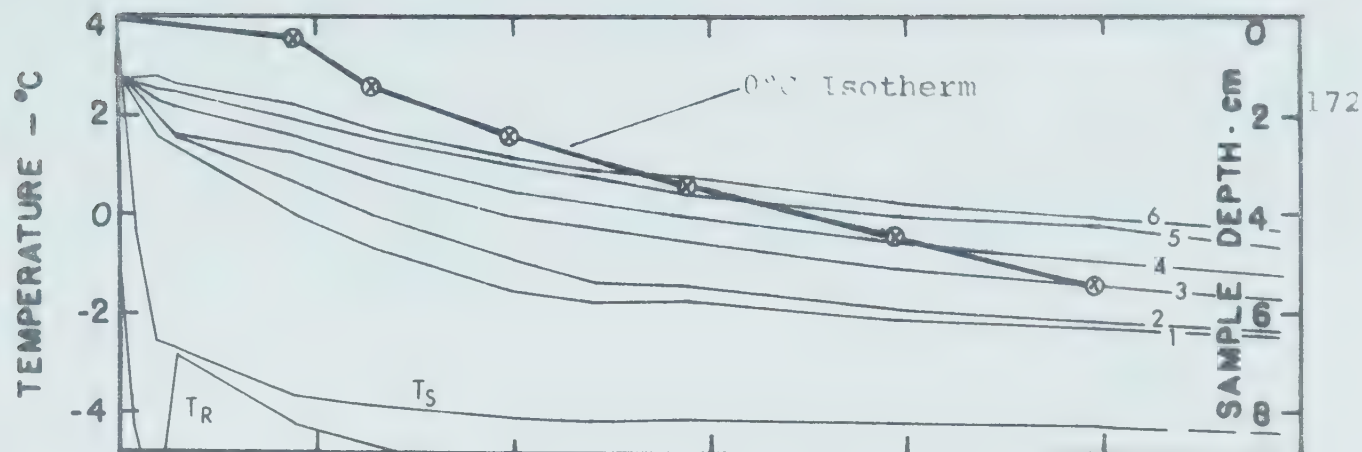


FIGURE E-3-2

APPENDIX F
SUMMARY OF DATA
DEVON SILT
(OVER CONSOLIDATED)

APPENDIX F

TABLE 1

Summary of Soil Mechanics Data

Devon Silt - Over Consolidated

Figure- Test	P_c Kg/cm ²	σ Kg/cm ²	U_b Kg/cm ²	Drainage	h_o cm	W_s gm	C_u	γ_d gm/cm ³
F-1-1	7.70	3.18	3.08	0	7.005	970.0	238	1.66
F-1-2	7.70	3.33	3.08	0	7.086	970.0	238	1.64
F-1-3	7.70	3.58	3.08	0	7.029	970.0	238	1.65
F-1-4	7.70	3.82	3.08	0	7.002	970.0	238	1.66
F-1-5	7.70	4.06	3.08	0	6.982	970.0	238	1.66
F-2-1	7.70	3.58	3.08	C	6.982	970.0	238	1.66
F-2-2	7.70	4.05	3.08	C	6.975	970.0	238	1.66
F-2-3	7.70	3.78	3.08	C	6.979	970.0	238	1.66
F-3-1	7.70	3.78	3.08	0	6.980	970.0	238	1.66
F-3-2	7.70	3.33	3.08	0	6.997	970.0	238	1.66
F-3-3	7.70	3.58	3.08	0	7.007	970.0	238	1.66
F-4-1	4.88	3.52	3.06	0	7.267	963.5	238	1.59
F-4-2	4.88	3.88	3.06	0	7.283	963.5	238	1.59
F-4-3	4.88	4.03	3.06	0	7.271	963.5	238	1.59
F-5-1	8.79	3.22	3.12	0	7.094	962.0	238	1.63
F-5-2	8.79	3.36	3.12	0	7.182	962.0	238	1.61
F-5-3	8.79	3.61	3.12	0	7.125	962.0	238	1.62
F-5-4	8.79	4.09	3.12	0	7.083	962.0	238	1.63
F-5-5	8.79	3.81	3.12	0	7.086	962.0	238	1.63

APPENDIX F

(TABLE 1 Continued)

Figure- Test	w _o %	e _o	S %	w _f %	e _f	n	C _v (cm ² /sec) x 10 ⁻³	k (cm/sec) x 10 ⁻⁶
F-1-1	50.0	1.331	100.5	22.9	0.614	0.380	2.6	0.123
F-1-2	-	-	-	23.6	0.631	0.387	-	-
F-1-3	-	-	-	23.1	0.620	0.382	-	-
F-1-4	-	-	-	22.9	0.614	0.380	-	-
F-1-5	-	-	-	22.8	0.609	0.379	-	-
F-2-1	-	-	-	22.8	0.609	0.379	-	-
F-2-2	-	-	-	22.7	0.607	0.378	-	-
F-2-3	-	-	-	22.7	0.607	0.378	-	-
F-3-1	-	-	-	22.7	0.607	0.378	-	-
F-3-2	-	-	-	22.9	0.614	0.380	-	-
F-3-3	-	-	-	22.9	0.614	0.380	-	-
F-4-1	50.2	1.342	100.0	25.6	0.686	0.407	2.94	0.197
F-4-2	-	-	-	25.8	0.690	0.407	-	-
F-4-3	-	-	-	25.7	0.687	0.407	-	-
F-5-1	51.1	1.331	102.0	24.2	0.647	0.393	5.13	0.201
F-5-2	-	-	-	24.8	0.666	0.400	-	-
F-5-3	-	-	-	24.4	0.654	0.394	-	-
F-5-4	-	-	-	24.0	0.645	0.391	-	-
F-5-5	-	-	-	24.0	0.645	0.391	-	-

0 - Open drainage
C - Closed drainage

APPENDIX F

TABLE 2

Summary of Freezing Test Data

Devon Silt - Over Consolidated

Note: + ΔV , -uporewater sucked in
 - ΔV , +uporewater expelled

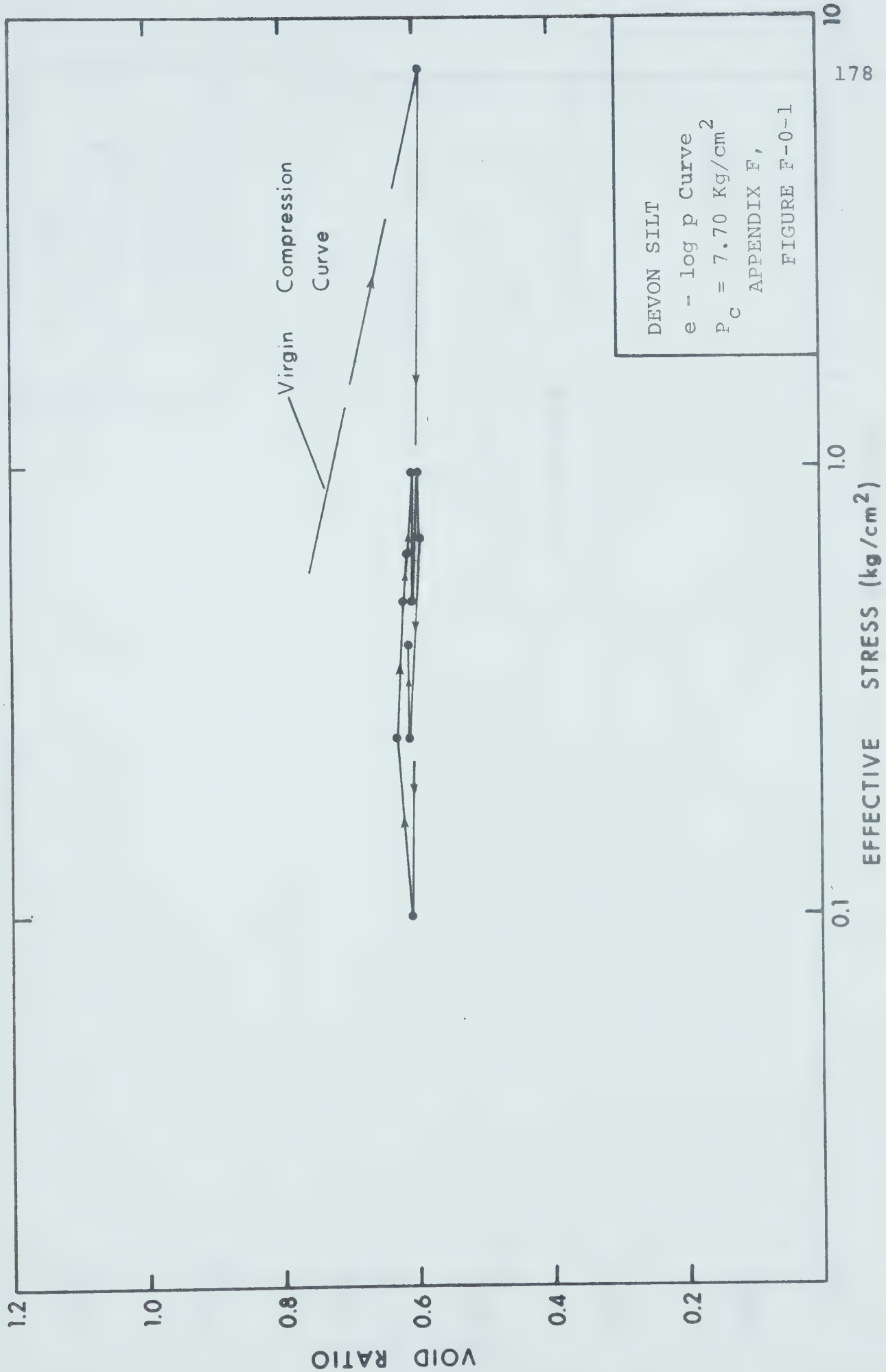
Figure- Test	T _b °C	t min	X thmc* cm	t min	X meas. cm	α_a cm/ $\sqrt{\text{min}}$ thmc* meas.
F-1-1	-4.44	330	5.405	-	-	0.299
F-1-2	-4.94	202	5.486	-	-	0.385
F-1-3	-4.44	164	5.429	-	-	0.384
F-1-4	-5.00	202	5.402	-	-	0.381
F-1-5	-4.79	206	5.382	-	-	0.375
F-2-1	-4.44	183	5.382	-	-	0.397
F-2-2	-4.94	178	5.375	-	-	0.402
F-2-3	-5.00	157	5.379	-	-	0.428
F-3-1	-9.72	110	5.380	-	-	0.514
F-3-2	-9.72	112	5.397	-	-	0.509
F-3-3	-9.78	100	5.407	124	4.429	0.541
F-4-1	**	92	3.667	-	-	0.382
F-4-2	-5.24	190	2.683	-	-	0.195
F-4-3	-4.72	-	-	-	-	-
F-5-1	-5.56	182	5.494	-	-	0.406
F-5-2	-4.78	226	5.582	-	-	0.371
F-5-3	-5.00	178	5.525	-	-	0.414
F-5-4	-5.17	155	5.483	-	-	0.441
F-5-5	-5.17	176	5.486	-	-	0.412
						0.338

APPENDIX F

(TABLE 2 Continued)

Figure - Test	ΔV 3 cm	at t = 160 min		
		Heave S, cm	Porewater Pressure, u, Kg/cm ²	Heave Pressure P _h , Kg/cm ²
F-1-1	+4.75	0.132	-	-
F-1-2	+2.24	0.107	-	-
F-1-3	+1.10	0.088	-	-
F-1-4	-0.22	0.068	-	-
F-1-5	-1.49	0.047	-	-
F-2-1	-	0.071	-0.05	-
F-2-2	-	0.067	+0.50	-
F-2-3	-	0.071	+0.14	-
F-3-1	-0.90*	0.092*	-	-
F-3-2	+2.80*	0.144*	-	-
F-3-3	+0.58*	0.127*	-	-
F-4-1	+5.80	0.156	-	-
F-4-2	+1.32	0.077	-	-
F-4-3	-0.88*	0.091*	-	-
F-5-1	+6.90	0.159	-	-
F-5-2	+2.90	0.107	-	-
F-5-3	+1.33	0.094	-	-
F-5-4	-1.12	0.066	-	-
F-5-5	-3.93	0.016	-	+1.62

** T_b = -7.36°C first 30 minutes of test * extrapolated to t = 160 min
 -4.83°C for remainder of test thmc* - thermocouple



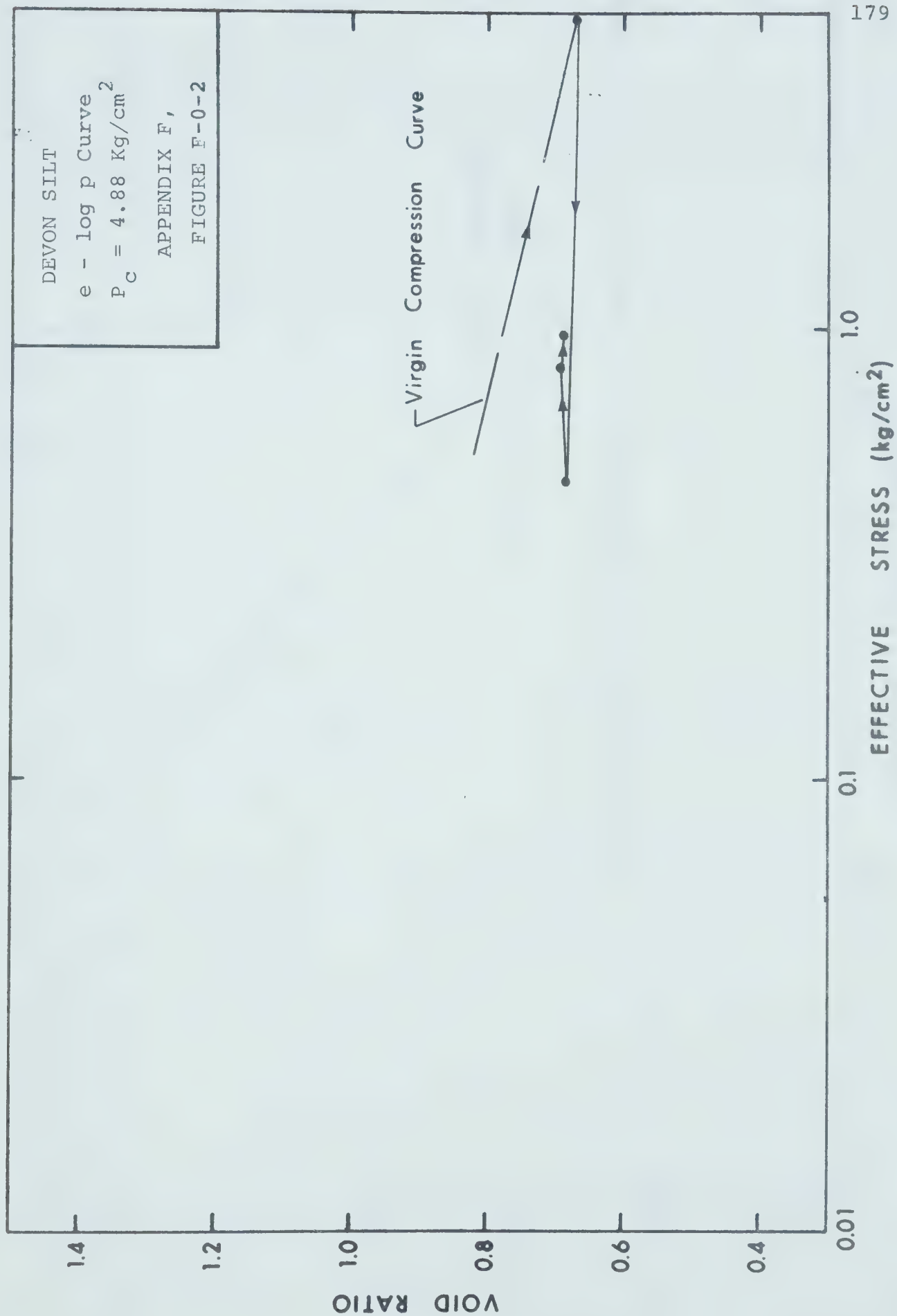
DEVON SILT

e - log p Curve

$P_C = 7.70 \text{ Kg/cm}^2$

APPENDIX F,

FIGURE F-0-1



DEVON SILT

$e - \log p$

$P_c = 7.70 \text{ Kg/cm}^2$

APPENDIX F,

FIGURE F-0-3

VOID RATIO

Virgin Compression
Curve

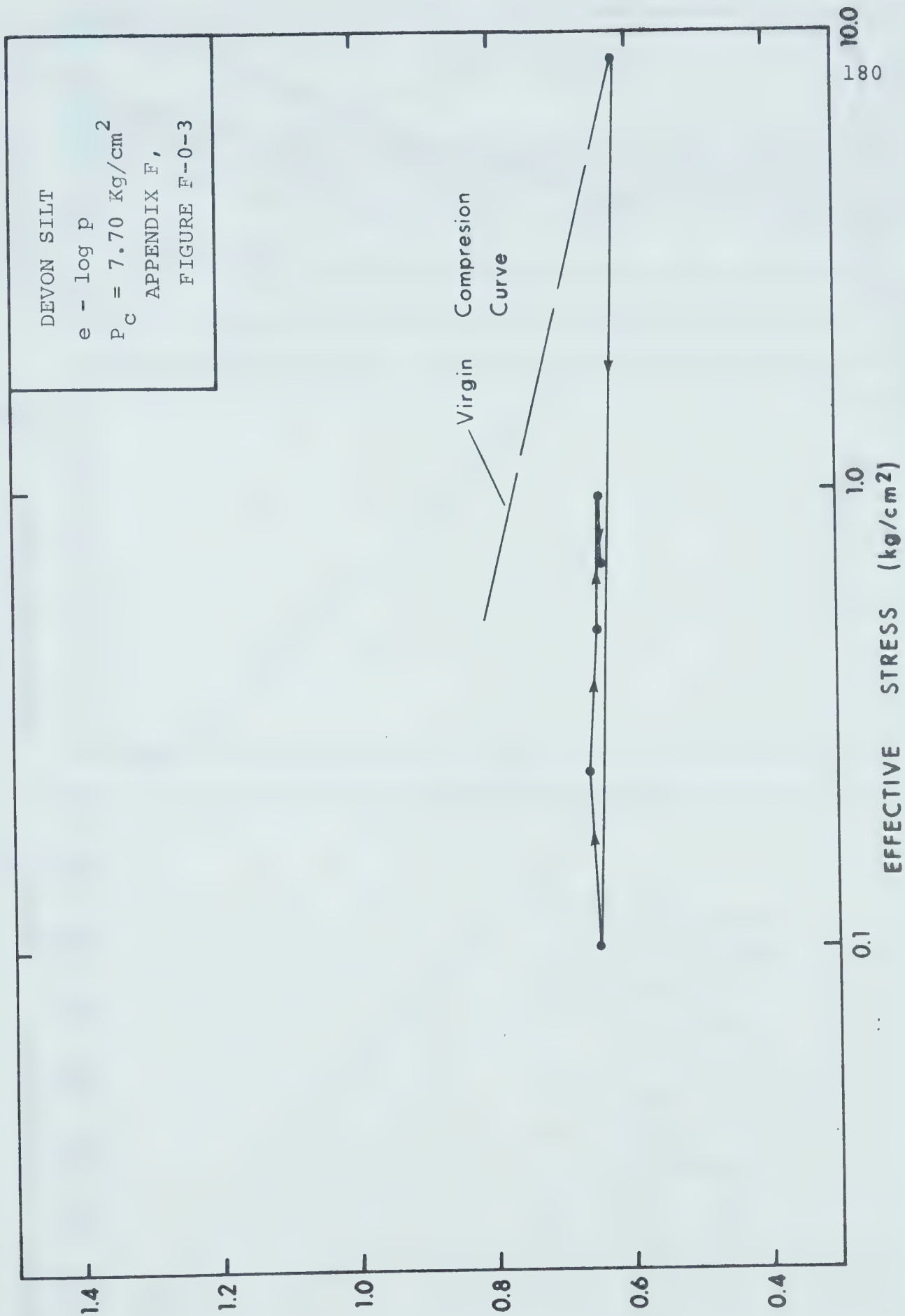
EFFECTIVE STRESS (kg/cm^2)

0.1

1.0

10.0

180



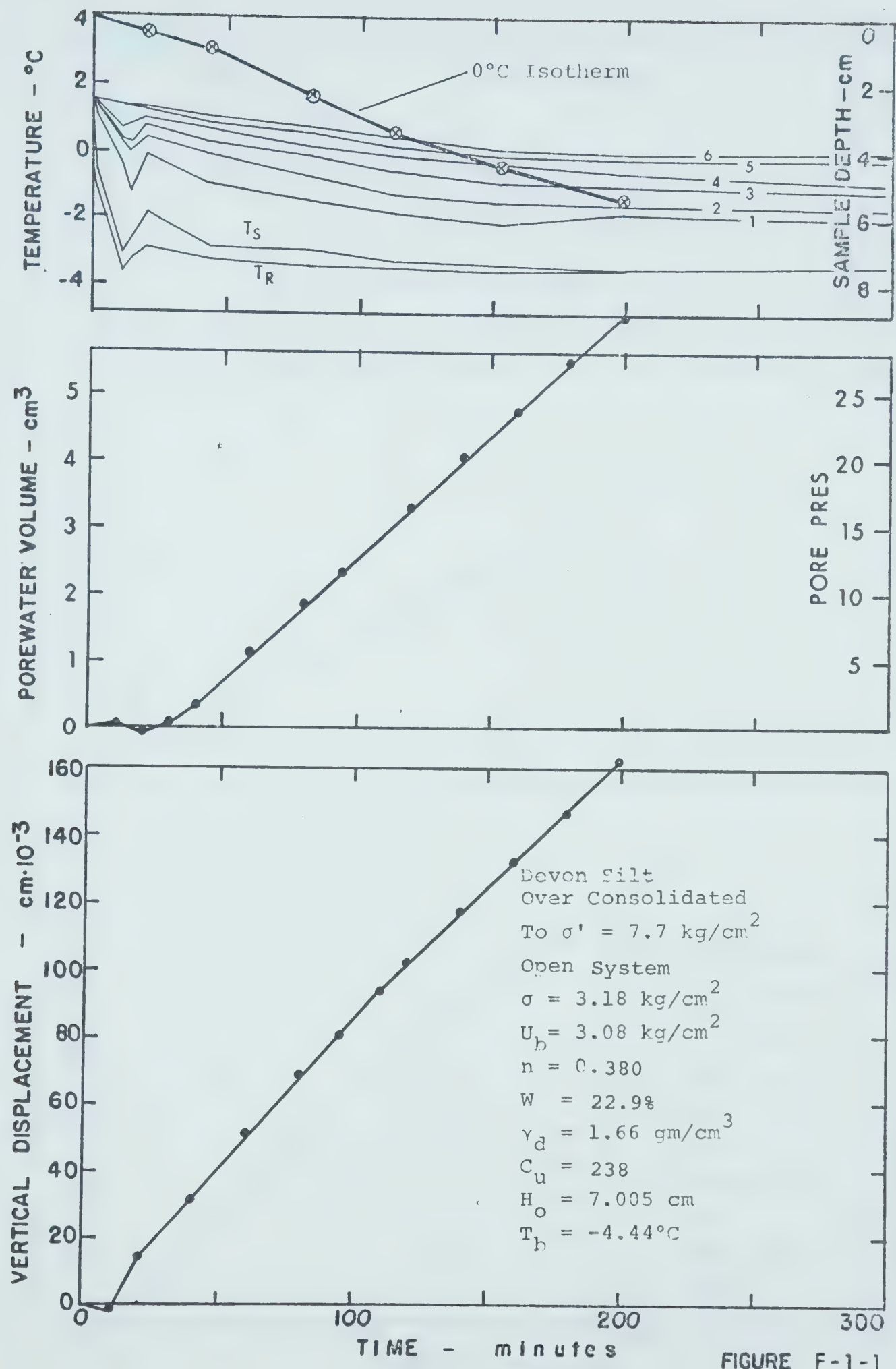


FIGURE F-1-1

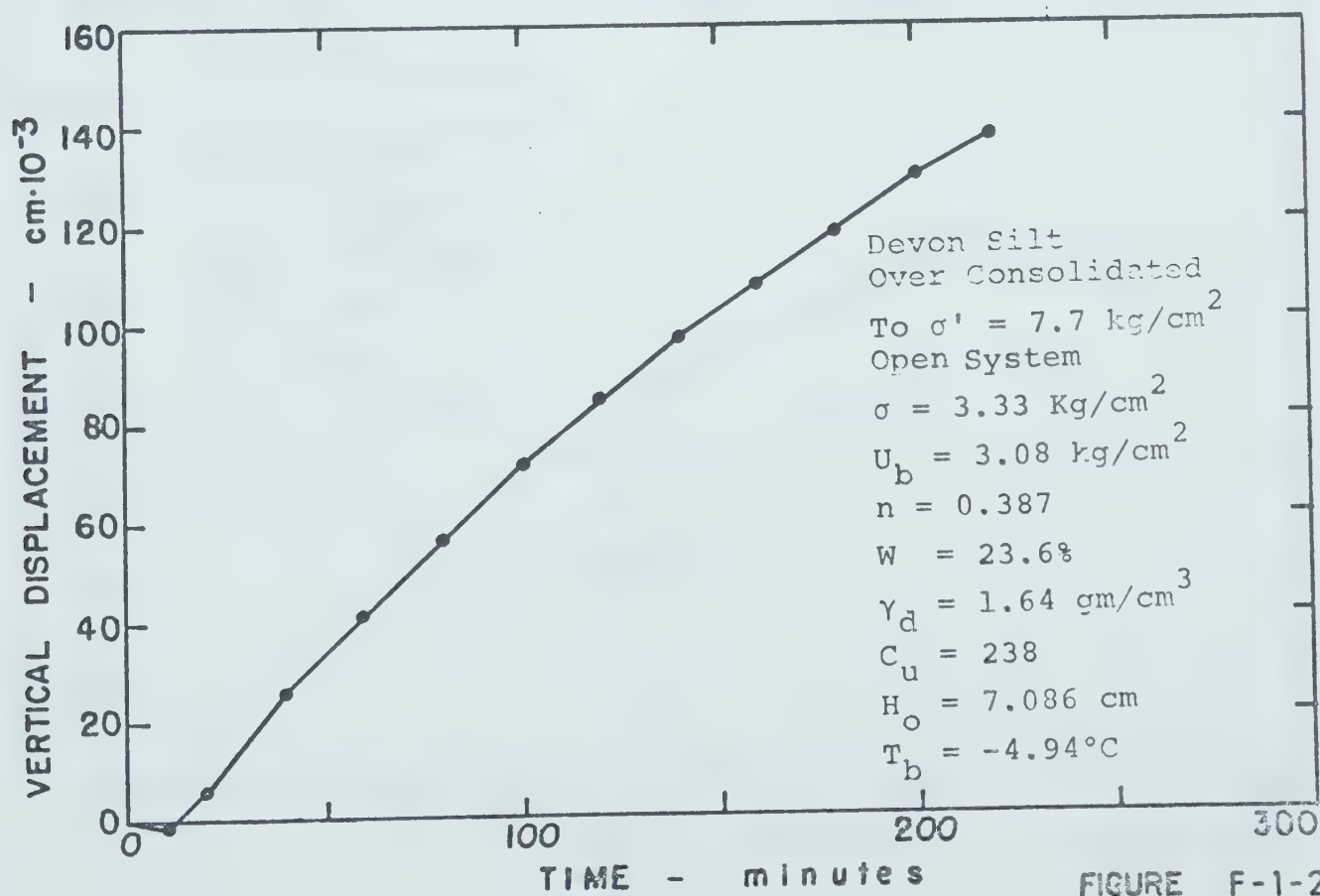
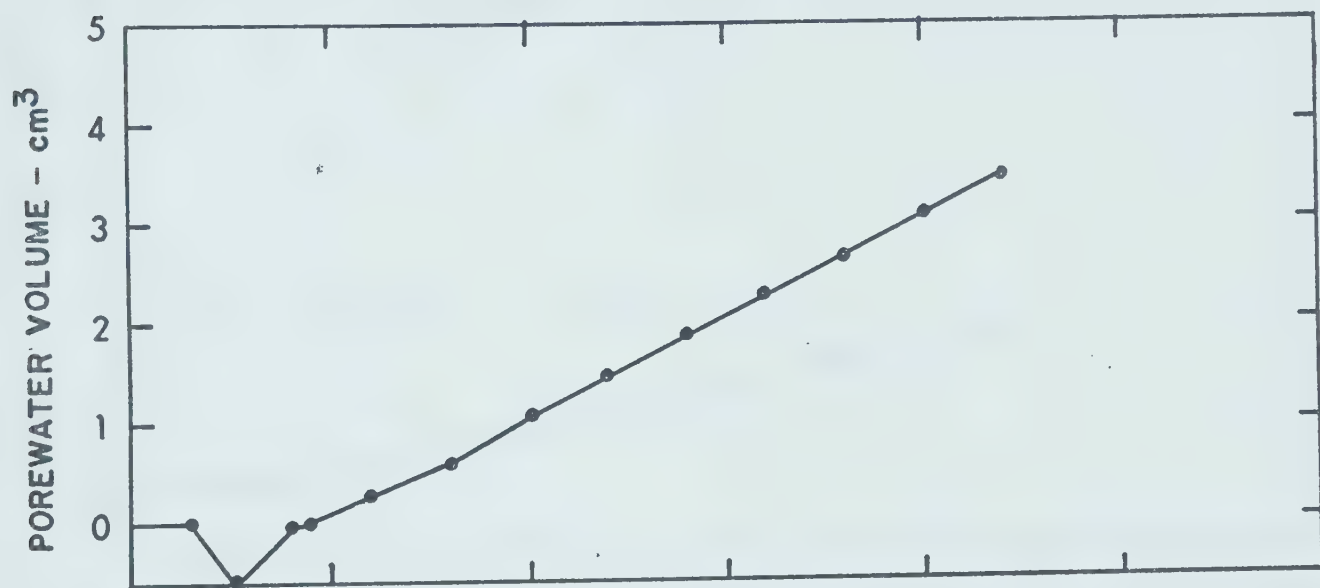
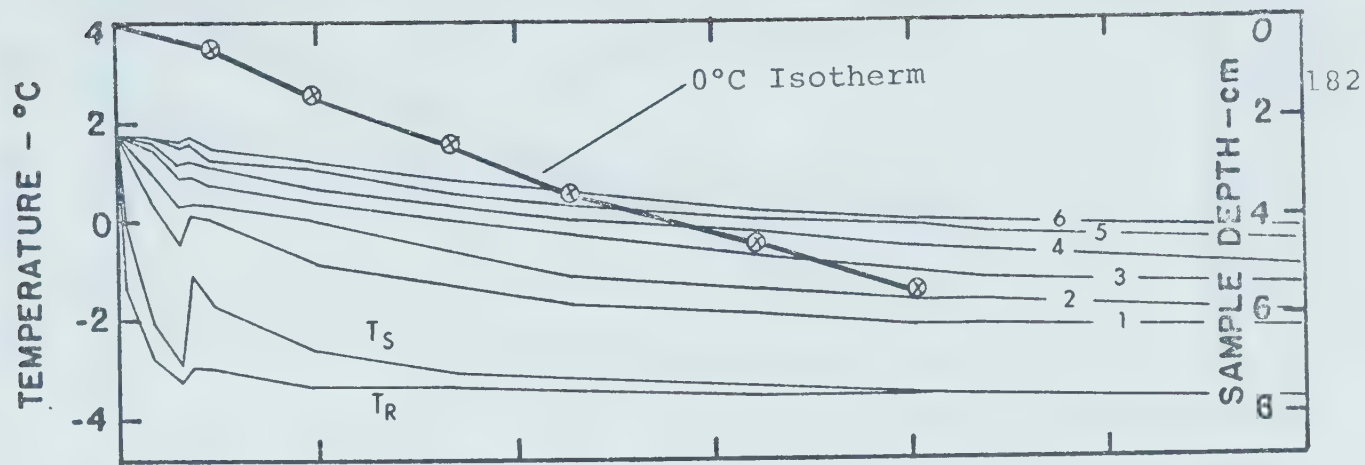


FIGURE F-1-2

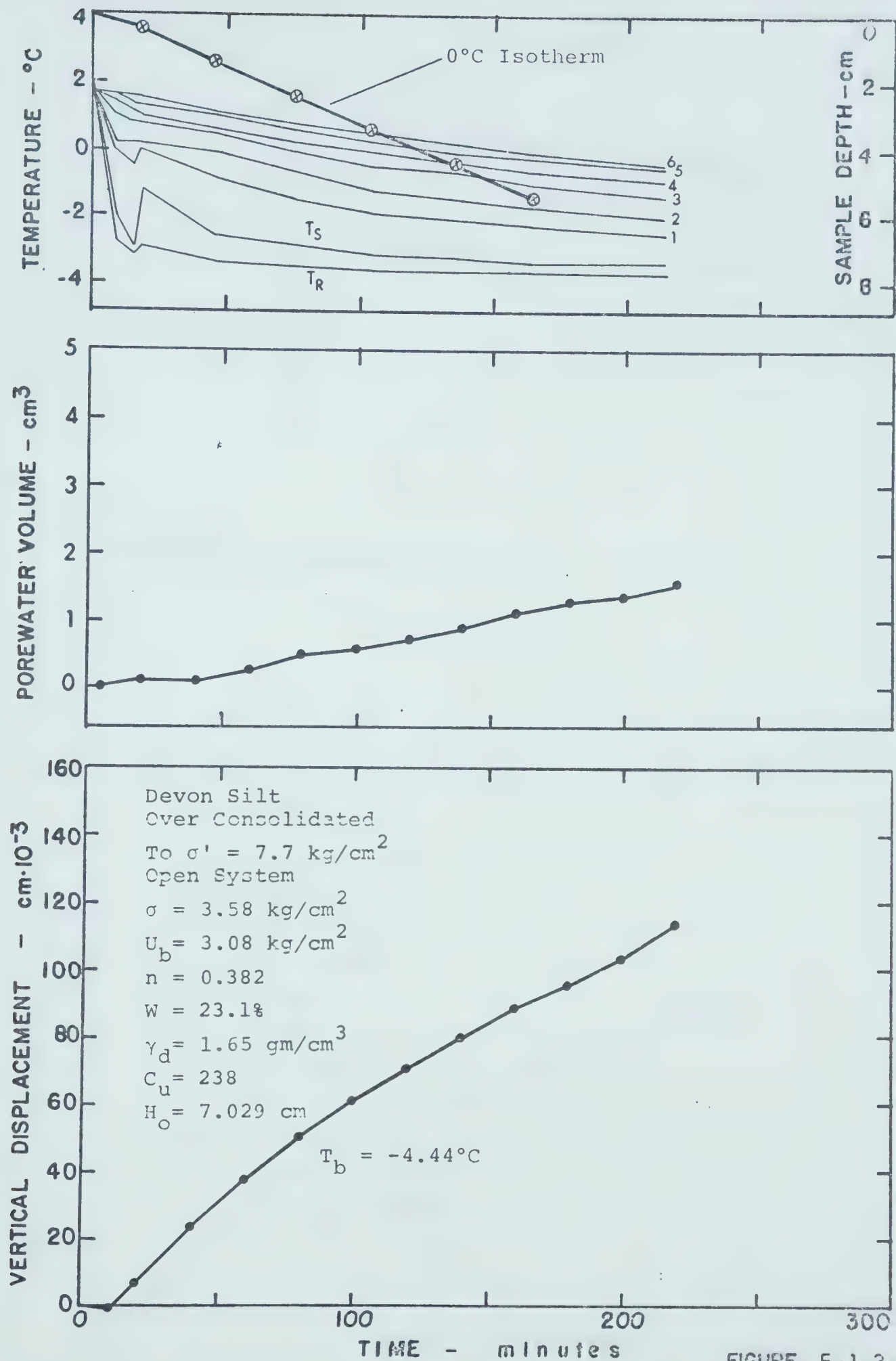


FIGURE F-1-3

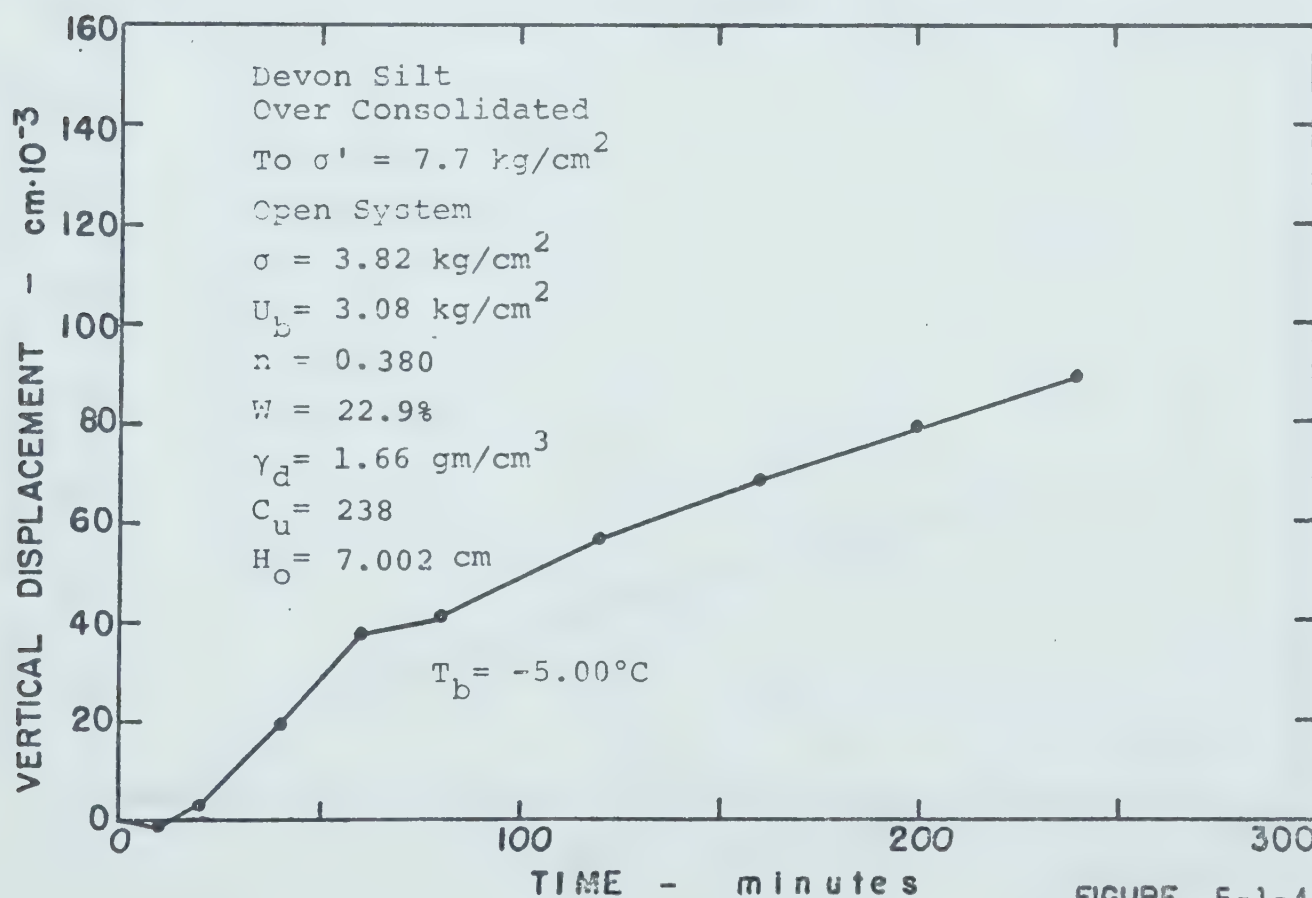
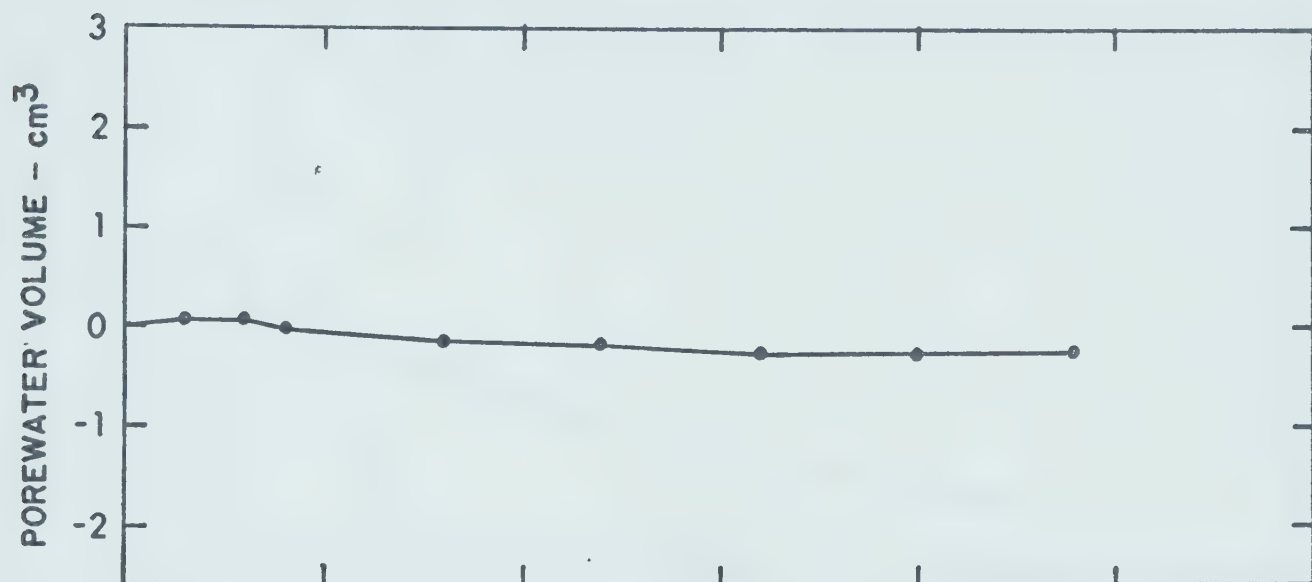
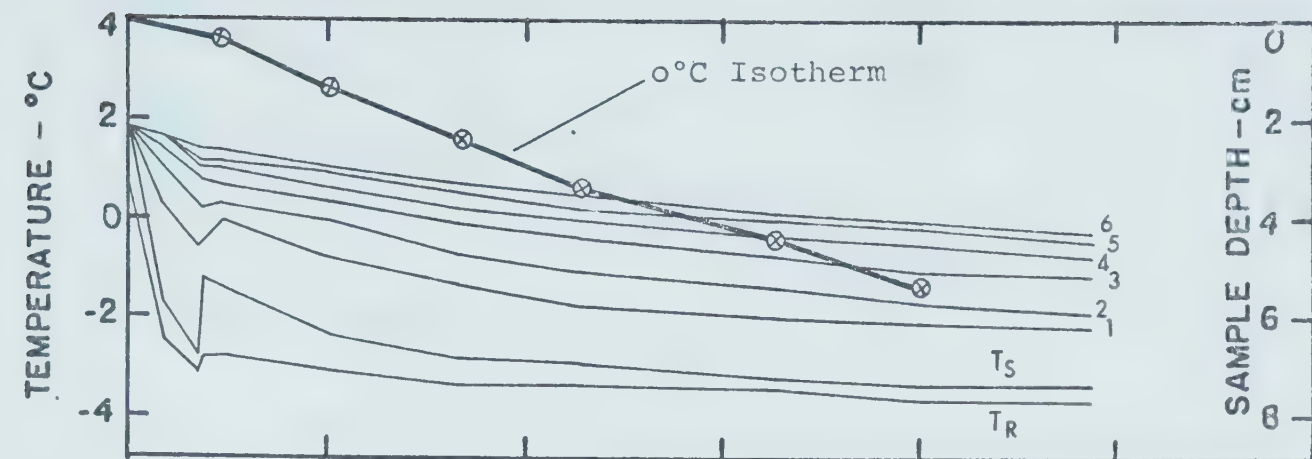


FIGURE F-1-4

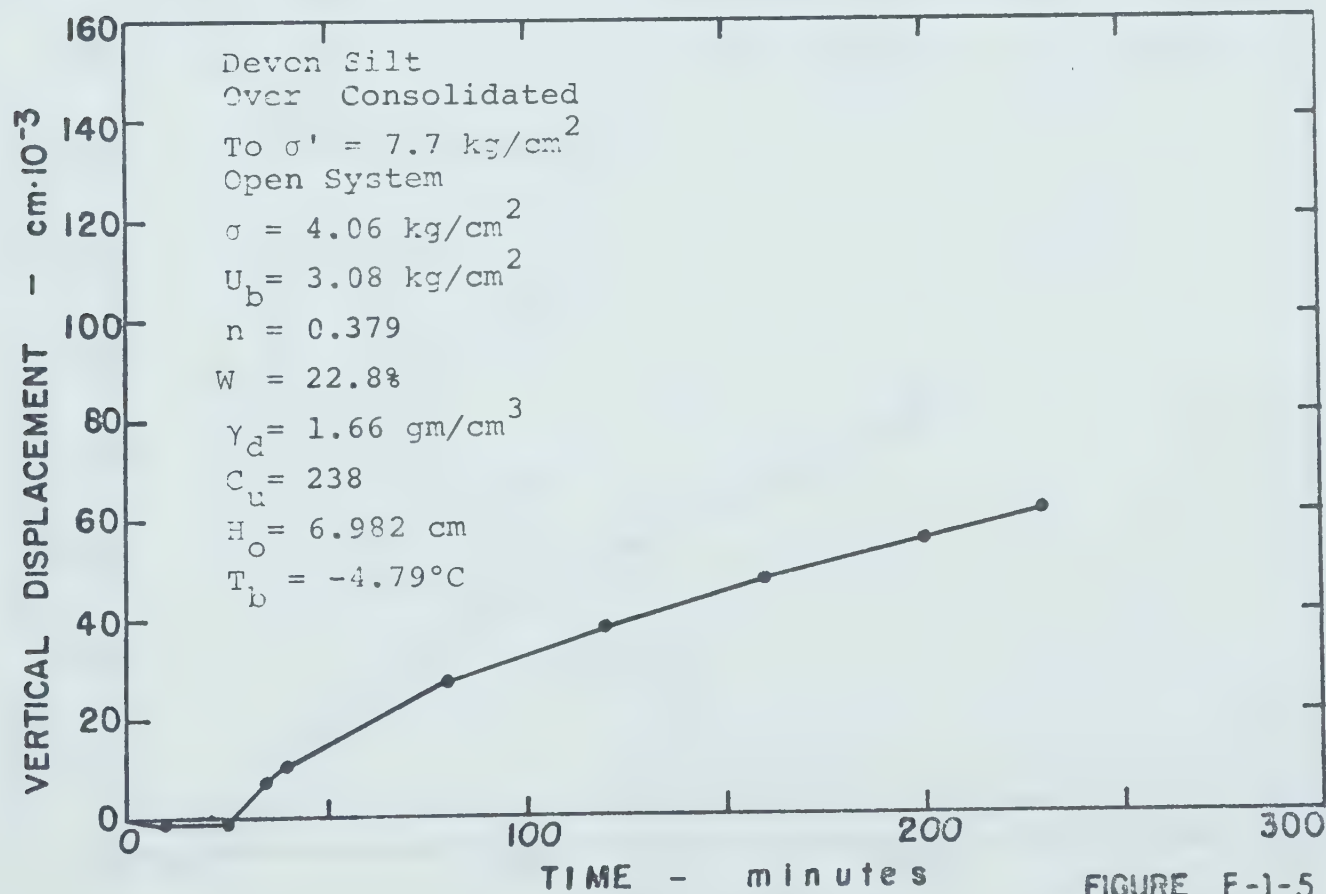
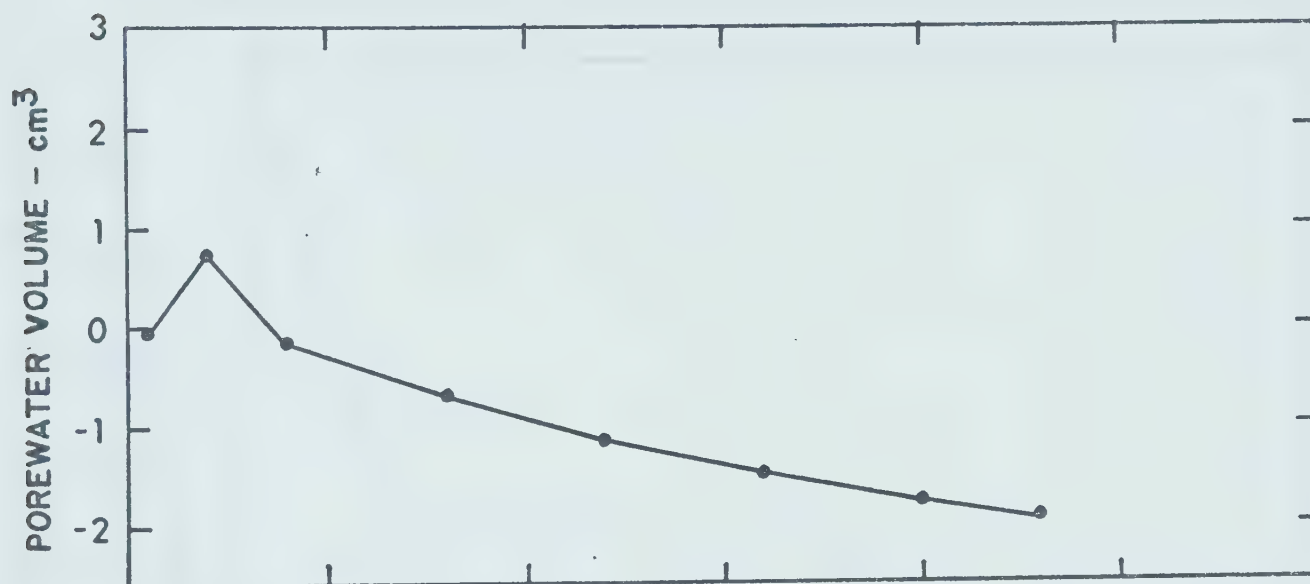
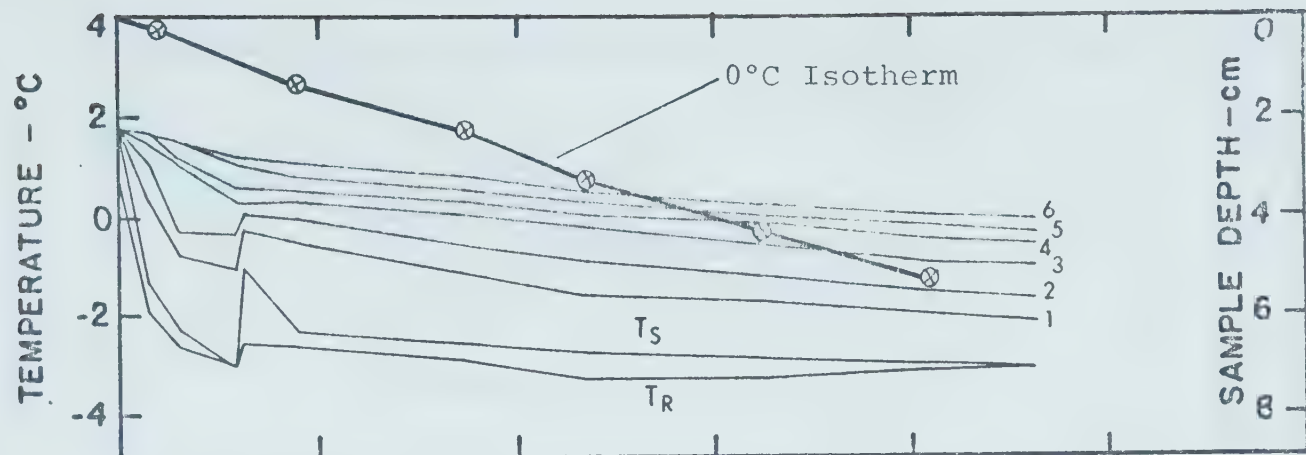


FIGURE F-1-5

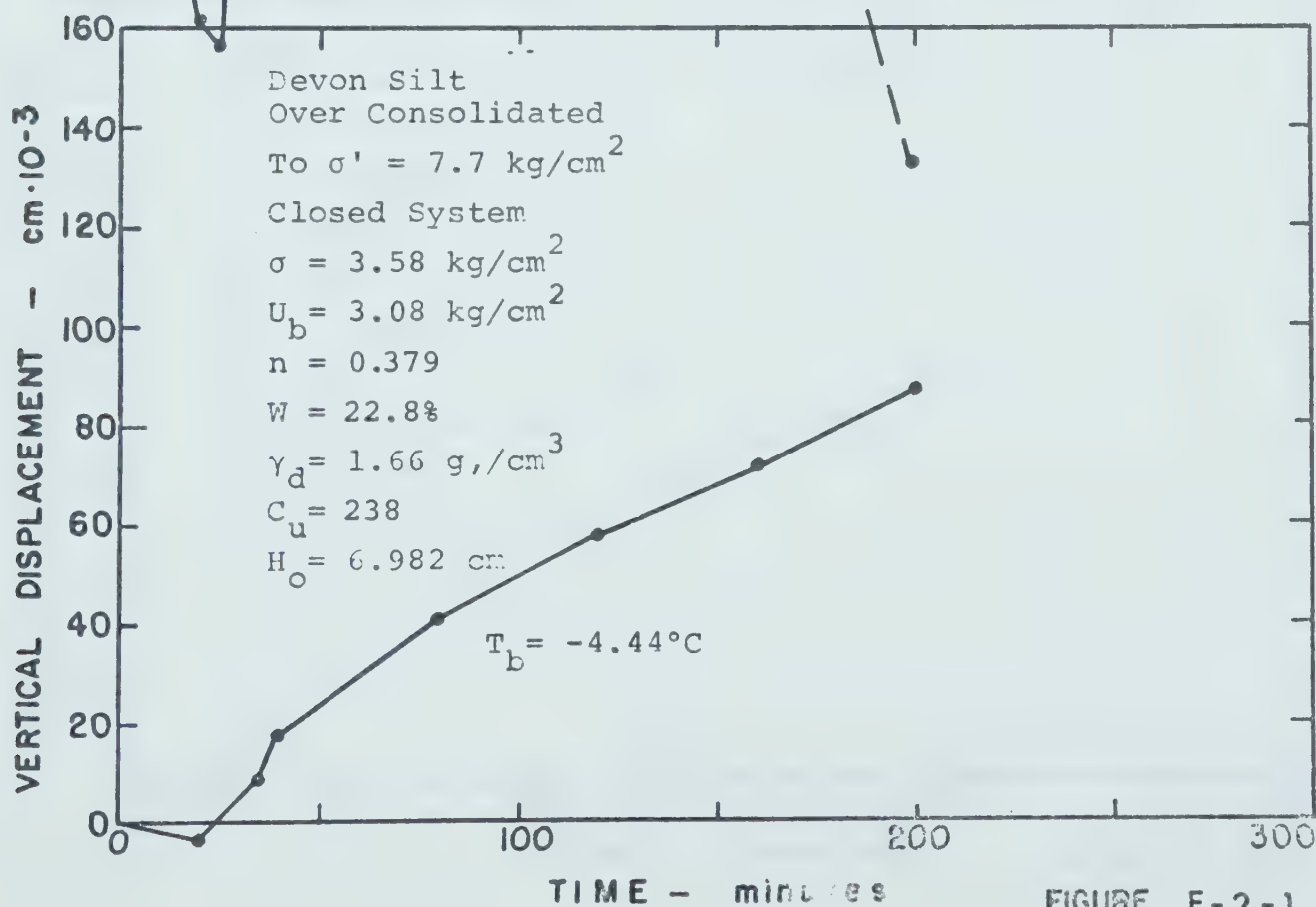
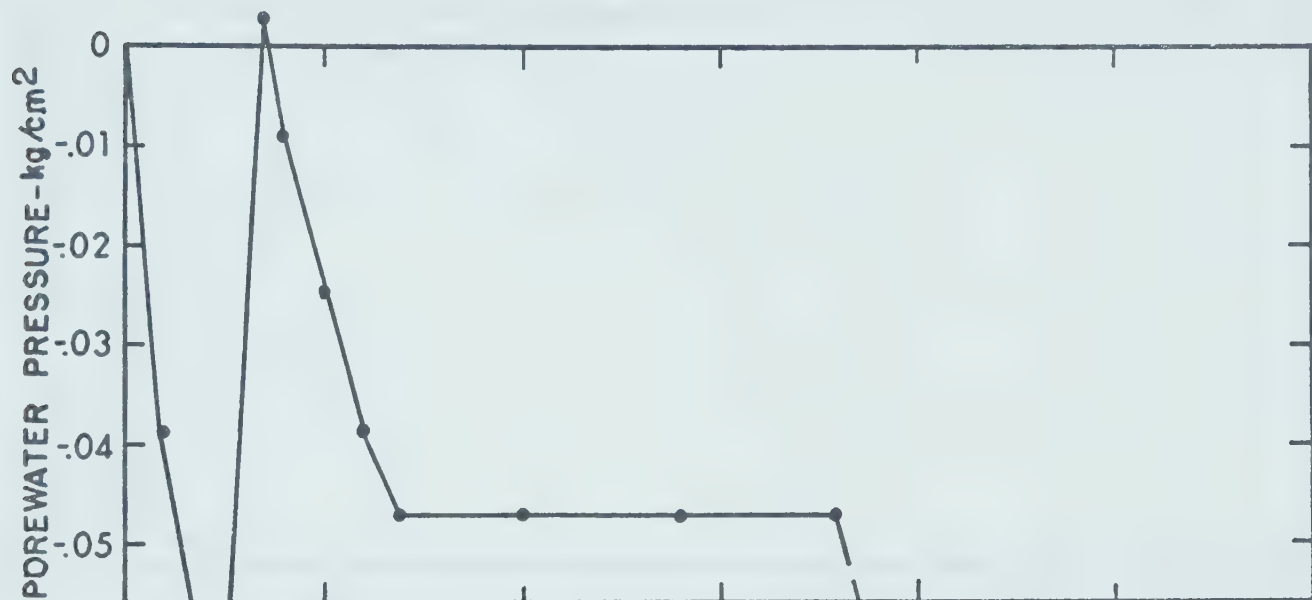
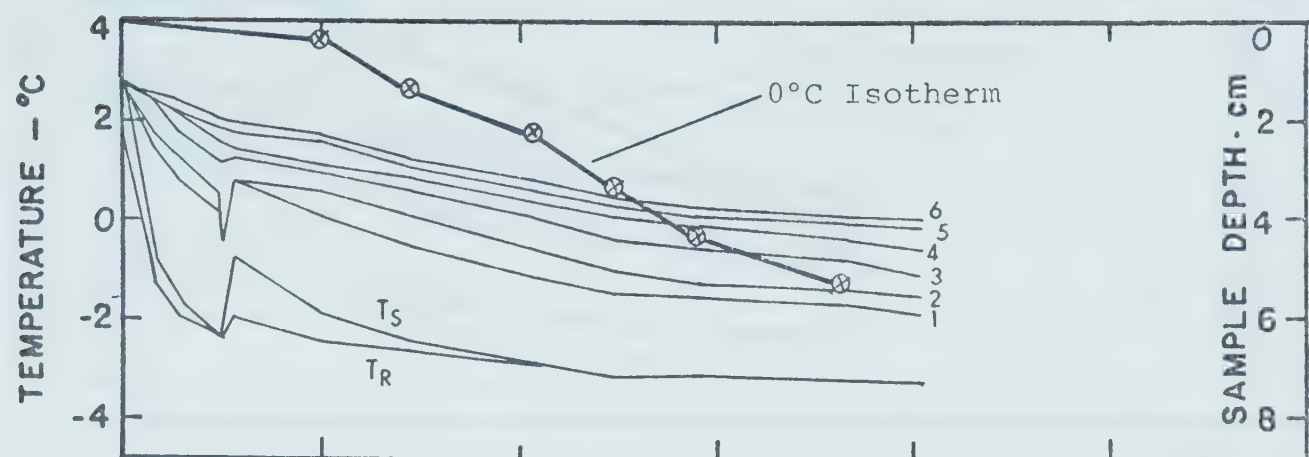


FIGURE F-2-1

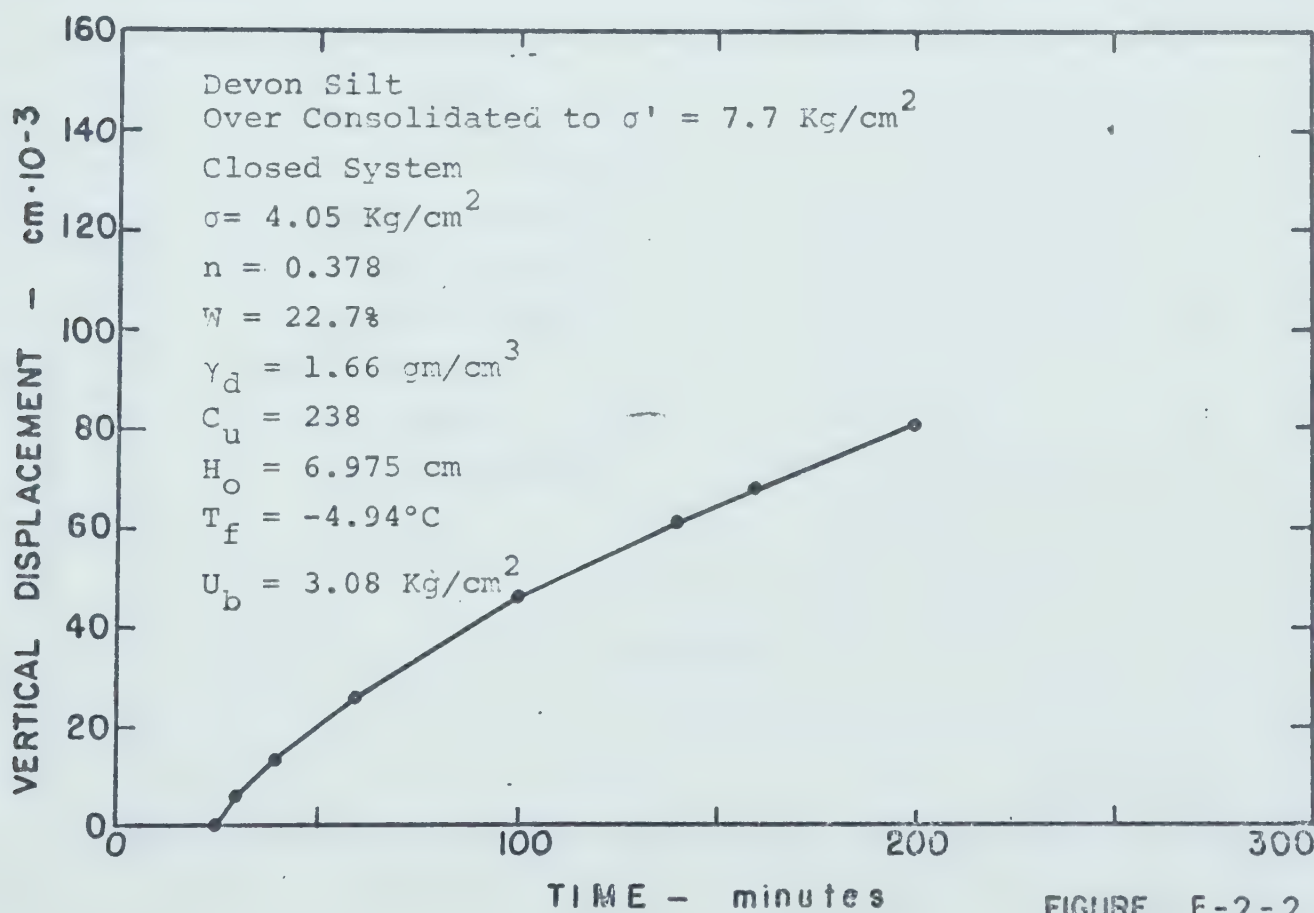
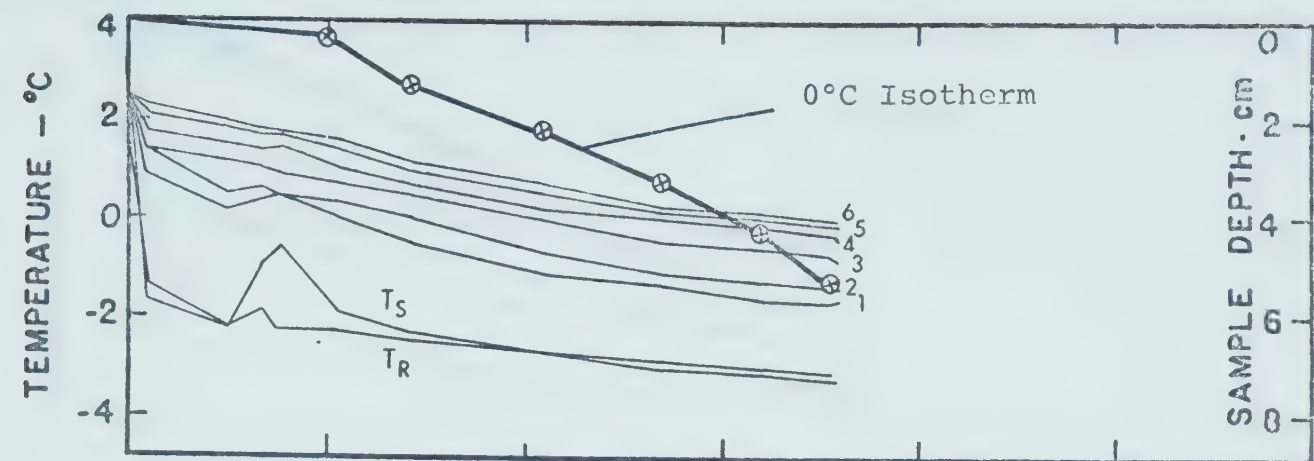


FIGURE F-2-2

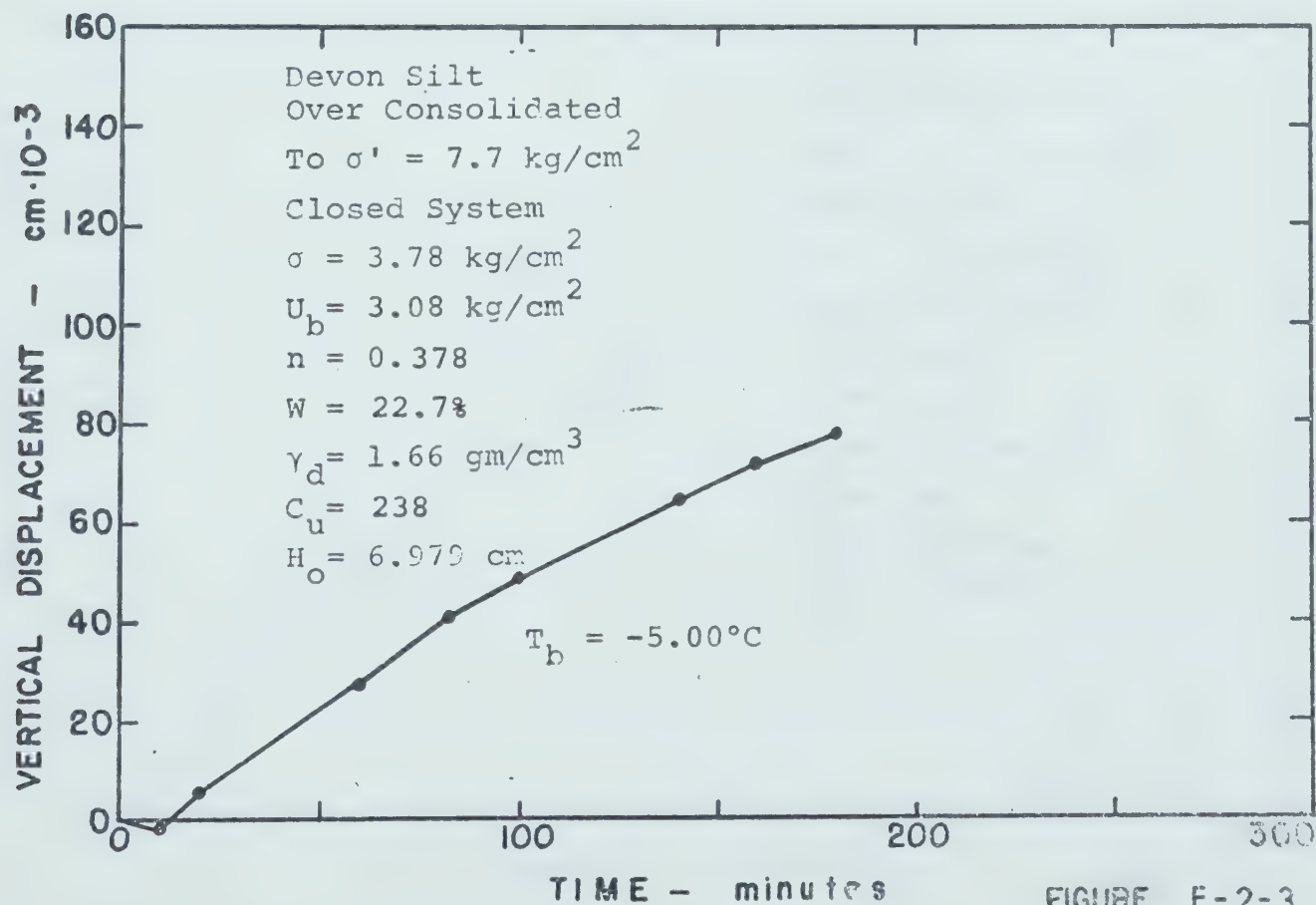
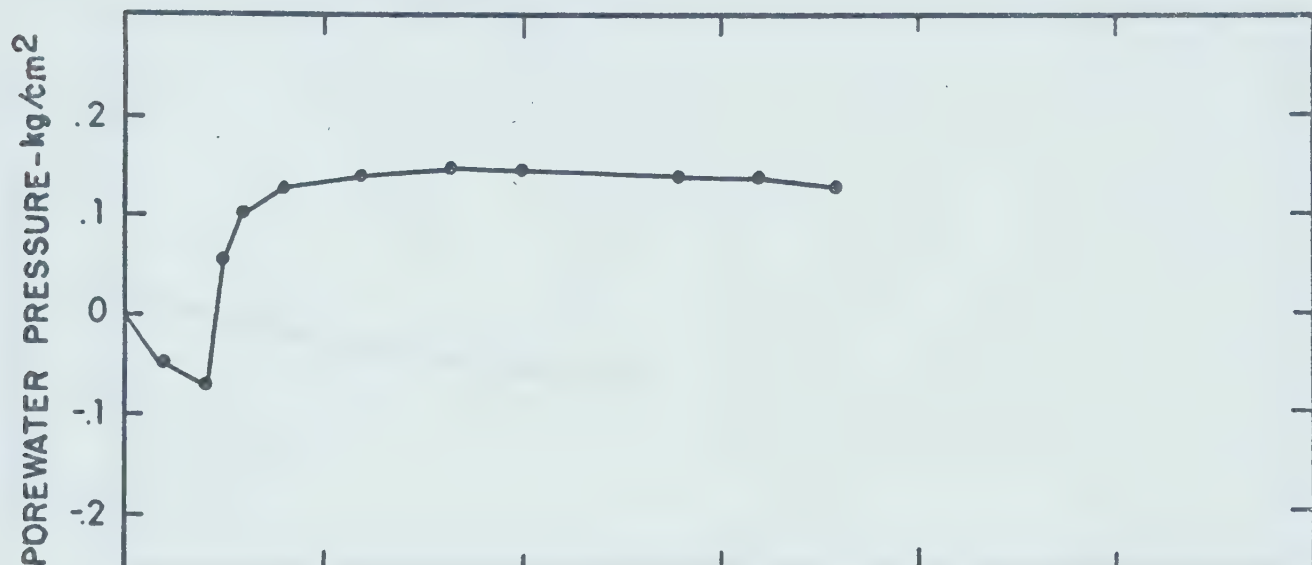
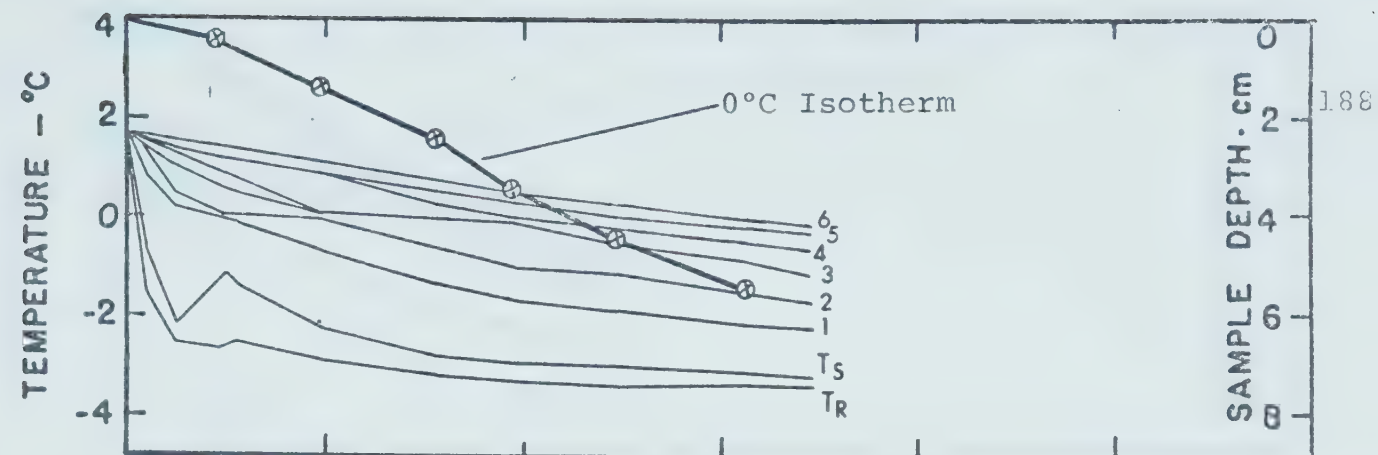


FIGURE F-2-3

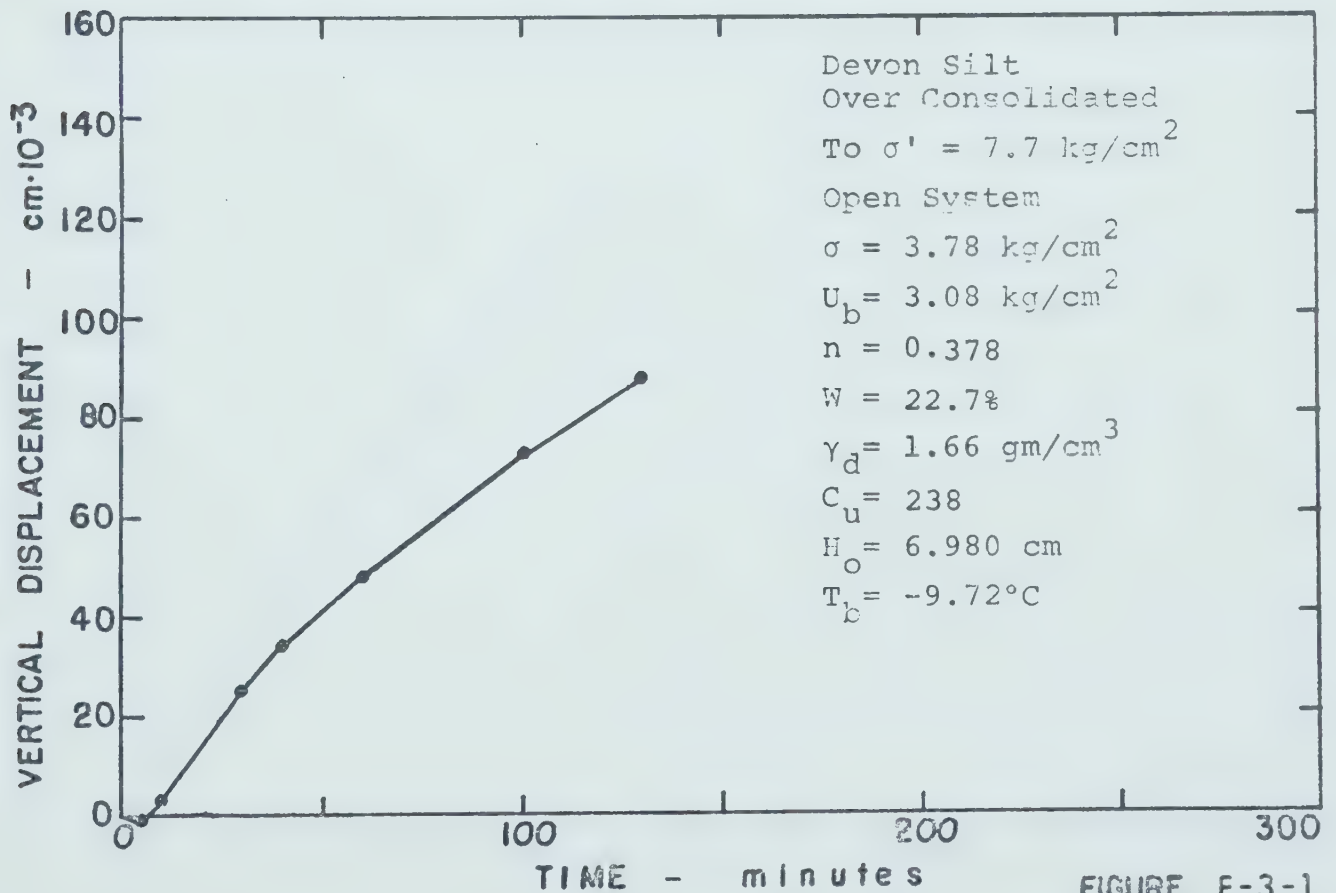
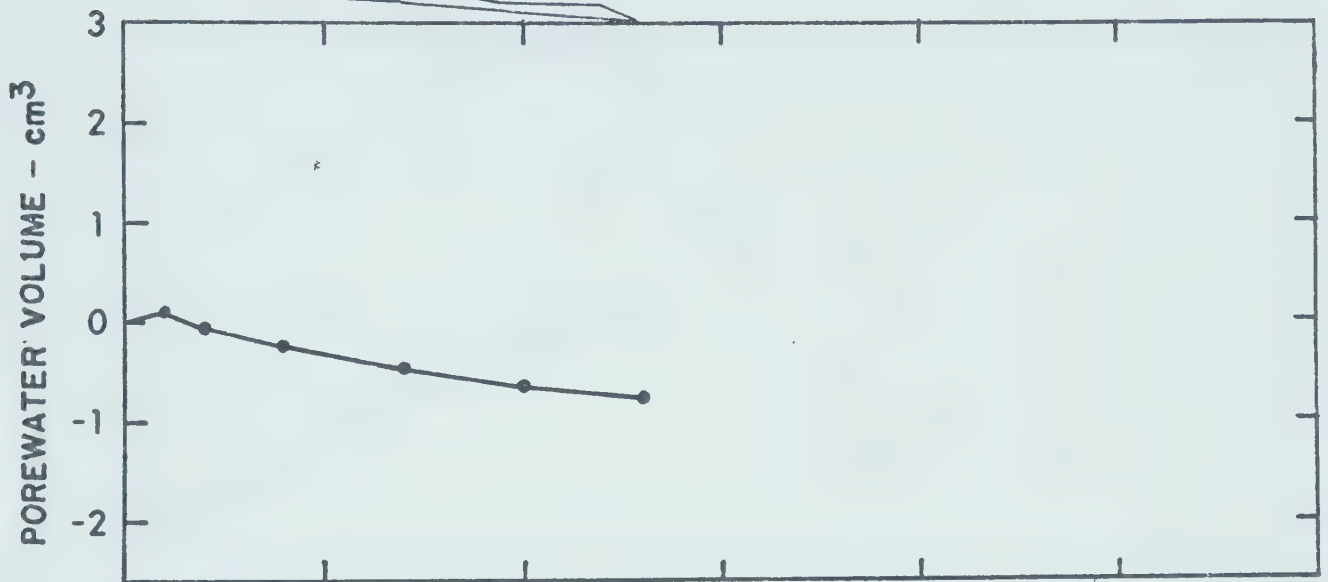
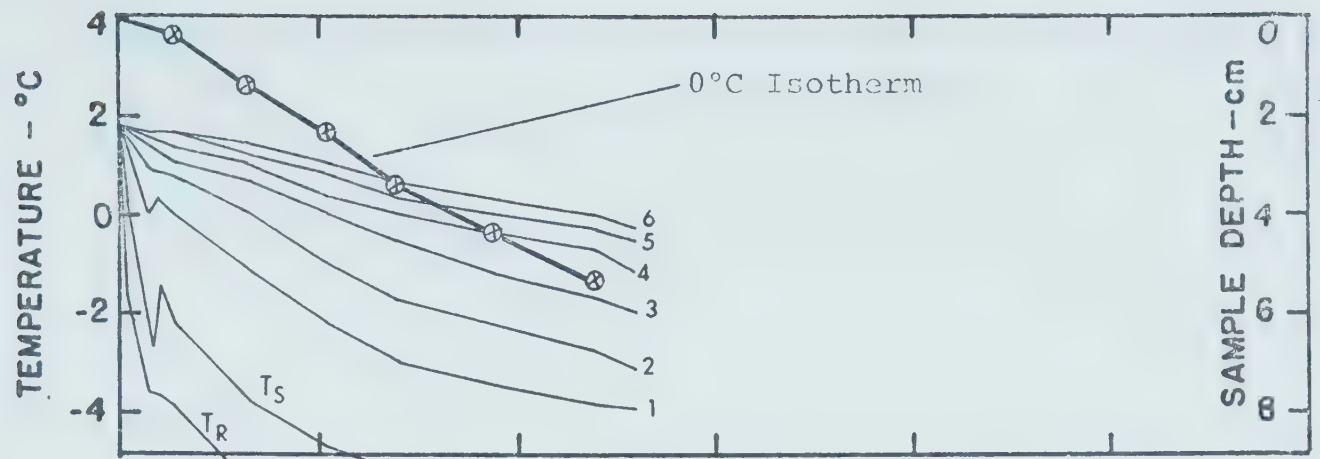


FIGURE F-3-1

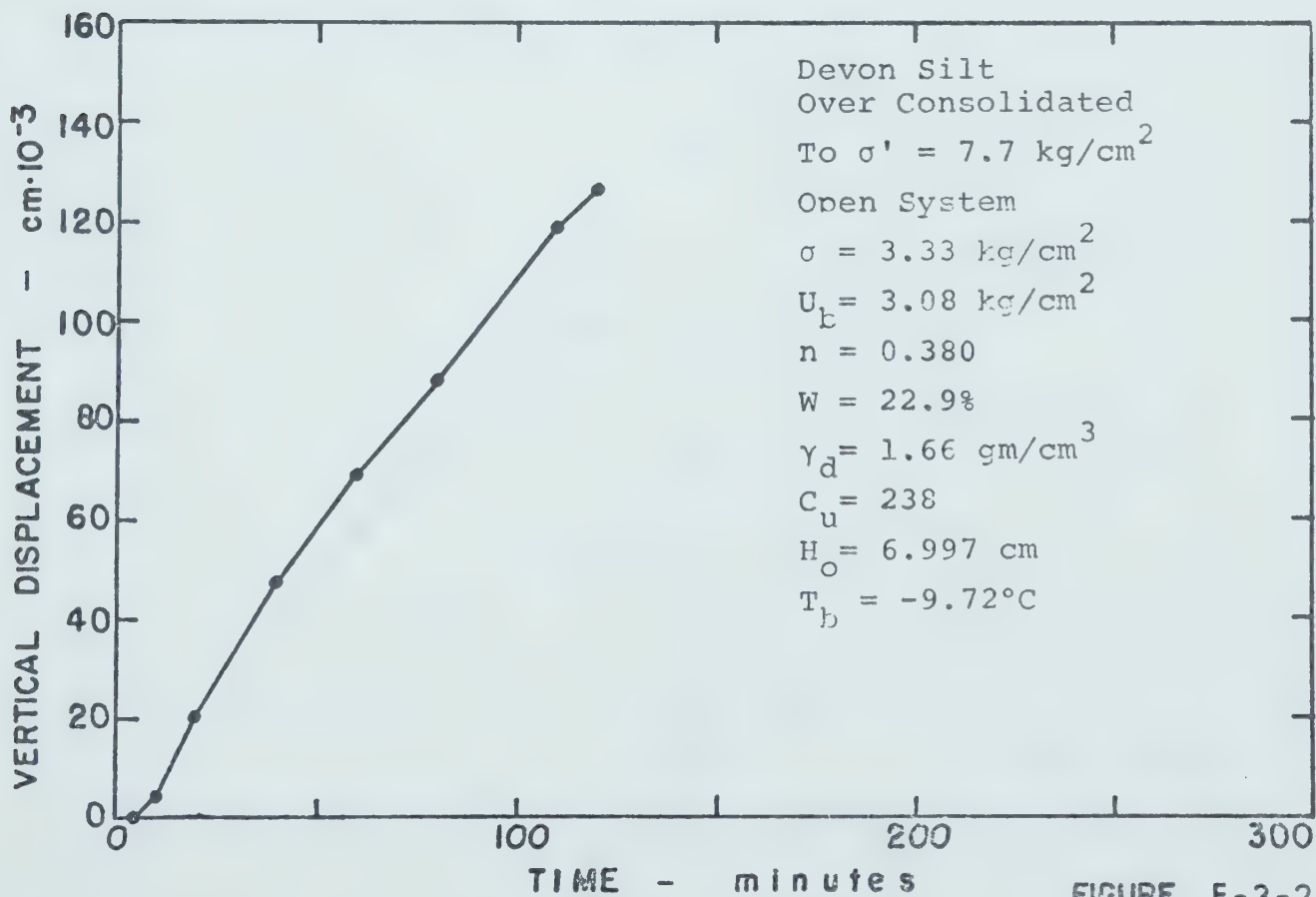
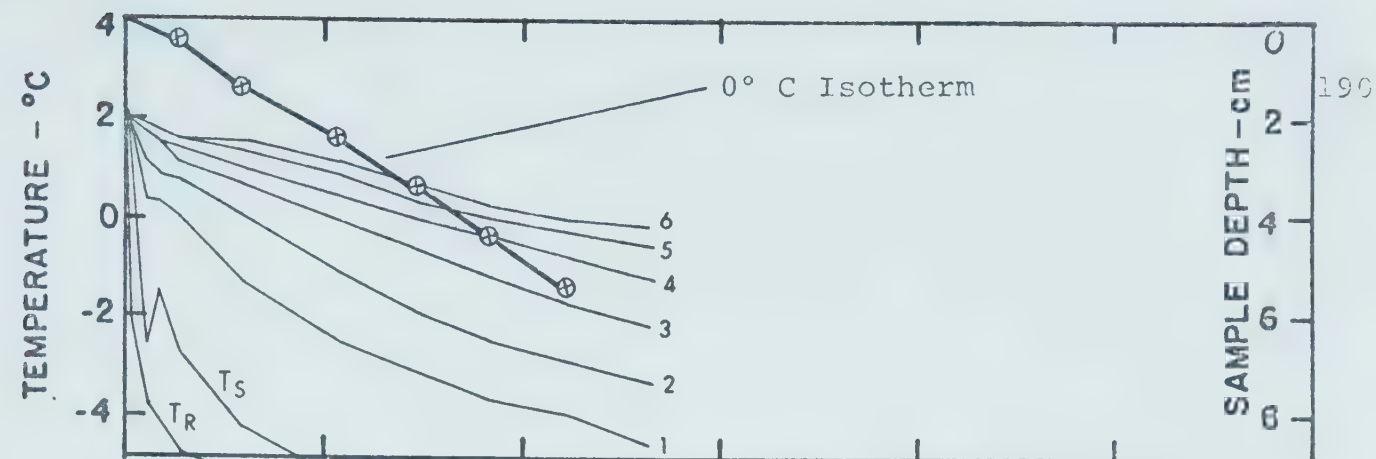


FIGURE F-3-2

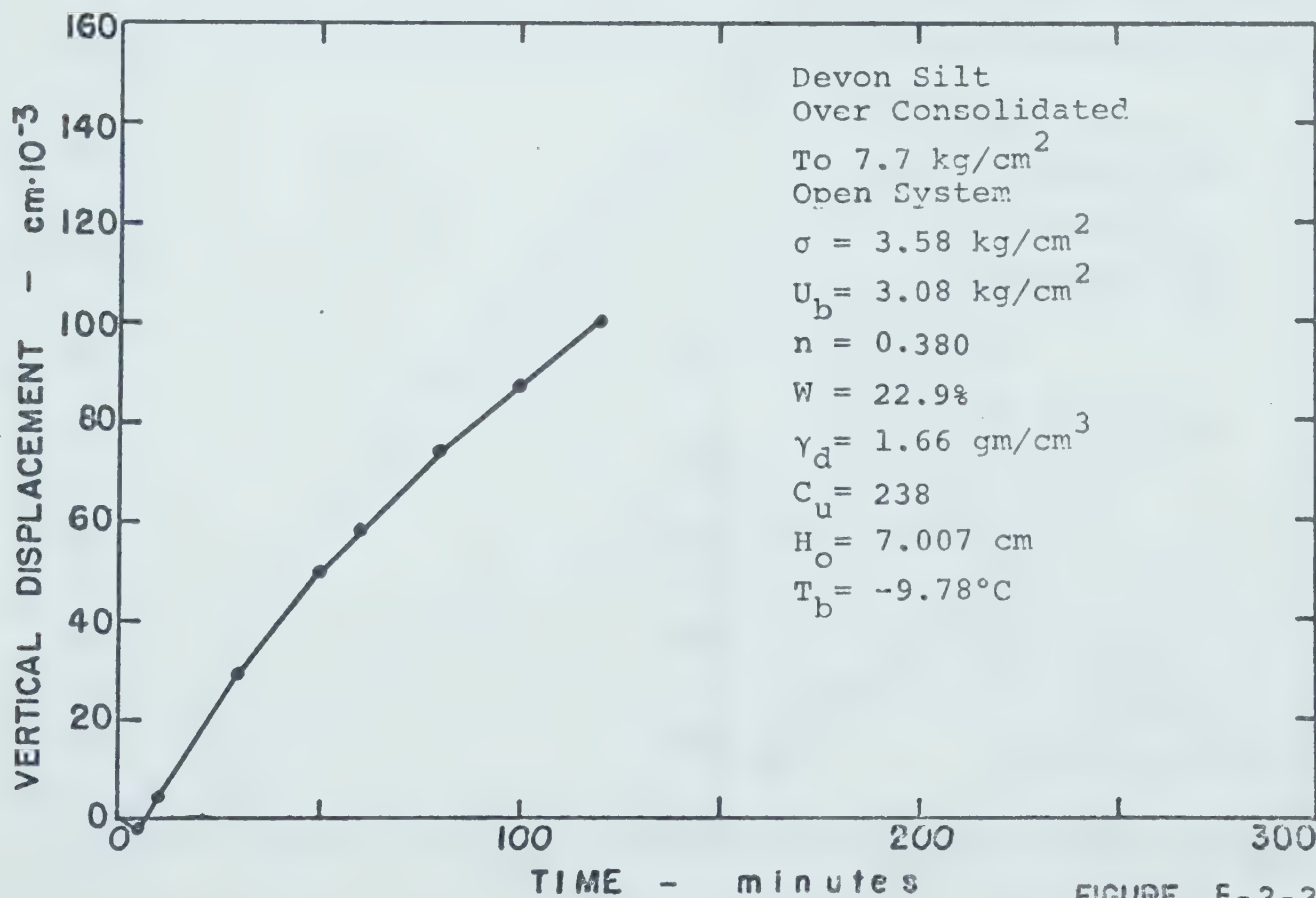
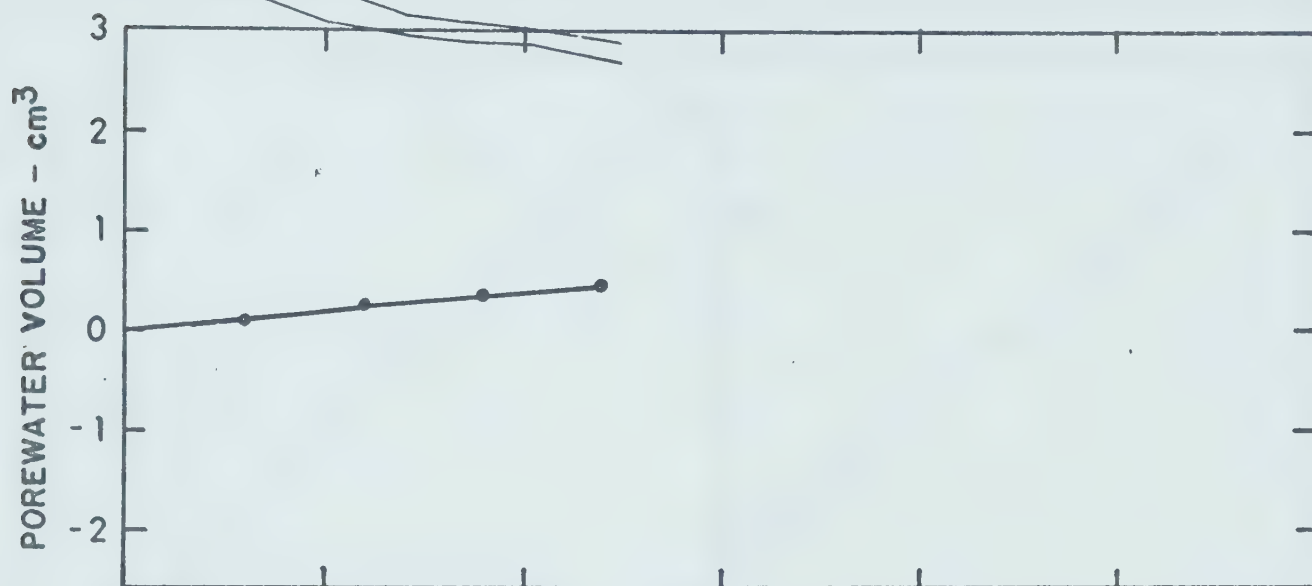
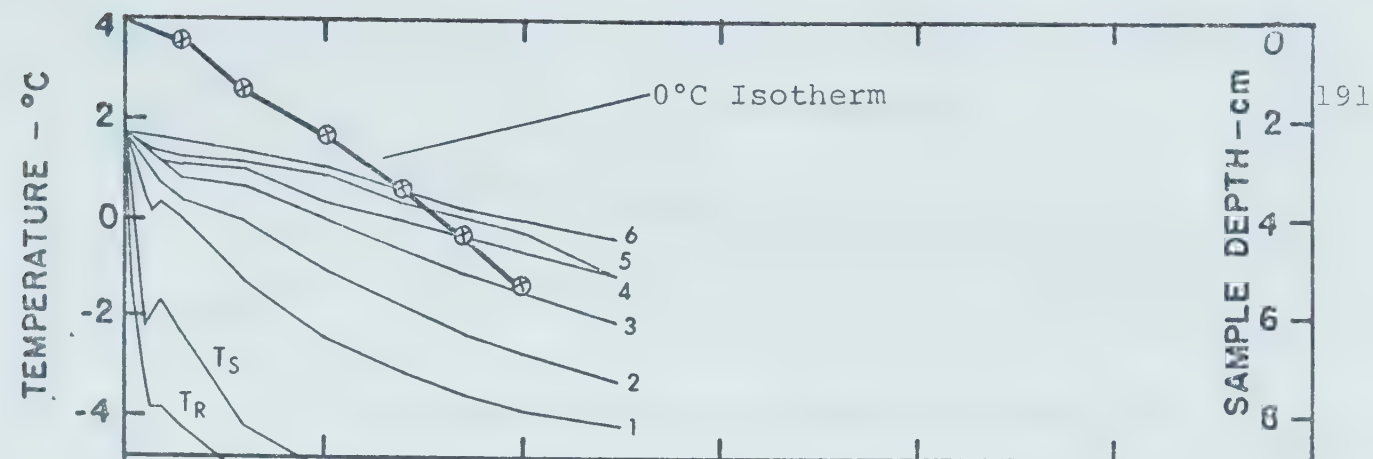


FIGURE F-3-3

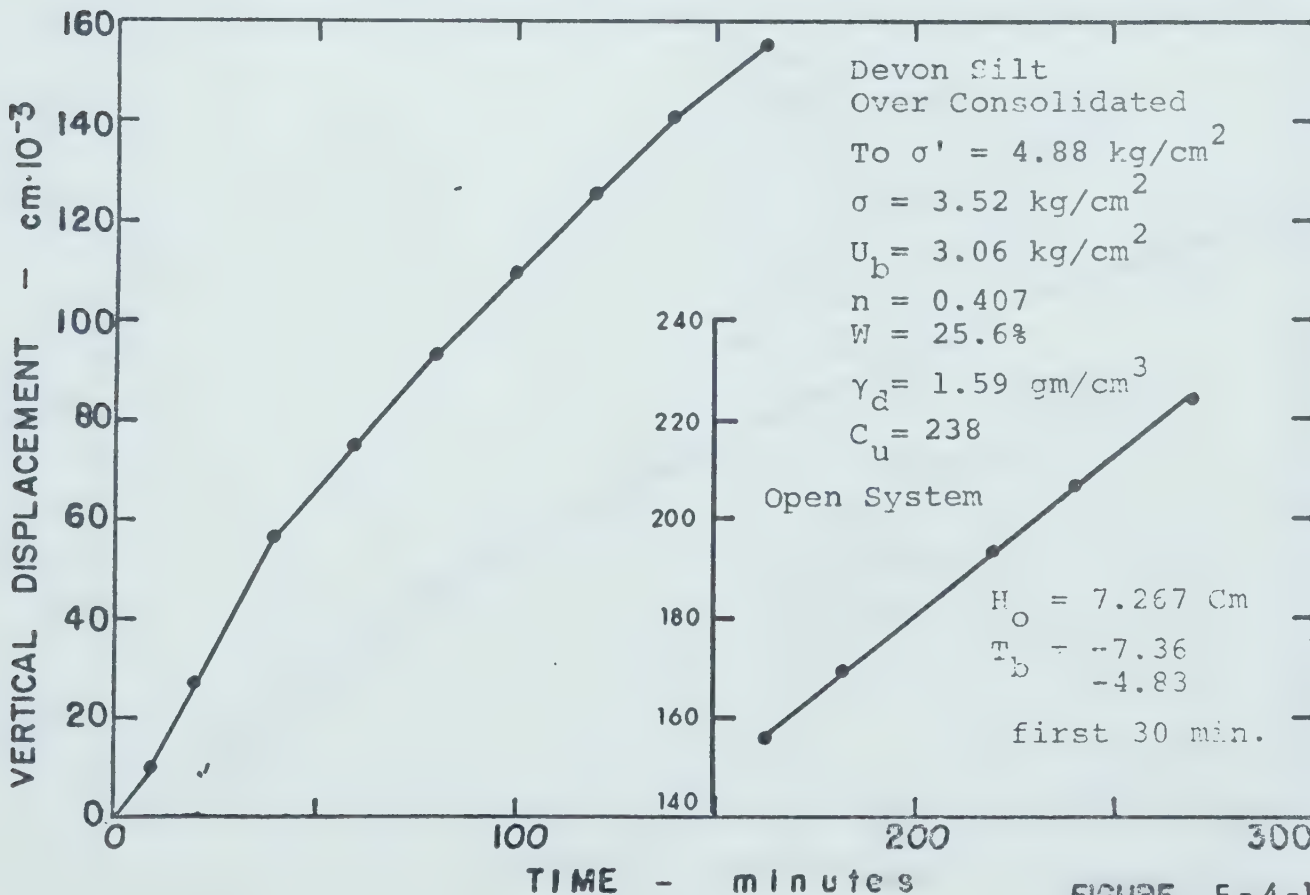
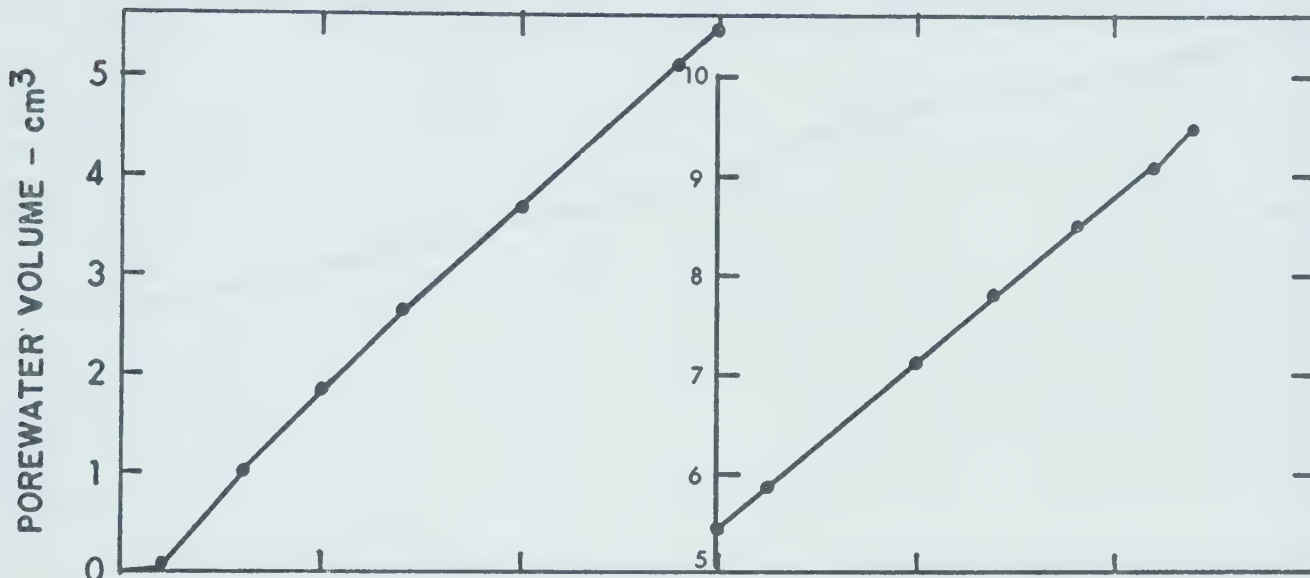
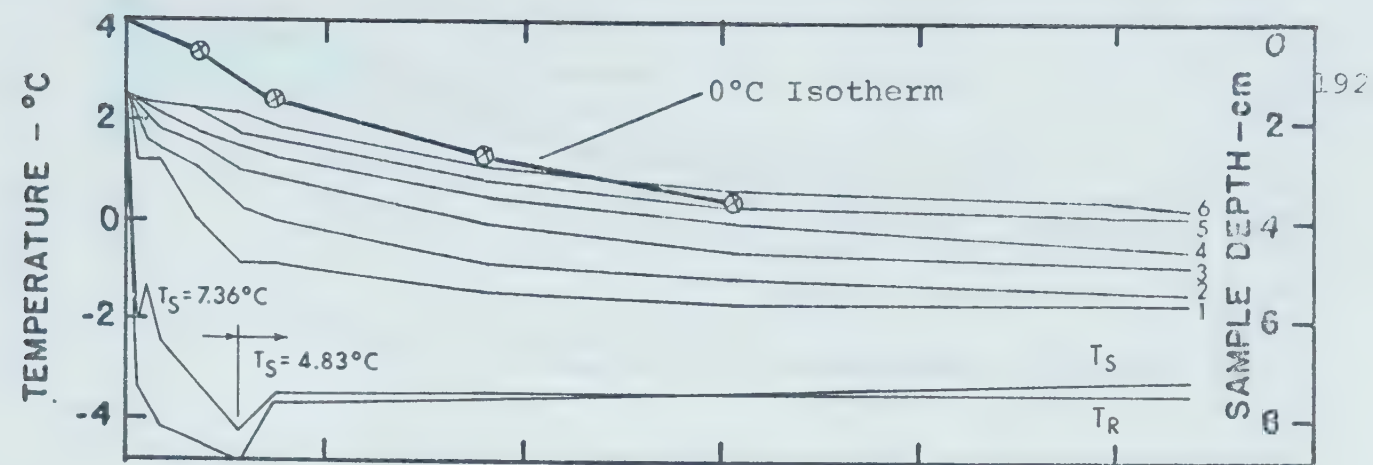


FIGURE F-4-1

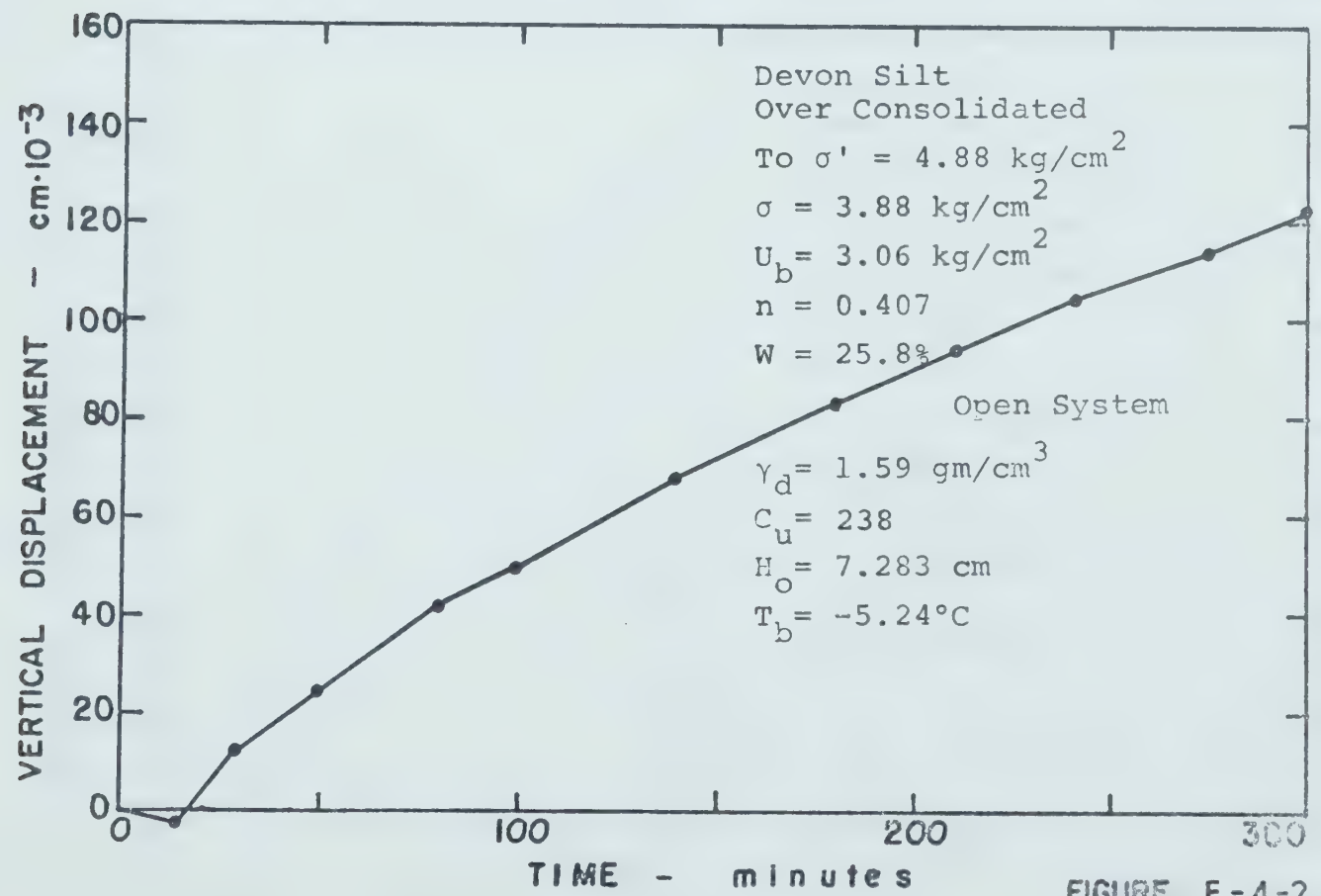
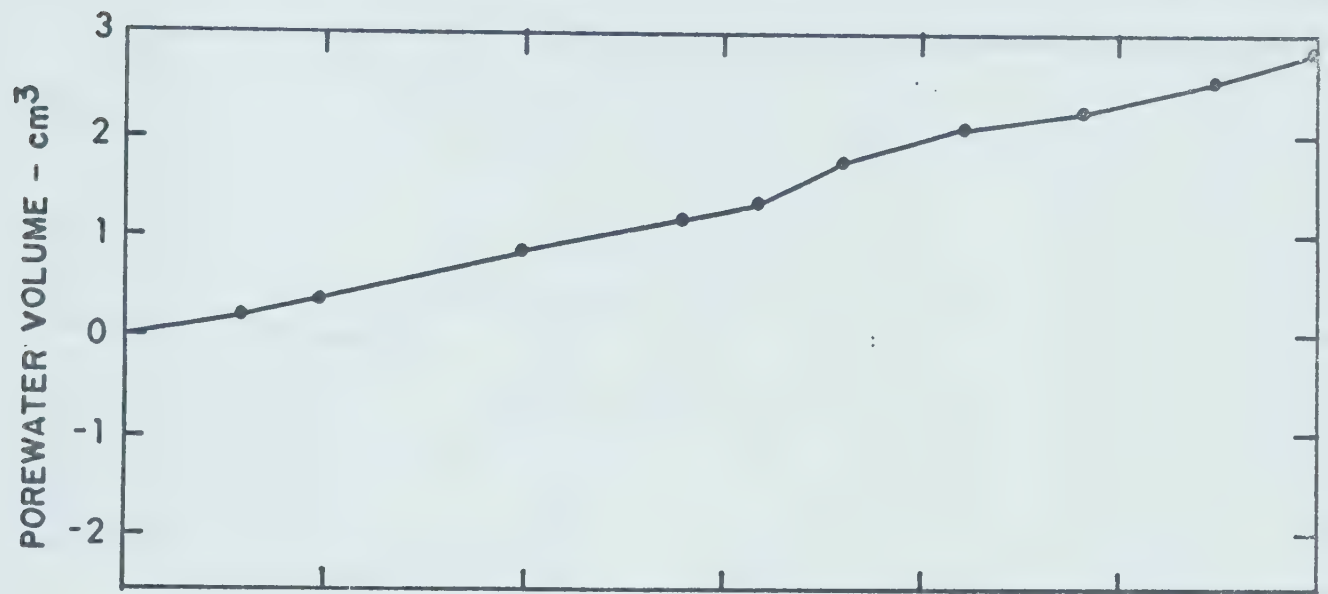
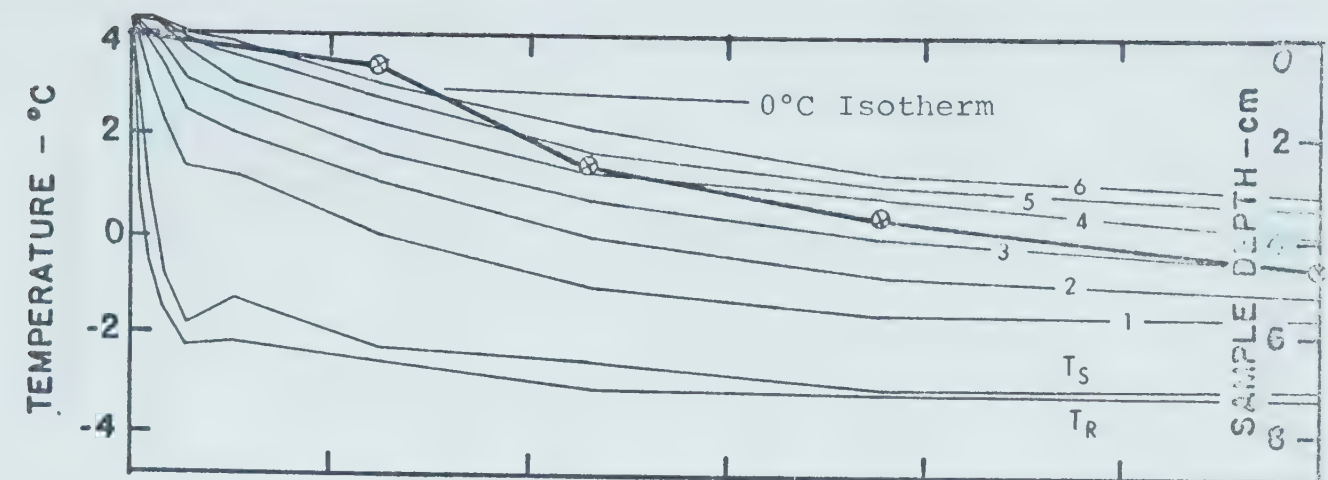


FIGURE F-4-2

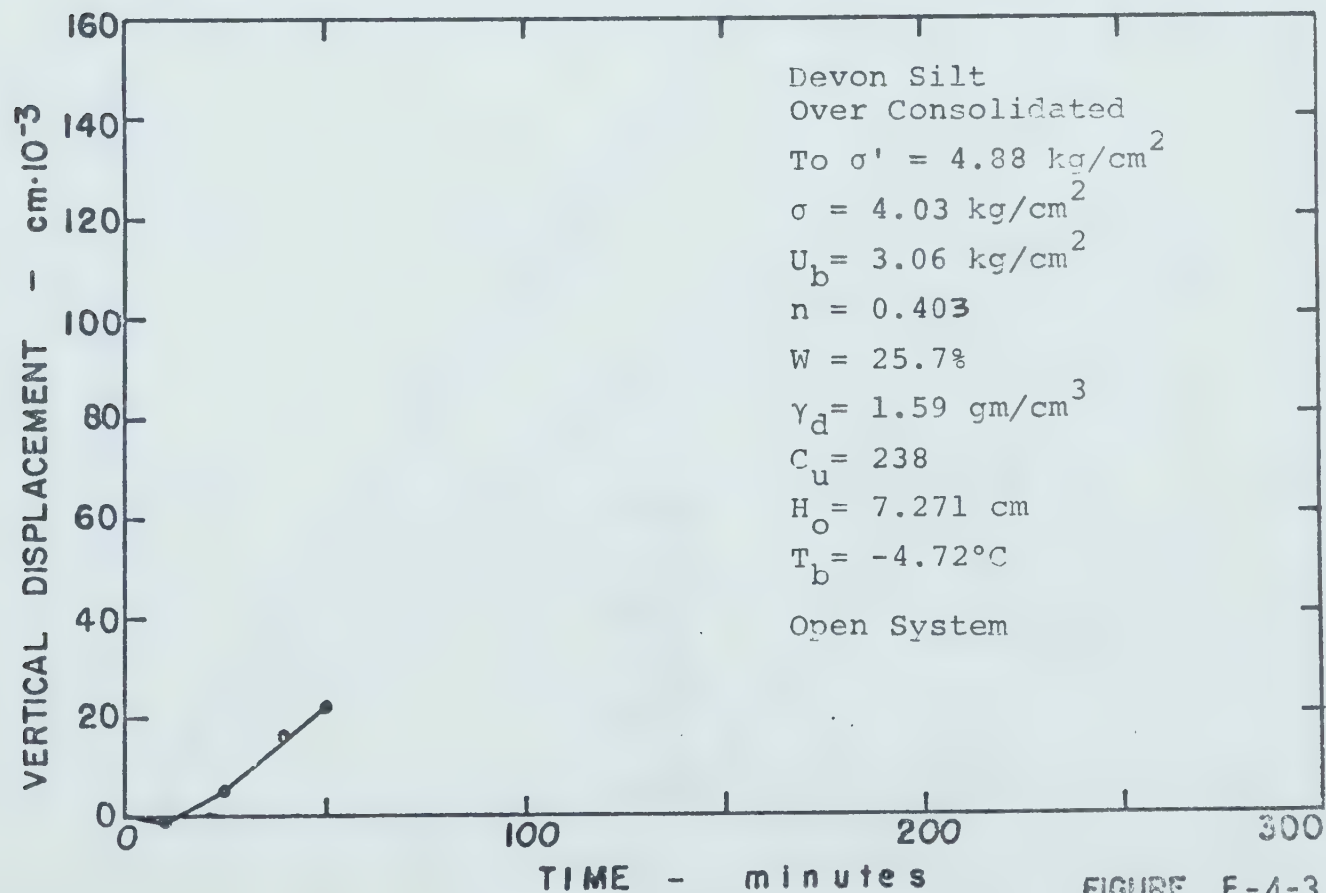
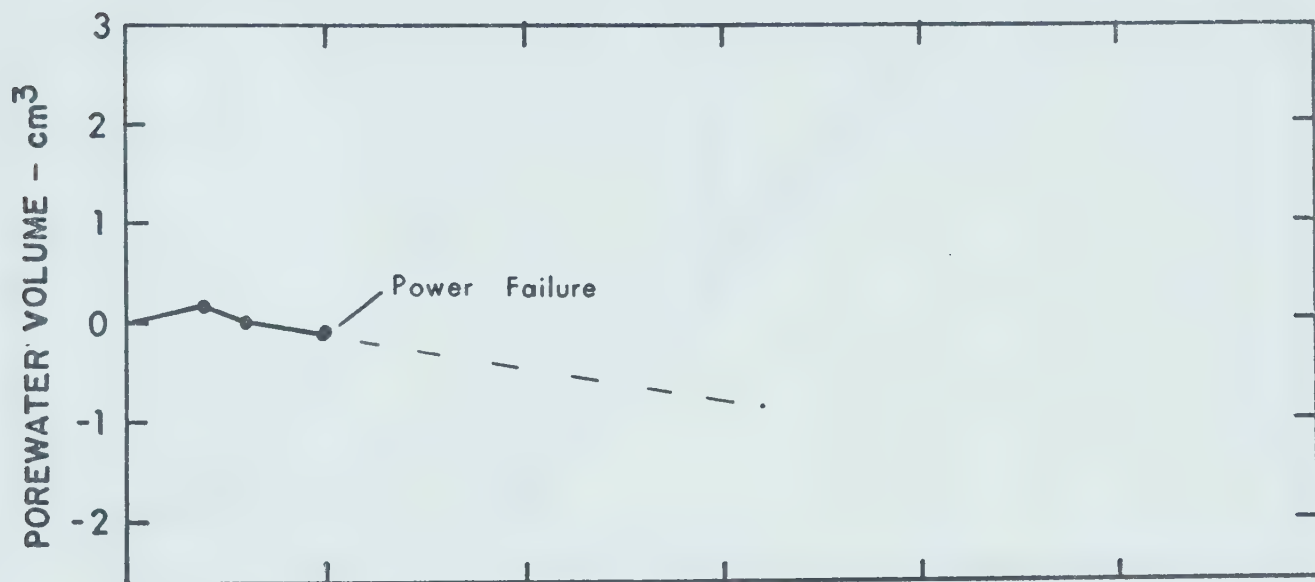
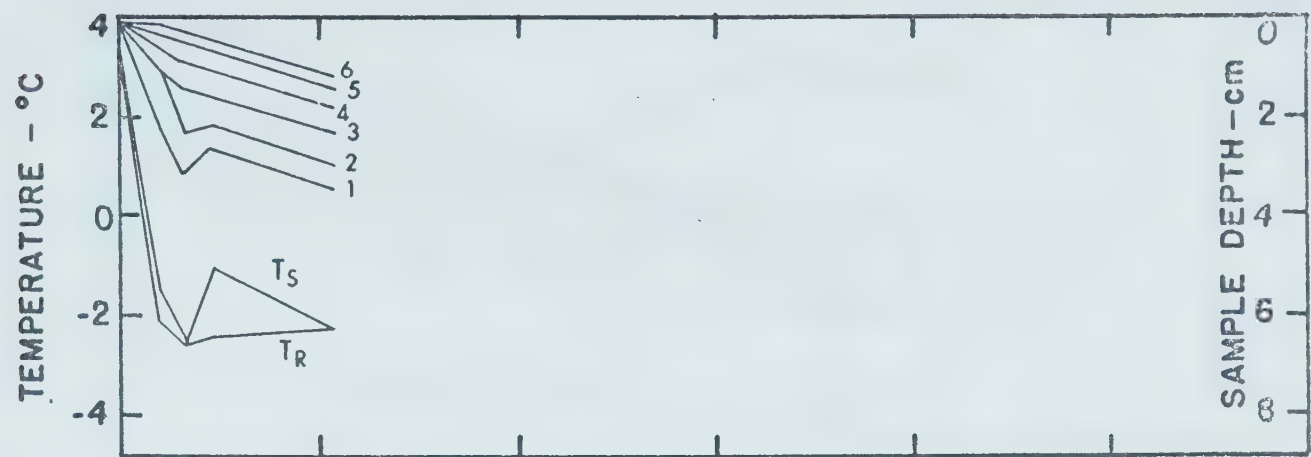


FIGURE F-4-3

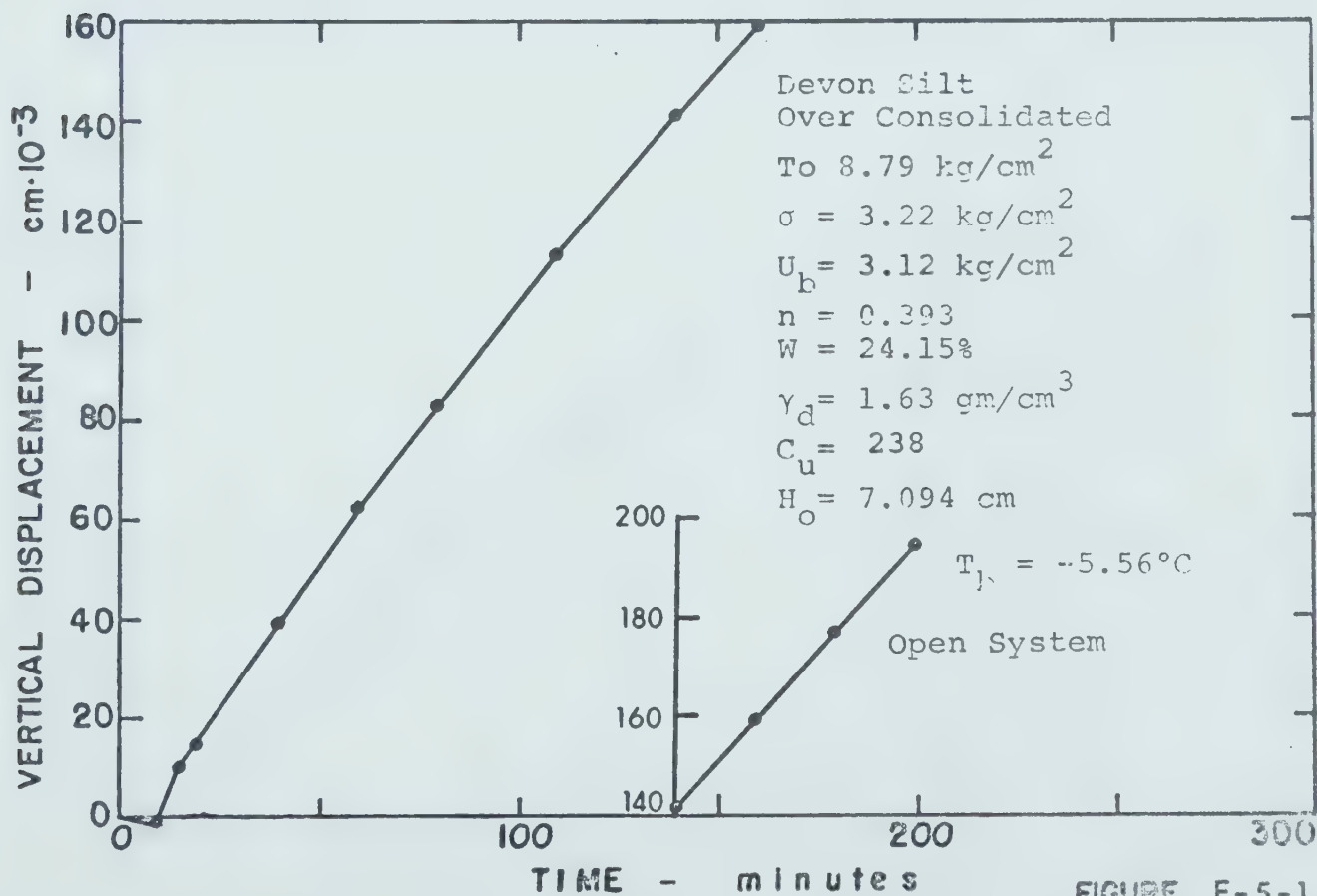
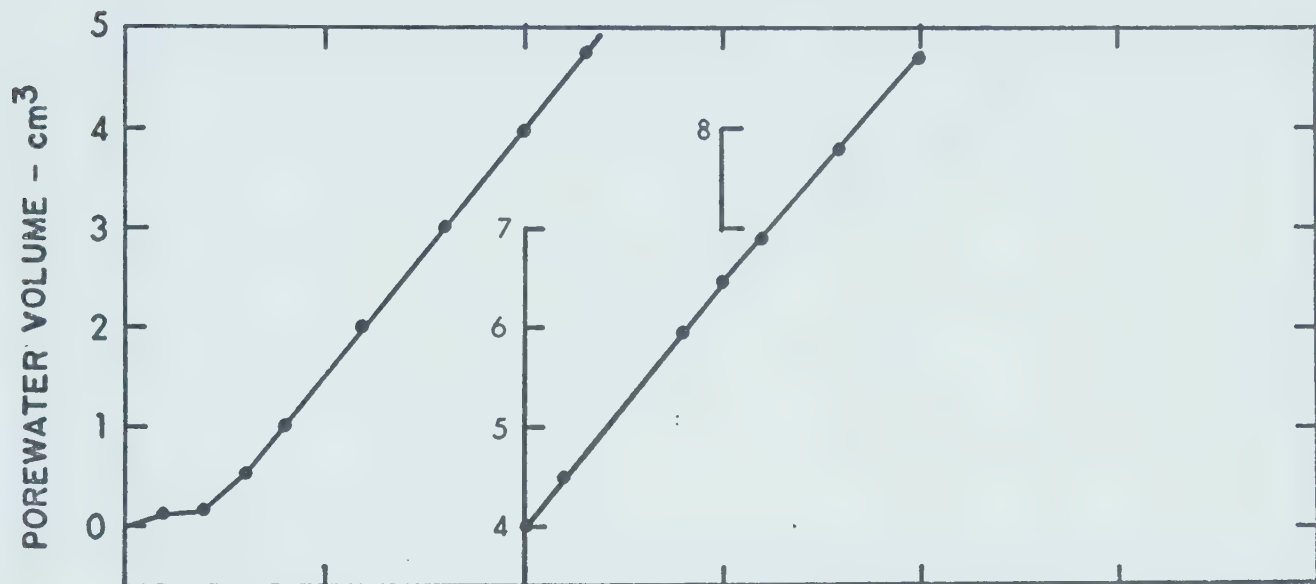
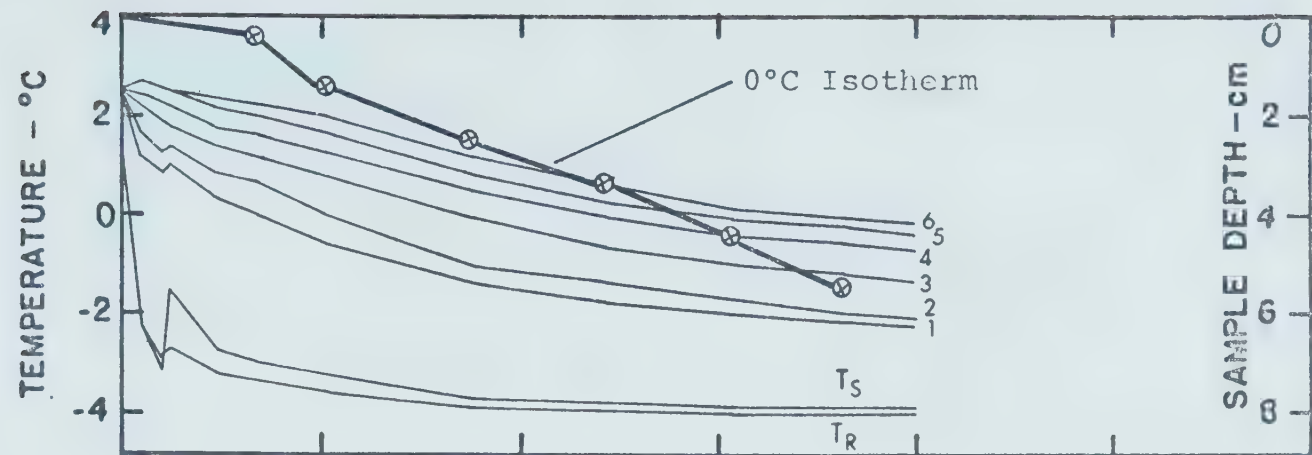


FIGURE F-5-1

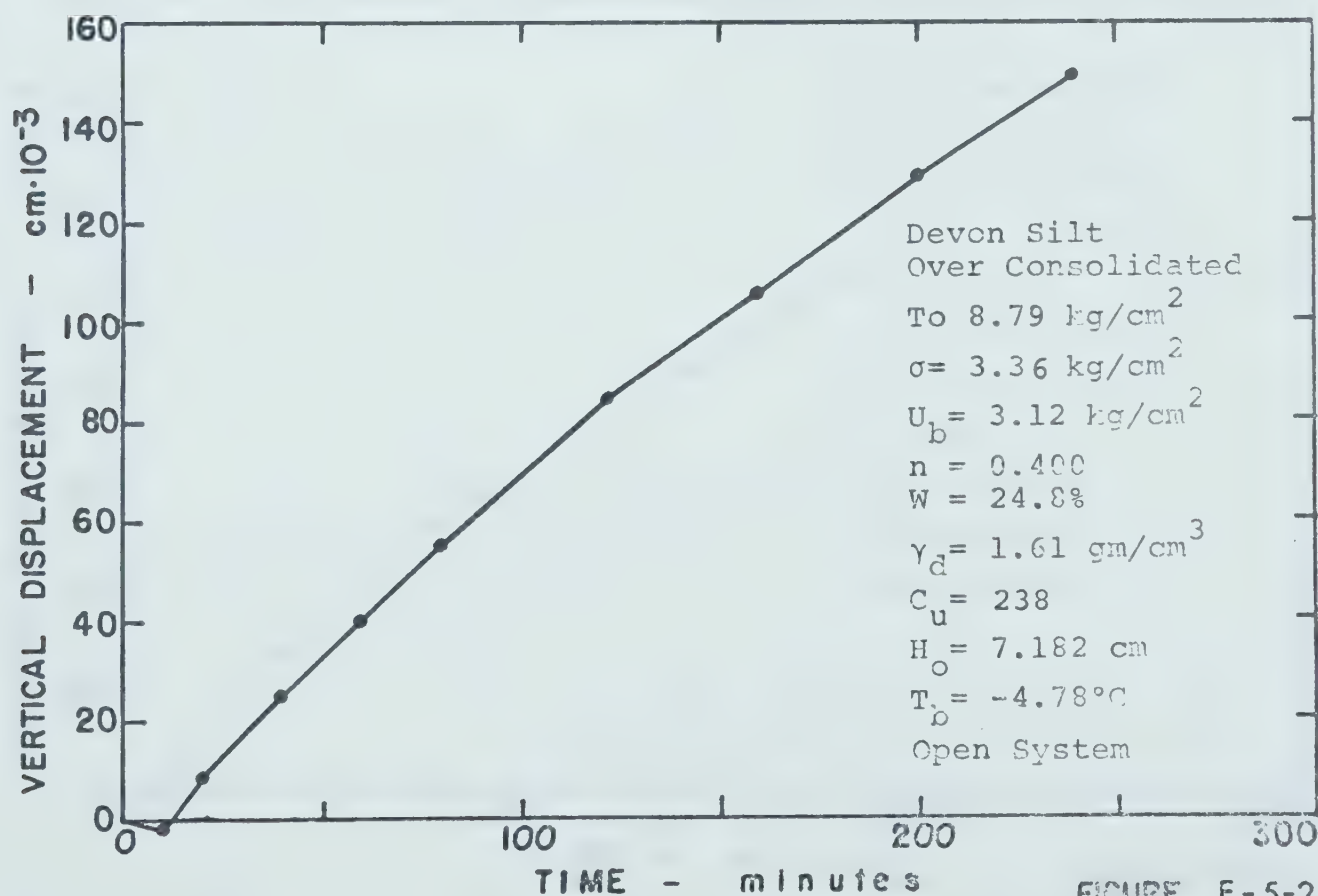
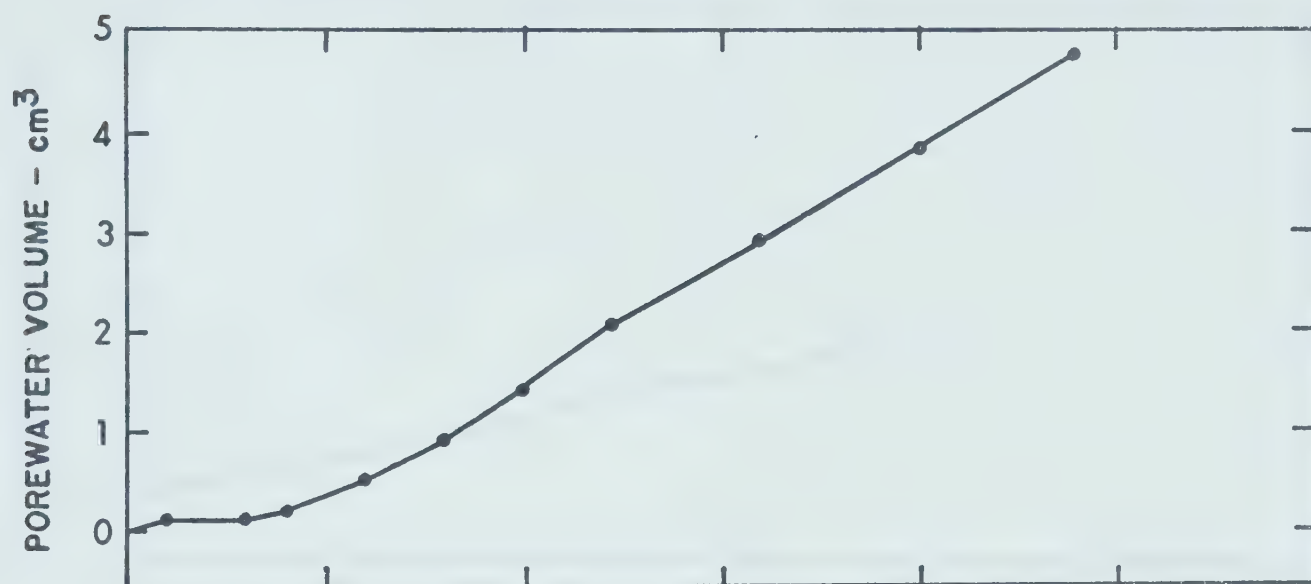
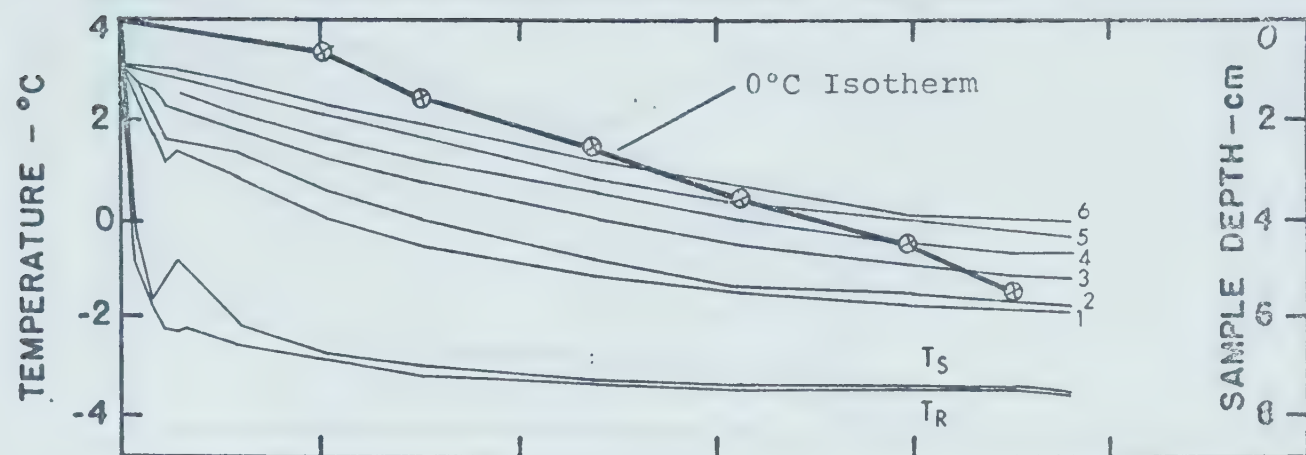


FIGURE F-5-2

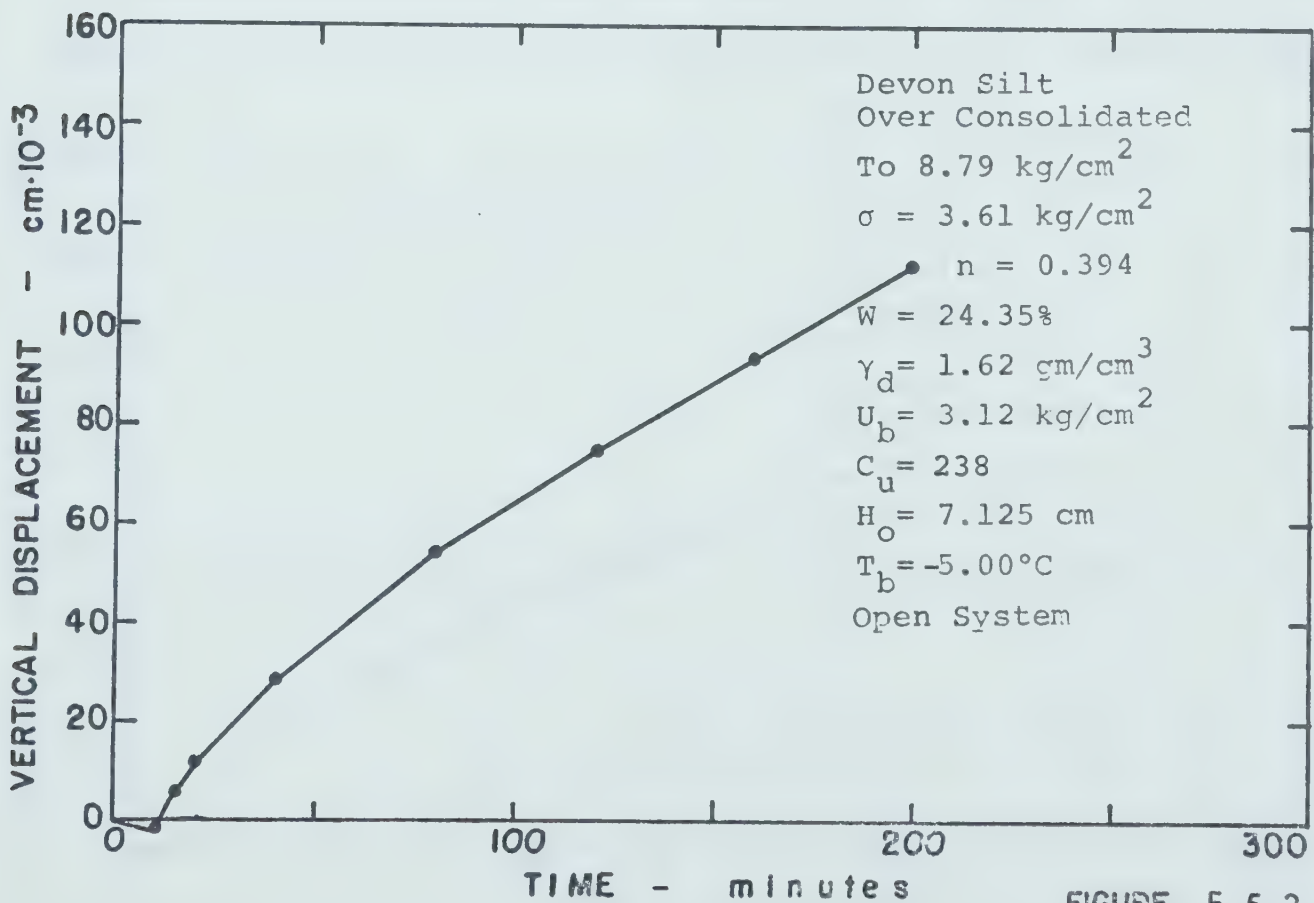
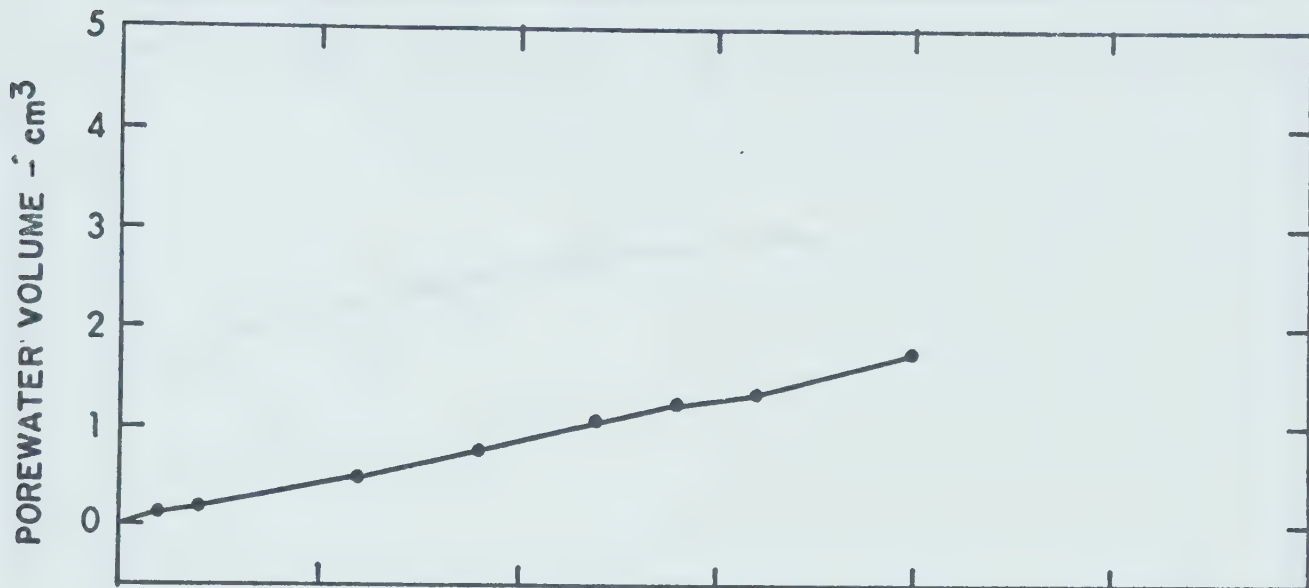
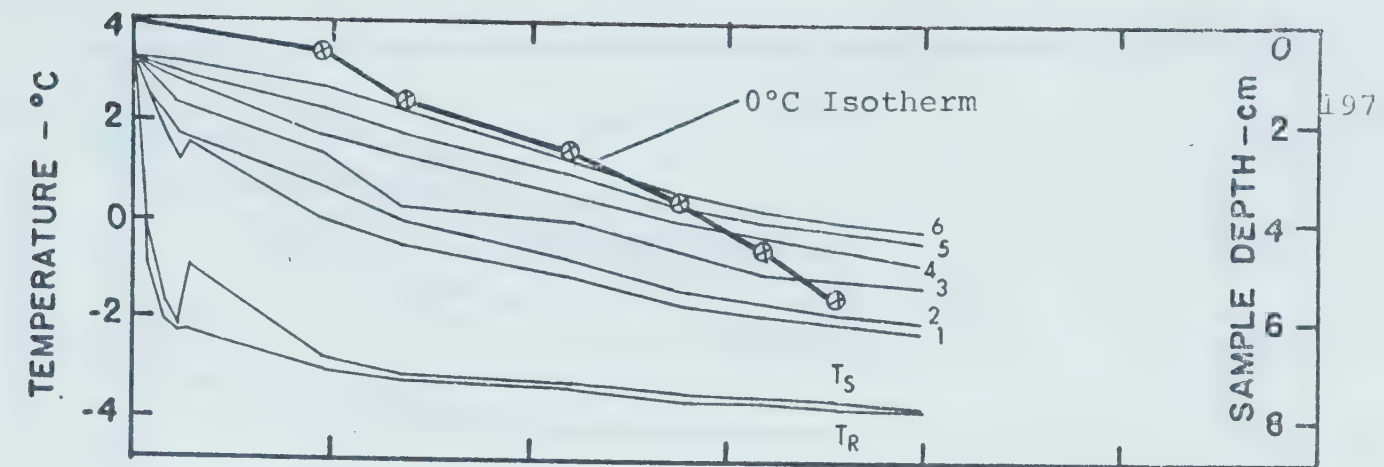


FIGURE F-5-3

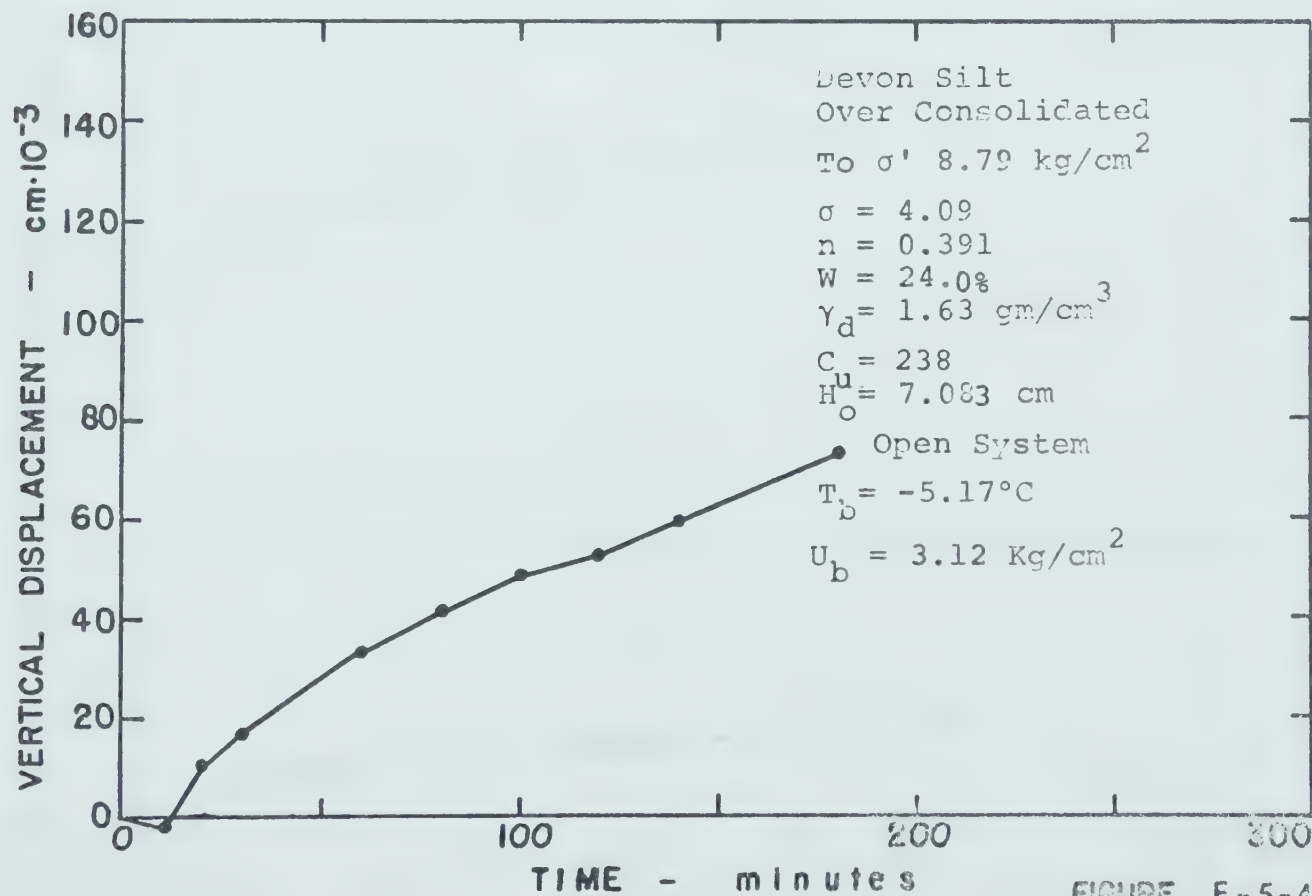
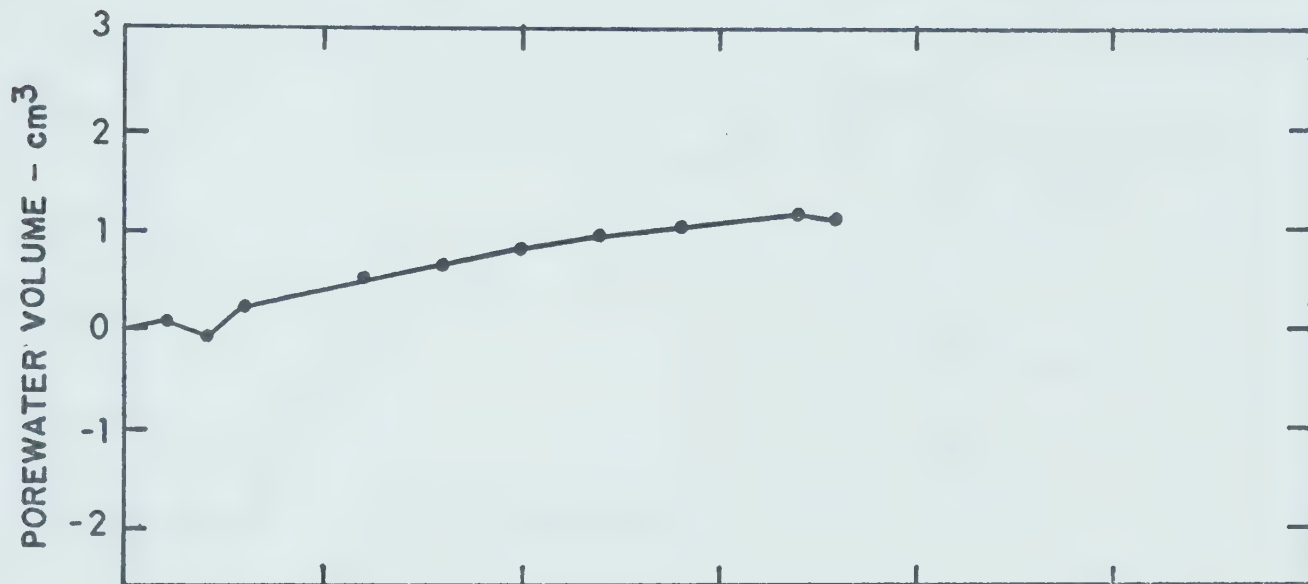
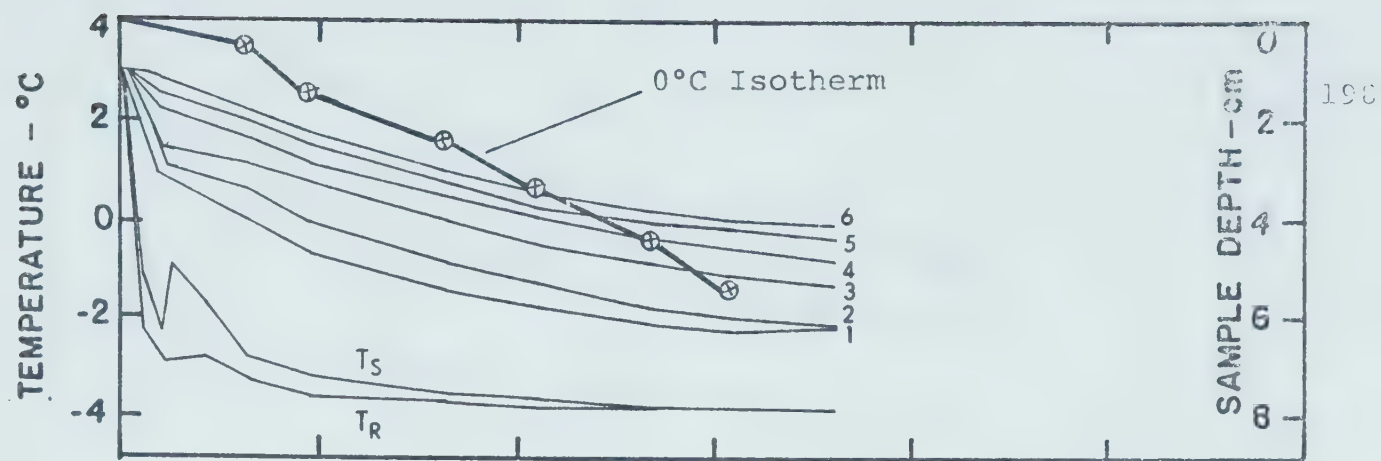


FIGURE F-5-4

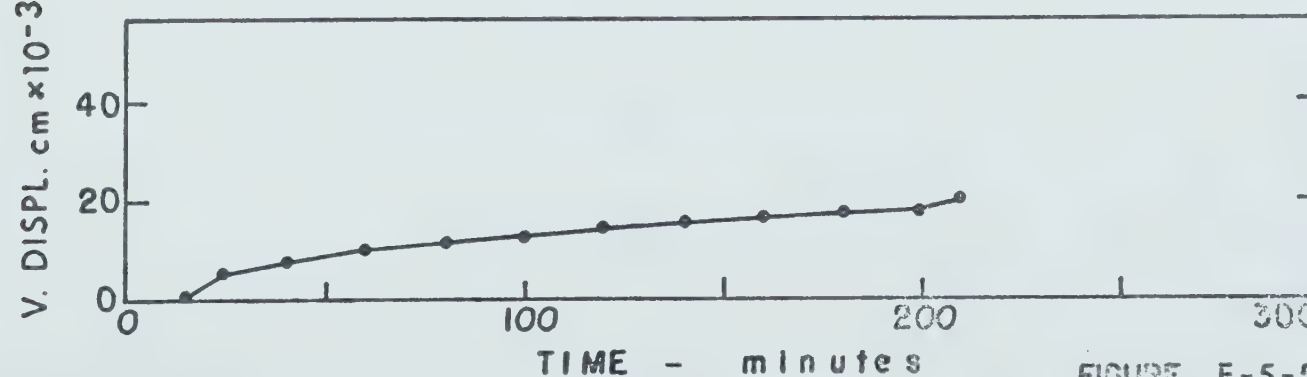
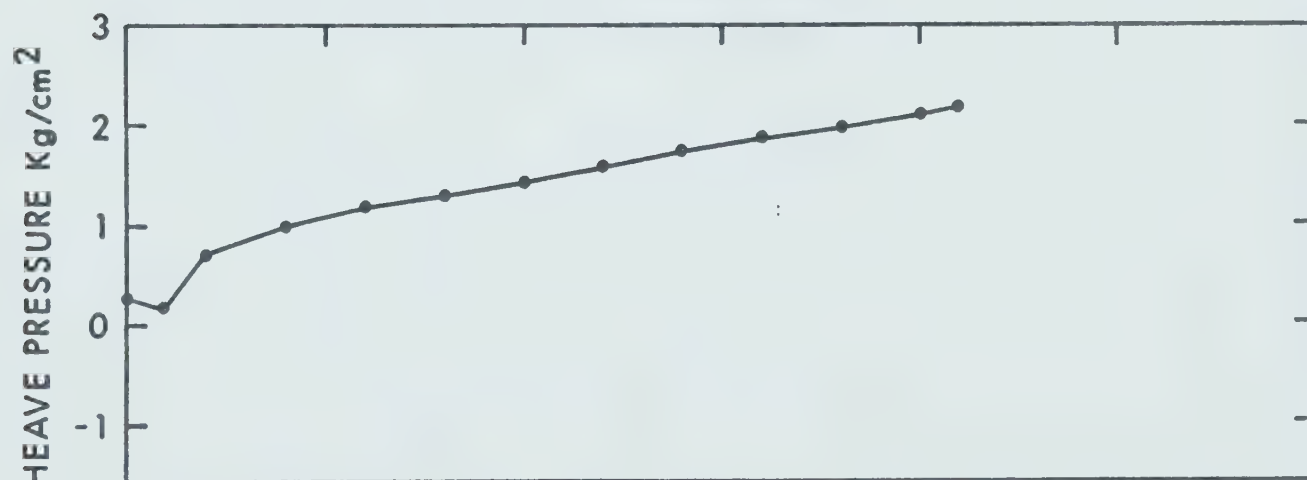
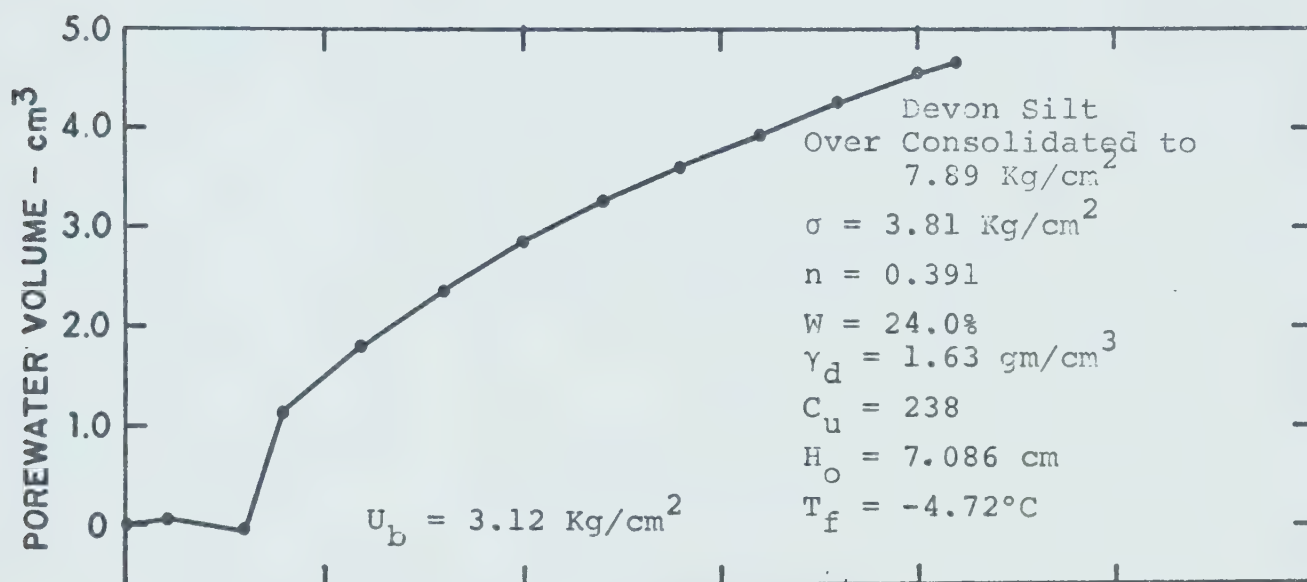
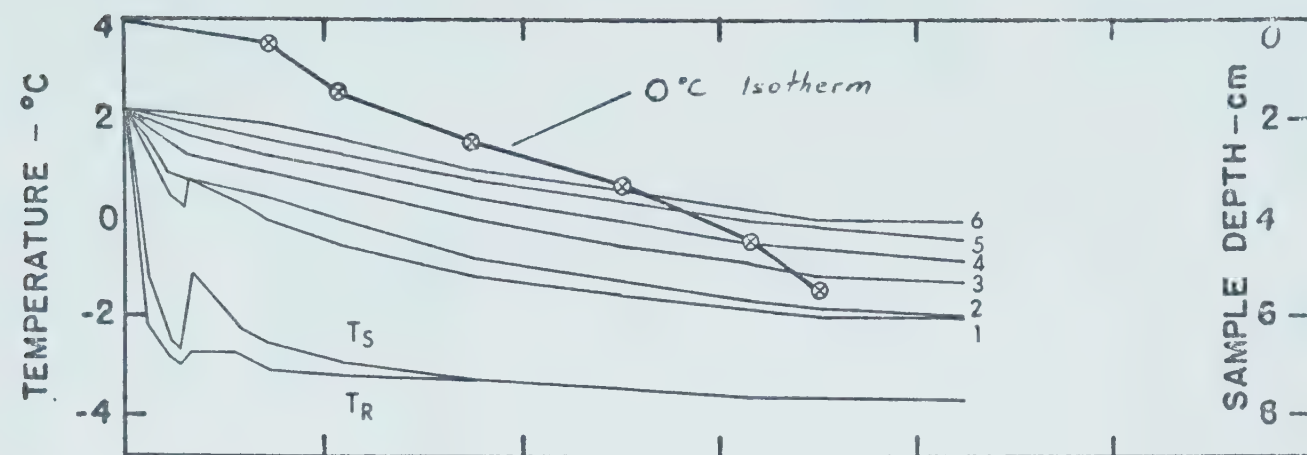


FIGURE F-5-5

APPENDIX G
SUMMARY OF DATA
MODIFIED DEVON SILT
(OVER CONSOLIDATED)

APPENDIX G

TABLE 1

Summary of Soil Mechanics Data

Modified Devon Silt - Over Consolidated

Figure- Test	P_c^2 Kg/cm ²	σ^2 Kg/cm ²	U_b^2 Kg/cm ²	Drainage	h_o cm	W_s gm	C_u	γ_d^3 gm/cm ³
G-1	7.70	3.07	2.97	0	6.433	843.0	353	1.57
G-2	7.70	3.21	2.97	0	6.550	843.0	353	1.54
G-3	7.70	3.46	2.97	0	6.503	843.0	353	1.55
G-4	7.70	3.70	2.97	0	6.422	843.0	353	1.57
G-5	7.70	3.95	2.97	0	6.326	843.0	353	1.60
G-6	7.70	4.19	2.97	0	6.304	843.0	353	1.61
G-7	7.70	5.90	2.97	0	6.227	843.0	353	1.62
G-8	7.70	5.21	2.97	0	6.223	843.0	353	1.62

APPENDIX G

(TABLE 1 Continued)

Figure- Test	W _O %	C _O	S %	W _f %	e _f	n	C _V cm ² /sec x10 ⁻³	k (cm/sec) x10 ⁻⁷
G-1	61.6	1.68	98.5	26.6	0.719	0.418	1.175	0.565
G-2	-	-	-	27.8	0.751	0.428	-	-
G-3	-	-	-	27.3	0.737	0.425	-	-
G-4	-	-	-	26.4	0.715	0.416	-	-
G-5	-	-	-	25.6	0.691	0.408	-	-
G-6	-	-	-	25.3	0.684	0.406	-	-
G-7	-	-	-	24.6	0.664	0.399	-	-
G-8	-	-	-	24.5	0.662	0.398	-	-

O - Open drainage

C - Closed drainage

APPENDIX G

TABLE 2

Summary of Freezing Test Data

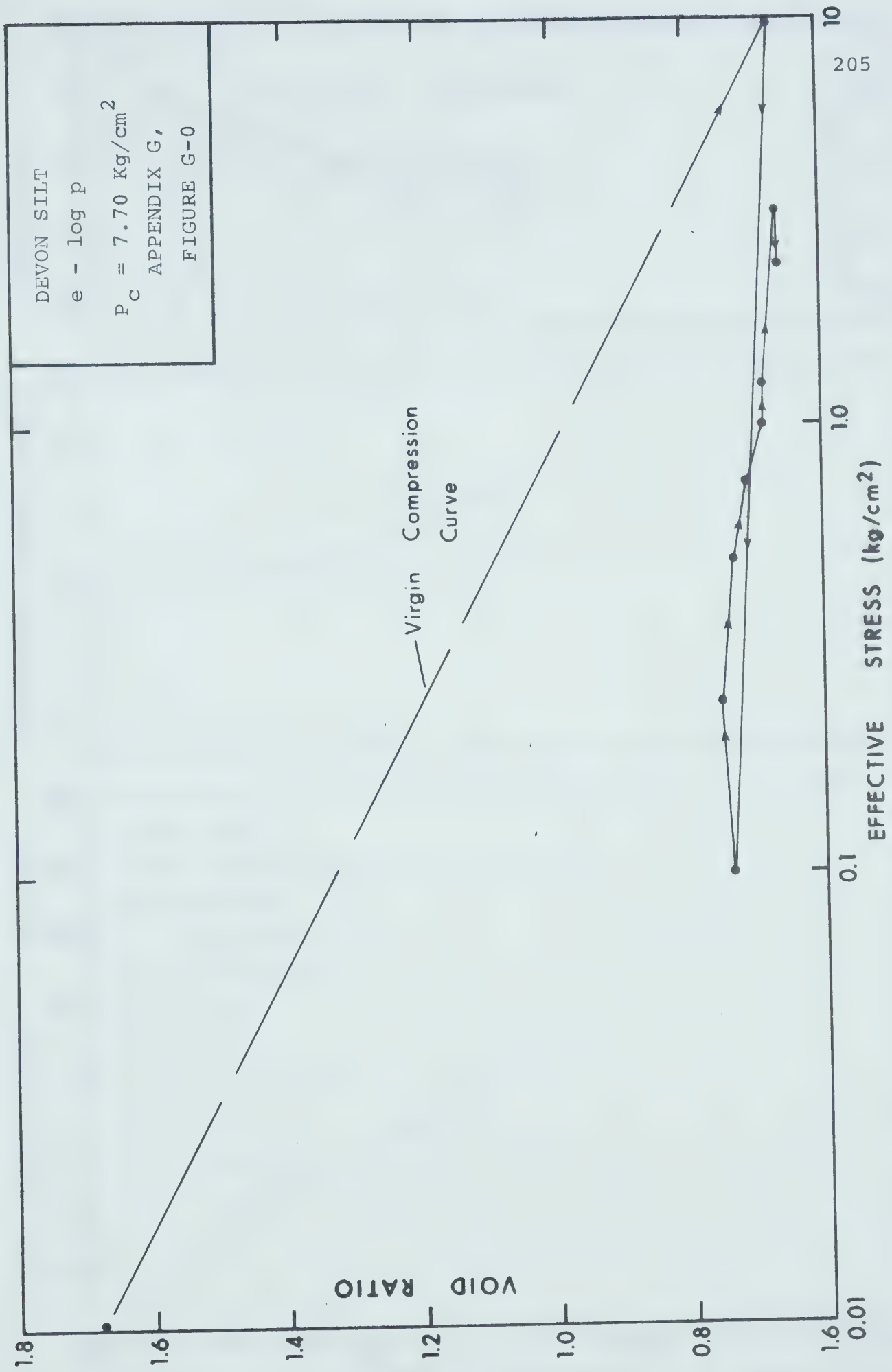
Modified Devon Silt - Over Consolidated

Figure- Test	T _b °C	t min	X thmc. cm	α_a cm/ $\sqrt{\text{min}}$ thmc.
G-1	-5.22	122	4.83	0.436
G-2	-4.87	166	4.95	0.417
G-3	-4.72	182	4.90	0.363
G-4	-4.79	164	4.82	0.376
G-5	-4.89	136	4.73	0.405
G-6	-5.00	149	4.70	0.384
G-7	-5.00	150	4.63	0.378
G-8	-4.50	172	3.62	0.276

APPENDIX G

(TABLE 2 Continued)

Figure Test	ΔV cm ³	at t = 160 min Heave S, cm	Heave Pressure P_h - Kg/cm ²
G-1	+1.40	0.085	-
G-2	+0.27	0.073	-
G-3	0.0	0.052	-
G-4	-1.01	0.058	-
G-5	+0.58	0.064	-
G-6	+0.50	0.063	-
G-7	-0.31	0.038	-
G-8	-0.52	0.010	+1.18
Porewater Expelled: $-\Delta V$ Porewater Sucked in: $+\Delta V$ thmc. - thermocouple			



DEVON SILT

$e - \log p$

$P_c = 7.70 \text{ Kg/cm}^2$

APPENDIX G,

FIGURE G-0

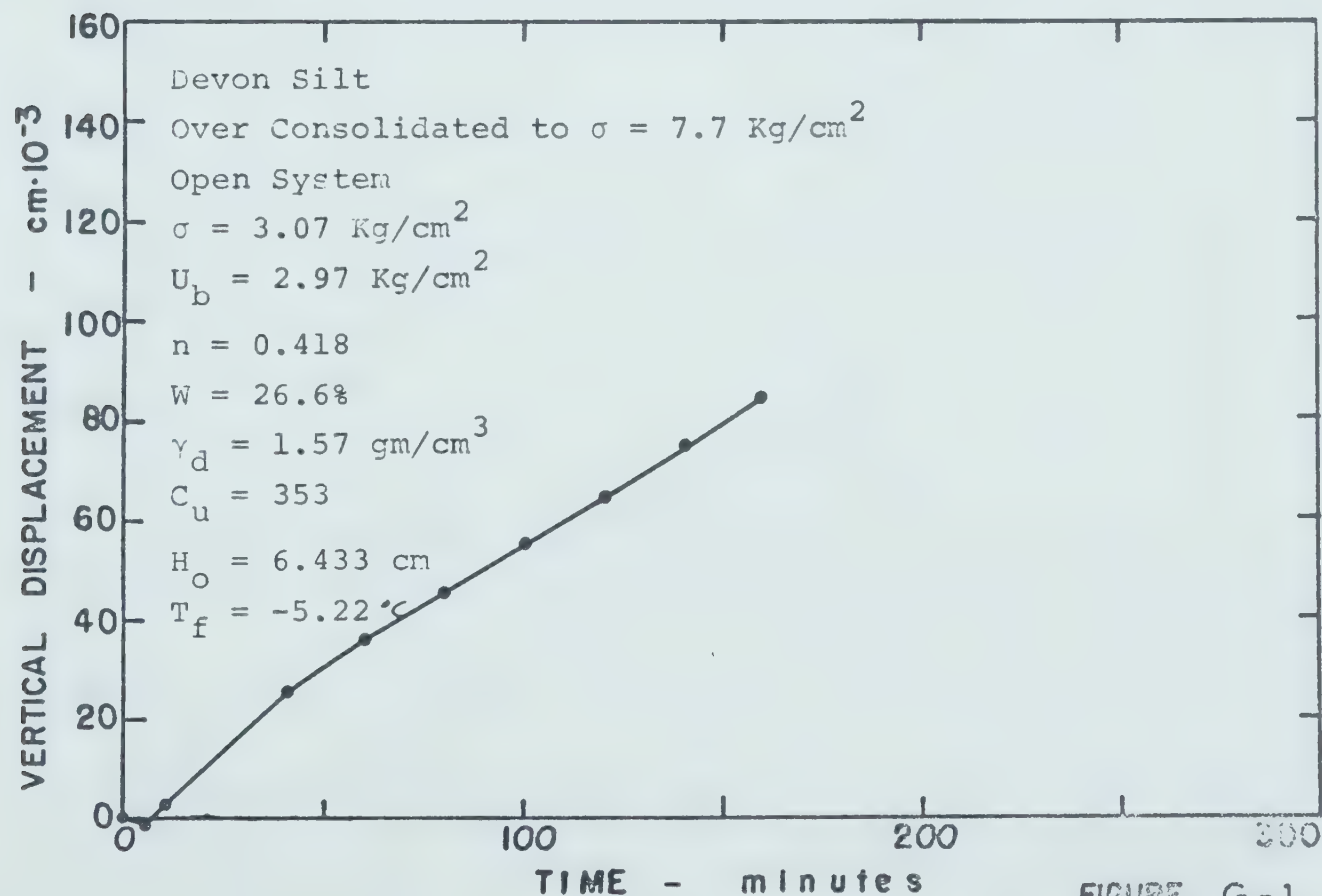
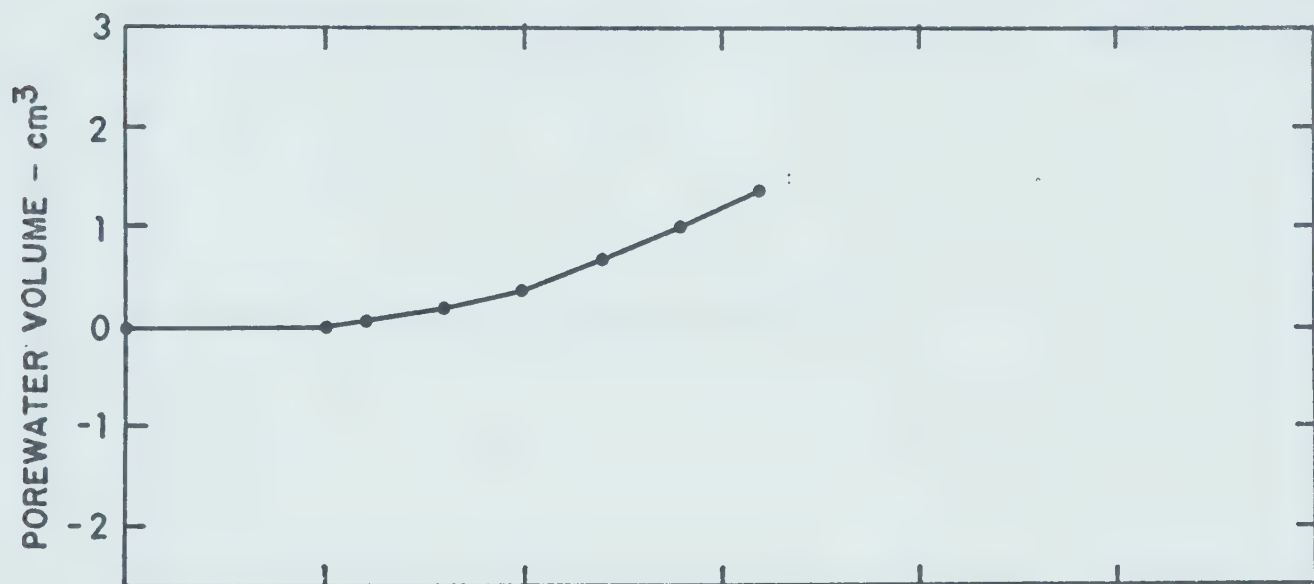
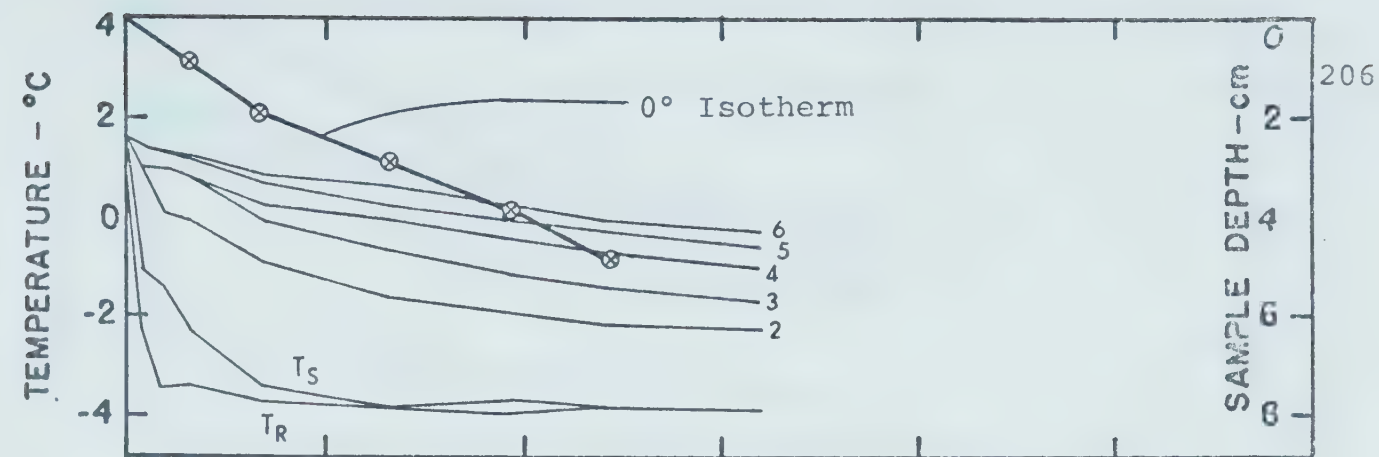


FIGURE G-1

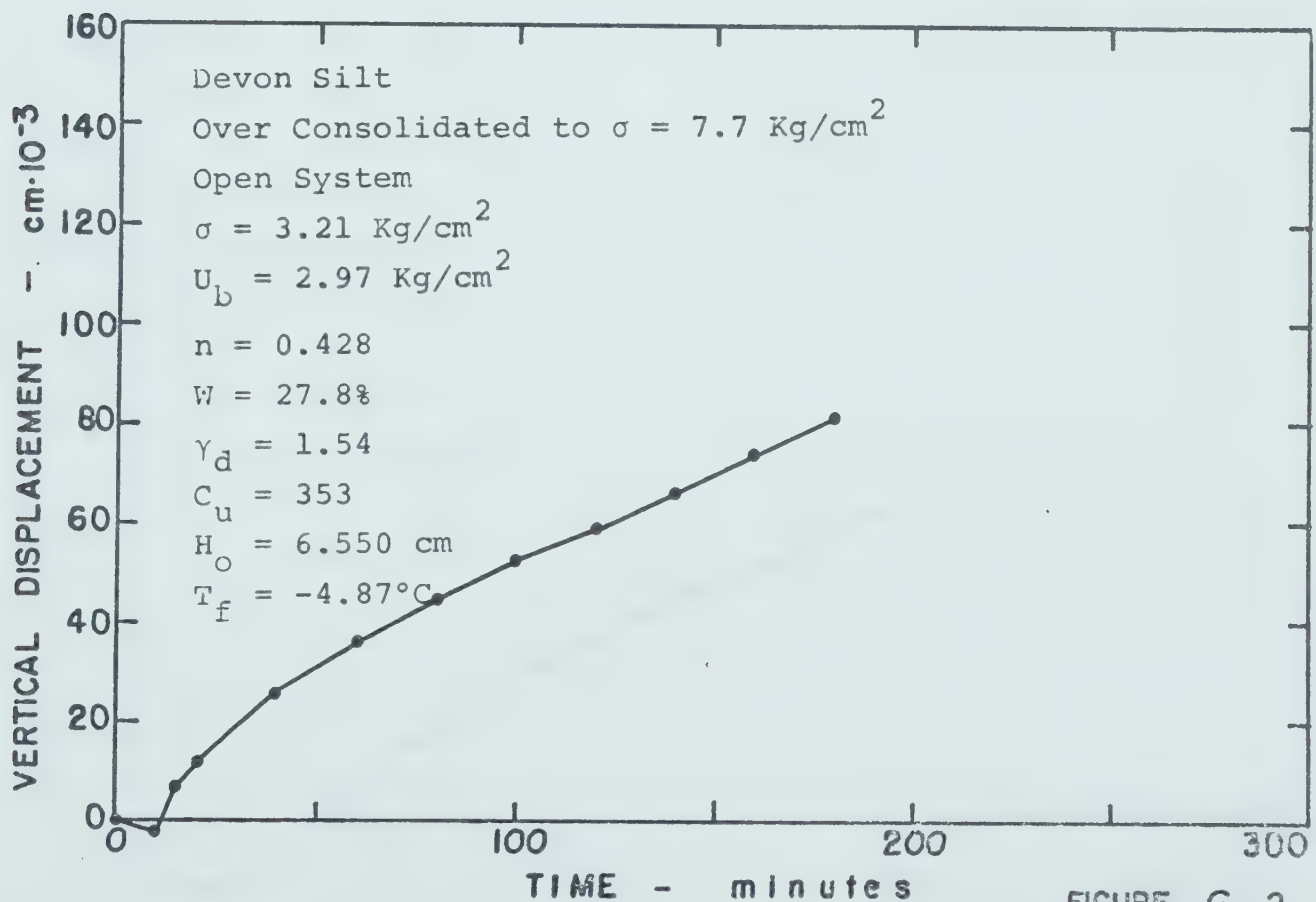
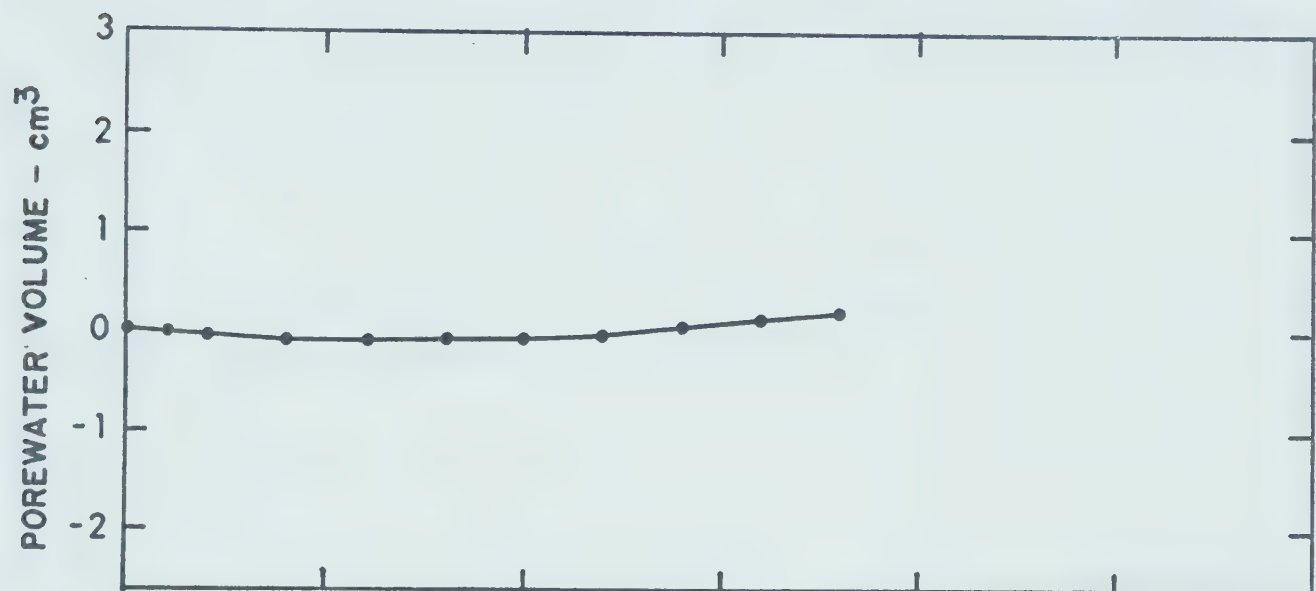
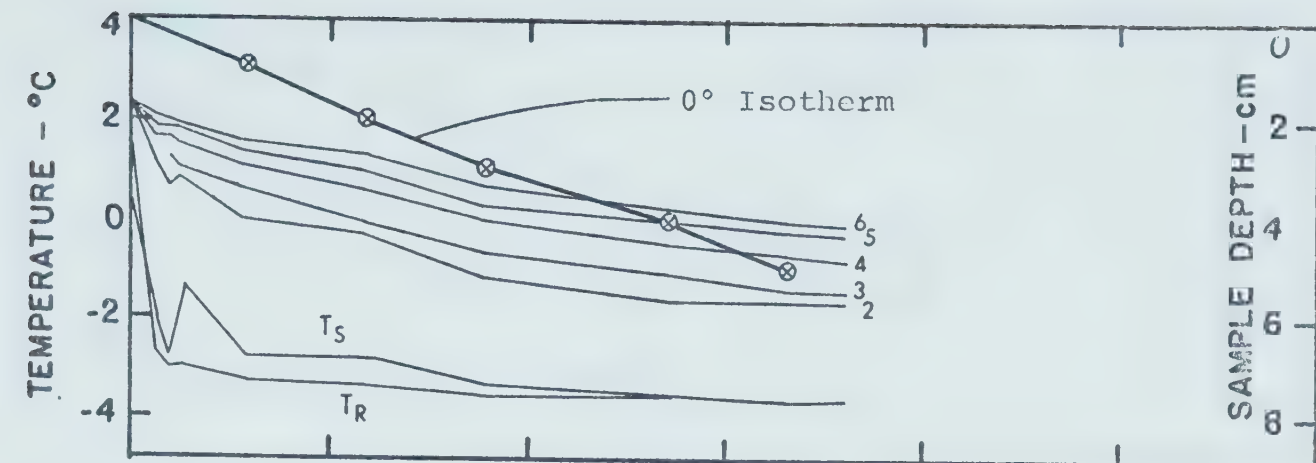


FIGURE G-2

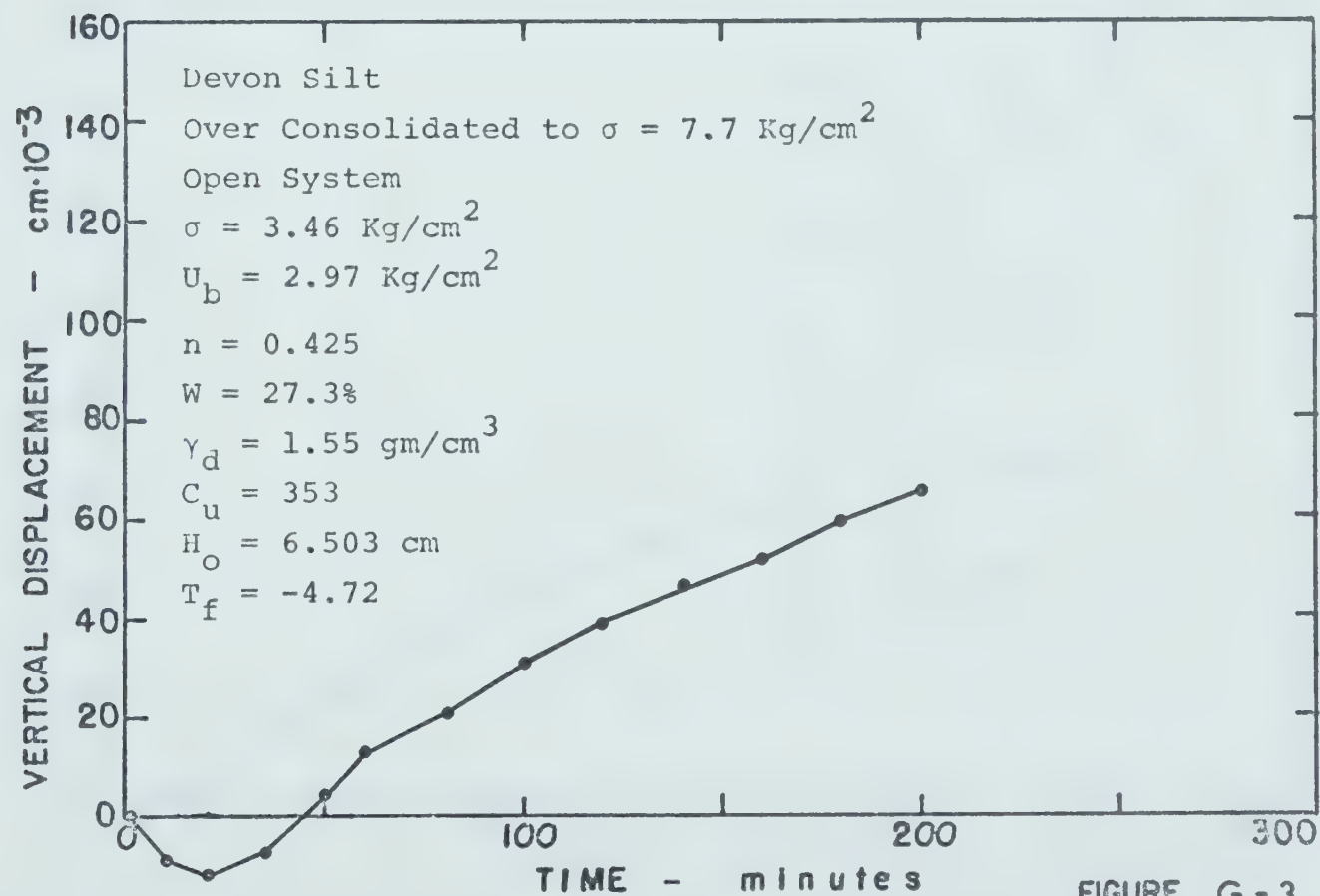
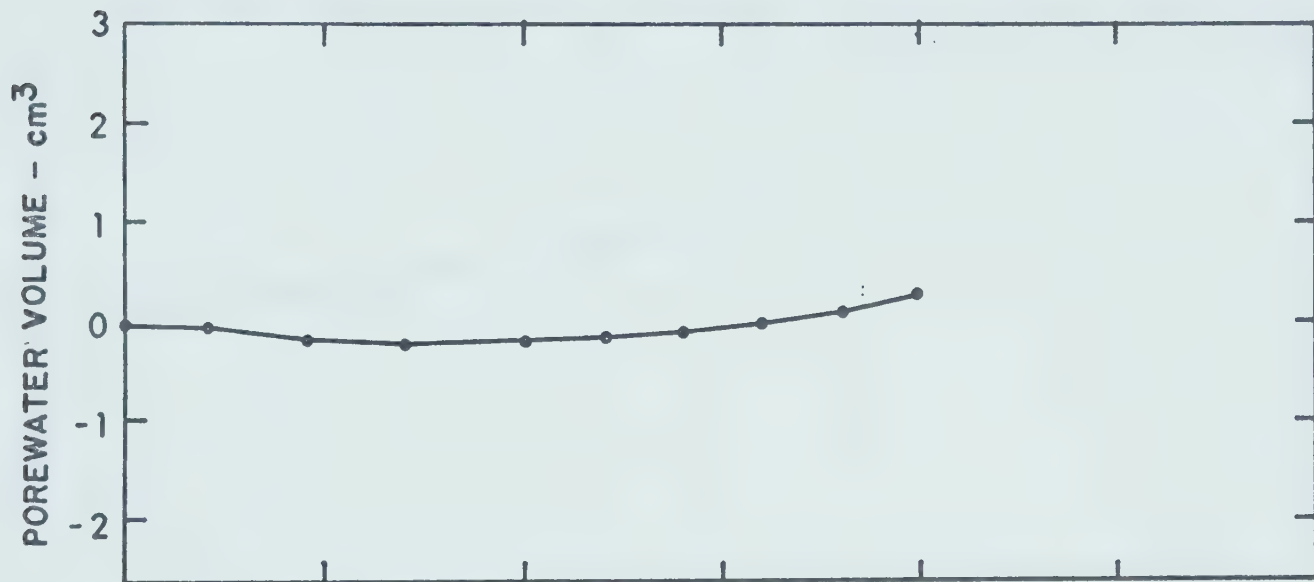
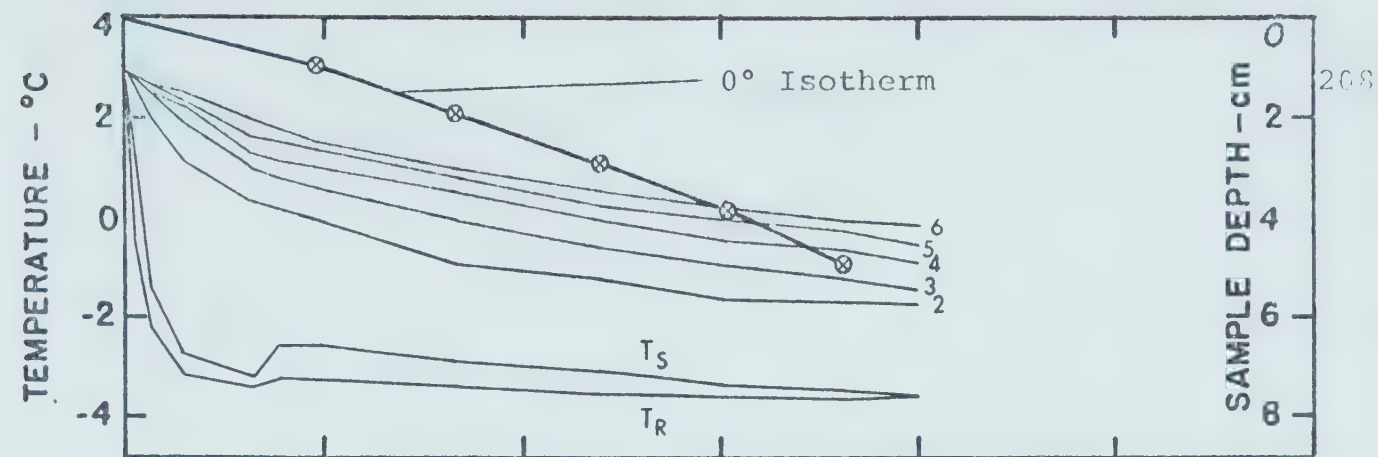


FIGURE G-3

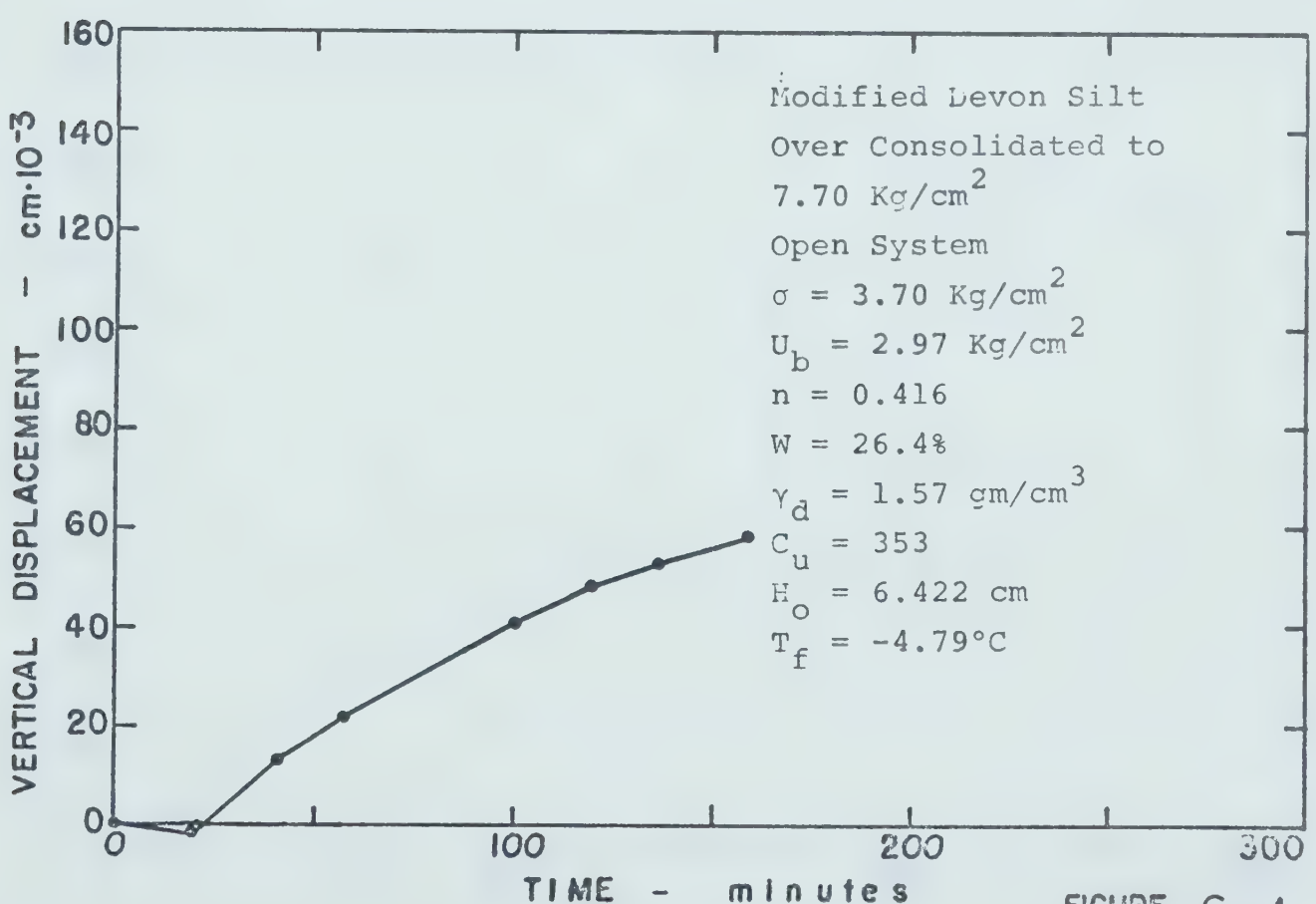
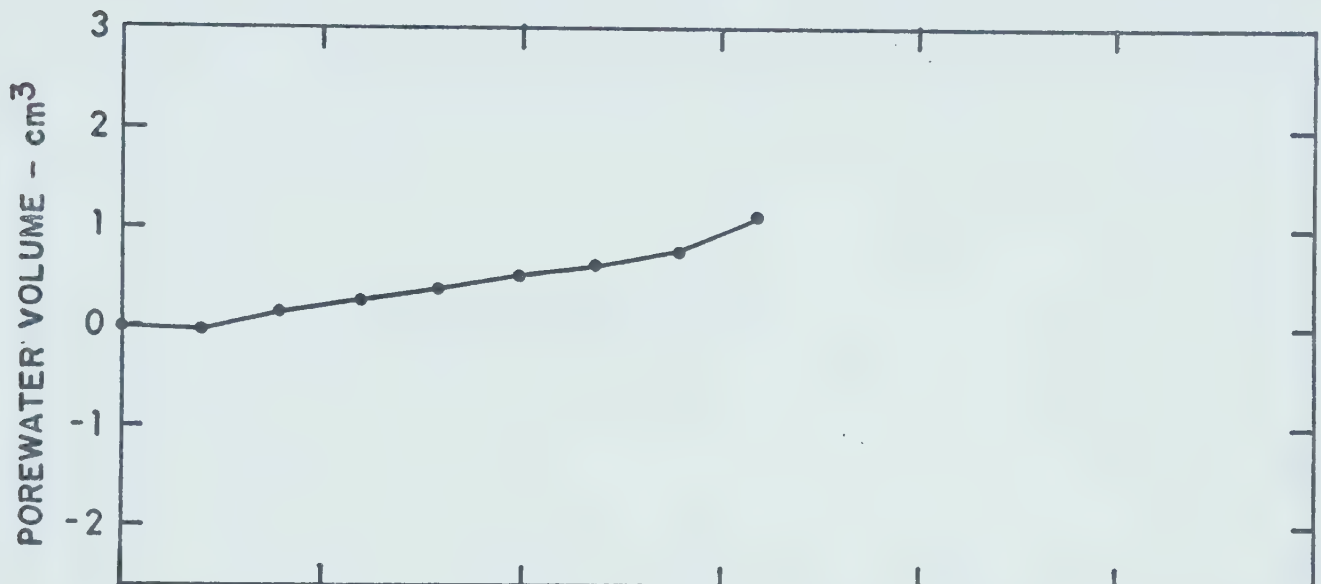
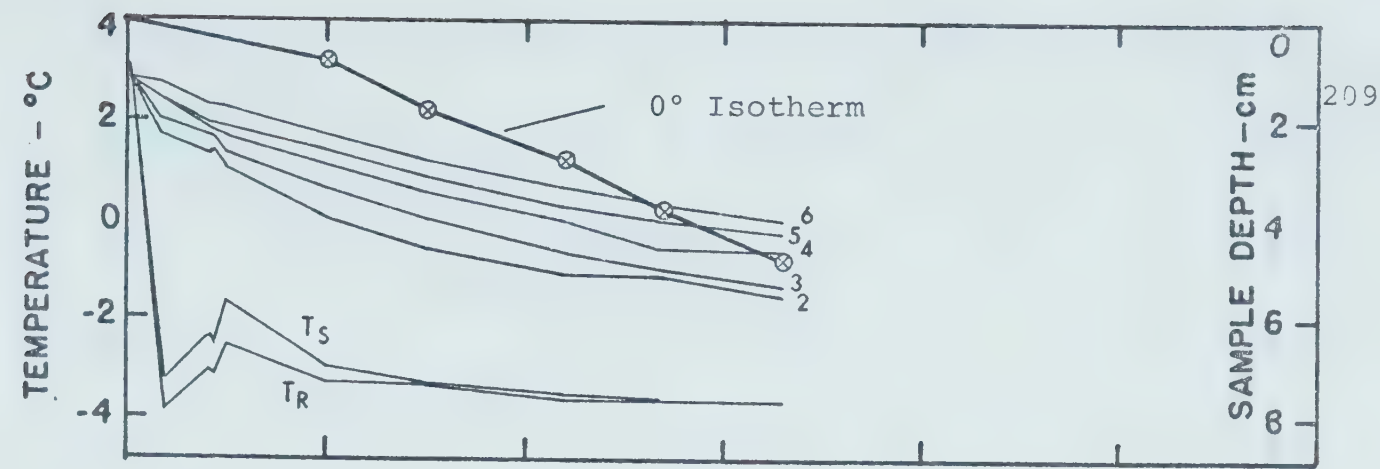


FIGURE G - 4

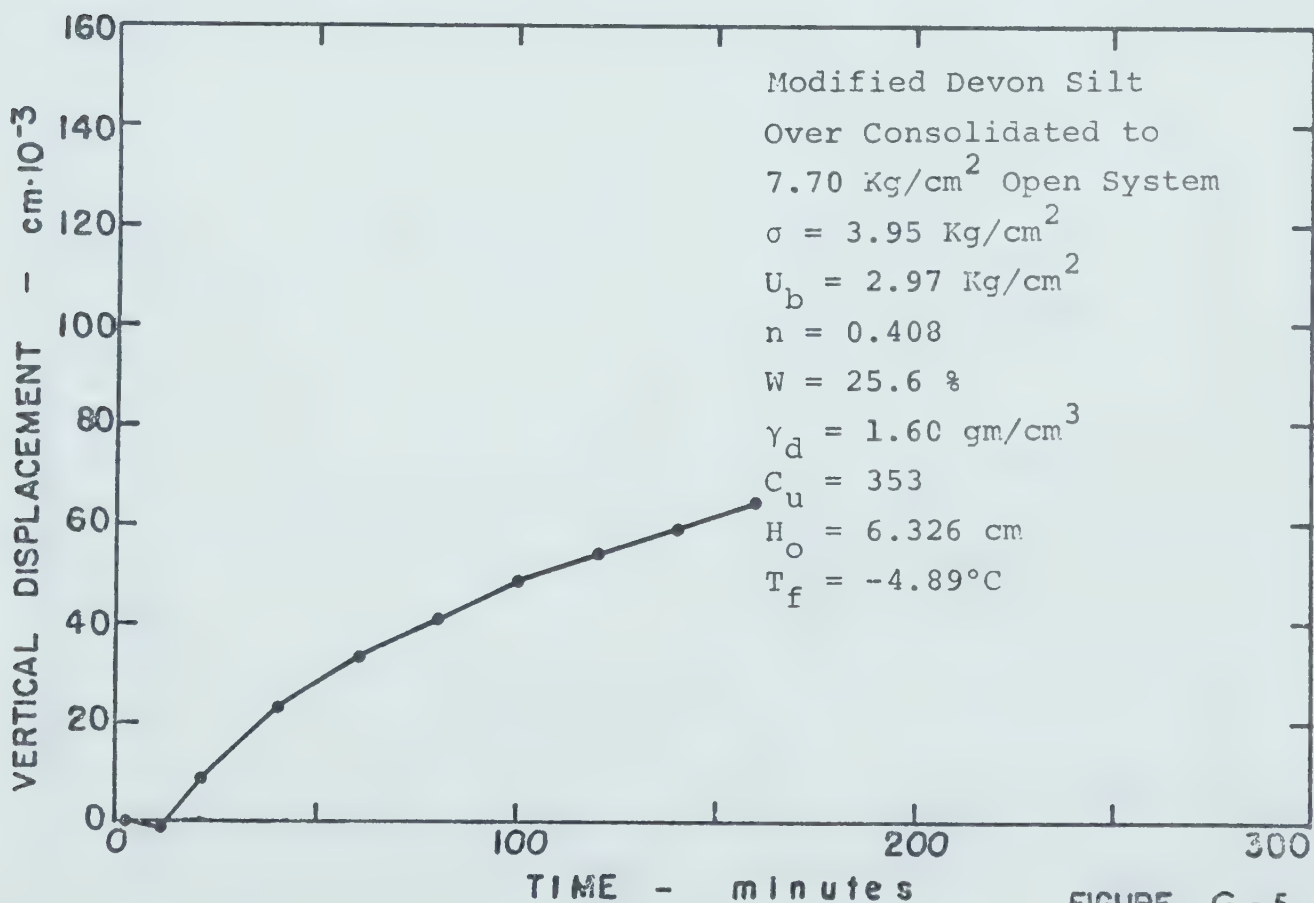
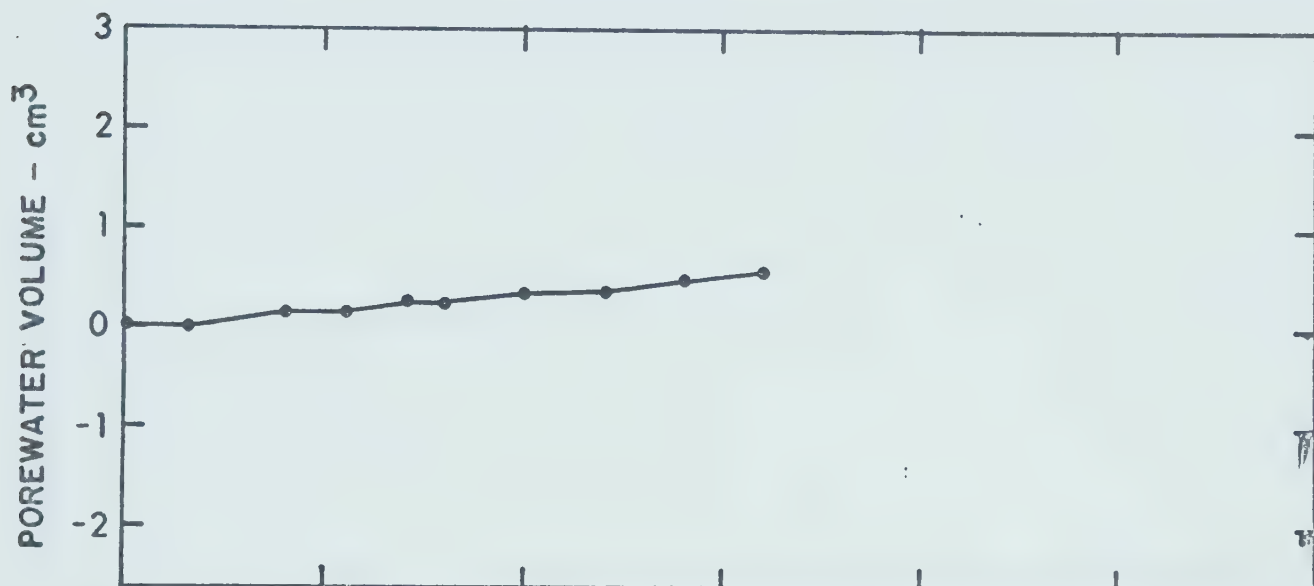
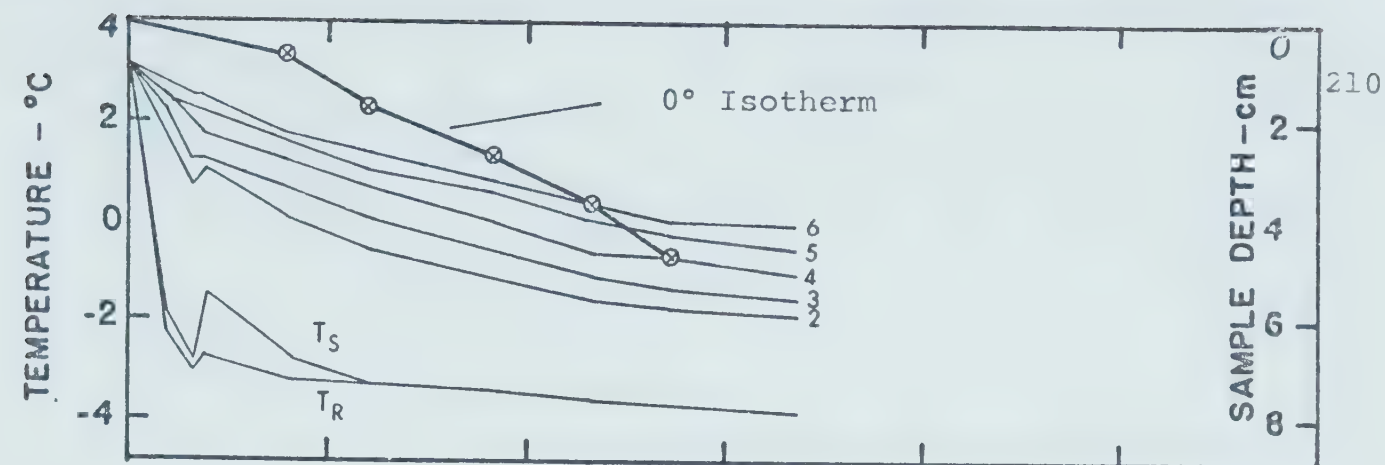


FIGURE G-5

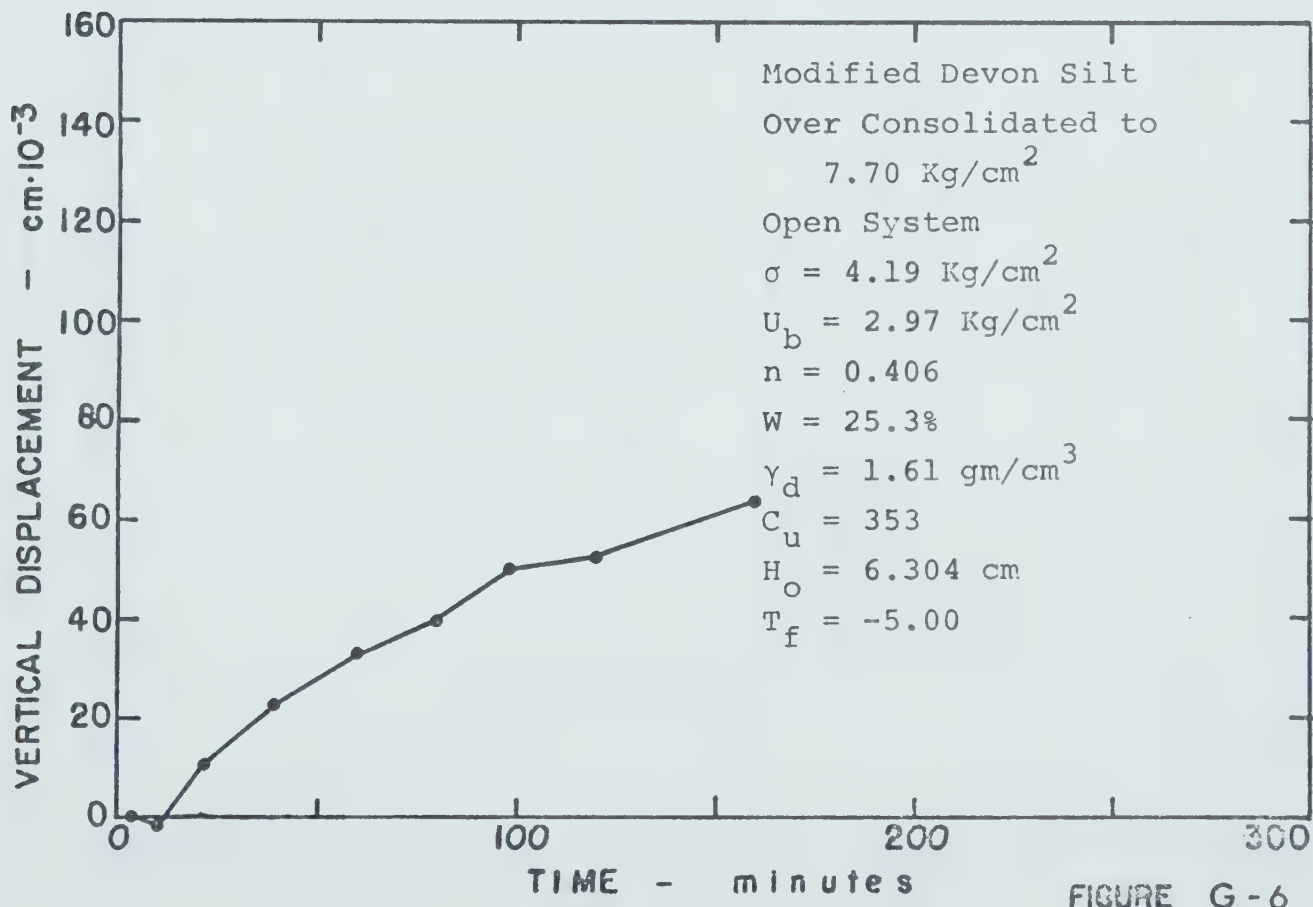
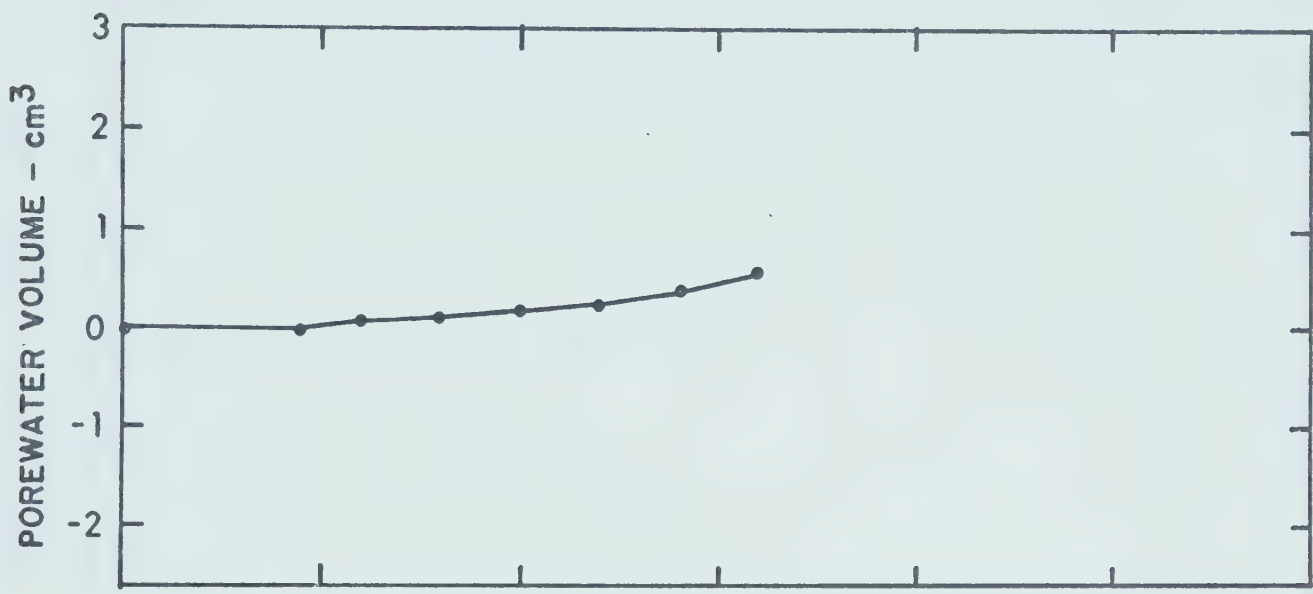
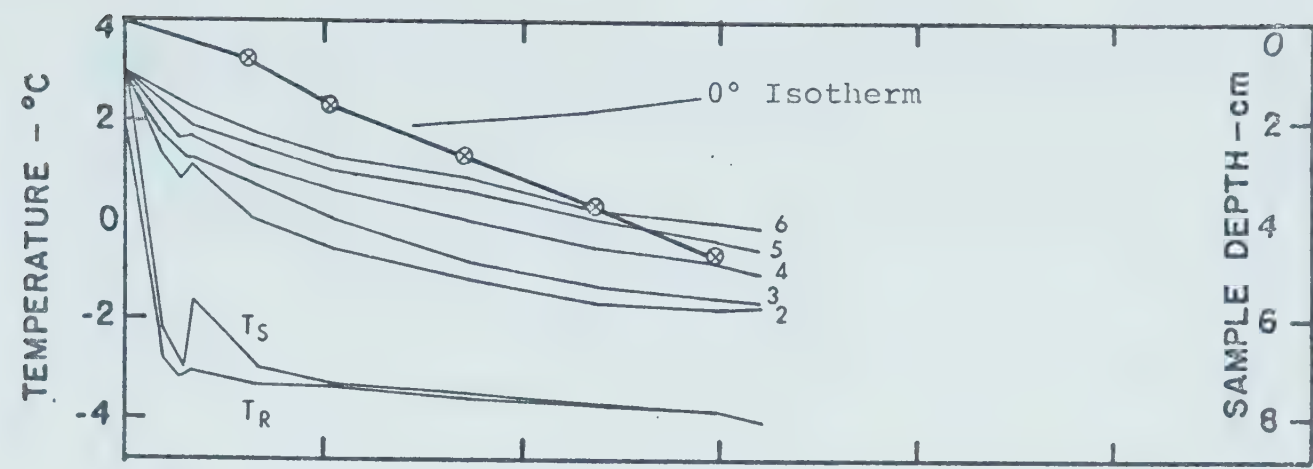


FIGURE G-6

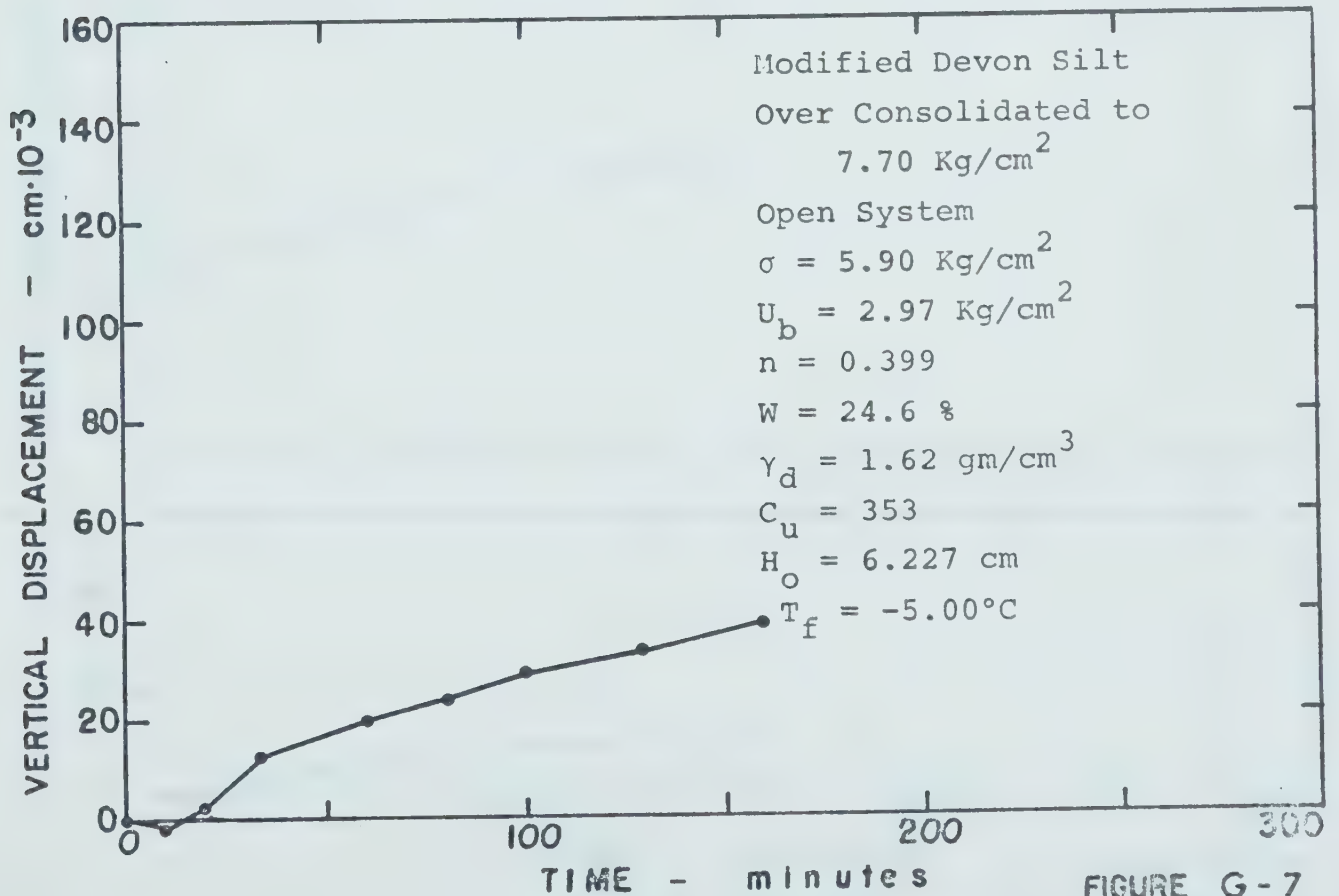
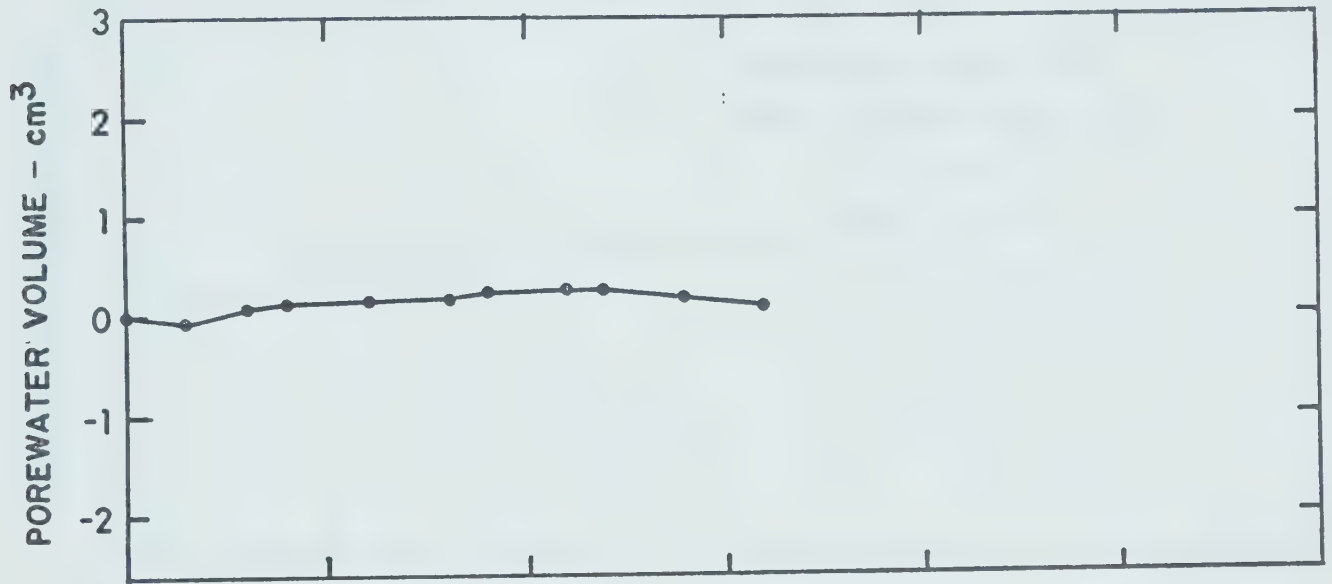
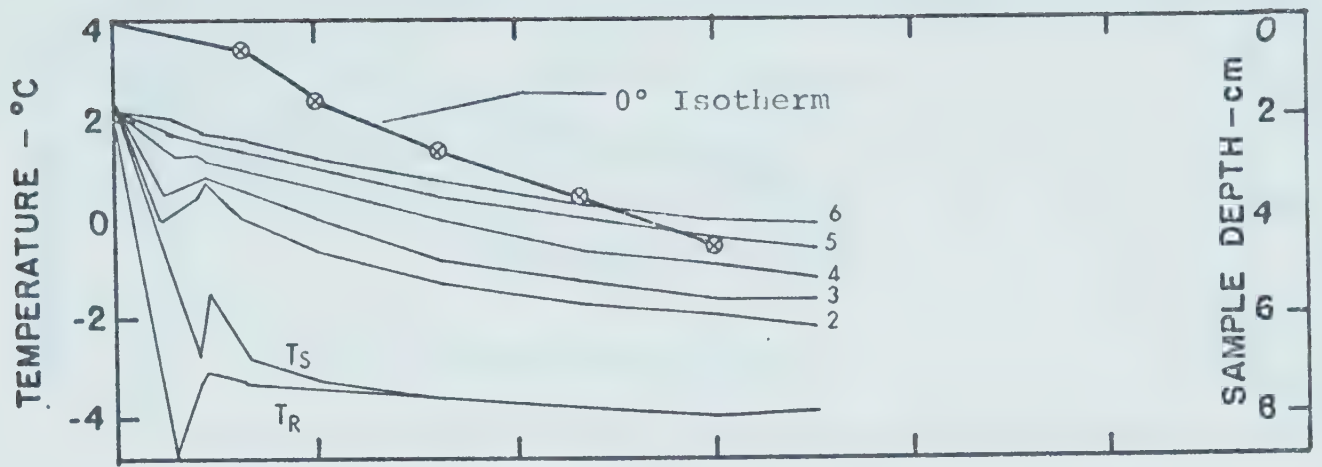


FIGURE G-7

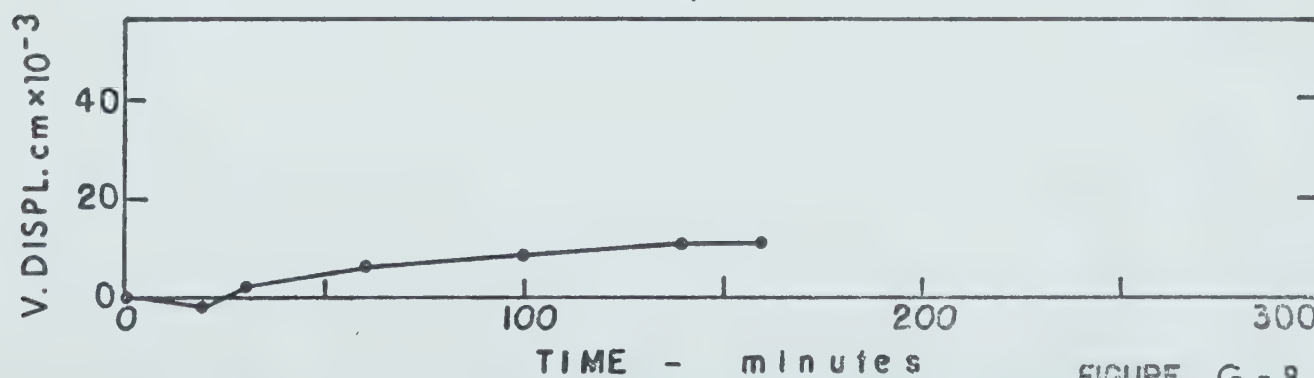
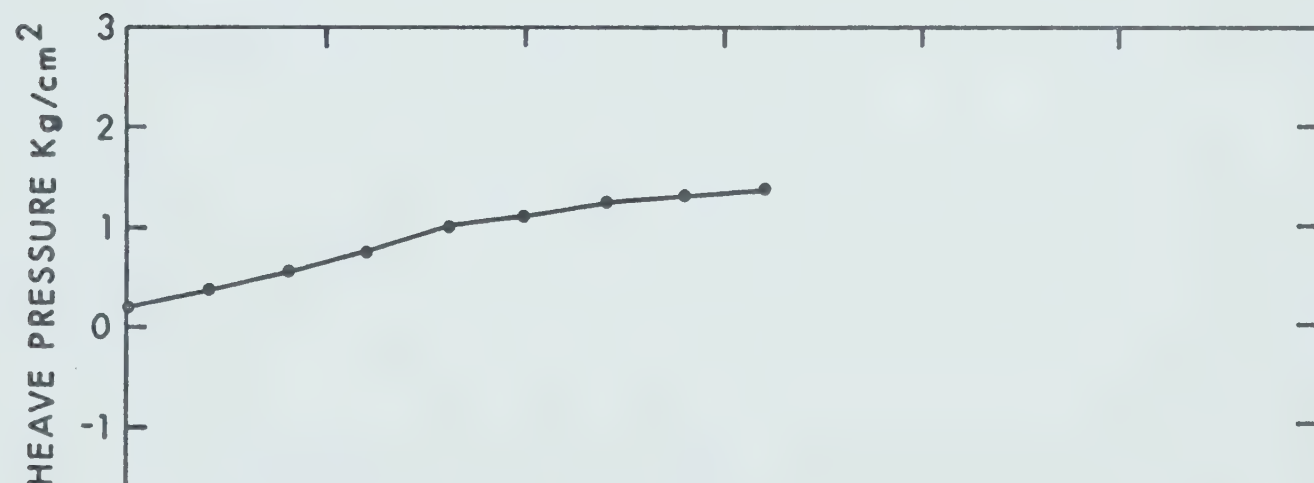
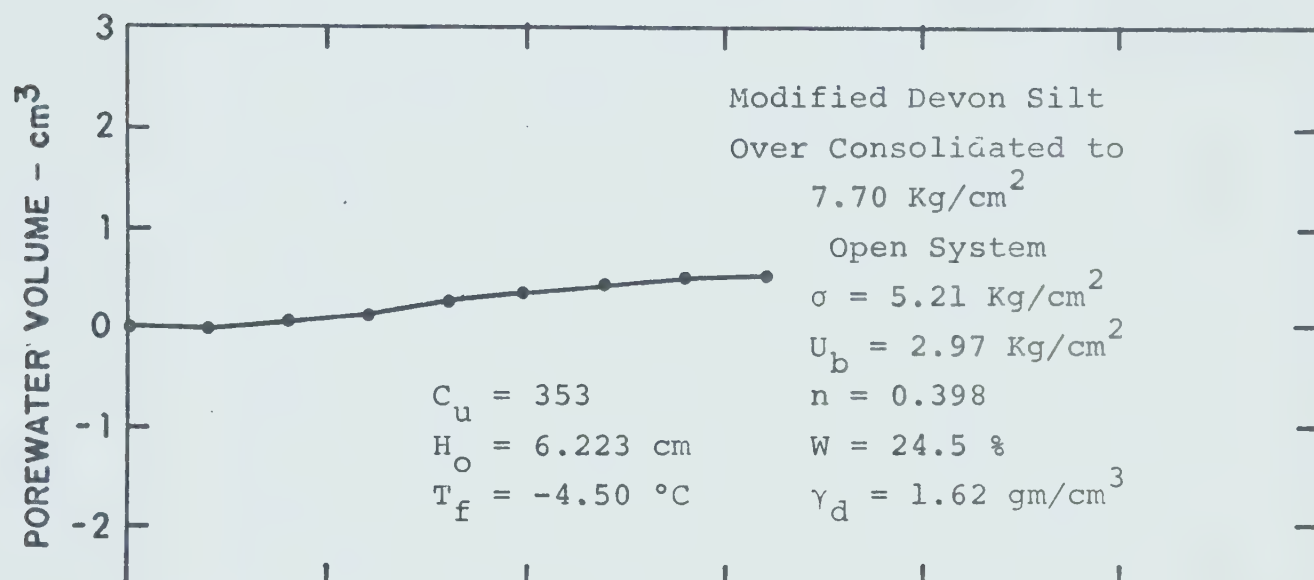
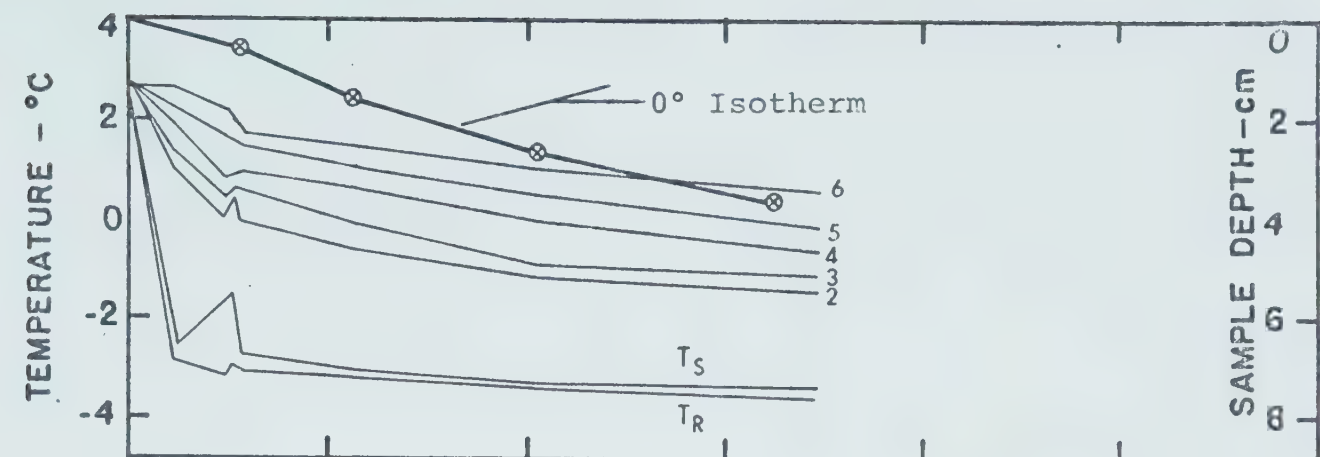


FIGURE G - 8

B30059